

PARABOLIC CATALAND

HABILITATIONSSCHRIFT

vorgelegt

dem Bereich Mathematik und Naturwissenschaften

der Technischen Universität Dresden

von

Dr. rer. nat. Henri Mühle

geboren am 15.07.1984 in Dresden

Eingereicht am: 04.02.2021

Wissenschaftlicher Vortrag und Aussprache,

sowie Probevorlesung am 06.10.2021

Die Habilitationsschrift wurde in der Zeit von Oktober 2019

bis Januar 2021 im Institut für Algebra angefertigt.

Für Paulina

Contents

Contents	v
List of Figures	ix
List of Tables	xiii
Acknowledgements	xv
Summary	xvii
Zusammenfassung	xix
Notation	xxi
Chapter 0. Prologue	1
Noncrossing partitions	1
Triangulations	2
Stack-sortable permutations	3
Dyck paths	3
Organization of this thesis	4
Chapter 1. Preliminaries	7
1.1. Posets and lattices	7
1.1.1. A notion of order	7
1.1.2. Diagrams and labelings	8
1.1.3. Duality and multichains	8
1.1.4. Zeta polynomial and Möbius function	9
1.1.5. Lattices	10
1.1.6. Distributivity	12
1.1.7. Semidistributivity	13
1.1.8. Trimness	15
1.1.9. Congruence-uniformity	18
1.1.10. The core label order	19
1.2. Coxeter groups	22
1.2.1. Coxeter systems	22
1.2.2. The geometric representation	24
1.2.3. Ordering a Coxeter group	27

1.2.4. Orienting a Coxeter group	30
Chapter 2. Cataland	33
2.1. Catalan numbers	33
2.2. Aligned elements	35
2.2.1. Cambrian lattices	38
2.3. Noncrossing partitions	43
2.4. Clusters	48
2.5. Nonnesting partitions	55
2.5.1. ν -Tamari lattices	57
2.6. Chapoton Triangles	59
Chapter 3. Parabolic Cataland: Origins	63
3.1. Parabolic quotients of Coxeter groups	63
3.2. Parabolic aligned elements	65
3.3. Parabolic noncrossing partitions	68
3.4. Parabolic clusters	70
3.5. Parabolic nonnesting partitions	71
3.6. Parabolic Chapoton triangles	73
Chapter 4. Parabolic Cataland: Linear type A	81
4.1. Definitions	81
4.1.1. Parabolic quotients of the symmetric group	81
4.1.2. The longest α -permutation	82
4.1.3. The root poset of \mathfrak{S}_α and α -Dyck paths	83
4.1.4. \bar{c} -clusters for \mathfrak{S}_α	85
4.1.5. \bar{c} -aligned elements for \mathfrak{S}_α	87
4.1.6. \bar{c} -noncrossing partitions for \mathfrak{S}_α	90
4.1.7. α -trees	91
4.2. Bijections	93
4.2.1. Noncrossing α -partitions and $(\alpha, 231)$ -avoiding permutations	94
4.2.2. Noncrossing α -partitions and α -Dyck paths	96
4.2.3. α -trees and $(\alpha, 231)$ -avoiding permutations	99
4.2.4. α -trees and noncrossing α -partitions	102
4.2.5. α -trees and α -Dyck paths	105
4.3. Posets	110
4.3.1. The weak order on $\mathfrak{S}_\alpha(231)$	110
4.3.2. The rotation order on $\text{Dyck}(\alpha)$	122
4.3.3. The core label order of $\mathbf{Tam}(\alpha)$	133
4.4. Chapoton triangles	137
4.5. Applications	141
4.5.1. A Hopf algebra on pipe dreams	141
4.5.2. A zeta map from diagonal harmonics	150
Chapter 5. Epilogue	161
5.1. Arbitrary type A	161
5.2. Linear type B	165
5.3. (α, m) -Tamari lattices	176
5.4. Parabolic multiclusters	182
Chapter A. Data	185
A.1. Parabolic Catalan numbers in rank 3	185

CONTENTS

vii

A.2. Parabolic Catalan numbers in rank 4	186
A.3. Answers to Research Challenge 3.3.4 in rank 4	188
Bibliography	189
Index	199
Declaration	203

List of Figures

1	A poset diagram together with an edge-labeling.....	8
2	The poset diagram of the Boolean lattice of order 3.....	11
3	Two lattices with five elements.....	12
4	A join-semidistributive lattice and related structures.....	14
5	An extremal lattice with its associated Galois graph.....	16
6	An extremal lattice that is not left modular.....	16
7	A directed graph associated with the lattice from Figure 5a and its lattice of orthogonal pairs.....	17
8	The smallest semidistributive lattice that is not congruence uniform.....	19
9	The core label order of the semidistributive lattice from Figure 8.....	20
10	A Coxeter matrix (left) and its associated Coxeter graph (right).....	23
11	Some Coxeter graphs.....	23
12	The finite crystallographic root systems of rank 2.....	26
13	The root poset of type A_4	27
14	The root posets of type B_4 and D_4	27
15	The finite crystallographic Coxeter groups of rank 2 ordered by weak order.....	28
16	The finite crystallographic Coxeter groups of rank 2 ordered by absolute order.....	29
17	A mutation of a Coxeter graph.....	31
18	The s_1s_2 -Cambrian lattices for the finite crystallographic Coxeter groups of rank 2. ...	39
19	The $s_2s_1s_3$ -Cambrian lattice of A_3	39
20	The $s_0s_1s_2$ -Cambrian lattice of B_3 as it arises as a lattice quotient of Weak (B_3).....	40
21	The componentwise order on $\text{Codes}(4)$	42
22	The lattice Nonc (4).....	43
23	The bijections involving permutations and noncrossing partitions for $n = 4$	45
24	Increasing flip orders of two subword complexes.....	51
25	A reduced pipe dream for $w = 54712683 \in \mathfrak{S}_8$	51
26	Labeling the boxes of the staircase shape for $n = 6$	52

27	The fourteen reduced pipe dreams for $w_{(4)}$	53
28	Illustration of a chute move.....	54
29	The chute order on $\text{Pipe}(4)$ realizing $\mathbf{Tam}(4)$	54
30	The nine ENENN-paths with peaks and valleys marked by blue squares and red circles, respectively.	55
31	Converting a Dyck path into a nonnesting partition, an order ideal and an antichain in the triangular poset for $n = 9$	56
32	The surrogate root posets for H_3 and $I_2(m)$	57
33	The four potential “fake” root posets for H_4	58
34	The rotation of a v -path for $v = \text{EEENENNEENEEN}$	59
35	The ENENN-Tamari lattice.....	59
36	The lattice $\mathbf{Weak}(B_3^{\{s_0, s_2\}})$	64
37	Some parabolic posets for A_3	68
38	The poset $\mathbf{Nonc}(B_3^{\{s_0, s_2\}}, s_0s_1s_2)$	69
39	Some parabolic root posets.	71
40	The ten nonnesting partitions of $A_3^{\{s_2\}}$	72
41	The eleven nonnesting partitions of $B_3^{\{s_0, s_2\}}$	72
42	The flip poset $\mathbf{Clus}(A_3^{\{s_2\}}, s_1s_2s_3)$	75
43	The lattice $\mathbf{Camb}(H_3^{\{s_2, s_3\}}, s_2s_1s_3)$	79
44	The poset $\mathbf{Nonc}(H_3^{\{s_2, s_3\}}, s_2s_1s_3)$	79
45	Right-flushing of an α -Dyck path produces a pipe dream for $w_{\langle \alpha \rangle}$	86
46	Illustrating the various traversals of a plane rooted tree.....	92
47	A plane rooted tree compatible with $\alpha = (3, 4, 2, 1, 4, 2)$	93
48	A commuting diagram of bijections.....	94
49	An illustration of the bijection Φ_{perm}	96
50	The α -path $\Phi_{\text{path}}(P)$, where $\alpha = (3, 4, 2, 1, 4, 2)$ and P is the noncrossing α -partition from Example 4.1.20.	98
51	An α -tree labeled in LR-postfix order for $\alpha = (3, 4, 2, 1, 4, 2)$, and the associated $(\alpha, 231)$ -avoiding permutation.	100
52	Illustration of the bijection from $\text{Tree}(\alpha)$ to $\text{Nonc}(\alpha)$	103
53	A labeled α -tree and its associated α -Dyck path.	106
54	The $(1, 2, 1)$ -Tamari lattices as it arises as a quotient lattice of $\mathbf{Weak}(\mathfrak{S}_{(1,2,1)})$	114
55	An illustration of Theorem 4.3.11.	115
56	Illustrating the inversion set of a join-irreducible $(\alpha, 231)$ -avoiding permutation.....	116
57	The lattice $\mathbf{Tam}((2, 1, 2))$	119
58	Two posets of join-irreducible α -permutations.	121
59	Galois graphs of two α -Tamari lattices.	122
60	The lattice $\mathbf{Tam}(v_{(1,2,1)})$	123
61	The lattice $\mathbf{Tam}(v_{(2,1,2)})$	124

62	Decoding the $(2, 3, 2, 1)$ -code $(2, 6, 0, 1, 3, 1, 1, 0)$.	127
63	The weak order on $\mathfrak{S}_{(1,2,1)}$, where the permutations are additionally labeled by their $(1, 2, 1)$ -codes.	129
64	Two α -Dyck paths for $\alpha = (2, 3, 2, 1)$.	129
65	Illustration of the map Υ for $\alpha = (2, 3, 2, 1)$.	131
66	The poset $\mathbf{CLO}(\mathbf{Tam}((1, 2, 1)))$.	135
67	The poset $\mathbf{CLO}(\mathbf{Tam}((2, 1, 2)))$.	136
68	Reversing the composition yields isomorphic core label orders.	137
69	The $(1, 2, 1)$ -Dyck paths together with their contribution to $\mathcal{H}_{(1,2,1)}(x, y)$.	138
70	The $(2, 1, 2)$ -Dyck paths together with their contribution to $\mathcal{H}_{(2,1,2)}(x, y)$.	138
71	The $(2, 1, 1)$ -Dyck paths together with their contribution to $\mathcal{H}_{(2,1,1)}(x, y)$.	141
72	Untangling a pipe dream at a global descent.	143
73	Two examples of the tangling of pipe dreams.	144
74	Illustrating the bijection from \mathcal{N}_n to $\text{Pipe}_n\langle\{\text{id}_1, \text{id}_2, \text{id}_3, \dots\}\rangle$ for $n = 16$.	146
75	A Dyck path and its image under the inverse zeta map.	152
76	The fourteen Dyck paths of semilength 4 together with various statistics.	153
77	The sets $\text{SteepPair}(3)$, $\text{LAC}(3)$ and $\text{BouncePair}(3)$ arranged according to Λ_{steep} and Ξ_{bounce} .	154
78	Illustration of the map Γ from $\text{SteepPair}(n)$ to $\text{BouncePair}(n)$ for $n = 16$.	155
79	The zeta map is a restriction of Γ .	156
80	An acyclic orientation, a Coxeter element and a barring for A_7 .	162
81	The two posets of (α, ε) -sortable permutations for $\alpha = (1, 2, 1)$.	163
82	The lattice $\mathbf{Camb}(A_3^{\{s_2\}}, s_2s_3s_1)$.	163
83	A ε -noncrossing α -partition together with its diagram and an (α, ε) -sortable permutation.	164
84	The root poset of type B_4 realized by vectors in \mathbb{R}^4 .	166
85	The lattice $\mathbf{Weak}(B_{\alpha^{(1)}}(231))$.	171
86	The lattice $\mathbf{Weak}(B_{\alpha^{(2)}}(231))$.	173
87	The core label order of $\mathbf{Weak}(B_{\alpha^{(1)}}(231))$.	173
88	The core label order of $\mathbf{Weak}(B_{\alpha^{(2)}}(231))$.	174
89	Interpreting order ideals in the type-B root posets as centrally symmetric Dyck paths.	174
90	The parabolic type-B Dyck paths for $\alpha = (0, 1, 2)$.	175
91	The parabolic type-B Dyck paths for $\alpha = (2, 1)$.	175
92	The elements of $\text{Paths}(v_{\alpha, 2})$ for $\alpha = (2, 1, 1)$.	179
93	The lattice $\mathbf{Tam}((2, 1, 1), 2)$.	180
94	The elements of $\text{Nonc}((2, 1, 1), 2)$.	181
95	The poset $\mathbf{Nonc}((2, 1, 1), 2)$.	181
96	The flip poset $\mathbf{Clus}(A_2, c, 2)$.	183
97	The flip poset of $\mathbf{Clus}(\mathfrak{S}_\alpha, c, 2)$ for $\alpha = (3, 1)$ and $c = s_2s_1s_3$.	184

List of Tables

1	The degrees, the Coxeter numbers and the Catalan numbers for the finite, irreducible Coxeter systems.	34
2	The subsets $J \subseteq S$ inducing a fully commutative quotient W^J	78
3	The various parabolic Catalan numbers in types A_3 , B_3 and H_3	185
4	The various parabolic Catalan numbers in types A_4 and B_4	186
5	The various parabolic Catalan numbers in type D_4	186
6	The various parabolic Catalan numbers in type F_4	187
7	The various parabolic Catalan numbers in type H_4	187
8	Answers to Research Challenge 3.3.4 for the crystallographic Coxeter groups of rank 4.	188

Acknowledgements

First and foremost I would like to thank Nathan Williams for sharing his constructions concerning Parabolic Cataland at an early stage and for being an inspirational collaborator and a good friend throughout the past years.

Secondly, I want to thank the Institute of Algebra at the Dresden University of Technology for hosting me in the past four and a half years. You may not be aware of how much this time has shaped me. I am particularly grateful to Manuel Bodirsky for being such a generous and supportive mentor.

I feel very fortunate that I had the chance to enjoy so many interesting, inspiring, and informative discussions with a lot of wonderful colleagues over my academic career. I have learned so much from you. I wish to mention Emily Barnard, Barbara Baumeister, François Bergeron, Cesar Ceballos, Camille Combe, Bérénice Delcroix-Oger, Wenjie Fang, Al Garver, Matthieu Josuat-Vergès, Christian Krattenthaler, Jean-Philippe Labbé, Erko Lehtonen, Thomas McConville, Philippe Nadeau, Jean-Christophe Novelli, Vincent Pilaud, Vivien Ripoll, Martin Rubey, Christian Stump, Eleni Tzanaki, Patrick Wegener. This list is certainly incomplete, and I apologize to anyone I have forgotten.

I am deeply grateful for being part of the algebraic combinatorics community, which gave me the chance to travel to so many places, to meet so many wonderful people and to acquire so many good memories.

A big shout out goes to my friends and family: you have all been very supportive, each in their own way. I am also much obliged to my team mates at Drehst'n Deckel and to all other Ultimate Frisbee players I had the pleasure to meet on (and off) the field. You have been providing a much needed contrast to my work.

Last but not least, I am especially happy about the two most important ladies in my life: Antje and Paulina, I hope you will always stay the way you are.

Summary

In the last few decades, combinatorial families exhibiting noncrossing or cluster phenomena have proven useful in understanding and connecting mathematical objects arising in seemingly unrelated branches of mathematics and theoretical physics.

These phenomena can be modeled in the context of Coxeter groups and play an important role in algebraic combinatorics. In finite type, such families are enumerated by generalized Catalan numbers.

In this thesis, we consider the extension of this theory to parabolic quotients of Coxeter groups. We outline the history, present the basic definitions and constructions, and provide a number of conjectures and research challenges arising in this context. We then solve these questions in linear type A and exhibit surprising connections of this theory to certain Hopf algebras and to the theory of diagonal harmonics. We end this thesis by proposing related directions for future research.

Zusammenfassung

Kombinatorische Familien, die nichtkreuzende oder Cluster-Phänomene aufweisen, haben sich in den letzten Jahrzehnten als wichtiges Werkzeug für das Verständnis und die Verbindung mathematischer Objekte aus scheinbar unverbundenen Teilgebieten der Mathematik und der theoretischen Physik erwiesen.

Diese Phänomene können im Zusammenhang mit Coxeter-Gruppen modelliert werden, und spielen eine wichtige Rolle in der algebraischen Kombinatorik. Im endlichen Fall werden derartige kombinatorische Familien von verallgemeinerten Catalanzahlen abgezählt.

In dieser Schrift betrachten wir eine Erweiterung dieser Theorie auf parabolische Quotienten von Coxeter-Gruppen. Wir stellen die historische Entwicklung und die grundlegenden Definitionen und Konstruktionen dar und präsentieren eine Reihe von Vermutungen und Forschungsfragen, die in diesem Zusammenhang entstehen. Anschließend lösen wir diese Fragen im sogenannten "linearen Typ A" und decken überraschende Zusammenhänge dieser Theorie zu bestimmten Hopf-Algebren und zur Theorie der diagonal-harmonischen Polynome auf. Am Ende dieser Schrift schlagen wir weiterführende Forschungsrichtungen vor.

Notation

$\mathbb{N}, \mathbb{Z}, \mathbb{Q}, \mathbb{R}, \mathbb{C}$	natural numbers, integers, rationals, reals, complex numbers
$[n], [a, b]$	the sets $\{1, 2, \dots, n\}$ resp. $\{a, a+1, \dots, b\}$
\mathbf{P}, \mathbf{Q}	posets
\mathbf{K}, \mathbf{L}	lattices
$\text{Covers}(\mathbf{P}), \text{Int}(\mathbf{P})$	set of edges resp. nonempty intervals
$\zeta_{\mathbf{P}}, \mu_{\mathbf{P}}$	zeta polynomial and Möbius function
$\hat{0}, \hat{1}$	least and greatest element of a bounded poset
$\text{JoinIrr}(\mathbf{L}), \text{MeetIrr}(\mathbf{L})$	join- and meet-irreducible elements
$\text{Galois}(\mathbf{L})$	Galois graph
$\Gamma(\mathbf{L})$	canonical join complex
$\mathbf{CLO}(\mathbf{L})$	core label order
$(W, S), \mathfrak{S}_n$	Coxeter system, symmetric group
Φ_W, Φ_W^+, Π_W	root system, positive roots, simple roots
$\mathbf{Weak}(W), \mathbf{Abs}(W)$	weak resp. absolute order
$\text{Inv}(w), \text{Cov}(w)$	inversions resp. cover inversions
$\text{Align}(W, c), \mathfrak{S}_n(231)$	c -aligned elements, 231-avoiding permutations
$\mathbf{Camb}(W, c), \mathbf{Tam}(n)$	c -Cambrian lattice, Tamari lattice
$\text{Nonc}(W, c), \text{Nonc}(n)$	c -noncrossing partitions, noncrossing set partitions
$\text{Clus}(W, c), \text{Pipe}(n)$	c -cluster complex, reduced pipe dreams for $1 \leq n \leq n+1$... 2
$\text{Paths}(m, n), \text{Dyck}(n)$	northeast paths, Dyck paths

CHAPTER 0

Prologue

In this thesis we invite the reader on a journey through *Parabolic Cataland*. We encounter various *parabolic Catalan families*, i.e., certain combinatorial objects defined on parabolic quotients of finite, irreducible Coxeter groups, and describe bijective, structural and enumerative connections among them.

The motivating example comes from the situation, when the quotient in question is the whole symmetric group. Then, the parabolic Catalan families recover *ordinary Catalan families*, i.e., combinatorial families enumerated by the *Catalan number*

$$\text{Cat}(n) = \frac{1}{n+1} \binom{2n}{n}.$$

There is a plethora of Catalan families, and four of them play a crucial role in our story: noncrossing set partitions, triangulations of a polygon, stack-sortable permutations and Dyck paths. We first highlight the importance of these objects by listing a number of applications and generalizations and by explaining that these families—in fact—live under the same roof.

Noncrossing partitions. The *noncrossing set partitions* are—as the name suggests—certain set partitions avoiding a particular entanglement of blocks. These were formally introduced by G. KREWERAS in [111], but have appeared before, e.g., under the name “planar rhyme schemes” [16]. Several researchers have exhibited a vast spectrum of structural and enumerative properties, most of them arising when ordering noncrossing partitions by refinement. The resulting partially ordered set is a geometric lattice, its order complex is a wedge of spheres. It is rank-symmetric (with rank sizes enumerated by the *Narayana numbers*) and admits a symmetric chain decomposition. The zeta polynomial of the lattice of noncrossing partitions recovers the *Fuß–Catalan numbers*, the maximal chains are in bijection with labeled trees and *parking functions*. See [4, 15, 121, 168] for expository articles on this matter.

Noncrossing partitions have found remarkably many applications outside combinatorics. For instance, they serve as a model to describe *free cumulants* in the theory of free probability [171, 172]. In particular, moments and free cumulants are related via Möbius inversion in the lattice of noncrossing partitions. Noncrossing partitions may also be used to describe connected components of *positroids*, i.e., certain matroids arising from totally nonnegative matrices [3], they can be used to compute the matrix of chromatic joins [41] and they arise as particular representations of a path quiver [159, 187]. Even outside of pure mathematics, noncrossing partitions have been successfully applied, e.g., as a model for certain secondary RNA structures in mathematical biology [93, 99, 156].

A huge step forward in understanding the nature of noncrossing partitions was achieved when P. BIANE and T. BRADY (independently) observed that the lattice of noncrossing partitions naturally arises as a certain interval in the Cayley graph of the symmetric group with respect to the generating set of all transpositions [24, 33]. This perspective was further solidified by D. BESSIS and others—building upon [28]—by considering the *dual braid monoid* associated with the Artin groups of finite, irreducible Coxeter systems [21, 34, 35, 137]. This monoid turns out to be a *Garside monoid*, i.e., its elements admit nice canonical forms and the word and conjugacy problems can be solved efficiently. The prototypical example is the classical braid group, where this construction is due to F. GARSIDE [80].

A key component in BESSIS' construction is the projection of the Artin group to the underlying Coxeter group, and the set of prefixes of a distinguished element, a *Coxeter element*. The subword order on this set of prefixes recovers the noncrossing partition lattice in the case of the classical braid group. This has two remarkable consequences: (i) we may uniformly construct analogues of noncrossing partition lattices for any *well-generated* complex reflection group; (ii) the invariant theory of these groups allows for the definition of analogues of the Catalan numbers in this setting.

What we have summarized in the previous two paragraphs is essentially the genesis of Coxeter–Catalan theory and was established within roughly a decade. One of the major results obtained with the help of noncrossing partitions is the proof that the universal cover of the complement of any complex reflection arrangement is contractible [23].

At about the same time V. REINER took a different approach and constructed generalizations of noncrossing partition lattices for some finite, irreducible Coxeter groups using the intersection lattice of the associated reflection arrangements [157], therefore reconnecting the algebraic noncrossing partitions with their combinatorial origin. His constructions are inspired by the correspondence between the intersection lattice of the braid arrangement and the partition lattice in type A, and provide combinatorial realizations of the noncrossing partition lattices in type B; it is perhaps the first article containing the uniform formula for the Coxeter–Catalan numbers. Noncrossing partitions of other types were later realized combinatorially, too [10, 22].

Triangulations. Triangulations of a polygon are one of the first (perhaps *the* first) Catalan objects ever considered. Their enumeration dates back (at least) to L. EULER.

We wish to approach triangulations from a rather different perspective, and consider a particular algebraic object: a *cluster algebra*. Cluster algebras were introduced by S. FOMIN and A. ZELEVINSKY as a combinatorial means to study total positivity in semisimple Lie groups. Loosely speaking, cluster algebras are quotients of some ring generated by a set of *clusters* with respect to certain *exchange relations* [72]. Combinatorially, cluster algebras possess the structure of a simplicial complex; the *cluster complex*. See [71] for more background.

In the last twenty years, exchange relations (and therefore cluster algebras) have been recognized to play a vital role in many areas of mathematics and mathematical physics, such as root systems, representation theory, higher Teichmüller theory, Poisson geometry, quantum field theory, string theory, integrable models and many more [1, 37, 38, 58, 59, 68, 69, 73, 74, 77, 81–83, 94, 104, 134, 163].

The cluster algebras with a finite number of clusters can be characterized via the Cartan–Killing classification of finite root systems [73]. Therefore, any finite cluster algebra corresponds to a finite Coxeter group. Moreover, the number of clusters in such a cluster algebra equals the corresponding Coxeter–Catalan number [74]. The cluster complex in type A is dual to the *associahedron* [74, 176]. It is well known that the associahedron can be realized as a simplicial complex whose vertices are triangulations and where two triangulations are adjacent if they are related by “flipping a diagonal”. This flip structure recovers the poset diagram of the *Tamari lattice*.

The exchange relations of a cluster algebra allow for the definition of a flip relation on the set of clusters, i.e., any cluster variable in a fixed cluster can be replaced by a particular other cluster variable so that a new cluster is obtained. For finite cluster algebras, this flip relation can be oriented in such a way that the reflexive and transitive closure yields a lattice; the *Cambrian lattice*. This flip relation identified the cluster complex as a special instance of the subword complexes first studied in the context of Schubert varieties [102, 103, 141].

Stack-sortable permutations. In an exercise of one of his famous books, D. KNUTH introduced a family of permutations that can be sorted by passing through a stack [101, Section 2.2.1]. These *stack-sortable permutations* can be characterized in terms of pattern-avoidance: they are exactly those permutations whose one-line notation does not contain a subword standardizing to 231. If we now order these 231-avoiding permutations by containment of their inversion sets, then we obtain a different realization of the Tamari lattice [31, Section 9].

Taking a lattice-theoretic point of view, N. READING introduced a method of sorting reduced words of a Coxeter group with respect to a Coxeter element [148, 149]. Ordering the *sortable* elements by the *weak order* yields a different realization of the Cambrian lattices [147, 149, 154].

Moreover, combining lattice-theoretic and geometric methods, READING established his sortable elements as a bridging component between noncrossing partitions and clusters [148], thus establishing that all of these objects are in bijection. A certain “cutting” relation on the the reflection arrangement of a finite, irreducible Coxeter group was then used to explain that the noncrossing partition lattice arises as a secondary (in some sense dual) structure on the corresponding Cambrian lattice [152]. This connection further strengthens the relationship between noncrossing partitions and clusters and beautifully underlines the coherence of Coxeter–Catalan theory.

Other generalizations and extensions of sortable elements include the sorting orders of [5] and the permutrees of [142].

Dyck paths. Northeast paths on an integer grid in their various forms have probably made their debut in the literature in the context of the *ballot problem*. An elegant method to enumerate such paths is the *reflection principle* attributed to D. ANDRÉ. As the name suggests, a *northeast path* is a lattice path using only steps in north or east direction starting at and relative to the origin. When all steps have unit length and the path never crosses the diagonal $x = y$, then such a path is a *Dyck path*. The reflection principle offers an elegant method to prove that Dyck paths are enumerated by the Catalan numbers.

A *rotation* of a Dyck path is a shift of a particular portion of the path one step to the left. The reflexive and transitive closure of this operation yields a partial order on the set of Dyck paths. In fact, this partial order is a lattice, and is yet another incarnation of the Tamari lattice.

If we label the north steps of a Dyck path by positive integers such that labels on consecutive north steps are increasing, then we obtain a parking function. This correspondence is in fact bijective, i.e., the set of all such labelings of all Dyck paths using $2n$ steps is precisely the set of parking functions of length n [87]. Since the maximal chains in the noncrossing partition lattice are indexed by parking functions, too, this exhibits an interesting connection between Dyck paths and noncrossing partitions which goes beyond a purely bijective one.

(Labeled) Dyck paths also play an important role in the theory of diagonal harmonics. The (now solved) Shuffle Conjecture asserts that the bigraded Hilbert series of the space of diagonal harmonic polynomials can be realized combinatorially as a sum over all parking functions with respect to two statistics (called “area” and “dinv”) [87]. Interestingly, the bigraded Hilbert series of the alternating component of this space can be realized in two different ways as a sum over unlabeled Dyck paths using two pairs of similar statistics (one pair of statistics is also called “area” and “dinv”, the other one is “bounce” and “area”). Both realizations are related by the so-called *zeta map*.

Restricting the set of all Dyck paths to those weakly above a fixed Dyck path v yields another fascinating structure: the v -Tamari lattice [144]. The relevance of these lattices for higher diagonal harmonics is for instance discussed in [20, 44].

There is a canonical way to partition the normal vectors to the hyperplanes in the reflection arrangement of a finite, irreducible Coxeter group such that each hyperplane contributes a *positive* and a *negative* normal vector. The set of positive normal vectors (also called *positive roots*) can be ordered such that two roots are comparable when their difference is a non-negative linear combination of *simple* roots. The resulting poset is the *root poset*. In type A , the root poset is of triangular shape, and from this perspective, Dyck paths trace out order ideals in this root poset. A. POSTNIKOV observed that the number of antichains in a root poset associated with a finite, irreducible Coxeter group is the appropriate Coxeter–Catalan number [157, Remark 2].

This perspective allows for a generalization of Dyck paths to other Coxeter groups, when—in general—there is no lattice path model for these objects. Using a particular torus arising from the coroot lattice, we can define analogues of parking functions for all *crystallographic* Coxeter groups, generalizing the combinatorial parking functions in type A . These objects apparently play an important role in the study of diagonal harmonics beyond type A [181].

Organization of this thesis. This thesis takes the interactions of the various Coxeter–Catalan objects mentioned above one step further. It is based on a construction of N. WILLIAMS, who considered Coxeter–Catalan objects for *parabolic quotients* of Coxeter groups in order to test the robustness of Coxeter–Catalan theory. While not all of the beautiful interactions mentioned above survive this generalization, there is a remarkable amount of results that seem to carry over almost verbatim to parabolic quotients. This thesis comprises the state-of-the-art of this theory.

In Chapter 1, we recall basic notions of order and lattice theory, as well as the fundamental definitions and results regarding Coxeter groups. While there are some original results in the lattice theory part, the majority of the statements is well known.

In Chapter 2, we describe the main components of *Cataland*, i.e., the Catalan families we have mentioned before, together with their main combinatorial, structural and enumerative properties.

Chapter 3 then introduces *Parabolic Cataland*, i.e., we define the extensions of the Catalan families encountered in Chapter 2 to parabolic quotients of Coxeter groups. These constructions are illustrated with lots of examples, and we present several conjectures and research challenges inspired from the ordinary case.

Chapter 4 is the heart of this thesis, and it contains a detailed study of Parabolic Cataland in linear type A , i.e., the case of the symmetric group with respect to the linear Coxeter element. This is also the case in which the prototypical, combinatorial results for ordinary Cataland were first obtained. We give concrete combinatorial models for the involved objects and solve almost all conjectures and research challenges that we have posed in Chapter 3. We also present two surprising applications of this theory involving Hopf algebras and diagonal harmonics.

Chapter 5 contains suggestions for combinatorial models in the other types as well as further generalizations and suggestions for follow-up research.

Appendix A provides some data regarding the various research challenges and conjectures posed in this thesis.

* * *

We recommend that readers sufficiently familiar with Coxeter theory start their journey in Chapter 2, where the origins of Cataland are presented, and refer to the appropriate places

of Chapter 1 whenever some unknown terminology is encountered. In general, we denote ordered sets in a boldface font.

Apart from this section, three green asterisks “* * *” indicate a thematic change from combinatorial considerations to algebraic considerations or vice versa.

Moreover, we have used the following color-coding: theorems are recognizable by a green background, conjectures and research challenges by an orange background and examples by a gray background.

CHAPTER 1

Preliminaries

1.1. Posets and lattices

In this thesis we mainly consider combinatorial families for which we have a means to compare any two of its members (where the answer may as well be that two such members are incomparable). Let us start by making this concept mathematically precise.

For more background and additional definitions concerning order theory, we recommend [56]. This book also covers a basic part of the lattice theory that we use here, and [75, 84] should cover the remaining ground.

1.1.1. A notion of order. The basic formal definition of “order” is the following.

Definition 1.1.1. Let M be a (finite) set. A binary relation $R \subseteq M \times M$ is an **order relation** if it has the following three properties.

- | | |
|--|----------------|
| If $a \in M$, then $(a, a) \in R$. | (Reflexivity) |
| If $(a, b) \in R$ and $(b, a) \in R$, then $a = b$. | (Antisymmetry) |
| If $(a, b) \in R$ and $(b, c) \in R$, then $(a, c) \in R$. | (Transitivity) |

Such an order relation allows us to compare two elements $a, b \in M$. It may be that a is *smaller* than b (if $(a, b) \in R$), or that a is *greater* than b (if $(b, a) \in R$), or that a and b are *incomparable* (if neither is the case).

Therefore, a set M equipped with an order relation R is a partially ordered set¹. In that case we normally say *poset* for short, and we write such a poset as a pair (M, R) .

We usually denote order relations by \leq , or some similar-looking symbols, in order to emphasize the ordering property of the relation. Throughout this section we fix a poset $\mathbf{P} = (P, \leq)$.

Remark 1.1.2. Recall that a binary relation $R \subseteq M \times M$ is **acyclic** if there does not exist an integer $k \geq 2$ and elements $m_1, m_2, \dots, m_k \in M$ such that $(m_1, m_2), (m_2, m_3), \dots, (m_{k-1}, m_k), (m_k, m_1) \in R$. It is an easy exercise to show that the reflexive and transitive closure of an acyclic relation is an order relation.

¹This order is “partial”, because we allow elements to be incomparable.

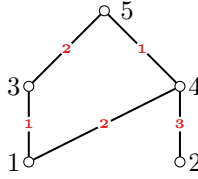


Figure 1. A poset diagram together with an edge-labeling.

Disclaimer 1.1.3. All posets considered in this thesis are finite.

If $\mathbf{Q} = (Q, \leq_Q)$ is another poset, then a map $f: P \rightarrow Q$ is *order preserving* if for all $a, b \in P$ with $a \leq b$ it holds that $f(a) \leq_Q f(b)$.

1.1.2. Diagrams and labelings. If $a \leq b$ and $a \neq b$, then we write $a < b$. A *cover relation* of \mathbf{P} is a pair (a, b) , for $a, b \in P$, such that $a < b$ and there does not exist $c \in P$ with $a < c < b$. In this case, we write $a \lessdot b$ instead of (a, b) . We then say that a is *is covered by* b , and b *covers* a . The *edge set* of \mathbf{P} is defined by

$$(1.1) \quad \text{Covers}(\mathbf{P}) \stackrel{\text{def}}{=} \{(a, b) \mid a, b \in P, a \lessdot b\}.$$

The (*poset*) *diagram* of \mathbf{P} is the directed graph $(P, \text{Covers}(\mathbf{P}))$, which is normally drawn in such a way that smaller elements (in \mathbf{P}) are drawn below greater ones. This enables us to omit orientations of edges; these can be recovered by following edges upwards.

Definition 1.1.4. Given a set Λ of labels, an *edge-labeling* of \mathbf{P} is a map $\lambda: \text{Covers}(\mathbf{P}) \rightarrow \Lambda$.

Edge-labelings are valuable tools in combinatorial order theory, because they can exhibit certain structural and topological properties of the underlying posets. We will encounter such edge-labelings later.

Example 1.1.5. Let us consider $M = \{1, 2, 3, 4, 5\}$ together with the order relation

$$R = \{(1, 1), (1, 3), (1, 4), (1, 5), (2, 2), (2, 4), (2, 5), (3, 3), (3, 5), (4, 4), (4, 5), (5, 5)\}.$$

The edge set of (M, R) is $\{(1, 3), (1, 4), (2, 4), (3, 5), (4, 5)\}$ and a poset diagram of (M, R) is shown in Figure 1. This figure additionally displays the edge-labeling λ , given by

$$\lambda(1, 3) = 1, \quad \lambda(1, 4) = 2, \quad \lambda(2, 4) = 3, \quad \lambda(3, 5) = 2, \quad \lambda(4, 5) = 1.$$

1.1.3. Duality and multichains. An important concept in order theory is *duality*. Loosely speaking, duality amounts to flipping the poset diagram upside-down. Strictly speaking, the *dual poset* of \mathbf{P} is

$$\mathbf{P}^d \stackrel{\text{def}}{=} (P, \geq),$$

where we have $a \geq b$ if and only if $b \leq a$. Many definitions from order theory have a “dual counterpart” as we can witness in the next paragraphs.

An element $a \in P$ is *minimal* (resp. *maximal*) if for every $b \in P$ with $b \leq a$ (resp. $a \leq b$) it follows that $b = a$. For $A \subseteq P$, an element $b \in P$ is a *lower bound* (resp. *upper bound*) of A if $b \leq a$ (resp. $a \leq b$) for all $a \in A$.

If \mathbf{P} has a unique minimal element (resp. a unique maximal element), then it is *lower bounded* (resp. *upper bounded*). If \mathbf{P} is both lower and upper bounded, then it is *bounded*.

Instead of “unique minimal element” (resp. “unique maximal element”) we usually say *least* element (resp. *greatest* element). Normally, we denote the least (resp. greatest) element of \mathbf{P} (if it exists) by $\hat{0}$ (resp. $\hat{1}$).

If \mathbf{P} is lower bounded (resp. upper bounded), then an *atom* (resp. *coatom*) is any element covering the least element (resp. covered by the greatest element).

An *order ideal* (resp. *order filter*) of \mathbf{P} is a set $A \subseteq \mathbf{P}$ such that for all $a \in A$ if $b \leq a$ (resp. $a \leq b$), then $b \in A$. For $A \subseteq \mathbf{P}$, the *order ideal generated by A* is the set

$$(1.2) \quad \mathbf{P}_{\leq A} \stackrel{\text{def}}{=} \{b \in \mathbf{P} \mid b \leq a \text{ for some } a \in A\}.$$

If $|A| = 1$, then we speak of *principal* order ideals (resp. *principal* order filters).

A *multichain* of \mathbf{P} is a tuple (c_1, c_2, \dots) such that $c_i \in \mathbf{P}$ for all i and $c_1 \leq c_2 \leq \dots$. The *size* of a multichain is the number of its members (counted with multiplicity). If all members of a multichain are distinct, then it is in fact a *chain*. A chain (c_1, c_2, \dots, c_k) of size k is *saturated* if $c_1 < c_2 < \dots < c_k$, and a saturated chain is *maximal* if c_1 is minimal and c_k is maximal in \mathbf{P} . The *length* of \mathbf{P} is one less than the maximum size of a maximal chain; denoted by $\text{len}(\mathbf{P})$. If \mathbf{P} is itself a chain of size n , then we normally write $\mathbf{Chain}(n)$ rather than \mathbf{P} .

If all maximal chains of \mathbf{P} have the same size, then \mathbf{P} is *graded*. Graded posets admit a *rank function*, defined by:

$$\text{rk}: \mathbf{P} \rightarrow \mathbb{N}, \quad a \mapsto \begin{cases} 0, & \text{if } a \text{ is minimal,} \\ \text{rk}(b) + 1, & \text{if } a \text{ is not minimal, and } b \text{ is such that } b < a. \end{cases}$$

This is well defined only if \mathbf{P} is finite and graded. In such a case it is guaranteed that every non-minimal element covers some element, and all elements covered by some fixed element have—recursively—the same rank. We may equivalently define the rank of a to be one less than the size of any saturated chain from some minimal element below a to a . If \mathbf{P} is graded, then the length of \mathbf{P} equals the rank of any maximal element of \mathbf{P} .

An *interval* of \mathbf{P} is a set of the form

$$[a, b] \stackrel{\text{def}}{=} \{c \in \mathbf{P} \mid a \leq c \leq b\}$$

for $a, b \in \mathbf{P}$ with $a \leq b$. Every interval of \mathbf{P} is itself a poset, and we may therefore restrict all concepts defined on \mathbf{P} to its intervals. Let $\text{Int}(\mathbf{P})$ denote the set of all nonempty intervals of \mathbf{P} .

Example 1.1.6. *The poset in Figure 1 has two minimal elements (1 and 2) and one maximal element (5). It has three maximal chains $\{1, 3, 5\}$, $\{1, 4, 5\}$ and $\{2, 4, 5\}$ —all of size 3—and is therefore graded by the rank function rk given by*

$$\text{rk}(1) = 0, \quad \text{rk}(2) = 0, \quad \text{rk}(3) = 1, \quad \text{rk}(4) = 1, \quad \text{rk}(5) = 2.$$

Moreover, this poset has twelve intervals, which are

$$[1, 1], \quad [2, 2], \quad [3, 3], \quad [4, 4], \quad [5, 5], \quad [1, 3], \quad [1, 4], \quad [2, 4], \quad [3, 5], \quad [4, 5], \quad [1, 5], \quad [2, 5].$$

1.1.4. Zeta polynomial and Möbius function. Now that we have defined multichains of a poset, it is an obvious question to ask *how many* multichains of given length exist. Let us denote by $\mathcal{Z}_{\mathbf{P}}(k)$ the number of multichains of \mathbf{P} of size $k-1$. It turns out that $\mathcal{Z}_{\mathbf{P}}(k)$ —when regarded as a function of k —is a polynomial over \mathbb{Z} ; the *zeta polynomial* of \mathbf{P} . The degree d of $\mathcal{Z}_{\mathbf{P}}$ is one less than the maximum size of a maximal chain in \mathbf{P} , and its leading coefficient equals the number of maximal chains of \mathbf{P} divided by $d!$; see [175, Section 3.12] for more background. It is clear from the definition that $\mathcal{Z}_{\mathbf{P}}(2)$ yields the cardinality of \mathbf{P} , and $\mathcal{Z}_{\mathbf{P}}(3)$ yields the number of nonempty intervals of \mathbf{P} .

Now, since $z_{\mathbf{P}}$ is a polynomial function over \mathbb{Z} it may well be evaluated at negative values, too. Surprisingly enough, the evaluation at $k = -1$ yields something meaningful when \mathbf{P} is bounded. Let us define the *Möbius function* of \mathbf{P} recursively as follows:

$$(1.3) \quad \mu_{\mathbf{P}}(a, b) \stackrel{\text{def}}{=} \begin{cases} 1, & \text{if } a = b, \\ -\sum_{a \leq c < b} \mu(a, c), & \text{if } a < b, \\ 0, & \text{otherwise.} \end{cases}$$

Proposition 1.1.7 ([175, Proposition 3.12.1(c)]). *If \mathbf{P} is bounded with least element $\hat{0}$ and greatest element $\hat{1}$, then*

$$z_{\mathbf{P}}(-1) = \mu_{\mathbf{P}}(\hat{0}, \hat{1}).$$

Remark 1.1.8. *One way to prove Proposition 1.1.7 uses the incidence algebra of \mathbf{P} introduced in [160]. This is the associative algebra consisting of all functions from the nonempty intervals of \mathbf{P} to the integers, together with pointwise addition and scalar multiplication and a certain convolution. The Möbius function is invertible as a member of this algebra, its inverse being the zeta function $z_{\mathbf{P}}$ that assigns 1 to each nonempty interval. It is straightforward to establish that in a bounded poset it holds that $z^k(\hat{0}, \hat{1}) = z_{\mathbf{P}}(k)$, from which the proposition follows.*

Example 1.1.9. *The poset in Figure 1 has rank 2, because all maximal chains have size 3. Since there are 3 maximal chains, the zeta polynomial of this poset is of the form $\frac{3}{2}k^2 + ak + b$. Since its cardinality is 5 and it has 12 intervals, we obtain $a = -\frac{1}{2}$ and $b = 0$, which yields the zeta polynomial*

$$z(k) = \frac{3}{2}k^2 - \frac{1}{2}k.$$

The Möbius function of this poset is given through the following assignments:

$$\begin{aligned} \mu(1, 1) = 1, \quad \mu(1, 3) = -1, \quad \mu(1, 4) = -1, \quad \mu(1, 5) = 1, \quad \mu(2, 2) = 1, \quad \mu(2, 4) = -1, \\ \mu(2, 5) = 0, \quad \mu(3, 3) = 1, \quad \mu(3, 5) = -1, \quad \mu(4, 4) = 1, \quad \mu(4, 5) = -1, \quad \mu(5, 5) = 1. \end{aligned}$$

If we restrict ourselves to the interval $[1, 5]$, then we find that the corresponding zeta polynomial is $z_{[1,5]}(k) = k^2$, and $z_{[1,5]}(-1) = 1 = \mu(1, 5)$.

1.1.5. Lattices. Let us pause for a moment and introduce an algebraic structure that will be of great importance on our journey.

Definition 1.1.10. *Let L be a (finite) set, together with two binary operations $\vee: L \times L \rightarrow L$, $\wedge: L \times L \rightarrow L$, and two constants $\hat{0}$ and $\hat{1}$. The algebraic structure $(L, \vee, \wedge, \hat{0}, \hat{1})$ is a **lattice** if the following axioms are satisfied for all $a, b, c \in L$:*

$$\begin{aligned} a \vee (b \vee c) &= (a \vee b) \vee c \quad \text{and} \quad a \wedge (b \wedge c) = (a \wedge b) \wedge c, & \text{(Associativity)} \\ a \vee b &= b \vee a \quad \text{and} \quad a \wedge b = b \wedge a, & \text{(Commutativity)} \\ a \vee (a \wedge b) &= a \quad \text{and} \quad a \wedge (a \vee b) = a, & \text{(Absorption)} \\ a \vee \hat{0} &= a \quad \text{and} \quad a \wedge \hat{1} = a. & \text{(Identity)} \end{aligned}$$

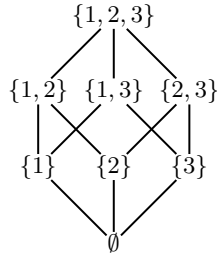


Figure 2. The poset diagram of the Boolean lattice of order 3.

One of the most natural examples of a lattice arises from the *power set* of a finite set M ; defined by $\wp(M) \stackrel{\text{def}}{=} \{A \mid A \subseteq M\}$. If $|M| = n$, then—without loss of generality—we may set $M = [n] \stackrel{\text{def}}{=} \{1, 2, \dots, n\}$, and call the structure

$$\mathbf{Bool}(n) \stackrel{\text{def}}{=} (\wp([n]), \cup, \cap, \emptyset, M)$$

the *Boolean lattice* of order n .

Since lattices are algebraic structures, we can unleash the full power of our algebraic toolkit on them, and, e.g., consider homomorphisms between lattices, sublattices or quotient lattices.

We are also able to reconnect lattices with the world of partially ordered sets, whose consideration we have briefly paused. In fact, it is an easy exercise to verify that, given a finite lattice $(L, \vee, \wedge, \hat{0}, \hat{1})$, the binary relation $R \subseteq L \times L$ defined by $(a, b) \in R$ if and only if $a \vee b = b$ is an order relation. Using the absorption axioms, we can equivalently write $(a, b) \in R$ if and only if $a \wedge b = a$.

Usually, we will denote the order relation coming from a lattice simply by \leq , rather than R . It follows readily from the identity axioms that a finite lattice—regarded as a poset—is bounded with least element $\hat{0}$ and greatest element $\hat{1}$. The partial order on $\mathbf{Bool}(n)$ is simply containment, and Figure 2 shows the Boolean lattice $\mathbf{Bool}(3)$ arranged as a poset diagram.

We may also characterize the posets which have an additional lattice structure. To that end, we define the *join* (resp. *meet*) of two elements of a poset $\mathbf{P} = (P, \leq)$ to be the unique smallest (resp. largest) element in \mathbf{P} that lies above (resp. below) them—if it exists. We normally denote the join by \vee and the meet by \wedge . If every two elements of \mathbf{P} have a join and a meet, then—by finiteness— \mathbf{P} must be bounded, and we denote the least element by $\hat{0}$ and the greatest element by $\hat{1}$. Under these conditions, we may verify that $\vee, \wedge, \hat{0}$ and $\hat{1}$ satisfy the axioms from Definition 1.1.10, and therefore $(P, \vee, \wedge, \hat{0}, \hat{1})$ is a lattice.

In the following we will not distinguish between the poset-theoretic and the algebraic nature of a poset that happens to be a lattice, and rather switch perspectives as we deem fit without explicit mention.

It may sometimes happen that a poset only satisfies half of the requirements for being a lattice. In that case, i.e., if every two elements of a poset have a join (resp. meet), then this poset is a *join-semilattice* (resp. *meet-semilattice*). The following lemma is classical.

Lemma 1.1.11. *Let $\mathbf{L} = (L, \leq)$ be a finite meet-semilattice. If \mathbf{L} has a greatest element, then \mathbf{L} is a lattice.*



Figure 3. Two lattices with five elements, with some perspective cover relations highlighted.

PROOF. Let $a, b \in L$. It remains to show that $a \vee b$ exists. Let M be the set of upper bounds of $\{a, b\}$. If L has a greatest element, then M is not empty. Since L is a meet-semilattice, any two elements of M have a meet, which means that M has a unique minimal element m . But m is exactly the join of a and b . \square

If $L = (L, \vee, \wedge, \hat{0}, \hat{1})$ is a lattice, then a subset $A \subseteq L$ is a *sublattice* if for all $a, b \in A$ it holds that $a \vee b \in A$ and $a \wedge b \in A$.

Moreover, an element $a \in L$ is *join irreducible* (resp. *meet irreducible*) if $a = \vee A$ (resp. $a = \wedge A$) implies $a \in A$. Let $\text{JoinIrr}(L)$ (resp. $\text{MeetIrr}(L)$) denote the set of join-irreducible (resp. meet-irreducible) elements of L .

Since L is finite, the join-irreducible (resp. meet-irreducible) elements are precisely those that cover (resp. are covered by) a unique element. If $j \in \text{JoinIrr}(L)$ (resp. $m \in \text{MeetIrr}(L)$), then this unique element is denoted by j_* (resp. m^*).

We call two cover relations $(a_1, b_1), (a_2, b_2) \in \text{Covers}(L)$ *perspective* if either $b_1 \vee a_2 = b_2$ and $b_1 \wedge a_2 = a_1$ or $a_1 \vee b_2 = b_1$ and $a_1 \wedge b_2 = a_2$; and we write $(a_1, b_1) \bar{\wedge} (a_2, b_2)$. See Figure 3 for an illustration. The next lemma is immediate.

Lemma 1.1.12. *Let $(a, b) \in \text{Covers}(L)$ and $j \in \text{JoinIrr}(L)$. If $(a, b) \bar{\wedge} (j_*, j)$, then $j \leq b$.*

We end by exhibiting a special family of irreducible elements. An *atom* (resp. *coatom*) is $a \in L$ with $\hat{0} < a$ (resp. $a < \hat{1}$). Let $\text{Atoms}(L)$ (resp. $\text{Coatoms}(L)$) denote the set of atoms (resp. coatoms) of L . Since L is finite, it follows that $\text{Atoms}(L) \subseteq \text{JoinIrr}(L)$ (resp. $\text{Coatoms}(L) \subseteq \text{MeetIrr}(L)$). A lattice is *nuclear* if $\vee \text{Atoms}(L) = \hat{1}$.

1.1.6. Distributivity. Another important class of lattices are *distributive lattices*, i.e., those lattices that satisfy the following two identities for all $a, b, c \in L$:

$$\begin{aligned} a \vee (b \wedge c) &= (a \vee b) \wedge (a \vee c), \\ a \wedge (b \vee c) &= (a \wedge b) \vee (a \wedge c). \end{aligned}$$

It is well known (and easy to check) that every Boolean lattice is distributive. Moreover—just like Boolean lattices—distributive lattices admit a beautiful presentation as set systems under inclusion.

Theorem 1.1.13 ([27]). *The set of order ideals of a finite poset under inclusion forms a distributive lattice. Conversely, every distributive lattice is isomorphic to the lattice of order ideals of its subposet of join-irreducible elements.*

Figure 3 shows two lattice with five elements, and it is quickly verified that neither of them is distributive. In fact, it follows from [26] that a lattice is distributive if and only if it does not contain N_5 or M_3 as a sublattice.

In next few sections, we introduce certain generalizations of distributive lattices. Throughout these sections we fix a finite lattice $\mathbf{L} = (L, \vee, \wedge, \hat{0}, \hat{1})$, and denote its partial order by \leq .

1.1.7. Semidistributivity. If every three elements $a, b, c \in L$ satisfy

$$(1.4) \quad a \vee b = a \vee c \text{ implies } a \vee b = a \vee (b \wedge c),$$

then \mathbf{L} is *join semidistributive*. Moreover, \mathbf{L} is *meet semidistributive* if \mathbf{L}^d is join semidistributive. A lattice that is both join and meet semidistributive is *semidistributive*. Semidistributive lattices were characterized by a means of forbidden sublattices in [55]. The lattice in Figure 3a is semidistributive, while the lattice in Figure 3b is not: its atoms do not satisfy (1.4). Moreover, it is immediately clear that every distributive lattice is semidistributive, too.

It was recently shown in [155] that finite semidistributive lattices can be uniquely represented as certain set systems under inclusion, in the spirit of Theorem 1.1.13.

Apart from the algebraic characterization given above, we can characterize join-semidistributive lattices also in terms of certain canonical representations. For $a \in L$, any set $A \subseteq L$ with $a = \bigvee A$ is a *join representation* of a . A join representation A_1 of a *refines* a join representation A_2 of a if $L_{\leq A_1} \subseteq L_{\leq A_2}$. If the set of join representations of a has a unique minimal element with respect to refinement, then this minimal element is the *canonical join representation* of a , denoted by $\text{Can}(a)$. The members of $\text{Can}(a)$ are the *canonical joinands* of a . (Canonical) meet representations are defined dually.

Theorem 1.1.14 ([75, Theorem 2.24]). *A finite lattice is join semidistributive if and only if every element admits a canonical join representation.*

Following [12], we may easily recognize the canonical join representations in a join-semidistributive lattice using the following edge labeling.

$$(1.5) \quad \lambda_{\text{jds}}: \text{Covers}(\mathbf{L}) \rightarrow \text{JoinIrr}(\mathbf{L}), \quad (a, b) \mapsto \min\{c \in L \mid a \vee c = b\}.$$

Proposition 1.1.15 ([12, Lemma 19(1)]). *Let $\mathbf{L} = (L, \leq)$ be a join-semidistributive lattice. For $a \in L$,*

$$\text{Can}(a) = \{\lambda_{\text{jds}}(a', a) \mid a' \lessdot a\}.$$

Figure 4a shows a join-semidistributive lattice labeled by (1.5). The reader may verify that Proposition 1.1.15 is satisfied. In fact, the labeling λ_{jds} is determined by the perspectivity relation.

Proposition 1.1.16. *Let \mathbf{L} be a join-semidistributive lattice and let $(a, b) \in \text{Covers}(\mathbf{L})$ and $j \in \text{JoinIrr}(\mathbf{L})$. Then, $\lambda_{\text{jds}}(a, b) = j$ if and only if $(a, b) \overline{\wedge} (j_*, j)$.*

PROOF. Suppose first that $\lambda_{\text{jds}}(a, b) = j$. By definition $a \vee j = b$ and thus $a \wedge j < j$. By minimality of j , it follows that $a \vee j_* < b$. Thus, $a \vee j_* = a$, since $a < b$. This implies that $a \wedge j = j_*$ which entails $(a, b) \overline{\wedge} (j_*, j)$.

Now, conversely, let $(a, b) \overline{\wedge} (j_*, j)$. By Lemma 1.1.12, $j \vee a = b$ and $j \wedge a = j_*$. Thus, $\lambda_{\text{jds}}(a, b) \leq j$. However, since $j_* \leq a$, we conclude that $\lambda_{\text{jds}}(a, b) \not\leq j_*$. Since $j \in \text{JoinIrr}(\mathbf{L})$, it follows that $\lambda_{\text{jds}}(a, b) = j$ as desired. \square

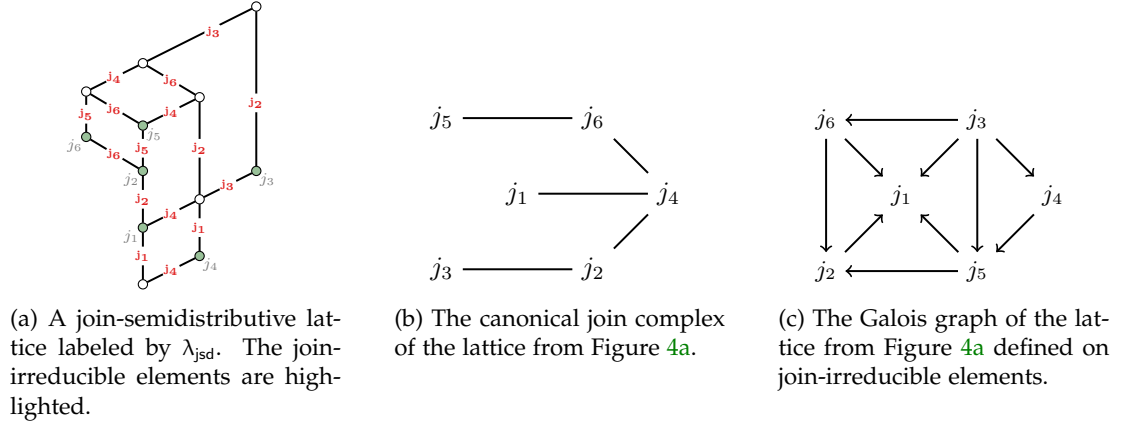


Figure 4. A join-semidistributive lattice and related structures.

Corollary 1.1.17. *Let $\mathbf{L} = (L, \leq)$ be a semidistributive lattice. The number of canonical joinands of $a \in L$ equals the number of elements covered by a .*

PROOF. Let $a \in L$, and let $b_1, b_2 \in L$ such that $b_1 \neq b_2$, $b_1 < a$, $b_2 < a$ and $\lambda_{\text{jsd}}(b_1, a) = k = \lambda_{\text{jsd}}(b_2, a)$. By Lemma 1.1.12, $k \leq a$ and by Proposition 1.1.16, $k \wedge b_1 = k_* = k \wedge b_2$. Since \mathbf{L} is meet semidistributive, $k_* = k \wedge (b_1 \vee b_2) = k \wedge a = k$, a contradiction. The claim follows from Proposition 1.1.15. \square

Lemma 1.1.18 ([75, Corollary 2.55]). *If \mathbf{L} is semidistributive, then $|\text{JoinIrr}(\mathbf{L})| = |\text{MeetIrr}(\mathbf{L})|$.*

According to [153, Proposition 2.2], the set of canonical join representations of \mathbf{L} forms a simplicial complex, the *canonical join complex*; denoted by $\Gamma(\mathbf{L})$. See [12, 13] for more work on the canonical join complex; Figure 4b shows the canonical join complex of the lattice in Figure 4a.

We now recall that the Möbius function of a join-semidistributive lattice takes only values in the set $\{-1, 0, 1\}$.

Proposition 1.1.19. *Let $\mathbf{L} = (L, \leq)$ be a join-semidistributive lattice, and let $M \subseteq \text{Coatoms}(\mathbf{L})$. If $\bigwedge M = \hat{0}$, then $M = \text{Coatoms}(\mathbf{L})$.*

PROOF. Suppose that $\bigwedge M = \hat{0}$. If $|M| = 1$, then $M = \{\hat{0}\} = \text{Coatoms}(\mathbf{L})$. Otherwise, pick $a \in \text{Coatoms}(\mathbf{L}) \setminus M$. Then, $a \vee m = \hat{1}$ for all $m \in M$, and consequently $\hat{1} = a \vee \bigwedge M = a \vee \hat{0} = a$, contradicting $a \in M$. Thus, $M = \text{Coatoms}(\mathbf{L})$. \square

Proposition 1.1.20. *If \mathbf{L} is join semidistributive, then*

$$\mu_{\mathbf{L}}(\hat{0}, \hat{1}) = \begin{cases} (-1)^{|\text{Coatoms}(\mathbf{L})|}, & \text{if } \bigwedge \text{Coatoms}(\mathbf{L}) = \hat{0}, \\ 0, & \text{otherwise.} \end{cases}$$

PROOF. ROTA'S Crosscut Theorem [160, Theorem 3] implies that

$$\mu_{\mathbf{L}}(\hat{0}, \hat{1}) = \sum_{M \subseteq \text{Coatoms}(\mathbf{L}) : \bigwedge M = \hat{0}} (-1)^{|M|}.$$

Proposition 1.1.19 states that this sum consists of at most one term, which yields the claim. \square

We say that a join-semidistributive lattice \mathbf{L} is *spherical* if $\mu_{\mathbf{L}}(\hat{0}, \hat{1}) \neq 0$.

1.1.8. Trimness. It is easy to verify that every finite lattice \mathbf{L} satisfies the following inequality:

$$\text{len}(\mathbf{L}) \leq \min\{|\text{JoinIrr}(\mathbf{L})|, |\text{MeetIrr}(\mathbf{L})|\}.$$

Following [118], we award a special name to lattices in which the equality

$$(1.6) \quad |\text{JoinIrr}(\mathbf{L})| = \text{len}(\mathbf{L}) = |\text{MeetIrr}(\mathbf{L})|$$

is true; we call them *extremal lattices*. It was shown in [118] that extremal lattices admit a presentation as finite set systems under inclusion in the spirit of Theorem 1.1.13, too. A recent article that utilizes this presentation in a combinatorial setting is [189].

In order to describe this presentation, we fix an extremal lattice \mathbf{L} of length n together with a maximal chain $c_0 < c_1 < \dots < c_n$. We may use this chain to order the sets $\text{JoinIrr}(\mathbf{L}) = \{j_1, j_2, \dots, j_n\}$ and $\text{MeetIrr}(\mathbf{L}) = \{m_1, m_2, \dots, m_n\}$ such that the following condition holds for all $s \in [n]$:

$$(1.7) \quad j_1 \vee j_2 \vee \dots \vee j_s = c_s = m_{s+1} \wedge m_{s+2} \wedge \dots \wedge m_n.$$

Definition 1.1.21. *Let \mathbf{L} be an extremal lattice of length n . Suppose that the join- and meet-irreducible elements of \mathbf{L} are labeled as in (1.7) with respect to some distinguished maximal chain. The **Galois graph** of \mathbf{L} is the directed graph $\text{Galois}(\mathbf{L})$ whose vertex set is $[n]$ and that has a directed edge $s \rightarrow t$ whenever $s \neq t$ and $j_s \not\leq m_t$.*

By construction, an edge $s \rightarrow t$ exists in $\text{Galois}(\mathbf{L})$ only if $s > t$. À priori, the Galois graph of \mathbf{L} depends on a choice of maximal chain which determines the order (1.7). However, [189, Proposition 2.5] states that different maximum-length maximal chains induce isomorphic Galois graphs. We may therefore drop the dependence on the chain in our notation.

If G is any directed graph on the vertex set M , then a pair (A, B) of subsets of M , with $A \cap B = \emptyset$, is an *orthogonal pair* if there are no edges from A to B . An orthogonal pair (A, B) is *maximal* if there is no orthogonal pair (A', B') such that $A \subseteq A'$ and $B \subseteq B'$ and $|A| + |B| < |A'| + |B'|$.

Theorem 1.1.22 ([118, Theorem 11]). *The set of maximal orthogonal pairs of a directed graph on $[n]$, in which $s \rightarrow t$ only if $s > t$, ordered by inclusion is an extremal lattice. Conversely, every extremal lattice is isomorphic to the lattice of maximal orthogonal pairs of its Galois graph.*

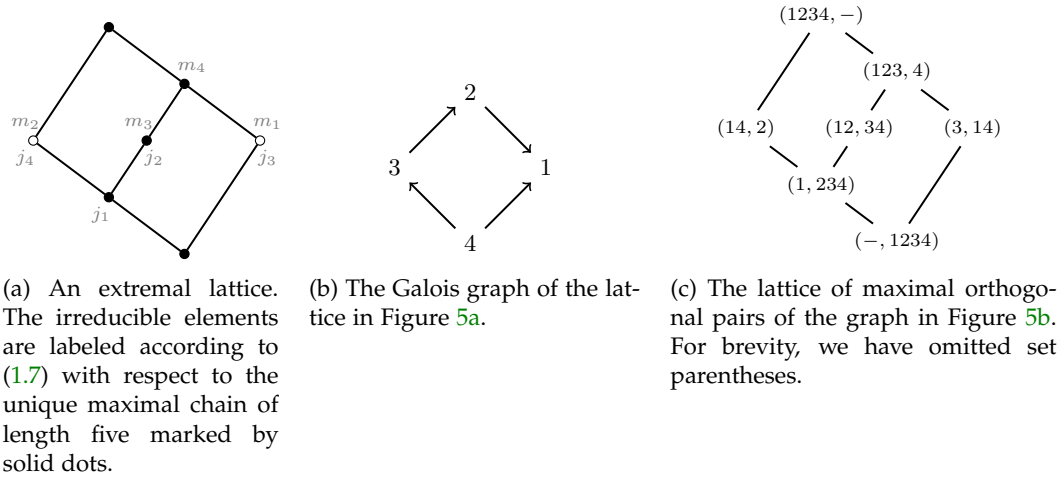


Figure 5. An extremal lattice with its associated Galois graph.

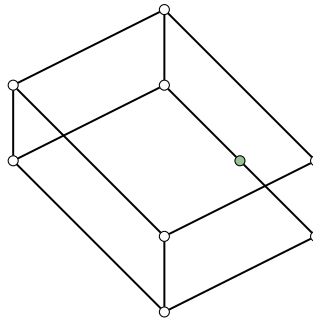


Figure 6. An extremal lattice that is not left modular. The highlighted element is not left modular, but belongs to the unique maximal chain of maximum length.

We observe that every distributive lattice is graded and extremal, and [118, Theorem 17] states that every graded, extremal lattice is distributive. Moreover, every interval of a distributive lattice is distributive, too.

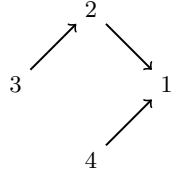
Thus, at a first glance, extremality may appear as an ungraded analogue of distributivity. However, [118, Theorem 14(ii)] states that every finite lattice can be embedded as an interval into an extremal lattice, which implies that extremality is not inherited by intervals. In order to fix this, [186] exhibits a subfamily of the extremal lattices which is closed under passing to intervals. Before we may formally define this, we need another concept.

If $b, c \in L$ with $b \leq c$, then every $a \in L$ satisfies the *modular inequality*

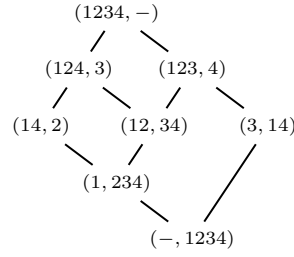
$$(1.8) \quad (b \vee a) \wedge c \geq b \vee (a \wedge c).$$

Any element a , which satisfies (1.8) with equality, is *left modular*. The least and the greatest element in a lattice are trivially left-modular. A lattice is *left modular* if it possesses a maximal chain of length $\text{len}(L)$ consisting entirely of left-modular elements. Left-modular lattices were studied in detail in [113, 114, 123, 185]. Figure 3b shows a left-modular lattice that is not extremal, and Figure 6 shows an extremal lattice that is not left modular.

A lattice that is both extremal and left modular is *trim*. Theorem 1 in [186] states that every interval of a trim lattice is trim, and every graded trim lattice is distributive. Thus,



(a) A directed graph on $[4]$ associated with the lattice from Figure 5a constructed via the condition in Corollary 1.1.25(i).



(b) The lattice of maximal orthogonal pairs of the directed graph from Figure 7a.

Figure 7. A directed graph associated with the lattice from Figure 5a and its lattice of orthogonal pairs.

trimness is a more suitable ungraded analogue of distributivity. We list a few constructions preserving trimness.

Proposition 1.1.23. *Let \mathbf{L} be a trim lattice. Then,*

- (i) *any interval of \mathbf{L} is trim;* [186, Theorem 1]
- (ii) *any sublattice of \mathbf{L} containing the left-modular chain is trim;* [186, Theorem 3]
- (iii) *any quotient lattice of \mathbf{L} is trim;* [189, Lemma 3.10]

Theorem 1.1.24 ([189, Theorem 1.4]). *Every extremal, semidistributive lattice is trim.*

Corollary 1.1.25 ([132, Corollary A.18]). *Let \mathbf{L} be an extremal, semidistributive lattice with $\text{len}(\mathbf{L}) = n$. Let C be a maximal chain of maximum length, and let the join- and meet-irreducible elements of \mathbf{L} be ordered as in (1.7) with respect to C .*

- (i) *For $s, t \in [n]$, $j_s \not\leq m_t$ if and only if $s \neq t$ and $j_t \leq j_{t*} \vee j_s$.*
- (ii) *If $j_t < j_s$, then there is a directed edge from s to t in $\text{Galois}(\mathbf{L})$.*

As a consequence of Corollary 1.1.25(ii), the poset $(\text{JoinIrr}(\mathbf{L}), \leq)^d$ is a subposet of the reflexive and transitive closure of $\text{Galois}(\mathbf{L})$ whenever \mathbf{L} is extremal and semidistributive.

Moreover, Corollary 1.1.25(i) allows for constructing the Galois graph of an extremal, semidistributive lattice by using only join-irreducible elements. The reader is invited to check that the lattice \mathbf{L} in Figure 5a is not semidistributive. The directed graph with vertex set $[4]$, which has an edge $s \rightarrow t$ if and only if $s \neq t$ and $j_t \leq j_{t*} \vee j_s$ is shown in Figure 7a, and it is *not* the Galois graph of \mathbf{L} . The lattice of maximal orthogonal pairs of this graph is shown in Figure 7b, and can be regarded as a semidistributive extension of \mathbf{L} .

We close this section with another remarkable property of extremal semidistributive lattices, which is illustrated in Figure 4.

Proposition 1.1.26 ([189, Corollary 6.8]). *Let \mathbf{L} be an extremal, semidistributive lattice. The complement of the undirected Galois graph $\text{Galois}(\mathbf{L})$ is isomorphic to the 1-skeleton of the canonical join complex $\Gamma(\mathbf{L})$.*

1.1.9. Congruence-uniformity. A *congruence relation* on \mathbf{L} is an equivalence relation $\Theta \subseteq \mathbf{L} \times \mathbf{L}$ such that for all $a_1, a_2, b_1, b_2 \in \mathbf{L}$ the following implication is true:

$$\text{if } (a_1, b_1), (a_2, b_2) \in \Theta, \text{ then } (a_1 \vee a_2, b_1 \vee b_2), (a_1 \wedge a_2, b_1 \wedge b_2) \in \Theta.$$

In other words, congruence relations are equivalence relations compatible with the lattice operations. The next lemma characterizes congruence relations combinatorially.

Lemma 1.1.27 ([147, Section 3]). *Let $\Theta \subseteq \mathbf{L} \times \mathbf{L}$ be an equivalence relation. Then, Θ is a congruence relation on \mathbf{L} if and only if all of the following hold.*

- (i) *Every equivalence class of Θ is an interval of \mathbf{L} .*
- (ii) *The map that sends each $a \in \mathbf{L}$ to the minimal element in $[a]_\Theta$ is order preserving.*
- (iii) *The map that sends each $a \in \mathbf{L}$ to the maximal element in $[a]_\Theta$ is order preserving.*

The *quotient lattice* of \mathbf{L} is

$$(1.9) \quad \mathbf{L}/\Theta \stackrel{\text{def}}{=} (\mathbf{L}/\Theta, \leq_\Theta),$$

where $\mathbf{L}/\Theta \stackrel{\text{def}}{=} \{[a]_\Theta \mid a \in \mathbf{L}\}$ and $[a]_\Theta \leq_\Theta [b]_\Theta$ if and only if there exist $c \in [a]_\Theta$ and $d \in [b]_\Theta$ such that $c \leq d$.

If $\mathbf{K} = (\mathbf{K}, \leq_{\mathbf{K}})$ is another lattice, then a map $f: \mathbf{K} \rightarrow \mathbf{L}$ is a *lattice homomorphism* if for all $a, b \in \mathbf{K}$ it holds that $f(a \vee_{\mathbf{K}} b) = f(a) \vee_{\mathbf{L}} f(b)$ and $f(a \wedge_{\mathbf{K}} b) = f(a) \wedge_{\mathbf{L}} f(b)$. Therefore, if Θ is a congruence relation on \mathbf{L} , then—by Lemma 1.1.27—the *(downward) projection*

$$(1.10) \quad \pi_\Theta^\downarrow: \mathbf{L} \rightarrow \mathbf{L}, \quad a \mapsto \bigwedge_{b \in [a]_\Theta} b$$

is a lattice homomorphism whose image is isomorphic to \mathbf{L}/Θ .

Let $\text{Con}(\mathbf{L})$ denote the set of all congruence relations on \mathbf{L} . By Disclaimer 1.1.3, the poset $(\text{Con}(\mathbf{L}), \subseteq)$ is in fact a distributive lattice [76].

Given $j \in \text{JoinIrr}(\mathbf{L})$, we say that $\Theta \in \text{Con}(\mathbf{L})$ *contracts* j if $(j_*, j) \in \Theta$.

Proposition 1.1.28 ([14, Proposition 4.11]). *Let \mathbf{L} be a join-semidistributive lattice and let $\Theta \in \text{Con}(\mathbf{L})$. If j is a canonical joinand of $a \in \mathbf{L}$ such that j is not contracted by Θ , then j is a canonical joinand of $\pi_\Theta^\downarrow(a)$ in \mathbf{L} . Moreover, if $\pi_\Theta^\downarrow(a) = a$, then none of the canonical joinands of a are contracted by Θ .*

For $(a, b) \in \text{Covers}(\mathbf{L})$ let $\text{cg}(a, b)$ denote the finest congruence relation on \mathbf{L} in which a and b are equivalent. If $b \in \text{JoinIrr}(\mathbf{L})$, then we simply write $\text{cg}(b)$ instead of $\text{cg}(b_*, b)$. The following result relates join-irreducible elements of \mathbf{L} and join-irreducible elements of $\text{Con}(\mathbf{L})$.

Theorem 1.1.29 ([85, Section 2.14],[75, Theorem 3.20]). *Let \mathbf{L} be a lattice, and let $\Theta \in \text{Con}(\mathbf{L})$. The following are equivalent.*

- (i) *Θ is join irreducible in $(\text{Con}(\mathbf{L}), \subseteq)$.*
- (ii) *$\Theta = \text{cg}(a, b)$ for some $(a, b) \in \text{Covers}(\mathbf{L})$.*
- (iii) *$\Theta = \text{cg}(j)$ for some $j \in \text{JoinIrr}(\mathbf{L})$.*

A direct consequence of Theorem 1.1.29 is that the map $j \mapsto \text{cg}(j)$ is surjective. However, in general it need not be injective. A lattice \mathbf{L} is *congruence uniform* if this map is a bijection for both \mathbf{L} and \mathbf{L}^d .

Congruence-uniform lattices were first considered in [122], where they were defined as those lattices that are bounded-homomorphic images of free lattices. The definition that we

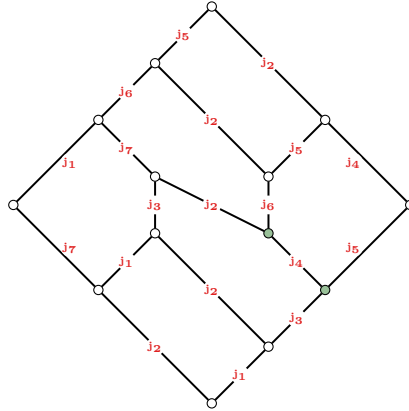


Figure 8. The smallest semidistributive lattice that is not congruence uniform, labeled by λ_{jsd} . The two highlighted join-irreducible elements induce the same congruence relation.

have just given is called “property P” in [57], and the equivalence of these two definitions is part of [57, Theorem 5.1]. Congruence-uniformity turns out to be a lattice property which sits properly inbetween distributivity and semidistributivity.

Theorem 1.1.30.

- (i) Every distributive lattice is congruence uniform. [64, Theorem 3]
- (ii) Every congruence-uniform lattice is semidistributive. [57, Lemma 4.2]

The smallest congruence-uniform lattice that is not distributive is the lattice N_5 from Figure 3a, and the smallest semidistributive lattice that is not congruence uniform is shown in Figure 8. Note that this lattice is also extremal and thus trim by Theorem 1.1.24.

We close this section with the following result, which states that the class of congruence-uniform lattices forms a *pseudovariety*.

Proposition 1.1.31 ([57, Theorem 4.1]). *The class of congruence-uniform lattices is closed under passing to sublattices, quotient lattices or (finitely many) direct products.*

1.1.10. The core label order. In this section, we introduce a method to reorder the elements of a lattice by means of an edge-labeling. The origins of this construction are due to N. READING in the context of hyperplane arrangements [152], and it was further developed for congruence-uniform lattices in [131]. We attempt a general definition here.

For any edge-labeling $\lambda: \text{Covers}(\mathbf{L}) \rightarrow \Lambda$ of \mathbf{L} , we call (\mathbf{L}, λ) a *labeled lattice*. For $a \in \mathbf{L}$, the *nucleus* of a is

$$a_{\downarrow} \stackrel{\text{def}}{=} a \wedge \bigwedge_{b \in \mathbf{L}: b < a} b.$$

This means, $\hat{0}_{\downarrow} = \hat{0}$ and—for $a \neq \hat{0}$ — a_{\downarrow} is the meet of the elements covered by a . The interval $[a_{\downarrow}, a]$ of \mathbf{L} is the *core* of a , and the *core label set*² of a is

$$\text{Sh}_{(\mathbf{L}, \lambda)}(a) \stackrel{\text{def}}{=} \{\lambda(c, d) \mid a_{\downarrow} \leq c < d \leq a\}.$$

²The notation Sh is meant to honor READING’s original construction in the context of hyperplane arrangements, in which core label sets correspond to sets of shard intersections.

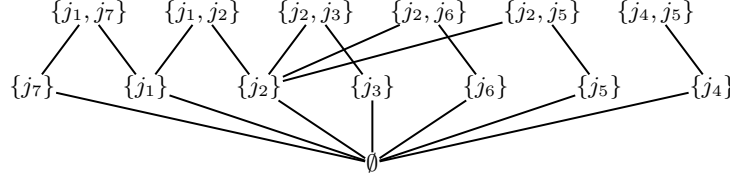


Figure 9. The core label order of the semidistributive lattice from Figure 8. The elements of this poset are the core label sets with respect to λ_{jdsd} .

In other words, the core label set of a lattice element a consists of all labels that appear in the core of a . Whenever no confusion may arise, we will drop the subscripts.

If the assignment $a \mapsto \text{Sh}_{(\mathbf{L}, \lambda)}(a)$ is injective, then we call λ a *core labeling*. In that case, the relation $\sqsubseteq_{(\mathbf{L}, \lambda)}$ —defined by $a \sqsubseteq_{(\mathbf{L}, \lambda)} b$ if and only if $\text{Sh}_{(\mathbf{L}, \lambda)}(a) \subseteq \text{Sh}_{(\mathbf{L}, \lambda)}(b)$ —is a partial order. Thus,

$$(1.11) \quad \mathbf{CLO}(\mathbf{L}, \lambda) \stackrel{\text{def}}{=} (\mathbf{L}, \sqsubseteq_{(\mathbf{L}, \lambda)})$$

is a poset, the *core label order* of \mathbf{L} . Figure 9 illustrates this construction. If λ is a core labeling, then (\mathbf{L}, λ) has the *intersection property* if for all $a, b \in \mathbf{L}$ there exists $c \in \mathbf{L}$ such that $\text{Sh}_{(\mathbf{L}, \lambda)}(a) \cap \text{Sh}_{(\mathbf{L}, \lambda)}(b) = \text{Sh}_{(\mathbf{L}, \lambda)}(c)$.

Theorem 1.1.32. *Let \mathbf{L} be a finite lattice, and let λ be a core labeling. Then, $\mathbf{CLO}(\mathbf{L}, \lambda)$ is a lattice if and only if \mathbf{L} has the intersection property and $\mathbf{CLO}(\mathbf{L}, \lambda)$ is bounded.*

PROOF. If \mathbf{L} has the intersection property, then the set $\{\text{Sh}(a) \mid a \in \mathbf{L}\}$ is closed under intersections, which means that $\mathbf{CLO}(\mathbf{L}, \lambda)$ is a meet-semilattice. By Lemma 1.1.11, $\mathbf{CLO}(\mathbf{L}, \lambda)$ is a lattice.

Conversely, if $\mathbf{CLO}(\mathbf{L}, \lambda)$ is a lattice, then it is clearly bounded. For $a, b \in \mathbf{L}$, let c be the meet of a and b in $\mathbf{CLO}(\mathbf{L}, \lambda)$. It follows that $\text{Sh}(c) \subseteq \text{Sh}(a) \cap \text{Sh}(b)$. On the other hand, if $j \in \text{Sh}(a) \cap \text{Sh}(b)$, then $\text{Sh}(j) = \{j\}$ since $j \in \text{JoinIrr}(\mathbf{L})$. It follows that $j \sqsubseteq_{(\mathbf{L}, \lambda)} a$ and $j \sqsubseteq_{(\mathbf{L}, \lambda)} b$, and therefore $j \sqsubseteq_{(\mathbf{L}, \lambda)} c$. But this implies that $j \in \text{Sh}(c)$; hence $\text{Sh}(c) = \text{Sh}(a) \cap \text{Sh}(b)$. Thus, \mathbf{L} has the intersection property. \square

Remark 1.1.33. *In fact, the proof of Theorem 1.1.32 suggests that $\mathbf{CLO}(\mathbf{L}, \lambda)$ is a meet-semilattice if and only if \mathbf{L} has the intersection property.*

We end this section with some results concerning the core label order of join-semidistributive lattices.

Lemma 1.1.34. *Let $\mathbf{L} = (\mathbf{L}, \leq)$ be a join-semidistributive lattice. Let $a, b \in \mathbf{L}$ and $j \in \text{JoinIrr}(\mathbf{L})$.*

- (i) *If $j \in \text{Sh}_{(\mathbf{L}, \lambda_{\text{jdsd}})}(a)$, then $j \leq a$.*
- (ii) *$a = \bigvee \text{Sh}_{(\mathbf{L}, \lambda_{\text{jdsd}})}(a)$.*
- (iii) *If $\text{Sh}_{(\mathbf{L}, \lambda_{\text{jdsd}})}(a) \subseteq \text{Sh}_{(\mathbf{L}, \lambda_{\text{jdsd}})}(b)$, then $a \leq b$.*
- (iv) *$\hat{1}$ is maximal in $\mathbf{CLO}(\mathbf{L}, \lambda_{\text{jdsd}})$.*

PROOF. (i) If $j \in \text{Sh}(a)$, then by Proposition 1.1.16 $(j_*, j) \bar{\wedge} (b_1, b_2)$ for some $a_\downarrow \leq b_1 < b_2 \leq a$. By Lemma 1.1.12, $j \leq b_2 \leq a$.

(ii) By (i), $j \leq a$ for all $j \in \text{Sh}(a)$, which implies $\bigvee \text{Sh}(a) \leq a$. By Proposition 1.1.15, we have $\text{Can}(a) \subseteq \text{Sh}(a)$, and we thus get $a = \bigvee \text{Can}(a) \leq \bigvee \text{Sh}(a)$. Together, this yields $a = \bigvee \text{Sh}(a)$.

(iii) By Proposition 1.1.15, $\text{Can}(a) \subseteq \text{Sh}(a)$. For $j \in \text{Sh}(a)$, $j \leq a$ by (i), which implies $\bigvee \text{Sh}(a) = \bigvee \text{Can}(a) = a$. If $\text{Sh}(a) \subseteq \text{Sh}(b)$, then $a = \bigvee \text{Sh}(a) \leq \bigvee \text{Sh}(b) = b$.

(iv) If there exists $a \in L$ with $\text{Sh}(\hat{1}) \subseteq \text{Sh}(a)$, then $\hat{1} \leq a$ by (ii). Since $\hat{1}$ is maximal in \mathbf{L} , we conclude $a = \hat{1}$. Therefore, $\hat{1}$ is maximal in $\mathbf{CLO}(\mathbf{L}, \lambda_{\text{jsd}})$. \square

Proposition 1.1.35. *The labeling λ_{jsd} from (1.5) of a join-semidistributive lattice is a core labeling.*

PROOF. Let $a, b \in L$ such that $\text{Sh}(a) = \text{Sh}(b)$. By Lemma 1.1.34(ii), $a = \bigvee \text{Sh}(a) = \bigvee \text{Sh}(b) = b$. Thus the assignment $a \mapsto \text{Sh}(a)$ is injective, and λ_{jsd} therefore is a core labeling. \square

Proposition 1.1.36. *Let \mathbf{L} be a join-semidistributive lattice. Then, $\mathbf{CLO}(\mathbf{L}, \lambda_{\text{jsd}})$ is bounded if and only if \mathbf{L} is spherical.*

PROOF. Observe that $\text{Sh}(\hat{0}) = \emptyset$, which implies that $\mathbf{CLO}(\mathbf{L}, \lambda_{\text{jsd}})$ has a least element. Now, suppose that \mathbf{L} is spherical, i.e., $\mu_{\mathbf{L}}(\hat{0}, \hat{1}) \neq 0$. By Proposition 1.1.20, $\bigwedge \text{Coatoms}(\mathbf{L}) = \hat{0}$, or in other words $\hat{1}_\downarrow = \hat{0}$. Consequently, $\text{Sh}(\hat{1}) = \text{JoinIrr}(\mathbf{L})$. Thus, for every $a \in L$ it holds that $\text{Sh}(a) \subseteq \text{Sh}(\hat{1})$, which means that $\hat{1}$ is the greatest element of $\mathbf{CLO}(\mathbf{L}, \lambda_{\text{jsd}})$.

Conversely, if $\mu_{\mathbf{L}}(\hat{0}, \hat{1}) = 0$, then $\bigwedge \text{Coatoms}(\mathbf{L}) = b > \hat{0}$ by Proposition 1.1.20. Since \mathbf{L} is finite, there exists $a \in \text{Atoms}(\mathbf{L})$ with $a \leq b$. For all $b_1, b_2 \in L$ with $b \leq b_1 < b_2$ it follows that $(\hat{0}, a)$ and (b_1, b_2) are not perspective, and by Proposition 1.1.16, $\lambda_{\text{jsd}}(b_1, b_2) \neq a$. Thus, $a \notin \text{Sh}(\hat{1})$. By Lemma 1.1.34(iv), $\hat{1}$ is maximal in $\mathbf{CLO}(\mathbf{L}, \lambda_{\text{jsd}})$, and it follows that a and $\hat{1}$ are incomparable in $\mathbf{CLO}(\mathbf{L}, \lambda_{\text{jsd}})$. This also implies that a and $\hat{1}$ do not have an upper bound in $\mathbf{CLO}(\mathbf{L}, \lambda_{\text{jsd}})$. Thus, $\mathbf{CLO}(\mathbf{L}, \lambda_{\text{jsd}})$ does not have a greatest element. \square

Corollary 1.1.37. *Let \mathbf{L} be a join-semidistributive lattice. Then, $\mathbf{CLO}(\mathbf{L}, \lambda_{\text{jsd}})$ is a lattice if and only if \mathbf{L} is spherical and has the intersection property.*

PROOF. This follows from Theorem 1.1.32 and Proposition 1.1.36. \square

We now explain how core label sets behave under lattice congruences.

Lemma 1.1.38. *Let $\mathbf{L} = (\mathbf{L}, \leq)$ be a join-semidistributive lattice and let $\Theta \in \text{Con}(\mathbf{L})$. Let Σ be the set of join-irreducible elements of \mathbf{L} contracted by Θ , and let $a \in \mathbf{L}$. If a is minimal in its congruence class, then the core label set $\text{Sh}_{(\mathbf{L}/\Theta, \lambda_{\text{jsd}})}([a]_{\Theta})$ is in bijection with $\text{Sh}_{(\mathbf{L}, \lambda_{\text{jsd}})}(a) \setminus \Sigma$.*

PROOF. In this proof, we write Sh for the core label sets in \mathbf{L} , and Sh_{Θ} for the core label sets in \mathbf{L}/Θ . The map

$$f: \text{JoinIrr}(\mathbf{L}) \setminus \Sigma \rightarrow \text{JoinIrr}(\mathbf{L}/\Theta), \quad j \mapsto [j]_{\Theta}$$

is by construction a bijection. Let $a \in \mathbf{L}$ which is minimal in its congruence class. If $j \in \text{Sh}(a)$, then we have $(j_*, j) \bar{\wedge} (b', b)$ for some $a_{\downarrow} \leq b' < b \leq a$.

If $j \in \Sigma$, then we have $(b', b) \in \Theta$, and therefore $[b']_{\Theta} = [b]_{\Theta}$. In particular we conclude $[j]_{\Theta} \notin \text{Sh}_{\Theta}([a]_{\Theta})$. If $j \notin \Sigma$, then we have $[b']_{\Theta} < [b]_{\Theta}$, and we conclude $[j]_{\Theta} \in \text{Sh}_{\Theta}([a]_{\Theta})$. It follows that f is the desired bijection from $\text{Sh}(a) \setminus \Sigma$ to $\text{Sh}_{\Theta}([a]_{\Theta})$. \square

Proposition 1.1.39. *Let \mathbf{L} be a join-semidistributive lattice with the intersection property. For every $\Theta \in \text{Con}(\mathbf{L})$ the quotient lattice \mathbf{L}/Θ has the intersection property, too.*

PROOF. In this proof, we write Sh for the core label sets in \mathbf{L} , and Sh_{Θ} for the core label sets in \mathbf{L}/Θ . Let $\Sigma = \{j \in \text{JoinIrr}(\mathbf{L}) \mid (j_*, j) \in \Theta\}$, and let f be the bijection from Lemma 1.1.38. Consequently, for $a \in \mathbf{L}$ we have $\text{Sh}_{\Theta}([a]_{\Theta}) = f(\text{Sh}(a) \setminus \Sigma)$.

Fix $a, b \in \mathbf{L}$ which are minimal in their respective congruence classes. Since \mathbf{L} has the intersection property we can find $c \in \mathbf{L}$ with $\text{Sh}(c) = \text{Sh}(a) \cap \text{Sh}(b)$. We then have

$$\begin{aligned} \text{Sh}_{\Theta}([a]_{\Theta}) \cap \text{Sh}_{\Theta}([b]_{\Theta}) &= f(\text{Sh}(a) \setminus \Sigma) \cap f(\text{Sh}(b) \setminus \Sigma) \\ &= f((\text{Sh}(a) \cap \text{Sh}(b)) \setminus \Sigma) \\ &= f(\text{Sh}(c) \setminus \Sigma) \\ &= \text{Sh}_{\Theta}([c]_{\Theta}). \end{aligned}$$

It follows that \mathbf{L}/Θ has the intersection property. \square

1.2. Coxeter groups

In this thesis we will mainly work with partial orders that arise in the context of Coxeter groups. This section recalls the basic definitions. We follow [29] and recommend [97] for further background.

1.2.1. Coxeter systems. Fix a finite set S , and consider a matrix $m: S \times S \rightarrow \mathbb{N} \cup \{\infty\}$. Such a matrix is a *Coxeter matrix* if for all $s, s' \in S$ it holds that $m(s, s') = m(s', s)$ and $m(s, s') = 1$ if and only if $s = s'$. Let

$$S_{\text{fin}}^2 \stackrel{\text{def}}{=} \{(s, s') \mid m(s, s') \neq \infty\}.$$

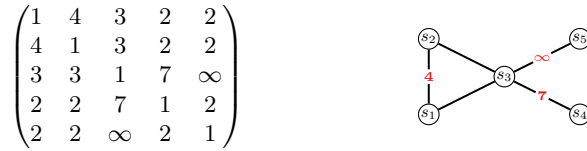


Figure 10. A Coxeter matrix (left) and its associated Coxeter graph (right).

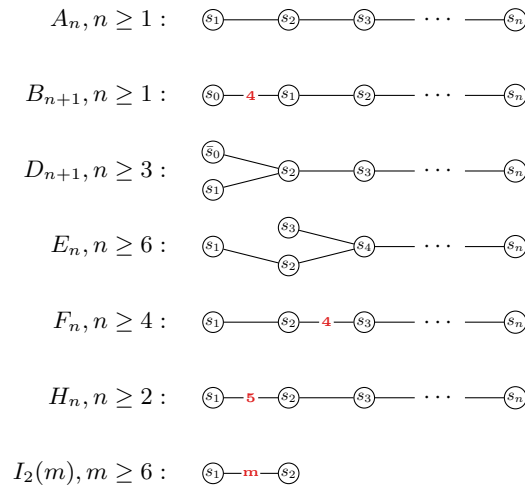


Figure 11. Some Coxeter graphs. The labels on the left will be used to denote the corresponding Coxeter group.

Definition 1.2.1. Let S be a finite set and let m be a Coxeter matrix. The **Coxeter group** associated with m is the group W given by the presentation

$$W \stackrel{\text{def}}{=} \langle S \mid (ss')^{m(s,s')} = e \text{ for all } (s, s') \in S_{\text{fin}}^2 \rangle.$$

The pair (W, S) is a **Coxeter system**, and the cardinality of S is the **rank** of W . Moreover, the elements of S are the **Coxeter generators** of W .

The defining conditions of a Coxeter matrix imply that the Coxeter generators are involutions and that two generators s, s' commute if and only if $m(s, s') = 2$. We denote the identity element of W by e .

The information contained in a Coxeter matrix can be recovered from the corresponding Coxeter system, and it can be stored efficiently in a labeled graph; the **Coxeter graph** associated with (W, S) . This is the graph $\Gamma_{(W,S)}$ whose vertex set is S and in which two vertices s and s' are connected by an edge if and only if $m(s, s') > 2$. Moreover, such an edge is labeled by $m(s, s')$, where we usually suppress the label 3. Figure 10 shows a Coxeter matrix and its associated Coxeter graph.

A Coxeter system is **irreducible** if its Coxeter graph is connected, and a Coxeter system is **finite** if its Coxeter group is finite. The classification of finite irreducible Coxeter systems goes back to H. S. M. COXETER [52], and relies on the geometric representation of Coxeter systems that we will review in Section 1.2.2. Figure 11 shows a list of Coxeter graphs which appear in this classification.

Theorem 1.2.2 ([52]). *Let (W, S) be an irreducible Coxeter system. The Coxeter group W is finite if and only if:*

- $W \cong A_n$ for $n \geq 1$;
- $W \cong B_n$ for $n \geq 2$;
- $W \cong D_n$ for $n \geq 4$;
- $W \cong E_n$ for $6 \leq n \leq 8$;
- $W \cong F_n$ for $n = 4$;
- $W \cong H_n$ for $3 \leq n \leq 4$;
- $W \cong I_2(m)$ for $m \geq 6$.

Example 1.2.3. *For $n \geq 1$, the Coxeter group A_n is isomorphic to the group of permutations of $[n + 1]$, i.e., the symmetric group $\mathfrak{S}_{[n+1]}$. The Coxeter generator s_i corresponds to the adjacent transposition $(i \ i+1)$.*

For $n \geq 2$, the Coxeter group B_n is isomorphic to the group of signed permutations of the set

$$\pm[n] \stackrel{\text{def}}{=} \{-n, \dots, -2, -1, 1, 2, \dots, n\}.$$

This group consists of permutations $w \in \mathfrak{S}_{\pm[n]}$ such that $w(-i) = -w(i)$ for all $i \in [n]$. The Coxeter generator s_0 corresponds to the transposition $(-1 \ 1)$, and the Coxeter generator s_i , for $i > 0$, corresponds to the permutation $(i \ i+1)(-i-1 \ -i)$.

For $n \geq 4$, the Coxeter group D_n is isomorphic to the group of signed permutations of $\pm[n]$ whose one-line notation involves an even number of signs, i.e., the kernel of the sign homomorphism on B_n . The Coxeter generator \bar{s}_0 corresponds to the permutation $(1 \ -2)(2 \ -1)$, and the Coxeter generator s_i , for $i > 0$, is the same as in B_n .

For $m \geq 3$, the Coxeter group $I_2(m)$ is isomorphic to the dihedral group of order $2m$. The Coxeter generators s_1 and s_2 correspond to reflections through two lines that intersect in an angle of $\frac{\pi}{m}$ radians.

Remark 1.2.4. *A Coxeter group may be realized through several different Coxeter systems. For instance, as abstract groups, there is an isomorphism $B_3 \cong A_1 \times A_3$, but the Coxeter graphs of B_3 and $A_1 \times A_3$ are clearly different.*

A finite Coxeter system is *crystallographic* if its Coxeter matrix contains only entries in $\{1, 2, 3, 4, 6\}$. The associated Coxeter groups are precisely the finite Weyl groups.

1.2.2. The geometric representation. A Coxeter group naturally acts on a real vector space. More precisely, let (W, S) be a Coxeter system of rank n and let V be an n -dimensional real vector space with basis $\{\mathbf{v}_s \mid s \in S\}$. We define a symmetric bilinear form on V by prescribing its value on the basis vectors:

$$(1.12) \quad B(\mathbf{v}_s, \mathbf{v}_{s'}) \stackrel{\text{def}}{=} \begin{cases} -\cos\left(\frac{\pi}{m(s, s')}\right), & \text{if } m(s, s') < \infty, \\ -1, & \text{if } m(s, s') = \infty. \end{cases}$$

It can be shown that B is positive semidefinite. In fact, B is positive definite if and only if W is finite [97, Theorem 6.4].

For $s \in S$ we may now define a linear transformation on V by

$$(1.13) \quad \sigma_s: V \rightarrow V, \quad \mathbf{v} \mapsto \mathbf{v} - 2B(\mathbf{v}, \mathbf{v}_s)\mathbf{v}_s.$$

Then, σ_s sends \mathbf{v}_s to its negative, fixes every vector orthogonal (with respect to B) to \mathbf{v}_s and preserves the bilinear form B .

The orthogonal complement of the line $\mathbb{R}\mathbf{v}_s$ is the *reflecting hyperplane* H_s . Thus, σ_s acts on V as a reflection through H_s , and the set $\{\sigma_s \mid s \in S\}$ of *simple reflections* generates a subgroup of the general linear group on V .

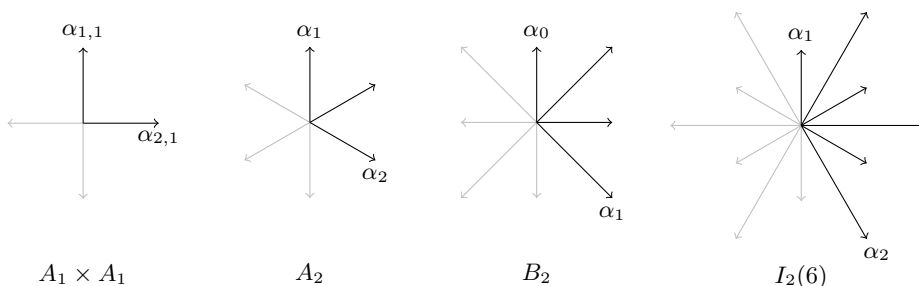


Figure 12. The finite crystallographic root systems of rank 2. The positive roots are drawn in black, the negative roots in gray. The simple root corresponding to the Coxeter generator s_i is labeled by α_i . The lengths of the roots are adjusted such that every root can be expressed as an integral linear combination of the simple roots.

Theorem 1.2.5 ([97, Proposition 5.3 and Corollary 5.4]). *There is a unique injective homomorphism $\sigma: W \rightarrow \text{GL}(V)$ which sends s to σ_s such that the group $\sigma(W)$ preserves the bilinear form B . Moreover, for $s, s' \in S$ the element ss' has order $m(s, s')$ in W .*

The homomorphism σ from Theorem 1.2.5 is the *geometric representation* of W . For $w \in W$ we simply write σ_w instead of $\sigma(w)$.

Moreover, for $s \in S$ and $w \in W$ the linear map $\sigma_{ws w^{-1}}$ acts as a reflection through the orthogonal complement of the real line spanned by $\sigma_w(\mathbf{v}_s)$. These are indeed all elements of $\sigma(W)$ which act on V as reflections [97, Section 5.7]. We therefore define the set of all *reflections* of the Coxeter system (W, S) by

$$(1.14) \quad T \stackrel{\text{def}}{=} \{ws w^{-1} \mid s \in S, w \in W\}.$$

By abuse of notation, we refer to the elements of S as simple reflections, too.

For $t \in T$, we denote by H_t the hyperplane in V fixed by the reflection σ_t . Then, another consequence of the previous observation is, that $\sigma(W)$ permutes the normal vectors to the hyperplanes H_t for $t \in T$.

We thus introduce a *root system* Φ_W of W to be a collection of unit vectors of V which is stable under the action of W . In view of the previous reasoning, Φ_W consists of two mutually inverse vectors per hyperplane H_t . Any root corresponding to a hyperplane H_s for $s \in S$ is *simple*, and the set of simple roots is Π_W .

We can partition $\Phi_W = \Phi_W^+ \uplus \Phi_W^-$ in such a way that Φ_W^+ contains precisely one root per reflecting hyperplane³. The elements of Φ_W^+ are *positive roots*, its negative counterparts *negative roots*.

Figure 12 shows all finite root systems of rank 2 corresponding to crystallographic Coxeter systems. The simple roots in these root systems are labeled according to the labels of the Coxeter generators of the corresponding Coxeter graphs; see Figure 11.

Consequently, the positive roots of W are in bijection with the reflections of W . Thus, for $t \in T$ we denote by α_t the corresponding positive root, and for $\alpha \in \Phi_W$ we denote by t_α the corresponding reflection.

³One such possibility is to consider a root positive if its expansion in terms of simple roots involves only nonnegative coefficients, see [97, Theorem 5.4].

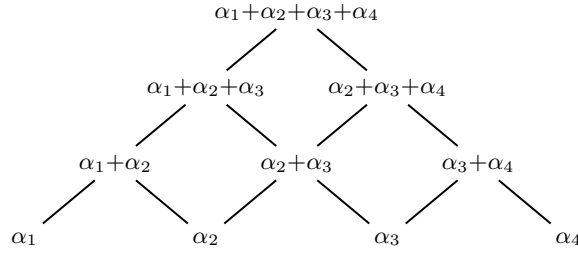
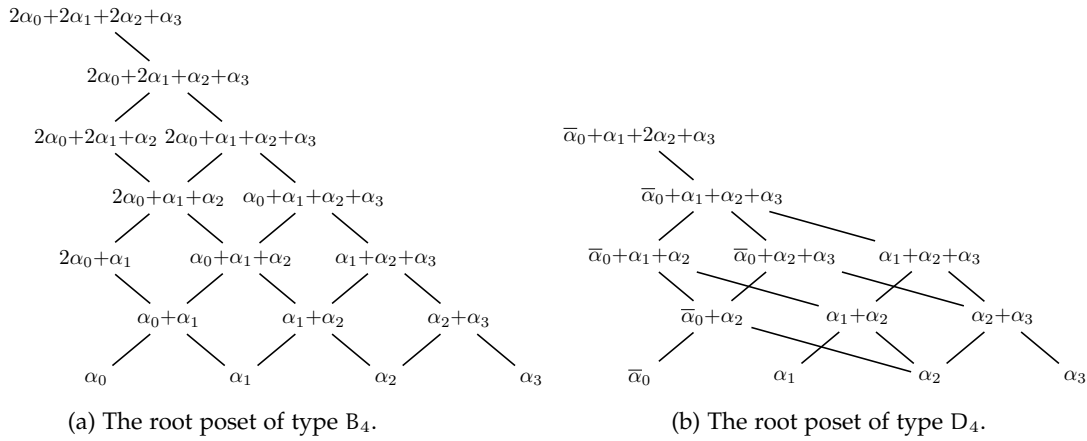


Figure 13. The root poset of type A_4 , where the simple roots are labeled according to the labeling of the Coxeter generators in Figure 11.



(a) The root poset of type B_4 .

(b) The root poset of type D_4 .

Figure 14. The root posets of type B_4 and D_4 . The labeling of the simple roots reflects the labeling of the Coxeter generators in Figure 11.

If W is crystallographic, then we can modify the lengths of the roots in such a way that every root can be expressed as a linear combination of simple roots with integral coefficients⁴. In this situation, we define the *root order* by setting

$$(1.15) \quad \alpha \preceq \beta \quad \text{if and only if} \quad \beta - \alpha \in \text{span}_{\mathbb{N}}(\Pi_W).$$

The partially ordered set (Φ_W^+, \preceq) is the *root poset* associated with W . By definition, the minimal elements of (Φ_W^+, \preceq) are precisely the simple roots. Figures 13 and 14 show the root posets of types A_4 , B_4 and D_4 .

1.2.3. Ordering a Coxeter group. We now return to considering Coxeter systems from an algebraic and combinatorial point of view, and occasionally comment on the geometric implications. Throughout this and the next section we fix a Coxeter system (W, S) .

Let $X \subseteq W$ be a generating set of W . Every $w \in W$ can be written as a word over the alphabet X , and any such word of minimal length is *X-reduced*. The number of letters in an X -reduced word is denoted by ℓ_X .

Using such a length function enables us to define a partial order on W , the *X-postfix order*, by setting

$$(1.16) \quad u \leq_X v \quad \text{if and only if} \quad \ell_X(u) + \ell_X(vu^{-1}) = \ell_X(v).$$

⁴In fact, this is possible if and *only* if W is crystallographic.

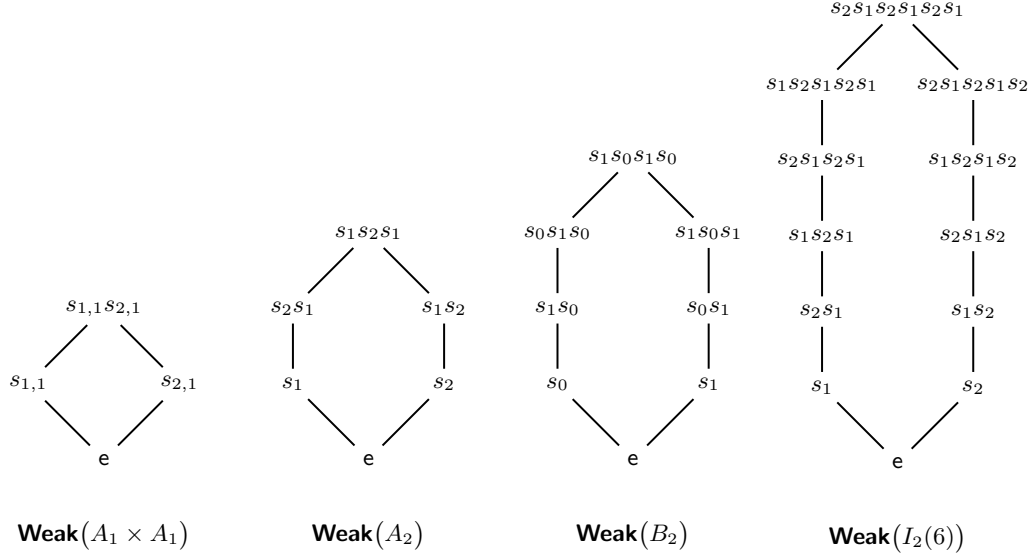


Figure 15. The finite crystallographic Coxeter groups of rank 2 ordered by weak order.

A cover relation $u \lessdot_X v$ in (W, \leq_X) is characterized by a unique generator $x \in X$ such that $v = xu$. Thus, the poset (W, \leq_X) is graded with rank function ℓ_X , and the maximal chains in an interval $[e, w]_X$ correspond bijectively to the X -reduced words for w .

The most relevant choices for X (within the scope of this thesis) are the set S of simple reflections and the set T of all reflections. The corresponding length functions are the *Coxeter length* (if $X = S$) and the *absolute length* (if $X = T$). The corresponding partial orders are the *(left) weak order* (if $X = S$; denoted by **Weak**(W) or \leq_{weak}) and the *absolute order* (if $X = T$; denoted by **Abs**(W) or \leq_{abs}).

Figures 15 and 16 show the finite crystallographic Coxeter systems of rank 2 ordered by weak and absolute order, respectively.

We may also order W by a subword order with respect to S -reduced words. This order is usually called *Bruhat order* (sometimes also *strong order*), and plays an important role in the study of Schubert varieties. In this thesis, however, Bruhat order will not be of major interest. Nevertheless, Bruhat order is *directed* in the sense that any two elements of W have an upper bound [29, Proposition 2.2.9]. This implies that if W is finite, then there exists a unique *longest element* with respect to ℓ_S ; denoted by w_\circ . In fact, the existence of a longest element characterizes finite Coxeter groups [29, Proposition 2.3.1].

Lastly, we will review another useful characterization of the weak order. A reflection $t \in T$ is a *(right) inversion* of $w \in W$ if $\ell_S(wt) < \ell_S(w)$. The set of all inversions of w is thus

$$(1.17) \quad \text{Inv}(w) \stackrel{\text{def}}{=} \{t \in T \mid \ell_S(wt) < \ell_S(w)\},$$

and it follows that $\ell_S(w) = |\text{Inv}(w)|$ [29, Corollary 1.4.5]. In particular, $\text{Inv}(w_\circ) = T$ [29, Proposition 2.3.2].

It turns out that weak order is equivalent to containment of inversion sets.

Proposition 1.2.6 ([29, Proposition 3.1.3]). *For $u, v \in W$, $u \leq_{\text{weak}} v$ if and only if $\text{Inv}(u) \subseteq \text{Inv}(v)$.*

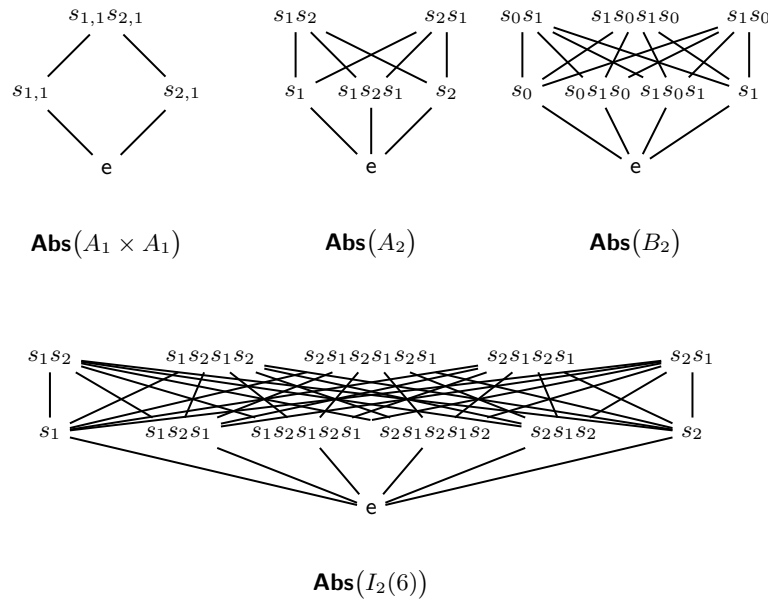


Figure 16. The finite crystallographic Coxeter groups of rank 2 ordered by absolute order. Note that the elements in each poset are labeled by S-reduced words.

A *finitary* poset is an (infinite) poset in which every principal order ideal is finite. Proposition 1.2.6 has the following consequence.

Theorem 1.2.7 ([29, Theorem 3.2.1]). *The poset $\mathbf{Weak}(W)$ is a finitary meet-semilattice. Moreover, $\mathbf{Weak}(W)$ is a lattice if and only if W is finite.*

Indeed, the only obstruction to (W, S) being a lattice is in general the lack of a greatest element. In fact, the weak order enjoys the following stronger properties.

Theorem 1.2.8 ([154, Theorem 8.1]). *Every principal order ideal in $\mathbf{Weak}(W)$ is semidistributive.*

Theorem 1.2.9 ([40, Theorem 6]). *Let (W, S) be a finite, irreducible Coxeter system. Then, $\mathbf{Weak}(W)$ is congruence uniform.*

In fact, we strongly suspect that the proof strategy applied in [40] applies almost verbatim to principal order ideals in $\mathbf{Weak}(W)$, thus strengthening Theorem 1.2.9 towards infinite Coxeter groups.

Remark 1.2.10. *The observant reader may wonder why we did not mention a subword order with respect to T-reduced words. Since T is by definition stable by conjugation, said reader may show that \leq_{abs} is in fact this subword order.*

Remark 1.2.11. *By inspection of Figure 16, we notice that there is no hope of $\mathbf{Abs}(W)$ being a semilattice for any natural choice of W . However, in Section 2.3 we will detail that certain maximal intervals in $\mathbf{Abs}(W)$ will be lattices whenever W is finite. These lattices will play a key role in the story of this thesis.*

1.2.4. Orienting a Coxeter group. Let $s, s' \in S$. A *braid move* is the replacement of the alternating string $ss'ss' \dots$ (of length $m(s, s')$) by the string $s'ss's \dots$ (of the same length). A *nil move* is the deletion of the string ss . By multiplying the letters of a word over S from left to right, any such word *evaluates* to an element of W . Coxeter systems admit the following *word property*, which goes back to H. MATSUMOTO and J. TITS [120, 190].

Theorem 1.2.12 ([29, Theorem 3.3.1]). *Let (W, S) be a Coxeter system and let $w \in W$. Any word over S that evaluates to w can be transformed into an S -reduced word for w by a sequence of braid and nil moves. Moreover, any two S -reduced words for w are related by a sequence of braid moves.*

We now want to emphasize a special family of elements of W . We say that $c \in W$ is a *Coxeter element* if $c = s_{\sigma(1)}s_{\sigma(2)} \cdots s_{\sigma(n)}$ for some permutation $\sigma \in \mathfrak{S}_n$. In fact, Theorem 1.2.12 implies that any S -reduced word of a Coxeter element is a permutation of S , because the only possible braid moves are commutations. Consequently, any two S -reduced words of a Coxeter element are related by a sequence of commutations. Another consequence of this is that any Coxeter element $c \in W$ satisfies $\ell_S(c) = n = \ell_T(c)$. This property in fact characterizes Coxeter elements.

Remark 1.2.13. *The study of Coxeter elements dates back to E. CARTAN and W. KILLING in the context of Lie algebras where they were studied as linear transformations in the geometric representation. Later, H. WEYL considered Coxeter elements as group elements and H. COXETER uncovered their importance in the invariant theory of a Coxeter group [53]. T. SPRINGER used the fact that Coxeter elements have an eigenvector that does not lie in any of the reflecting hyperplanes of W and considered the more general regular elements [173]. In [21, 28], it was shown that the role Coxeter elements play in the so-called dual braid presentation of a Coxeter group is analogous to the role of the longest element in the usual Coxeter presentation. [80] explains how this perspective helps solving the word problem in braid groups.*

A Coxeter element $c \in W$ induces an *orientation* of the Coxeter graph $\Gamma_{(W, S)}$ by setting $s \rightarrow s'$ if and only if s is to the left of s' in any S -reduced word of c . This is well defined since any two S -reduced words for c are related by a sequence of commutations, and commuting generators are not adjacent in $\Gamma_{(W, S)}$. By abuse of terminology, we use the term *orientation* also for Coxeter systems, and of course mean the corresponding orientation of $\Gamma_{(W, S)}$.

By definition, an S -reduced word for c induces a linear order on S , and—therefore—the associated orientation of (W, S) is acyclic. Coxeter elements and acyclic orientations of the Coxeter graph are in bijection

Theorem 1.2.14 ([167, Theorem 1.5]). *Let (W, S) be a Coxeter system. The set of acyclic orientations of $\Gamma_{(W, S)}$ is in bijection with the set of Coxeter elements of W .*

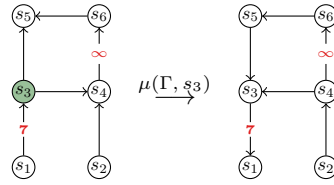


Figure 17. A mutation of a Coxeter graph.

In view of Theorem 1.2.2, the Coxeter graph of a finite, irreducible Coxeter system is a tree, and every orientation of a tree is acyclic. If such a Coxeter graph has k edges, then there exist 2^k Coxeter elements by Theorem 1.2.14.

For a moment, let us consider an arbitrary directed graph $D = (V, E)$. A *sink* (resp. *source*) of D is a vertex without outgoing (resp. incoming) edges. It is quickly verified that any acyclic directed graph has at least one source and one sink. The *mutation* of D at $v \in V$ is the directed graph $\mu(D, v) = (V, E')$, where E' is obtained from E by reversing the direction of all edges incident to v . Figure 17 displays a mutation in a Coxeter graph.

Now, let $c \in W$ be a Coxeter element and let $\Gamma_{(W,S)}^c$ denote the corresponding acyclic orientation of the Coxeter graph. A letter $s \in S$ is *initial* (resp. *final*) in c if there exists an S -reduced word for c which starts (resp. ends) with s . Clearly, the initial (resp. final) generators of c are precisely the sources (resp. sinks) of $\Gamma_{(W,S)}^c$.

For a Coxeter element $c \in W$ and an initial generator $s \in S$, the *rotation* of c by s is the Coxeter element scs , in which s is final. Clearly, a rotation of c by an initial generator corresponds to a mutation of $\Gamma_{(W,S)}^c$ by a source.

Conjugating a Coxeter element is nothing but a sequence of rotations by initial generators, and therefore corresponds to a sequence of mutations of the corresponding orientation. This, in fact, amounts to a characterization of conjugacy of Coxeter elements.

Theorem 1.2.15 ([63, Theorem 1.1]). *Let (W, S) be a Coxeter system and let c, c' be two Coxeter elements of W . Then, c and c' are conjugate if and only if $\Gamma_{(W,S)}^c$ and $\Gamma_{(W,S)}^{c'}$ are related by a sequence of mutations.*

It is straightforward to verify that any two orientations of a tree are related by a sequence of mutations. Since the Coxeter graphs of finite, irreducible Coxeter systems are trees, we obtain the next result.

Corollary 1.2.16 ([97, Proposition 3.16]). *Any two Coxeter elements in a finite, irreducible Coxeter system are conjugate.*

CHAPTER 2

Cataland

From now on, we mainly consider finite, irreducible Coxeter systems. In those situations, where results and constructions extend to infinite Coxeter systems, we add an appropriate comment.

So, throughout this section, let (W, S) be a finite Coxeter system. It turns out that there is a canonical way to associate a certain integer with W , and there is an astonishing amount of combinatorial families associated with (W, S) whose cardinality is precisely this number.

We summarize these constructions, as well as their interactions, under the name *Cataland*. This term was coined in N. WILLIAMS' thesis [192], and has since gained traction. The purpose of this thesis is to explore the uncharted territory outside Cataland. It turns out that in doing so we discover new bridges and connections to well-established research areas, that were barely visible from inside Cataland.

2.1. Catalan numbers

Let (W, S) be a Coxeter system and let $X \subseteq W$ be a generating set of W . The generating series of ℓ_X is given by

$$(2.1) \quad W_X(q) \stackrel{\text{def}}{=} \sum_{w \in W} q^{\ell_X(w)}.$$

As explained in Section 1.2.3, we are mainly concerned with the cases $X = S$ and $X = T$. If (W, S) is finite and irreducible, the generating series $W_S(q)$ and $W_T(q)$ admit nice factorizations.

Theorem 2.1.1. *Let (W, S) be a finite, irreducible Coxeter system of rank n . There exist positive integers e_1, e_2, \dots, e_n such that*

$$W_S(q) = \prod_{i=1}^n (1 + q + q^2 + \dots + q^{e_i}), \quad [49, 170]$$

$$W_T(q) = \prod_{i=1}^n (1 + qe_i). \quad [166, \text{Theorem 5.3}]$$

W	$\text{Deg}(W)$	h_W	$\text{Cat}(W)$
A_n	$2, 3, \dots, n+1$	$n+1$	$\frac{1}{n+2} \binom{2n+2}{n+1}$
B_n	$2, 4, \dots, 2n$	$2n$	$\binom{2n}{n}$
D_n	$2, 4, \dots, 2n-2, n$	$2n-2$	$\frac{3n-2}{n} \binom{2n-2}{n-1}$
E_6	$2, 5, 6, 8, 9, 12$	12	833
E_7	$2, 6, 8, 10, 12, 14, 18$	18	4160
E_8	$2, 8, 12, 14, 18, 20, 24, 30$	30	25080
F_4	$2, 6, 8, 12$	12	105
H_3	$2, 6, 10$	10	32
H_4	$2, 12, 20, 30$	30	280
$I_2(m)$	$2, m$	m	$m+2$

Table 1. The degrees, the Coxeter numbers and the Catalan numbers for the finite, irreducible Coxeter systems.

Corollary 2.1.2. *If (W, S) is a finite, irreducible Coxeter system of rank n , then*

$$|W| = \prod_{i=1}^n (e_i + 1) \quad \text{and} \quad |T| = \sum_{i=1}^n e_i.$$

Because of this stunning connection, the numbers e_1, e_2, \dots, e_n appearing in Theorem 2.1.1 deserve a special name; they are the *exponents* of (W, S) . For convenience, we define the *degrees* of (W, S) by $d_i \stackrel{\text{def}}{=} e_i + 1$. Let $\text{Deg}(W) \stackrel{\text{def}}{=} \{d_1, d_2, \dots, d_n\}$ denote the set of degrees of (W, S) , and let $h_W \stackrel{\text{def}}{=} \max \text{Deg}(W)$ be the *Coxeter number* of (W, S) . Table 1 lists the degrees and the Coxeter numbers of the finite, irreducible Coxeter systems.

Remark 2.1.3. *The exponents of (W, S) further emphasize the importance of the Coxeter elements in this whole story. By Corollary 1.2.16 any two Coxeter elements are conjugate and therefore have the same order in W . According to [53], the order of any Coxeter element of W is precisely h_W . If ζ is a primitive h_W^{th} root of unity, then the eigenvalues of any Coxeter element (in the geometric representation) are $\zeta^{e_1}, \zeta^{e_2}, \dots, \zeta^{e_n}$.*

Remark 2.1.4. *Given a linear representation of a finite Coxeter group W on a real vector space V , we may consider the algebra A of polynomial functions on V . Then, W naturally acts on A , which gives rise to the ring of polynomial invariants A^W . It was shown in [48] that A^W is a polynomial algebra, and every homogeneous choice of algebraically independent generators has degrees d_1, d_2, \dots, d_n , which justifies the terminology degrees for these numbers.*

However, we do not plan on studying these generating series in greater detail, we simply use them as a convenient means to define the exponents and degrees of finite, irreducible Coxeter systems. This, in turn, brings us to one of the main definitions in this thesis.

Definition 2.1.5 ([157, Remark 2]). Let (W, S) be a finite, irreducible Coxeter system. The W -Catalan number is

$$\text{Cat}(W) \stackrel{\text{def}}{=} \prod_{d \in \text{Deg}(W)} \frac{d + h_W}{d}.$$

Table 1 lists the W -Catalan numbers for the finite, irreducible Coxeter systems. We observe that the eponymous instance comes from type A , which recovers the ordinary *Catalan numbers*:

$$\text{Cat}(n) \stackrel{\text{def}}{=} \frac{1}{n+1} \binom{2n}{n} = \text{Cat}(A_{n-1}).$$

For now, it is quite astonishing that $\text{Cat}(W)$ appears to be an integer in every instance. In the next few sections, however, we give several explanations of this integrality property. More precisely, a W -Catalan family is a set of combinatorial objects indexed by a Coxeter group W (and possibly a Coxeter element c) whose cardinality is $\text{Cat}(W)$. We exhibit four W -Catalan families, and in each case we give a combinatorial interpretation in type A .

2.2. Aligned elements

Let $n > 0$ be an integer. Recall that the *symmetric group* of permutations of $[n]$ is denoted by \mathfrak{S}_n . For $w \in \mathfrak{S}_n$ and $i \in [n]$ we usually write w_i instead of $w(i)$.

A permutation $w \in \mathfrak{S}_n$ has a *231-pattern* if there exist indices $1 \leq i < j < k \leq n$ such that $w_k < w_i < w_j$. A permutation without a 231-pattern is *231-avoiding*. Let us write $\mathfrak{S}_n(231)$ for the set of all 231-avoiding permutations.

Proposition 2.2.1 ([101, Section 2.2.1, Exercises 4 and 5]). For $n > 0$, the cardinality of $\mathfrak{S}_n(231)$ is $\text{Cat}(n)$.

For $w \in \mathfrak{S}_n$ we define its *inversion set* by

$$(2.2) \quad \text{Inv}(w) \stackrel{\text{def}}{=} \{(i, j) \mid 1 \leq i < j \leq n \text{ and } w_i > w_j\}.$$

Let $w \in \mathfrak{S}_n$ such that $(i, k) \in \text{Inv}(w)$, and let $j \in \{i+1, i+2, \dots, k-1\}$. Then, clearly, $(i, j) \in \text{Inv}(w)$ or $(j, k) \in \text{Inv}(w)$. The inversion set of w is *aligned* if $(i, k) \in \text{Inv}(w)$ implies $(i, j) \in \text{Inv}(w)$ for all $i < j < k$.

Lemma 2.2.2 ([31, Lemma 9.8]). A permutation $w \in \mathfrak{S}_n$ is 231-avoiding if and only if $\text{Inv}(w)$ is aligned.

Let us rest for a moment and reinterpret the “aligned” condition in an order-theoretic way. By Example 1.2.3, the symmetric group \mathfrak{S}_n is isomorphic to the Coxeter group A_{n-1} , where the Coxeter generator s_i corresponds to the adjacent transposition $(i \ i+1)$. Thus, the set of all reflections of A_{n-1} corresponds to the set of all transpositions of \mathfrak{S}_n . Hence, the inversion sets defined in (2.2) recover precisely the type- A instance of the inversion sets for Coxeter systems defined in (1.17).

If we fix the *lexicographic order* on the transpositions—defined by $(i, j) \prec (i', j')$ if and only if either $i < i'$ or $i = i'$ and $j < j'$ —then $\text{Inv}(w)$ is aligned if for every $1 \leq i < k \leq n$:

$$(2.3) \quad (i, k) \in \text{Inv}(w) \text{ implies } (i, j) \in \text{Inv}(w) \text{ for all } (i, j) \prec (i, k).$$

Thus, by considering a *different* linear order on the transpositions, we would obtain a *different* “aligned” condition for \mathfrak{S}_n .

notation of $w \in \mathfrak{S}_n$ from left to right. At the i^{th} step we remove elements from the top of the stack until we find an element larger than w_i , and subsequently put w_i on top of the stack. The elements we have removed (if any) are written in a list in order of their removal.

It can then be verified that $w \in \mathfrak{S}_n(231)$ if and only if the output list of the above algorithm applied to w is linearly ordered. For this reason, 231-avoiding permutations are also called **stack-sortable** permutations.

Remark 2.2.10. N. READING gave an intriguing characterization of the c -aligned elements using the structure of their c -sorting words.

To that end, we collect the letters of the c -sorting word of $w \in W$ appearing in the i^{th} copy of c in ${}^\infty c$ (read from right to left) into a set, say X_i . Then, w is **c -sortable** if $X_1 \supseteq X_2 \supseteq \dots$, see [148, 149]. The equivalence of c -sortability and c -alignment is [148, Theorem 4.1].

Remark 2.2.11. In [154], N. READING and D. SPEYER proposed an analogous construction for c -alignment (and c -sortability) to infinite Coxeter groups. While the definition of c -sortability does not differ significantly from the finite case, the definition of c -alignment is much more intricate.

2.2.1. Cambrian lattices. We have just identified a distinguished subset for every finite, irreducible Coxeter system (W, S) and every Coxeter element $c \in W$. Following the spirit of this thesis, we want to study the behaviour of this set when partially ordered, and according to Section 1.2.3 we are mainly concerned with weak and absolute order. While $\text{Align}(W, c)$ under absolute order does not appear to exhibit nice properties, the poset $\mathbf{Weak}(\text{Align}(W, c))$ is exceptionally well behaved.

Let us dive right into this topic with the main definition of this section.

Definition 2.2.12 ([149]). Let (W, S) be a finite, irreducible Coxeter system and let $c \in W$ be a Coxeter element. The **c -Cambrian lattice** of W is

$$(2.7) \quad \mathbf{Camb}(W, c) \stackrel{\text{def}}{=} \mathbf{Weak}(\text{Align}(W, c)).$$

Figure 18 shows the $s_1 s_2$ -Cambrian lattices of the finite crystallographic Coxeter systems of rank 2. Figure 19 shows a Cambrian lattice of the Coxeter group A_3 ; the elements are given by their corresponding c -sorting words. Let us record the most relevant properties of the Cambrian lattices from our perspective.

Theorem 2.2.13. Let (W, S) be a finite, irreducible Coxeter system and let $c \in W$ be a Coxeter element. Then, $\mathbf{Camb}(W, c)$ is:

- (i) a quotient lattice of $\mathbf{Weak}(W)$; [149, Theorem 1.1]
- (ii) a sublattice of $\mathbf{Weak}(W)$; [149, Theorem 1.2]
- (iii) congruence uniform; Proposition 1.1.31 & Theorem 1.2.9
- (iv) trim. [98, Theorem 4.17]

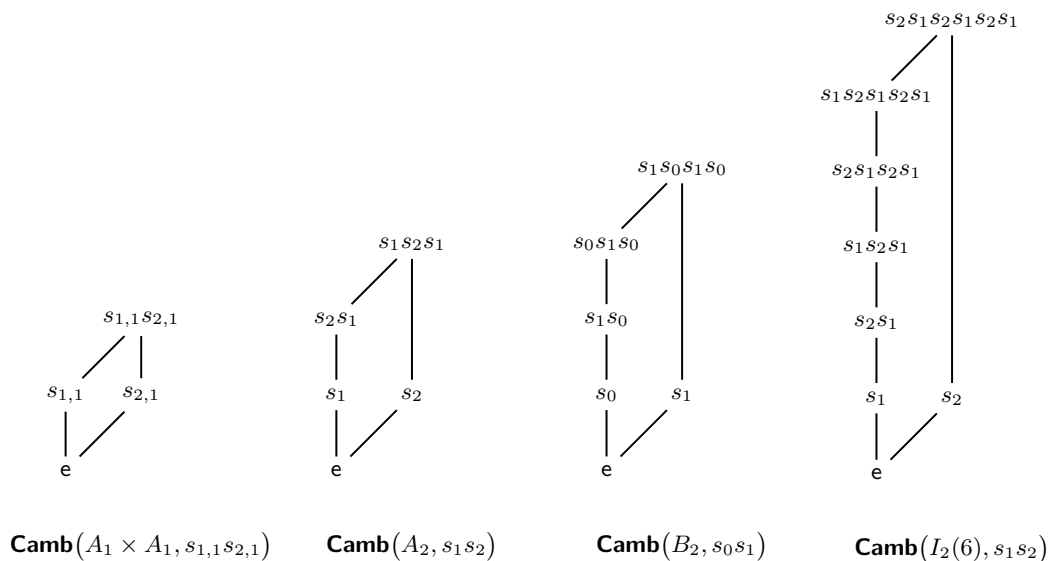


Figure 18. The s_1s_2 -Cambrian lattices for the finite crystallographic Coxeter groups of rank 2.

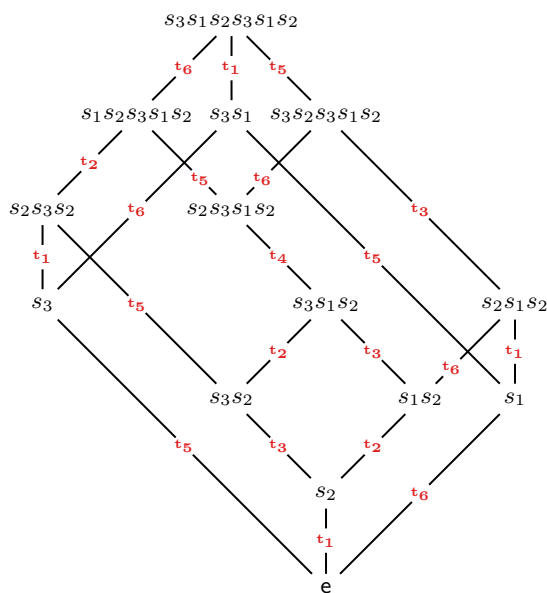


Figure 19. The $s_2s_1s_3$ -Cambrian lattice of A_3 . The edge-labels are explained in Example 2.3.14.

The key component in proving Theorem 2.2.13(i) is the fact that for each $w \in W$ there exists a unique maximal c -aligned element below w in weak order [149, Proposition 3.2]. This gives rise to a *projection map*

$$(2.8) \quad \pi_c^\perp: W \rightarrow \text{Align}(W, c), \quad w \mapsto \bigvee \{w' \in \text{Align}(W, c) \mid w' \leq_{\text{weak}} w\},$$

poset is a meet-semilattice, and properties (i)–(iii) of Theorem 2.2.13 carry over to principal order ideals. Trimness of principal order ideals of the Cambrian semilattices was established in [127]. A topological study of the Cambrian semilattices was conducted in [100].

By Theorem 2.2.13, $\mathbf{Camb}(W, c)$ is congruence uniform, and thus semidistributive by Theorem 1.1.30(ii). Therefore, every c -aligned element admits a canonical join representation by Theorem 1.1.14. In fact, there is a nice, compact description of these canonical join representations. For $w \in W$, a *cover inversion*⁵ is an inversion $t \in \text{Inv}(w)$ such that there exists $s \in S$ with $sw = wt$. The name stems from the fact that cover inversions precisely describe the cover relations in $\mathbf{Weak}(W)$. We write $\text{Cov}(w)$ for the set of cover inversions of w .

Lemma 2.2.16. *For $w \in W$, the number of elements covered by w is $|\text{Cov}(w)|$.*

PROOF. This is immediate by construction. □

Theorem 8.3 in [154] states that for every $w \in \text{Align}(W, c)$ and every $t \in \text{Cov}(w)$, there exists a unique element $j_t \in \text{Align}(W, c)$ with $\text{Cov}(j_t) = \{t\}$. By Lemma 2.2.16, j_t is join irreducible as an element of $\mathbf{Camb}(W, c)$.

Theorem 2.2.17 ([154, Theorem 8.1 and Proposition 8.2]). *Let $w \in \text{Align}(W, c)$. Then,*

$$\text{Can}(w) = \{j_t \mid t \in \text{Cov}(w)\}.$$

* * *

The main part of this thesis is devoted to the combinatorial study of a generalization of the members of Cataland in type A. We therefore want to spend a few moments to recall a combinatorial construction of the Cambrian lattices of Λ_{n-1} with respect to the *linear*⁶ Coxeter element

$$(2.9) \quad \bar{c} \stackrel{\text{def}}{=} s_1 s_2 \cdots s_{n-1}.$$

By Example 2.2.7, the \bar{c} -aligned elements of Λ_{n-1} are precisely the 231-avoiding permutations of \mathfrak{S}_n . The weak order on \mathfrak{S}_n is the containment order on inversion sets. We recall an encoding due to A. BJÖRNER and M. WACHS that is equivalent to the projection map $\pi_{\bar{c}}^\downarrow$ from (2.8) in the sense that the preimages of $\pi_{\bar{c}}^\downarrow$ are precisely the permutations with the same encoding.

Following [31, Definition 9.9], for $w \in \mathfrak{S}_n$ we define the *BW-code* of w by $\text{cd}(w) = (c_1, c_2, \dots, c_n)$, where

$$c_i \stackrel{\text{def}}{=} \max\{k \mid w_i > w_{i+1}, w_i > w_{i+2}, \dots, w_i > w_{i+k}\}.$$

Let $\text{Codes}(n) \stackrel{\text{def}}{=} \{\text{cd}(w) \mid w \in \mathfrak{S}_n\}$. Definition 9.1 in [31] states that an integer tuple (c_1, c_2, \dots, c_n) belongs to $\text{Codes}(n)$ if and only if $0 \leq c_i \leq n - i$ and $c_{k+i} \leq c_k - i$ for all $k \in [n - 2]$ and $i \in [c_k]$.

⁵Perhaps these elements are better known under the name “cover reflections”. However, we have chosen to call them “cover inversions” to emphasize the fact that they are inversions, not just arbitrary reflections.

⁶The name reflects the fact that the orientation of the Coxeter graph of Λ_{n-1} corresponding to \bar{c} is the linear orientation from left to right.

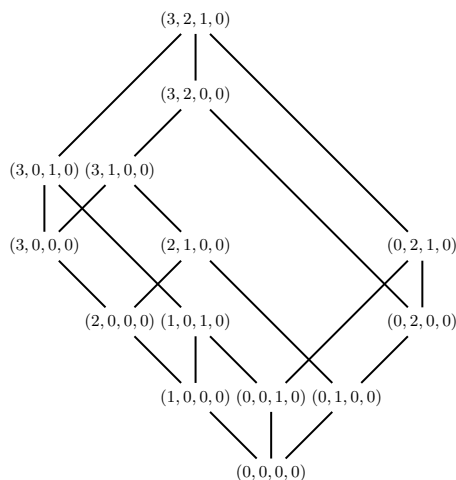


Figure 21. The componentwise order on Codes(4).

Proposition 2.2.18 ([31, Proposition 9.10]). *For $n > 0$, the map $cd: \mathfrak{S}_n(231) \rightarrow \text{Codes}(n)$ is a bijection, which converts the weak order on permutations to the componentwise order on integer tuples.*

Consequently, the componentwise order on Codes(n) is a lattice. This lattice has occurred in the literature in various incarnations throughout the last six decades; we have just seen two. The most well-known incarnation is probably the rotation order on binary trees, which is usually referred to as the *Tamari lattice* $\text{Tam}(n)$; first introduced in [182]. Figure 21 shows $\text{Tam}(4)$ realized by the componentwise order on the elements of Codes(4).

Remark 2.2.19. *A classical way to encode a permutation $w \in \mathfrak{S}_n$ is the *Lehmer code*, which is the integer tuple $l(w) = (l_1, l_2, \dots, l_n)$, where $l_i = |\{j \mid j > i, w_j < w_i\}|$ [112]. More precisely, the i^{th} entry in the Lehmer code counts inversions of w of the form (i, \cdot) . The Lehmer encoding uniquely determines a permutation.*

The BW-codes defined above can be regarded as a “consecutive” version of the Lehmer code. This encoding does no longer uniquely determine the permutation. However, it identifies 231-avoiding permutations as the permutations with the minimal number of inversions among all permutations with the same BW-encoding, and the componentwise order on the BW-codes agrees with the weak order on the corresponding 231-avoiding permutations.

Remark 2.2.20. *Very recently, the BW-codes have been recovered in the study of certain combinatorial Hopf algebras as special instances of so-called δ -cliffs [50]. The combinatorial Hopf algebra associated with the BW-codes is known under the name *Loday–Ronco algebra* and was introduced in [115]. See also Section 4.5.1.*

It is straightforward to verify that a cover inversion of $w \in \mathfrak{S}_n$ is a *descent* of w , i.e., a pair (i, j) such that $i < j$ and $w_i = w_j + 1$. By Theorem 2.2.17, the canonical join representation of $w \in \mathfrak{S}_n(231)$ can thus be identified with the descent set of w . This brings us to our next main object.

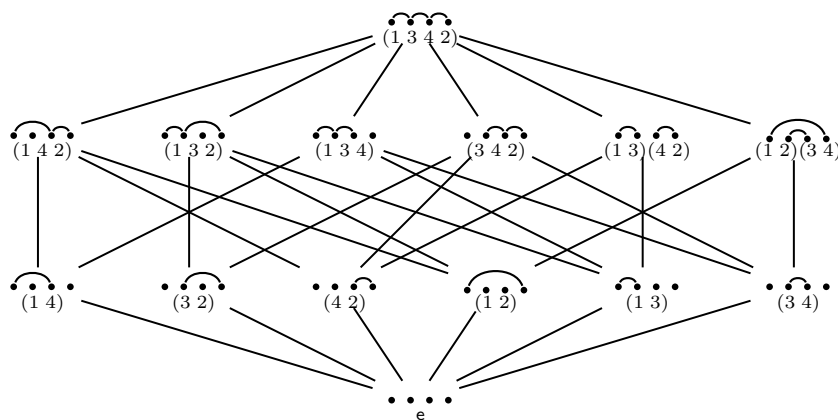


Figure 22. The lattice $\mathbf{Nonc}(4)$. Its elements are also labeled by the corresponding c -noncrossing A_3 -partitions for $c = s_2s_1s_3$, proving that this lattice is isomorphic to $\mathbf{Nonc}(A_3, c)$.

2.3. Noncrossing partitions

Let $n > 0$ be an integer. A *set partition* is a collection $P = \{B_1, B_2, \dots, B_k\}$ of nonempty, mutually disjoint subsets of $[n]$ —called *blocks*—such that $\bigcup_{i=1}^k B_i = [n]$. The collection of all ordinary partitions of $[n]$ is denoted by Π_n . In view of the things to come, we will normally use the term *ordinary partitions* rather than set partitions.

Two consecutive elements in a block of P form a *bump*, and we consider bumps to be ordered pairs, where the smaller entry comes first. We graphically represent P by drawing n nodes—labeled from 1 through n —on a horizontal line and connecting two nodes by an arc if their labels correspond to a bump of P .

An ordinary partition is *noncrossing* if its diagram P can be drawn such that no two arcs intersect each other in their interior. In other words, $P \in \Pi_n$ is noncrossing if whenever (a_1, b_1) and (a_2, b_2) are bumps of P and $a_1 < a_2$, then either $b_1 < a_2$ or $b_2 < b_1$. We write $\mathbf{Nonc}(n)$ for the set of all noncrossing set partitions of $[n]$.

Proposition 2.3.1 ([111, Corollaire 4.2]). *For $n > 0$, the cardinality of $\mathbf{Nonc}(n)$ is $\text{Cat}(n)$.*

The next result establishes a bijective correspondence between 231-avoiding permutations and noncrossing partitions, and was independently discovered in [153].

Proposition 2.3.2 ([192, Proposition 5.3.5]). *Let $n > 0$ and $w \in \mathfrak{S}_n(231)$. There exists a unique $P \in \mathbf{Nonc}(n)$ such that the cover inversions of w correspond to the bumps of P .*

Ordinary partitions are naturally ordered by *refinement*, i.e., if $P, P' \in \Pi_n$, then P *refines* P' —written $P \leq_{\text{ref}} P'$ —if every block of P is contained in some block of P' . It is easy to see that $(\Pi_n, \leq_{\text{ref}})$ is a lattice. This property is inherited by $\mathbf{Nonc}(n) \stackrel{\text{def}}{=} (\mathbf{Nonc}(n), \leq_{\text{ref}})$, and is illustrated in Figure 22 for $n = 4$.

Theorem 2.3.3 ([111, Théorème 1]). *For $n > 0$, the poset $\mathbf{Nonc}(n)$ is a lattice. Moreover, it is a meet-subsemilattice of $(\Pi_n, \leq_{\text{ref}})$.*

Note that our definition of ordinary noncrossing partitions implicitly depends on the linear order $1 < 2 < \dots < n$ of $[n]$. However, we could have done equally well without this choice of linear order, had we just defined noncrossing partitions as a collection of mutually nonintersecting arcs. In doing so, we could in fact label the nodes of the diagram of an ordinary noncrossing partition with respect to *any* linear order of $[n]$. In Figure 22, we have labeled the ordinary noncrossing partitions for $n = 4$ with respect to the order $1 < 3 < 4 < 2$.

Let $a_1 = 1$ and fix a linear order $a_1 < a_2 < \dots < a_n$ on $[n] = \{a_1, a_2, \dots, a_n\}$ ⁷. Due to this ordering, for any $P \in \Pi_n$ there exists a unique permutation $w \in \mathfrak{S}_n$ whose cycles correspond to the blocks of P . More precisely, if $\{a_{i_1}, a_{i_2}, \dots, a_{i_k}\}$ is a block of P with $i_1 < i_2 < \dots < i_k$, then $(a_{i_1} a_{i_2} \dots a_{i_k})$ is a cycle of w . This map has the following property.

Theorem 2.3.4 ([24, Theorem 1]). *Let $c = (a_1 a_2 \dots a_n)$ be an n -cycle of \mathfrak{S}_n , where $a_1 = 1$. The map that sends blocks to cycles is a bijection from $\text{Nonc}(n)$ to $\{w \in \mathfrak{S}_n \mid w \leq_{\text{abs}} c\}$. Moreover, this map converts the refinement order on partitions to the absolute order on permutations.*

Theorem 2.3.4 was recovered from an algebraic point of view in [33]. Figure 23 illustrates the bijections described in Proposition 2.3.2 and Theorem 2.3.4 for $n = 4$.

* * *

Recall from Example 1.2.3 that \mathfrak{S}_n is isomorphic to the Coxeter group A_{n-1} , with the Coxeter generator s_i corresponding to the adjacent transposition $(i \ i+1)$. It is quickly verified that every Coxeter element of A_{n-1} corresponds to an n -cycle.

With our current knowledge, the following definition seems to come out of thin air. Its only apparent justification is that its restriction to type A is in accordance with Theorem 2.3.4.

Definition 2.3.5. *Let (W, S) be a finite, irreducible Coxeter system and let $c \in W$ be a Coxeter element. We define the set of **c -noncrossing W -partitions** by*

$$\text{Nonc}(W, c) \stackrel{\text{def}}{=} \{w \in W \mid w \leq_{\text{abs}} c\}.$$

*Moreover, we define **Nonc** $(W, c) \stackrel{\text{def}}{=} \mathbf{Abs}(\text{Nonc}(W, c))$.*

Figure 22 shows the lattice $\mathbf{Nonc}(A_3, c)$, where $c = s_2 s_1 s_3$. Combinatorial realizations for $\text{Nonc}(B_n, c)$ and $\text{Nonc}(D_n, c)$ in terms of ordinary noncrossing partitions were given in [10, 157].

Lemma 2.3.6. *The poset **Nonc** (W, c) is graded.*

PROOF. The absolute order admits—by definition—the rank function ℓ_{\top} . Since $\mathbf{Nonc}(W, c)$ is an interval in $\mathbf{Abs}(W)$ it inherits this rank function. \square

We spend the remainder of this section explaining that this indeed is a reasonable definition, and we first observe that the cardinality of $\text{Nonc}(W, c)$ is independent of c , and is indeed the correct W -Catalan number.

⁷The position of the 1 is fixed to break the cyclic symmetry.

$w \in \mathfrak{S}_4(231)$	$P \in \text{Nonc}_4$	$w \leq_T (1\ 3\ 4\ 2)$
1234	$\begin{array}{c} \bullet \bullet \bullet \bullet \\ 1\ 3\ 4\ 2 \end{array}$	$()$
2134	$\begin{array}{c} \frown \bullet \bullet \\ 1\ 3\ 4\ 2 \end{array}$	$(1\ 3)$
3124	$\begin{array}{c} \frown \bullet \bullet \\ 1\ 3\ 4\ 2 \end{array}$	$(1\ 4)$
4123	$\begin{array}{c} \frown \bullet \bullet \\ 1\ 3\ 4\ 2 \end{array}$	$(1\ 2)$
1324	$\begin{array}{c} \bullet \frown \bullet \\ 1\ 3\ 4\ 2 \end{array}$	$(3\ 4)$
1423	$\begin{array}{c} \bullet \frown \bullet \\ 1\ 3\ 4\ 2 \end{array}$	$(3\ 2)$
1243	$\begin{array}{c} \bullet \bullet \frown \\ 1\ 3\ 4\ 2 \end{array}$	$(4\ 2)$
3214	$\begin{array}{c} \frown \bullet \bullet \\ 1\ 3\ 4\ 2 \end{array}$	$(1\ 3\ 4)$
4312	$\begin{array}{c} \frown \bullet \bullet \\ 1\ 3\ 4\ 2 \end{array}$	$(1\ 3\ 2)$
2143	$\begin{array}{c} \frown \frown \\ 1\ 3\ 4\ 2 \end{array}$	$(1\ 3)(4\ 2)$
4132	$\begin{array}{c} \frown \frown \\ 1\ 3\ 4\ 2 \end{array}$	$(1\ 4\ 2)$
4213	$\begin{array}{c} \frown \frown \\ 1\ 3\ 4\ 2 \end{array}$	$(1\ 2)(3\ 4)$
1432	$\begin{array}{c} \bullet \frown \frown \\ 1\ 3\ 4\ 2 \end{array}$	$(3\ 4\ 2)$
4321	$\begin{array}{c} \frown \frown \frown \\ 1\ 3\ 4\ 2 \end{array}$	$(1\ 3\ 4\ 2)$

Figure 23. The bijections involving permutations and noncrossing partitions for $n = 4$.

Theorem 2.3.7 ([10, 21, 111, 157]). *Let (W, S) be a finite, irreducible Coxeter system and let $c \in W$ be a Coxeter element. Then,*

$$|\text{Nonc}(W, c)| = \text{Cat}(W).$$

Theorems 2.2.8 and 2.3.7 imply that the sets $\text{Align}(W, c)$ and $\text{Nonc}(W, c)$ are equinumerous, and this fact cries for a bijective explanation. Indeed, the bijection from Proposition 2.3.2 extends to all types⁸. Let $w \in \text{Align}(W, c)$ with $\text{Cov}(w) = \{t_1, t_2, \dots, t_k\}$, where the cover inversions are ordered according to $\text{Inv}(w_o(c))$, i.e., $t_i \prec_c t_j$ if and only if $i < j$. We define a map

$$(2.10) \quad \text{nc}_c: \text{Align}(W, c) \rightarrow \text{Nonc}(W, c), \quad w \mapsto t_1 t_2 \cdots t_k.$$

Theorem 2.3.8 ([148, Theorem 6.1]). *The map nc_c is a bijection for every finite, irreducible Coxeter system (W, S) and every Coxeter element $c \in W$.*

⁸Our exposition may give the impression that Theorem 2.2.8 was known prior to Theorem 2.3.7. This is not at all the case. In fact, Theorem 2.3.7 was proven first in a case-by-case fashion, and Theorem 2.2.8 was subsequently concluded (uniformly) via the map nc_c .

Example 2.3.9. Let us illustrate Theorem 2.3.8 in case of $W = B_2$, $c = s_1s_0$. The c -sorting word of the longest element of B_2 is $w_o(c) = s_0s_1s_0s_1$, and its inversion set is

$$\text{Inv}(w_o) = \left\{ \underbrace{s_1}_{t_1}, \underbrace{s_1s_0s_1}_{t_2}, \underbrace{s_0s_1s_0}_{t_3}, \underbrace{s_0}_{t_4} \right\}$$

where the inversions are ordered according to $\text{Inv}(w_o(c))$, i.e., $t_1 \prec_c t_2 \prec_c t_3 \prec_c t_4$. Comparing with Figure 12, we find $\alpha_{t_4} = \alpha_0$ and $\alpha_{t_1} = \alpha_1$. It follows that $\alpha_{t_2} = \alpha_0 + \alpha_1$ and $\alpha_{t_3} = 2\alpha_0 + \alpha_1$.

According to Definition 2.2.6, $w \in B_2$ is c -aligned if whenever it has t_2 or t_3 as inversions it needs to have t_1 as an inversion, too.

The eight elements of B_2 are listed in the following table, together with their inversion and cover inversion sets and—if they are c -aligned—with their image under nc_c .

$w \in B_2$	$\text{Inv}(w)$	$w \in \text{Align}(B_2, c)?$	$\text{Cov}(w)$	$\text{nc}_c(w)$
e	\emptyset	yes	\emptyset	e
s_0	$\{t_4\}$	yes	$\{t_4\}$	s_0
s_1	$\{t_1\}$	yes	$\{t_1\}$	s_1
s_0s_1	$\{t_1, t_2\}$	yes	$\{t_2\}$	$s_1s_0s_1$
s_1s_0	$\{t_4, t_3\}$	no	$\{t_3\}$	—
$s_0s_1s_0$	$\{t_4, t_3, t_2\}$	no	$\{t_2\}$	—
$s_1s_0s_1$	$\{t_1, t_2, t_3\}$	yes	$\{t_3\}$	$s_0s_1s_0$
$s_0s_1s_0s_1$	$\{t_1, t_2, t_3, t_4\}$	yes	$\{t_1, t_4\}$	s_1s_0

We conclude that the definition of the set $\text{Nonc}(W, c)$ fits nicely into the enumerative part of this story. We will now see that it also fits exceptionally well into the structural aspect.

Recall that the set T is by definition stable under W -conjugation. This implies that the length function ℓ_T (and thus the partial order \leq_{abs}) is invariant under W -conjugation. It follows that the structure of $\text{Nonc}(W, c)$ does not depend on the choice of c .

Corollary 2.3.10. Let $c, c' \in W$ be two Coxeter elements. Then, $\text{Nonc}(W, c) \cong \text{Nonc}(W, c')$.

PROOF. By Corollary 1.2.16, c and c' are W -conjugate. The claim follows since \leq_{abs} is invariant under W -conjugation. \square

By Theorem 2.3.3 $\text{Nonc}(A_{n-1}, c)$ is a lattice, and—perhaps somewhat surprisingly—this property extends to all types, too.

Theorem 2.3.11 ([35, Theorem 7.8]). The poset $\text{Nonc}(W, c)$ is a lattice for every finite, irreducible Coxeter system (W, S) and every Coxeter element $c \in W$.

Special cases of Theorem 2.3.11 were proven earlier in [10, 21, 111, 157] exploiting the combinatorial realizations of these posets in terms of ordinary noncrossing partitions. We wish to emphasize that the proof of Theorem 2.3.11 given in [35] is *uniform*, i.e., it works simultaneously for all finite, irreducible Coxeter systems. Its key component is an isomorphism from $\text{Nonc}(W, c)$ —for a particular Coxeter element c —to a collection of simplicial spheres which converts absolute order into containment order.

In a similar spirit, but from a completely different viewpoint, another remarkable uniform proof of Theorem 2.3.11 was given in [152] and exhibits $\mathbf{Nonc}(W, c)$ as the core label order of $\mathbf{Camb}(W, c)$; see Section 1.1.10. Let us recall this construction.

By Theorem 2.2.17, the canonical join representation of $w \in \text{Align}(W, c)$ can be identified with the set $\text{Cov}(w)$, and we may thus consider the following (well-defined) edge-labeling of $\mathbf{Camb}(W, c)$:

$$(2.11) \quad \lambda_c: \text{Covers}(\mathbf{Camb}(W, c)) \rightarrow T, \quad (u, v) \mapsto t,$$

where t is the unique element of $\text{Cov}(v) \setminus \text{Inv}(u)$. The labeling λ_c is equivalent to the labeling λ_{jisd} of $\mathbf{Camb}(W, c)$ considered as a semidistributive lattice. By Proposition 1.1.35, the core label order of $\mathbf{Camb}(W, c)$ is well defined.

For $w \in \text{Align}(W, c)$, we may define the subgroup $W_{\text{Cov}(w)} = \langle \text{Cov}(w) \rangle$ generated by the cover inversions of w . By [152, Proposition 4.7], the set of reflections of $W_{\text{Cov}(w)}$ agrees with the labels appearing in the core of w in $\mathbf{Camb}(W, c)$, i.e.,

$$\{t \in T \mid t \in W_{\text{Cov}(w)}\} = \text{Sh}_{(\mathbf{Camb}(W, c), \lambda_c)}(w).$$

Proposition 2.3.12 ([180, Theorem 2.10.5]). *For $u, v \in W$, $\text{Sh}_{(\mathbf{Weak}(W), \lambda_{\text{jisd}})}(u) \subseteq \text{Sh}_{(\mathbf{Weak}(W), \lambda_{\text{jisd}})}(v)$ if and only if $\text{Inv}(u) \subseteq \text{Inv}(v)$ and $W_{\text{Cov}(u)} \subseteq W_{\text{Cov}(v)}$.*

As a consequence, the containment order on $\{W_{\text{Cov}(w)} \mid w \in \text{Align}(W, c)\}$ is isomorphic to the core label order of $\mathbf{Camb}(W, c)$. This implies the following result.

Theorem 2.3.13 ([152, Theorem 8.5]). *Let (W, S) be a finite, irreducible Coxeter system and let $c \in W$ be a Coxeter element. The bijection nc_c extends to an isomorphism from $\mathbf{CLO}(\mathbf{Camb}(W, c))$ to $\mathbf{Nonc}(W, c)$.*

Example 2.3.14. *Let $W = A_3$ and $c = s_2s_1s_3$. The c -sorting word of w_o is*

$$\mathbf{w}_o(c) = s_3s_1s_2s_3s_1s_2,$$

and its inversion set is

$$\text{Inv}(w_o) = \left\{ \underbrace{s_2}_{t_1}, \underbrace{s_2s_1s_2}_{t_2}, \underbrace{s_2s_3s_2}_{t_3}, \underbrace{s_3s_1s_2s_3s_1}_{t_4}, \underbrace{s_3}_{t_5}, \underbrace{s_1}_{t_6} \right\},$$

whose entries are ordered according to $\text{Inv}(w_o(c))$. The c -Cambrian lattice of A_3 is displayed in Figure 19, where the edges are labeled by λ_c . The following table shows the inversion and cover inversion sets of the elements of $\text{Align}(A_3, c)$ together with their images under nc_c (given as permutations of [4] in cycle notation) and the sets of reflections in the subgroup of A_3 generated by the cover inversions.

w	$\text{Inv}(w)$	$\text{Cov}(w)$	$\text{nc}_c(w)$	$T \cap W_{\text{Cov}(w)}$
e	\emptyset	\emptyset	$()$	\emptyset
s_1	$\{t_6\}$	$\{t_6\}$	$(1\ 2)$	$\{t_6\}$
s_2	$\{t_1\}$	$\{t_1\}$	$(3\ 2)$	$\{t_1\}$
s_3	$\{t_5\}$	$\{t_5\}$	$(3\ 4)$	$\{t_5\}$
s_1s_2	$\{t_1, t_2\}$	$\{t_2\}$	$(1\ 3)$	$\{t_2\}$
s_3s_1	$\{t_5, t_6\}$	$\{t_5, t_6\}$	$(1\ 2)(3\ 4)$	$\{t_5, t_6\}$
s_3s_2	$\{t_1, t_3\}$	$\{t_3\}$	$(4\ 2)$	$\{t_3\}$

$s_2s_1s_2$	$\{t_1, t_2, t_6\}$	$\{t_1, t_6\}$	$(1\ 3\ 2)$	$\{t_1, t_2, t_6\}$
$s_3s_1s_2$	$\{t_1, t_2, t_3\}$	$\{t_2, t_3\}$	$(1\ 3)(4\ 2)$	$\{t_2, t_3\}$
$s_2s_3s_2$	$\{t_1, t_3, t_5\}$	$\{t_1, t_5\}$	$(2\ 3\ 4)$	$\{t_1, t_3, t_5\}$
$s_2s_3s_1s_2$	$\{t_1, t_2, t_3, t_4\}$	$\{t_4\}$	$(1\ 4)$	$\{t_4\}$
$s_3s_2s_3s_1s_2$	$\{t_1, t_2, t_3, t_4, t_6\}$	$\{t_3, t_6\}$	$(1\ 4\ 2)$	$\{t_3, t_4, t_6\}$
$s_1s_2s_3s_1s_2$	$\{t_1, t_2, t_3, t_4, t_5\}$	$\{t_2, t_5\}$	$(1\ 3\ 4)$	$\{t_2, t_4, t_6\}$
$s_3s_1s_2s_3s_1s_2$	$\{t_1, t_2, t_3, t_4, t_5, t_6\}$	$\{t_1, t_5, t_6\}$	$(1\ 3\ 4\ 2)$	$\{t_1, t_2, t_3, t_4, t_5, t_6\}$

We can verify in Figure 22 that for every $w \in \text{Align}(A_3, c)$, the set $W_{\text{Cov}(w)}$ agrees with the principal order ideal of $\text{Nonc}(A_3, c)$ generated by $\text{nc}_c(w)$, which illustrates Theorem 2.3.13.

2.4. Clusters

In Section 2.2.1 we have defined the c -Cambrian lattices by the weak order on c -aligned elements. In this section we introduce another realization of these lattices as certain flip posets on subword complexes.

Let (W, S) be a Coxeter system, and let S^* denote the set of words over the alphabet S . For $Q \in S^*$ and $w \in W$, the *subword complex* $\text{Subw}(W; Q, w)$ is the simplicial complex whose facets are the complements of the positions of the S -reduced words for w in Q [103, Definition 1.8.1], see also [102]. The *Demazure product* on (W, S) is the map $\delta: S^* \rightarrow W$ defined recursively by

$$(2.12) \quad \delta(e) = e \quad \text{and} \quad \delta(Qs) \mapsto \begin{cases} \delta(Qs), & \text{if } \ell_S(\delta(Q)s) = \ell_S(\delta(Q)) + 1, \\ \delta(Q), & \text{if } \ell_S(\delta(Q)s) = \ell_S(\delta(Q)) - 1. \end{cases}$$

Theorem 2.4.1 ([102, Theorem 3.7]). *For $Q \in S^*$ and $w \in W$, the subword complex $\text{Subw}(W; Q, w)$ is homotopy equivalent to either a ball or a sphere. It is homotopy equivalent to a sphere if and only if $\delta(Q) = w$.*

Example 2.4.2. *Let $W = B_3$ and $c = s_0s_1s_2$. Consider $w \in B_3$ given by $w(c) = s_1s_0s_2s_1s_0s_2s_1$, and $Q = s_0s_1s_2s_0s_1s_2s_0s_1s_2s_0s_1s_2$. The S -reduced words for w are*

$$s_1s_2s_0s_1s_2s_0s_1, \quad s_1s_0s_2s_1s_2s_0s_1, \quad s_1s_0s_1s_2s_1s_0s_1, \quad s_1s_0s_2s_1s_0s_2s_1, \quad s_1s_2s_0s_1s_0s_2s_1.$$

There are eleven occurrences of S -reduced words for w as subwords of Q :

$$\begin{aligned} & s_0s_1s_2s_0s_1s_2s_0s_1s_2s_0s_1s_2, \quad s_0s_1s_2s_0s_1s_2s_0s_1s_2s_0s_1s_2, \quad s_0s_1s_2s_0s_1s_2s_0s_1s_2s_0s_1s_2, \\ & s_0s_1s_2s_0s_1s_2s_0s_1s_2s_0s_1s_2, \quad s_0s_1s_2s_0s_1s_2s_0s_1s_2s_0s_1s_2, \quad s_0s_1s_2s_0s_1s_2s_0s_1s_2s_0s_1s_2, \\ & s_0s_1s_2s_0s_1s_2s_0s_1s_2s_0s_1s_2, \quad s_0s_1s_2s_0s_1s_2s_0s_1s_2s_0s_1s_2, \quad s_0s_1s_2s_0s_1s_2s_0s_1s_2s_0s_1s_2, \\ & s_0s_1s_2s_0s_1s_2s_0s_1s_2s_0s_1s_2, \quad s_0s_1s_2s_0s_1s_2s_0s_1s_2s_0s_1s_2. \end{aligned}$$

The facets of $\text{Subw}(B_3; Q, w)$ are thus

$$\begin{aligned} & \{1, 9, 10, 11, 12\}, \quad \{1, 8, 9, 10, 12\}, \quad \{1, 7, 8, 9, 12\}, \quad \{1, 6, 7, 8, 12\}, \quad \{1, 5, 6, 7, 12\}, \\ & \{1, 4, 5, 6, 12\}, \quad \{1, 3, 4, 5, 12\}, \quad \{1, 2, 3, 4, 12\}, \quad \{1, 3, 5, 7, 12\}, \quad \{1, 3, 7, 9, 12\}, \\ & \{1, 6, 8, 10, 12\}. \end{aligned}$$

Since Q contains an S -reduced word for w as an initial segment, it follows that $\delta(Q) = w$. Thus, by Theorem 2.4.1, $\text{Subw}(B_3; Q, w)$ is homotopy equivalent to a ball.

Question 6.4 in [102] asks whether any spherical subword complex can be realized as a convex polytope, and affirmative answers for certain classes of subword complexes have been given in [19, 43, 138, 139, 141, 165, 178]. A particular class of spherical subword complexes are obtained from a Coxeter element $c \in W$. If Q is a word in S^* , then we denote by \bar{Q} the *reverse* word, i.e., the word Q read from right to left.

Definition 2.4.3 ([43, Theorem 2.2]). *Let (W, S) be a finite, irreducible Coxeter system and let $c \in W$ be a Coxeter element. The **c-cluster complex** is the subword complex*

$$\text{Clus}(W, c) \stackrel{\text{def}}{=} \text{Subw}(W; \overline{c\mathbf{w}_o(c)}, \mathbf{w}_o),$$

*for any S -reduced word c for c . The facets of $\text{Clus}(W, c)$ are the **c-clusters**.*

Remark 2.4.4. *Originally, the c -cluster complex of W was defined in [74] in the context of finite type cluster algebras. More precisely, the vertices of the c -cluster complex correspond to the **almost positive roots** of W , i.e., the elements in $\Phi_W^+ \uplus (-\Pi_W)$. Two such almost positive roots belong to a face if they satisfy a certain compatibility condition depending on c [74, Section 3.1].*

Recall from Section 2.2 that every S -reduced word for a Coxeter element $c \in W$ induces a linear order $\alpha_1 \prec_c \alpha_2 \prec_c \cdots \prec_c \alpha_n$ of the simple roots and that the c -sorting word of \mathbf{w}_o induces a linear order $\beta_1 \prec_c \beta_2 \prec_c \cdots \prec_c \beta_N$ on the positive roots. Theorem 2.2 in [43] states that the map

$$i \mapsto \begin{cases} -\alpha_i, & \text{if } 1 \leq i \leq n, \\ \beta_{i-n}, & \text{if } n < i \leq N+n \end{cases}$$

is an isomorphism from the subword realizations of the c -cluster complex to the root realization.

Proposition 2.4.5 ([119, Proposition 4.10]). *Let $c, c' \in W$ be two Coxeter elements. Then, $\text{Clus}(W, c) \cong \text{Clus}(W, c')$.*

Theorem 2.4.6 ([74, Proposition 3.8]). *Let (W, S) be a finite, irreducible Coxeter system and let $c \in W$ be a Coxeter element. Then, the number of facets of $\text{Clus}(W, c)$ is $\text{Cat}(W)$.*

Let us briefly describe a bijection from the c -aligned elements of W to the c -clusters of W following [148, Section 8]. For $w \in \text{Align}(W, c)$, let $\mathbf{w}(c) = a_1 a_2 \cdots a_k$ be the c -sorting word for w . Given $s \in S$, the *last reflection* for s in w is either the formal negative $-s$ if s does not occur in $\mathbf{w}(c)$ or $a_k a_{k-1} \cdots a_{k-i+1} \cdots a_{k-1} a_k$, where a_{k-i+1} is the left-most occurrence of s in $\mathbf{w}(c)$.

Since c linearly orders S and $\mathbf{w}_o(c)$ linearly orders T we consider the following relabeling of the last reflections. Let $S = \{s_1, s_2, \dots, s_n\}$, where the indices indicate the linear order on S induced by c , and let $T = \{t_1, t_2, \dots, t_N\}$, where the indices indicate the inversion order $\text{Inv}(\mathbf{w}_o(c))$. For $w \in \text{Align}(W, c)$ and $s \in S$, let \hat{s} be the last reflection for s in w . If $\hat{s} = -s_i$, then we identify \hat{s} with i , and if $\hat{s} = t_j$, then we identify \hat{s} with $n + j$. Let $\text{cl}_c(w)$ denote the set of last reflections of w under this identification.

Theorem 2.4.7 ([148, Theorem 8.1]). *Let (W, S) be a finite, irreducible Coxeter system and let $c \in W$ be a Coxeter element. The assignment $w \mapsto \text{cl}_c(w)$ is a bijection from $\text{Align}(W, c)$ to the set of facets of $\text{Clus}(W, c)$.*

Example 2.4.8. We illustrate Theorem 2.4.7 by continuing Example 2.3.9. Let $W = B_2$ and $c = s_1 s_0$. There are two S -reduced words for w_o , namely $w_{o1} = s_0 s_1 s_0 s_1$ and $w_{o2} = s_1 s_0 s_1 s_0$; and $w_{o1} = w_o(c)$. Then, we set $Q = s_1 s_0 s_1 s_0 s_1 s_0$, and there are six occurrences of an S -reduced word for w_o in Q :

$$s_1 s_0 s_1 s_0 s_1 s_0, \quad s_1 s_0 s_1 s_0 s_1 s_0.$$

The facets of $\text{Clus}(B_2, c)$ are thus $\{\{1, 2\}, \{1, 6\}, \{2, 3\}, \{3, 4\}, \{4, 5\}, \{5, 6\}\}$.

According to Example 2.3.9, $\text{Inv}(w_o(c))$ is $t_1 \prec_c t_2 \prec_c t_3 \prec_c t_4$, with $t_1 = s_1$, $t_2 = s_1 s_0 s_1$, $t_3 = s_0 s_1 s_0$, $t_4 = s_0$. The eight elements of B_2 are listed below, together with their last reflections and—if they are c -aligned—with their image under cl_c .

$w \in B_2$	$w \in \text{Align}(B_2, c)$	last reflections of w	$cl_c(w)$
e	yes	$-s_1, -s_0$	$\{1, 2\}$
s_0	yes	$-s_1, t_4$	$\{1, 6\}$
s_1	yes	$-s_0, t_1$	$\{2, 3\}$
$s_0 s_1$	yes	t_1, t_2	$\{3, 4\}$
$s_1 s_0$	no	t_3, t_4	—
$s_0 s_1 s_0$	no	t_2, t_3	—
$s_1 s_0 s_1$	yes	t_2, t_3	$\{4, 5\}$
$s_0 s_1 s_0 s_1$	yes	t_3, t_4	$\{5, 6\}$

Theorem 1.2.12 implies that there is a canonical way to partially order the facets of a subword complex. Indeed, for any facet $I \in \text{Subw}(W; Q, w)$ and any $i \in I$ there exists a unique facet $J \in \text{Subw}(W; Q, w)$ and a unique $j \in J$ such that $I \setminus \{i\} = J \setminus \{j\}$. In this situation we say that the facets I and J are related by a *flip*. If $i < j$, then this flip is *increasing*, and we write $I \leq_{\text{flip}} J$. This is, clearly, an acyclic binary relation on the set of facets of $\text{Subw}(W; Q, w)$, and can thus be extended to a partial order \leq_{flip} . Increasing flip orders on (spherical) subword complexes were intensively studied in [140, 141]. Figures 24a and 24b show the increasing flip orders on the facets of the subword complexes from Examples 2.4.2 and 2.4.8.

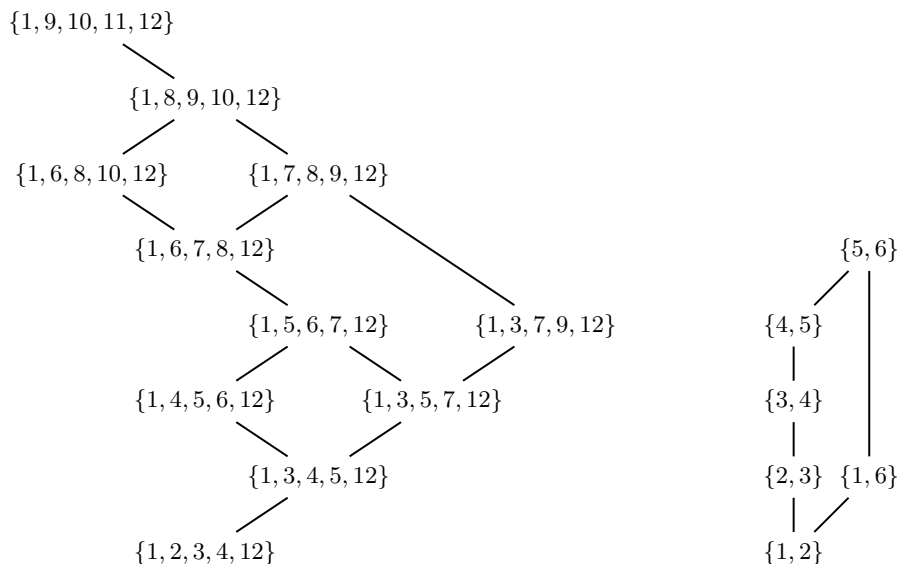
We now remark that we have previously encountered the increasing flip order on the c -cluster complex of W in the guise of the (dual of the) c -Cambrian lattice. This claim can be illustrated by comparing Figures 18 and 24b. Note that we have to consider the dual of $\text{Camb}(W, c)$, because we use left weak order.

Theorem 2.4.9 ([141, Corollary 6.3.2]). *Let (W, S) be a finite, irreducible Coxeter system and let $c \in W$ be a Coxeter element. The increasing flip order on $\text{Clus}(W, c)$ is isomorphic to the dual of $\text{Camb}(W, c)$.*

* * *

We finish this section by giving a combinatorial interpretation of the \bar{c} -clusters of A_{n-1} . A *Ferrers shape* is a sequence $\lambda = (\lambda_1, \lambda_2, \dots, \lambda_k)$ of integers satisfying $\lambda_1 \geq \lambda_2 \geq \dots \geq \lambda_k$. We graphically represent a Ferrers shape by drawing λ_k unit boxes in a row, then draw λ_{k-1} unit boxes left-aligned on top of the previous row, and so on. A *staircase shape* of order n is a Ferrers shape of the form $(n, n-1, \dots, 1)$ for some n .

According to [17, 70], a *pipe dream* for $w \in \mathfrak{S}_n$ is a filling of a staircase shape of order n with elbows (\curvearrowright) and crosses ($+$) such that the strand entering in the i^{th} row from the left exits in



(a) The increasing flip order on the subword complex from Example 2.4.2.

(b) The increasing flip order on the subword complex from Example 2.4.8.

Figure 24. Increasing flip orders of two subword complexes.

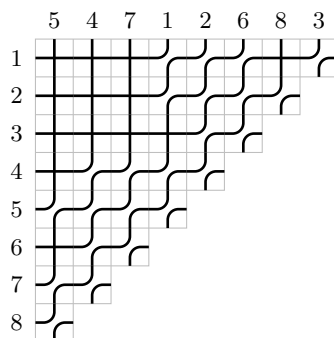


Figure 25. A reduced pipe dream for $w = 54712683 \in \mathfrak{S}_8$.

the $(w_i^{-1})^{\text{th}}$ column to the top. A pipe dream is *reduced* if no two strands cross more than once. Let $\text{Pipe}(w)$ denote the set of reduced pipe dreams for w . See Figure 25 for an illustration. By design, the last boxes in each row are filled with elbows, and each cross corresponds to a unique inversion of w . In fact, if we label the boxes appropriately, the crosses determine a reduced factorization of w into adjacent transpositions.

Remark 2.4.10. *Pipe dreams were initially defined to aid the understanding and computation of Schubert polynomials, which form an important basis of the polynomial ring $\mathbb{Z}[x_1, x_2, \dots]$ and represent special elements of the cohomology ring of a flag variety. See [25] for more background.*

	10	14	17	19	20	
5	9	13	16	18		
4	8	12	15			
3	7	11				
2	6					
1						

Figure 26. Labeling the boxes of the staircase shape for $n = 6$.

We now consider the permutation $w_{\langle n \rangle} \stackrel{\text{def}}{=} 1 \ n+1 \ n \ \dots \ 2 \in \mathfrak{S}_{n+1}$, and abbreviate $\text{Pipe}(n) \stackrel{\text{def}}{=} \text{Pipe}(w_{\langle n \rangle})$. This permutation is special in that the cardinality of $\text{Pipe}(n)$ is a Catalan number.

Proposition 2.4.11 ([193, Proposition 1]). *For $n > 0$, the number of reduced pipe dreams of $w_{\langle n \rangle}$ is $\text{Cat}(n)$.*

Let us describe a bijection from $\text{Pipe}(n)$ to the \bar{c} -clusters of A_{n-1} . Note that in any reduced pipe dream for $w_{\langle n \rangle}$, the top-left box always contains an elbow. We label the boxes of the staircase shape as illustrated in Figure 26 for $n = 6$. The $n - 1 + \binom{n}{2}$ labeled boxes are precisely those that can contain a cross in a reduced pipe dream for $w_{\langle n \rangle}$. Note further that in A_{n-1} , the word $\overline{c}w_{\circ}(\bar{c})$ has precisely $n - 1 + \binom{n}{2}$ letters, and every reduced factorization of $w_{\langle n \rangle}$ into adjacent transpositions of \mathfrak{S}_{n+1} corresponds to a unique reduced S-factorization of $w_{\circ} \in A_{n-1}$ by sending $(i \ i+1)$ to s_{i-1} . This establishes the following result, which is illustrated in Figure 27 for $n = 4$.

Theorem 2.4.12 ([65, Section 2]). *Let $n > 0$. For $P \in \text{Pipe}(n)$, the set of labels of the boxes containing the elbows of P is a facet of $\text{Clus}(A_{n-1}, \bar{c})$, and this correspondence is bijective.*

Following the spirit of this thesis, we now define a partial order on the set of pipe dreams for w . A rectangular region inside a Ferrers shape filled with crosses and elbows is *chutable* if it is filled with crosses except for the northwest, southwest and southeast corners. A *chute move*—denoted by \prec_{chute} —takes a chutable rectangle and exchanges the elbow from the southwest corner with the cross from the northeast corner [17, 161]. Figure 28 illustrates this process.

It is quickly verified that a chute move does not change the permutation w , which entails that being related by a chute move is an acyclic binary relation on the set of pipe dreams for w . Thus, this relation may be extended to a partial order; denoted by \preceq_{chute} . If $w = w_{\langle n \rangle}$, then Theorem 2.4.12 implies that chute moves correspond precisely to increasing flips in the \bar{c} -cluster complex of type A, which yields another realization of $\mathbf{Tam}(n)$ as the lattice of chute moves on $\text{Pipe}(n)$. See Figure 29 for an illustration. Structurally, it is believed that the chute move posets are always lattices.

Conjecture 2.4.13 ([161, Conjecture 2.8]). *For every $n > 0$ and $w \in \mathfrak{S}_n$, the poset $(\text{Pipe}(w), \preceq_{\text{chute}})$ is a lattice.*

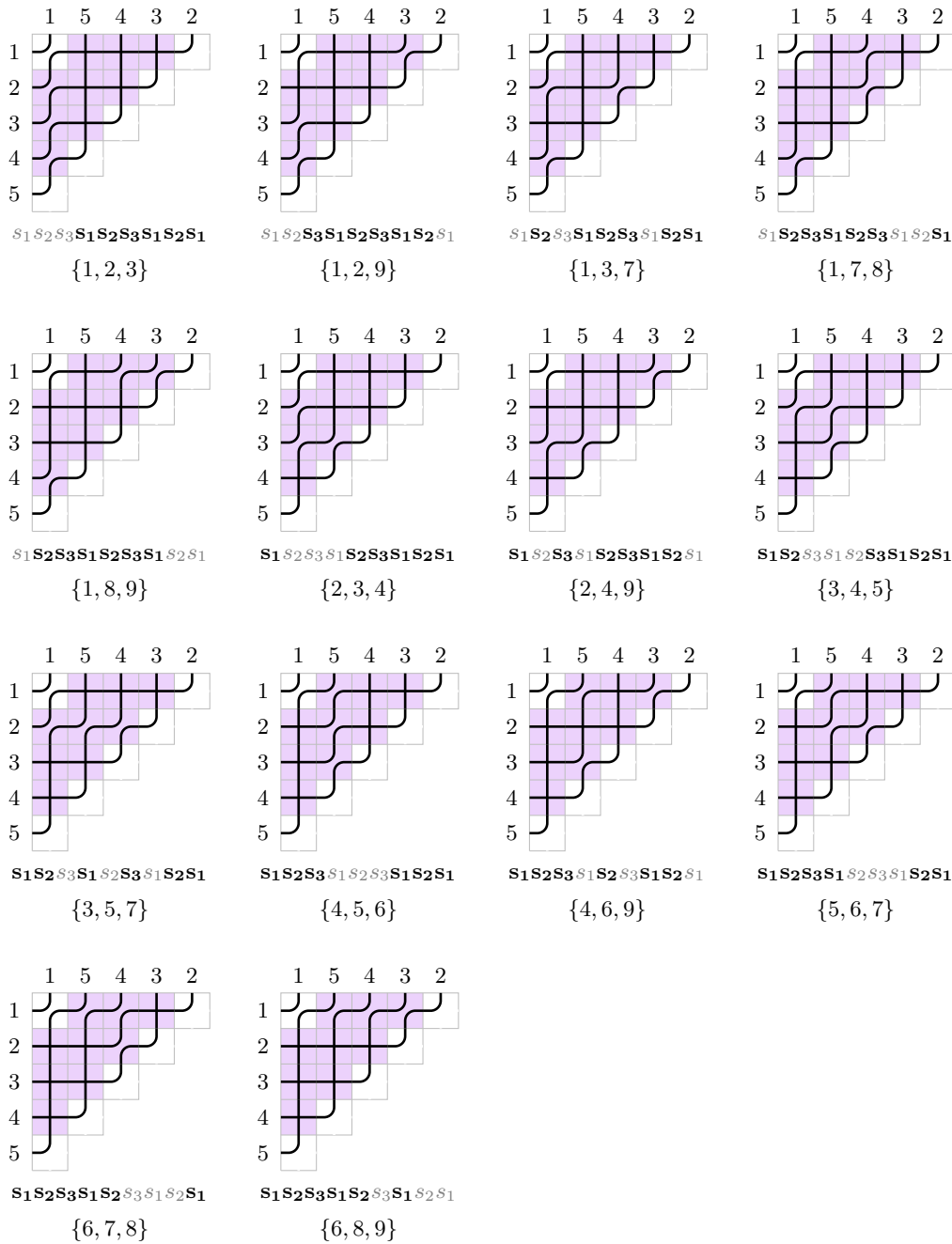


Figure 27. The fourteen reduced pipe dreams for $w_{(4)}$. Each pipe dream is additionally labeled by the S-reduced word for $w_o \in A_3$ it represents in $\vec{c}w_o(\vec{c})$ and the corresponding facet of $\text{Clus}(A_3, \vec{c})$.

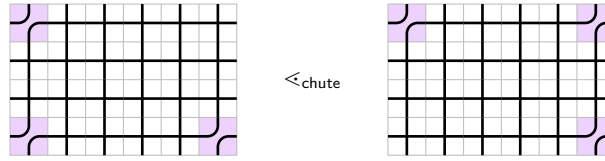


Figure 28. Illustration of a chute move.

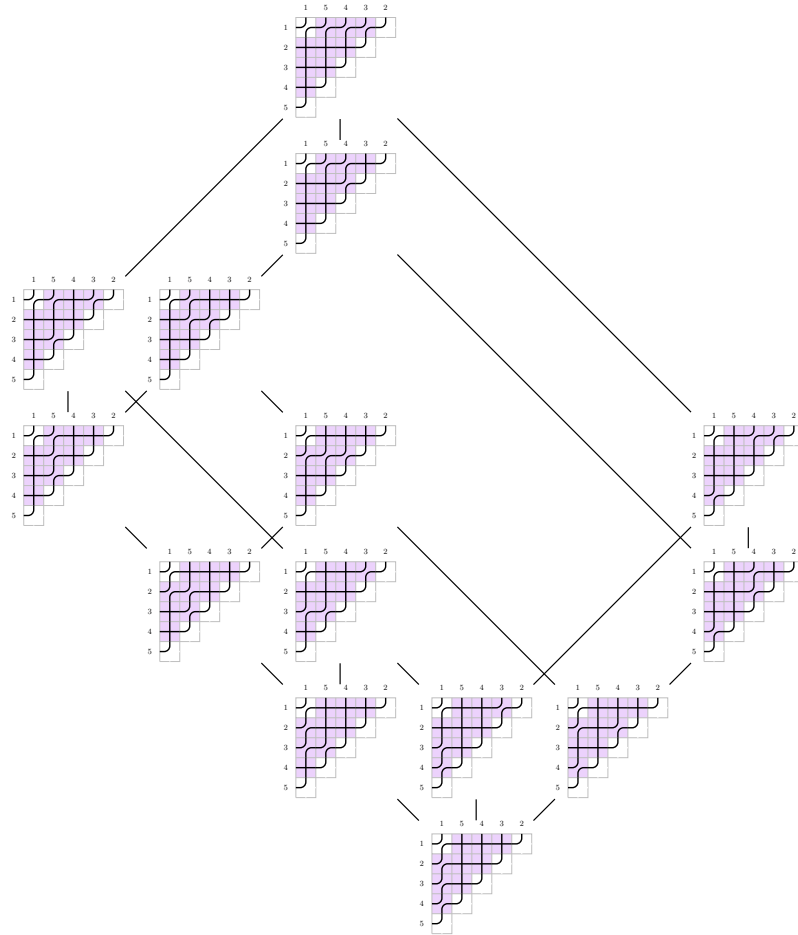


Figure 29. The chute order on $\text{Pipe}(4)$ realizing $\mathbf{Tam}(4)$.

Conjecture 2.4.13 has been verified in the following cases. For $u \in \mathfrak{S}_m$ and $v \in \mathfrak{S}_n$, their sum is the permutation $u \oplus v \in \mathfrak{S}_{m+n}$ defined by

$$(2.13) \quad (u \oplus v)_i \stackrel{\text{def}}{=} \begin{cases} u_i, & \text{if } i \leq m, \\ v_i + m, & \text{if } i > m. \end{cases}$$

Theorem 2.4.14 ([44, Theorem 41]). *Let $n > 0$. If $w \in \mathfrak{S}_n$ is $w = 1 \oplus u$, where u is 132-avoiding, then $(\text{Pipe}(w), \leq_{\text{chute}})$ is a lattice.*

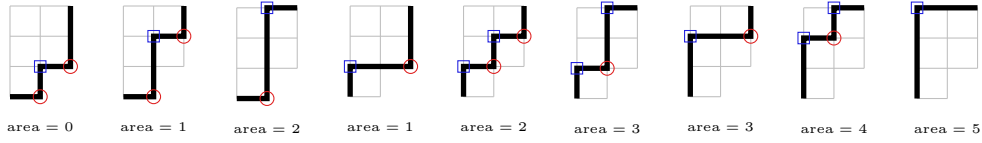


Figure 30. The nine ENENN-paths with peaks and valleys marked by blue squares and red circles, respectively.

The proof of Theorem 2.4.14 realizes the chute posets of pipe dreams via a rotation order on certain lattice paths. We will describe this construction in the next section.

2.5. Nonnesting partitions

We now deviate slightly from the algebraic constructions of the previous sections, and exhibit another W -Catalan family defined on certain sets of positive roots. In order to motivate this construction, we start purely combinatorially by considering certain lattice paths. Along the way we exhibit yet another realization of the Tamari lattice.

A *northeast path* is a lattice path in \mathbb{N}^2 which starts at the origin and uses only unit steps in north or east direction. Consequently, a northeast path can be written as a word over the alphabet $\{N, E\}$. We write $\text{Paths}(m, n)$ for the set of northeast paths with m east steps and n north steps, i.e., the set of northeast paths ending at (m, n) . For $p \in \text{Paths}(m, n)$ its *reverse* path is obtained by reading p backwards and swapping north and east steps, and is denoted by \bar{p} .

A *peak* (resp. *valley*) of $p \in \text{Paths}(m, n)$ is a coordinate on p which is preceded by a north step (resp. east step) and followed by an east step (resp. north step). We denote by $\text{peak}(p)$ (resp. $\text{valley}(p)$) the number of peaks (resp. valleys) of p .

Let $v \in \text{Paths}(m, n)$. Any $p \in \text{Paths}(m, n)$ which stays weakly above v and weakly below the path $N^n E^m$ is a *v -path*; and the set of all v -paths is denoted by $\text{Paths}(v)$. The *area* of p is the number of coordinates $(i - \frac{1}{2}, j - \frac{1}{2})$, for $i \in [m]$ and $j \in [n]$, above v and below p ; denoted by $\text{area}(p)$. In other words, a v -path stays inside the Ferrers shape traced out by v , and the area statistic counts the boxes below the path. Figure 30 illustrates these definitions for $v = \text{ENENN}$.

A *Dyck path* of semilength n is an element of $\text{Dyck}(n) \stackrel{\text{def}}{=} \text{Paths}((NE)^n)$. J. SEGNER proved that the Catalan numbers satisfy the following recurrence relation [164]:

$$(2.14) \quad \text{Cat}(n) = \sum_{i=0}^{n-1} \text{Cat}(i)\text{Cat}(n-1-i),$$

and it is easy to decompose the set of Dyck paths of semilength n in an analogous manner, thus proving the next statement.

Proposition 2.5.1. *For $n > 0$, the number of Dyck paths of semilength n is $\text{Cat}(n)$.*

By construction, the peaks of $p \in \text{Dyck}(n)$ can be identified with pairs (i, j) for some $0 \leq i < j \leq n$. By converting a peak (i, j) with $i + 1 < j$ to a bump $(i + 1, j)$, one can naturally associate a set partition of $[n]$ with p . It is easy to show that the set partitions so obtained are *nonnesting*, i.e., if (a_1, b_1) and (a_2, b_2) are bumps and $a_1 < a_2$, then $b_1 < b_2$. In fact, this map is a bijection from $\text{Dyck}(n)$ to the set $\text{Nonn}(n)$ of all nonnesting set partitions of $[n]$.

Even though nonnesting partitions are eponymous for this section, we now turn to a different object that is much better suited to generalize to finite Coxeter groups. Note that the coordinates $(i - \frac{1}{2}, j - \frac{1}{2})$ which are inside the $n \times n$ -rectangular region in \mathbb{N}^2 , whose bottom

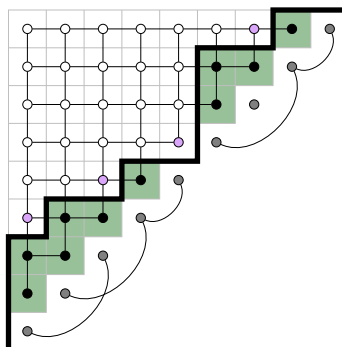


Figure 31. Converting a Dyck path into a nonnesting partition, an order ideal and an antichain in the triangular poset for $n = 9$.

left corner is the origin, and above the path $(NE)^n$ are those of the form $1 \leq i < j \leq n$. By connecting these coordinates with horizontal and vertical line segments of unit length, we recover the poset diagram—rotated by 45 degrees counterclockwise—of the *triangular poset*, defined by

$$(2.15) \quad \Delta_n \stackrel{\text{def}}{=} \left(\{(i, j) \mid 1 \leq i < j \leq n\}, \preceq \right),$$

where $(a_1, b_1) \preceq (a_2, b_2)$ if and only if $a_1 \geq a_2$ and $b_1 \leq b_2$.

Now, every Dyck path of semilength n traces out an order ideal of Δ_n , and this is clearly a bijection. Moreover, the minimal elements of the complement of an order ideal form an *antichain*, i.e., a set of pairwise incomparable elements, and this is again a bijective correspondence. Figure 31 illustrates the three bijections we have just described.

* * *

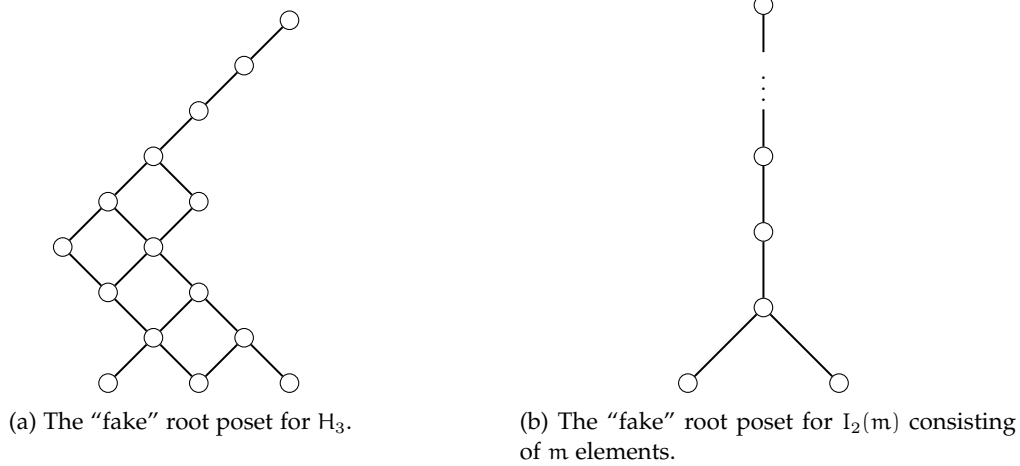
By inspection of Figure 13, we observe that the triangular poset Δ_n is isomorphic to the root poset of A_{n-1} via the map

$$(i, j) \mapsto \alpha_i + \alpha_{i+1} + \cdots + \alpha_{j-1}.$$

This implies that the number of order ideals (and thus the number of antichains) of the root poset of type A is exactly the type-A Catalan number. A. POSTNIKOV observed that this extends to all crystallographic groups.

Theorem 2.5.2 ([157, Remark 2]). *Let (W, S) be a finite, irreducible crystallographic Coxeter system. The number of antichains of the root poset (Φ_W^+, \preceq) is $\text{Cat}(W)$.*

Remark 2.5.3. *In general, the positive roots of noncrystallographic Coxeter systems need not be expressible as integral linear combinations of the simple roots. Therefore, our definition of the root poset does not immediately extend to noncrystallographic Coxeter systems. However, D. ARMSTRONG suggested two surrogate posets for H_3 and $I_2(m)$ with $m \notin \{2, 3, 4, 6\}$ [4, Open Problem 5.4.4]. We have drawn them in Figure 32. The number of order ideals in these “fake” root posets is the correct Catalan number, and they have some other properties desirable for root posets. We therefore mean these posets when we consider “root posets” for H_3 or $I_2(m)$.*

Figure 32. The surrogate root posets for H_3 and $I_2(m)$.

For H_4 , an exhaustive computer search showed that no such surrogate exists [54]. However, [54, Figure 5] shows four posets with 60 elements that satisfy a remarkable amount of properties common to root posets. We have reproduced these posets in Figure 33.

Definition 2.5.4. Let (W, S) be a finite, irreducible Coxeter system other than H_4 . The **nonnesting W -partitions** are the antichains of (Φ_W^+, \preceq) .

We write $\text{Nonn}(W)$ for the set of nonnesting W -partitions. A uniform bijection between nonnesting and noncrossing W -partitions was given in [7]. Other bijections using combinatorial or geometric interpretations were given for instance in [8, 51, 67, 117, 179].

2.5.1. v -Tamari lattices. Let us return for a moment to the set of v -paths for some $v \in \text{Paths}(m, n)$. Let $p \in \text{Paths}(v)$ and let (i, j) be any lattice point on p . The *distance* of (i, j) from v is

$$\text{dist}_v(p, (i, j)) \stackrel{\text{def}}{=} \max\{a - i \mid (a, j) \text{ is a lattice point on } p\}.$$

If (i, j) is a valley of p , then we define the *rotation* of p by (i, j) to be the v -path q constructed from p by swapping the east step preceding (i, j) with the segment of p between (i, j) and the next lattice point (i', j') (after (i, j)) on p with $\text{dist}_v(p, (i, j)) = \text{dist}_v(p, (i', j'))$. In that situation, we write $p \leq_v q$. Since the area of q is strictly bigger than the area of p , it follows that \leq_v is an acyclic binary relation and its reflexive and transitive closure therefore is a partial order; denoted by \leq_v .

The poset $\mathbf{Tam}(v) \stackrel{\text{def}}{=} (\text{Paths}(v), \leq_v)$ is the *v -Tamari lattice*. If $v = (\text{NE})^n$, then $\mathbf{Tam}(v)$ recovers the ordinary Tamari lattice $\mathbf{Tam}(n)$ ⁹. Figure 34 illustrates the rotation of a v -path, and Figure 35 shows $\mathbf{Tam}(\text{ENENN})$.

Theorem 2.5.5 ([144, Theorems 1–3]). Let $m, n > 0$ be integers and let $v \in \text{Paths}(m, n)$.

(i) $\mathbf{Tam}(v)$ is a lattice.

⁹Note that the ordinary Tamari lattice is indexed by an integer, while the v -Tamari lattice is indexed by a northeast path.

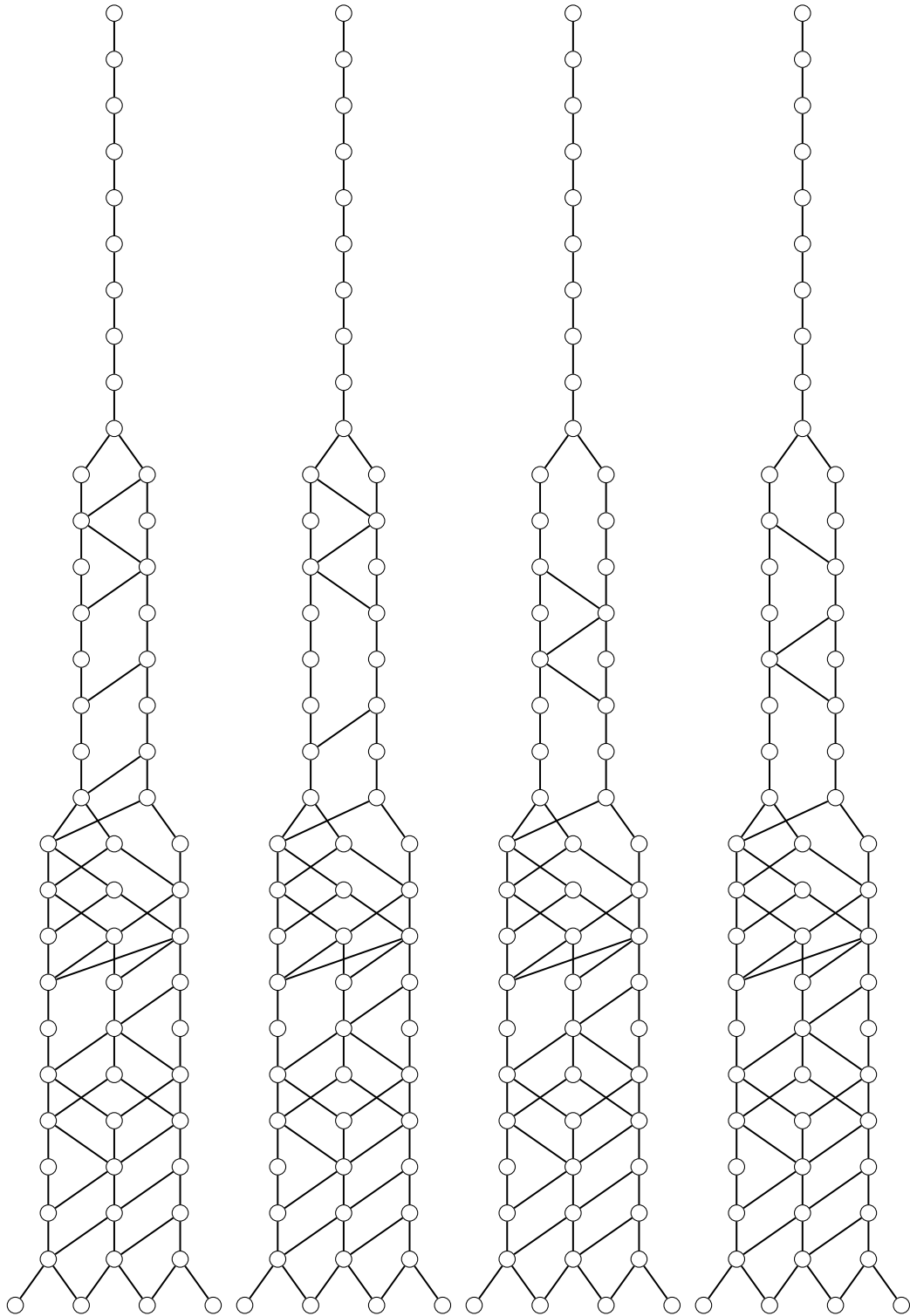


Figure 33. The four potential "fake" root posets for H_4 exhibited in [54, Figure 5].

for a finite, irreducible Coxeter system (W, S) and a Coxeter element $c \in W$ we define three bivariate polynomials.

The *M-triangle* is the generating function of the Möbius function in $\mathbf{Nonc}(W, c)$ according to rank:

$$(2.16) \quad \mathcal{M}_W(x, y) \stackrel{\text{def}}{=} \sum_{p, q \in \mathbf{Nonc}(W, c)} \mu_{\mathbf{Nonc}(W, c)}(p, q) x^{\text{rk}(p)} y^{\text{rk}(q)}.$$

By definition, the Möbius function of a poset is a structural invariant. Since the noncrossing partition lattices for different Coxeter elements are isomorphic by Corollary 2.3.10, the M-triangle does not depend on the choice of c . Moreover, the M-triangle is well defined, since $\mathbf{Nonc}(W, c)$ is graded by Lemma 2.3.6.

Let A be a face of the cluster complex $\text{Clus}(W, c)$. If n denotes the rank of W and N denotes the number of reflections of W , then by Definition 2.4.3 A is a subset of $[n + N]$. We consider the two maps

$$\begin{aligned} \text{pos}: \wp([N + n]) &\rightarrow \mathbb{N}, & A &\mapsto |A \cap \{n+1, n+2, \dots, N + n\}|, \\ \text{neg}: \wp([N + n]) &\rightarrow \mathbb{N}, & A &\mapsto |A \cap [n]|. \end{aligned}$$

The *F-triangle* is the generating function of the faces of $\text{Clus}(W, c)$ with respect to these maps:

$$(2.17) \quad \mathcal{F}_W(x, y) \stackrel{\text{def}}{=} \sum_{A \in \text{Clus}(W, c)} x^{\text{pos}(A)} y^{\text{neg}(A)}.$$

Again, by Proposition 2.4.5, the F-triangle does not depend on the choice of Coxeter element.

Finally, assume that $W \neq H_4$. For $A \in \text{Nonn}(W)$, we denote by $\min(A)$ the number of minimal elements of (Φ_W^+, \preceq) contained in A . The *H-triangle* is the refined generating function of nonnesting partitions with respect to size:

$$(2.18) \quad \mathcal{H}_W(x, y) \stackrel{\text{def}}{=} \sum_{A \in \text{Nonn}(W)} x^{|A|} y^{\min(A)}.$$

Example 2.6.1. Let us illustrate these definitions for $W = A_3$. Figure 22 shows $\mathbf{Nonc}(A_3, c)$, and we find that the corresponding M-triangle is

$$\mathcal{M}_{A_3}(x, y) = x^3 y^3 - 6x^2 y^3 + 10xy^3 + 6x^2 y^2 - 5y^3 - 16xy^2 + 10y^2 + 6xy - 6y + 1.$$

The nonnesting partitions of A_3 can be recovered from Figure 13 by restricting to the order ideal generated by $\alpha_1 + \alpha_2 + \alpha_3$, and we find that the corresponding H-triangle is

$$\mathcal{H}_{A_3}(x, y) = x^3 y^3 + 3x^2 y^2 + 2x^2 y + x^2 + 3xy + 3x + 1.$$

The fourteen \bar{c} -clusters of A_3 are displayed in Figure 27, so that we find the F-triangle to be

$$\mathcal{F}_{A_3}(x, y) = 5x^3 + 5x^2 y + 3xy^2 + y^3 + 10x^2 + 8xy + 3y^2 + 6x + 3y + 1.$$

Referring to these polynomials as “triangles” comes from the fact that if we arrange their coefficients in a square matrix, where the entry in position (i, j) corresponds to the coefficient of $x^{i-1} y^{j-1}$, then the non-zero entries are arranged in a triangular shape. The three polynomials from Example 2.6.1 can be represented as follows:

$$\mathcal{M}_{A_3}(x, y) = \begin{pmatrix} 1 \\ x \\ x^2 \\ x^3 \end{pmatrix}^T \begin{pmatrix} 1 & -6 & 10 & -5 \\ 0 & 6 & -16 & 10 \\ 0 & 0 & 6 & -6 \\ 0 & 0 & 0 & 1 \end{pmatrix} \begin{pmatrix} 1 \\ y \\ y^2 \\ y^3 \end{pmatrix},$$

$$\mathcal{H}_{A_3}(x, y) = \begin{pmatrix} 1 \\ x \\ x^2 \\ x^3 \end{pmatrix}^T \begin{pmatrix} 1 & 0 & 0 & 0 \\ 3 & 3 & 0 & 0 \\ 1 & 2 & 3 & 0 \\ 0 & 0 & 0 & 1 \end{pmatrix} \begin{pmatrix} 1 \\ y \\ y^2 \\ y^3 \end{pmatrix},$$

$$\mathcal{F}_{A_3}(x, y) = \begin{pmatrix} 1 \\ x \\ x^2 \\ x^3 \end{pmatrix}^T \begin{pmatrix} 1 & 3 & 3 & 1 \\ 6 & 8 & 3 & 0 \\ 10 & 3 & 0 & 0 \\ 5 & 0 & 0 & 0 \end{pmatrix} \begin{pmatrix} 1 \\ y \\ y^2 \\ y^3 \end{pmatrix}.$$

Most suprisingly, the M-, H- and F-triangles can be obtained from one another by an invertible substitution of variables. This correspondence can be verified for A_3 directly using the polynomials from Example 2.6.1.

Theorem 2.6.2 ([9, 105, 106, 109, 183, 191]). *Let (W, S) be a finite, irreducible Coxeter system. If $r = |S|$, then*

$$\begin{aligned} \mathcal{F}_W(x, y) &= y^r \mathcal{M}_W \left(\frac{y+1}{y-x}, \frac{y-x}{y} \right) \\ &= x^r \mathcal{H}_W(x, y) \left(\frac{x+1}{x}, \frac{y+1}{x+1} \right), \\ \mathcal{H}_W(x, y) &= (x(y-1)+1)^r \mathcal{M}_W \left(\frac{y}{y-1}, \frac{x(y-1)}{x(y-1)+1} \right) \\ &= (x-1)^r \mathcal{F}_W \left(\frac{1}{x-1}, \frac{x(y-1)+1}{x-1} \right), \\ \mathcal{M}_W(x, y) &= (xy-1)^r \mathcal{F}_W \left(\frac{1-y}{xy-1}, \frac{1}{xy-1} \right) \\ &= (1-y)^r \mathcal{H}_W \left(\frac{y(x-1)}{1-y}, \frac{x}{x-1} \right). \end{aligned}$$

Remark 2.6.3. *In fact, Theorem 2.6.2 is proven (in the given references) for the crystallographic Coxeter groups. Using the surrogate root posets in the noncrystallographic types, see Figures 32 and 33, we can show that this correspondence extends to these types, too.*

More precisely, if $W = I_2(m)$, it is easily verified that

$$\begin{aligned} \mathcal{F}_{I_2(m)}(x, y) &= (m-1)x^2 + 2xy + y^2 + mx + 2y + 1, \\ \mathcal{H}_{I_2(m)}(x, y) &= x^2y^2 + 2xy + (m-2)x + 1, \\ \mathcal{M}_{I_2(m)}(x, y) &= x^2y^2 - mxy^2 + mxy + (m-1)y^2 - my + 1. \end{aligned}$$

If $W = H_3$, then we obtain

$$\begin{aligned} \mathcal{F}_{H_3}(x, y) &= 21x^3 + 7x^2y + 3xy^2 + y^3 + 35x^2 + 10xy + 3y^2 + 15x + 3y + 1, \\ \mathcal{H}_{H_3}(x, y) &= x^3y^3 + 3x^2y^2 + 4x^2y + 8x^2 + 3xy + 12x + 1, \\ \mathcal{M}_{H_3}(x, y) &= x^3y^3 - 15x^2y^3 + 15x^2y^2 + 35xy^3 - 50xy^2 - 21y^3 + 15xy + 35y^2 \\ &\quad - 15y + 1. \end{aligned}$$

If $W = H_4$, then we obtain

$$\begin{aligned} \mathcal{F}_{H_4}(x, y) &= 232x^4 + 32x^3y + 11x^2y^2 + 4xy^3 + y^4 + 480x^3 + 59x^2y + 17xy^2 + 4y^3 \\ &\quad + 307x^2 + 31xy + 6y^2 + 60x + 4y + 1, \end{aligned}$$

$$\mathcal{H}_{\mathbb{H}_4}(x, y) = x^4y^4 + 4x^3y^3 + 5x^3y^2 + 9x^3y + 6x^2y^2 + 42x^3 + 19x^2y + 133x^2 + 4xy + 56x + 1,$$

$$\mathcal{M}_{\mathbb{H}_4}(x, y) = x^4y^4 - 60x^3y^4 + 60x^3y^3 + 307x^2y^4 - 465x^2y^3 - 480xy^4 + 158x^2y^2 + 885xy^3 + 232y^4 - 465xy^2 - 480y^3 + 60xy + 307y^2 - 60y + 1.$$

Note that all four posets from Figure 33 yield the same H-triangle.

We can verify that these triples of polynomials satisfy the relations stated in Theorem 2.6.2.

CHAPTER 3

Parabolic Cataland: Origins

The previous chapter exhibits various enumerative and structural interactions between the families $\text{Align}(W, c)$, $\text{Nonc}(W, c)$, $\text{Clus}(W, c)$ and $\text{Nonn}(W)$. A most remarkable property is that these four families are equinumerous (independently of the choice of Coxeter element), and their cardinality is given by $\text{Cat}(W)$; see Theorems 2.2.8, 2.3.7, 2.4.6 and 2.5.2.

In his thesis [192], N. WILLIAMS set out to test the robustness of this connection by attempting to extend it to parabolic quotients of W . To that end, he defined analogues of $\text{Align}(W, c)$, $\text{Nonc}(W, c)$, $\text{Clus}(W, c)$ and $\text{Nonn}(W)$ for these quotients and compared their enumeration with respect to different Coxeter elements. Computer experiments suggest that such a well-defined *parabolic Catalan number* exists when W is of type A_n , B_n , H_3 or $I_2(m)$.

Remark 3.0.1. *The finite, irreducible Coxeter groups of type A_n , B_n , H_3 or $I_2(m)$ are nowadays called the **coincidental** types, because they share several remarkable properties that distinguish them from the other finite, irreducible Coxeter groups. Instances of these properties can be found in [14, 43, 62, 89, 92, 95, 96, 126, 150, 158, 174, 192].*

We first define parabolic quotients of Coxeter groups, and then recall WILLIAMS' constructions of parabolic analogues of $\text{Align}(W, c)$, $\text{Nonc}(W, c)$, $\text{Clus}(W, c)$ and $\text{Nonn}(W)$. We then present some numerology and pose structural conjectures about these sets and their interactions. We then properly investigate Parabolic Cataland in linear type A , and suggest combinatorial models in other types.

3.1. Parabolic quotients of Coxeter groups

Let (W, S) be a Coxeter system. Any $J \subseteq S$ naturally generates a subgroup W_J of W . This is again a Coxeter group whose Coxeter diagram is the subgraph of $\Gamma_{(W, S)}$ induced by the vertices in J . Subgroups of W of this form are *parabolic subgroups*.

The *parabolic quotient* of W by J is the set W^J of minimal length representatives (with respect to ℓ_S) of the left cosets of W_J in W , i.e.,

$$(3.1) \quad W^J \stackrel{\text{def}}{=} \{w \in W \mid \ell_S(ws) > \ell_S(w) \text{ for all } s \in J\}.$$

In other words, W^J consists of all elements of W for which no S -reduced word ends in some $s \in J$.

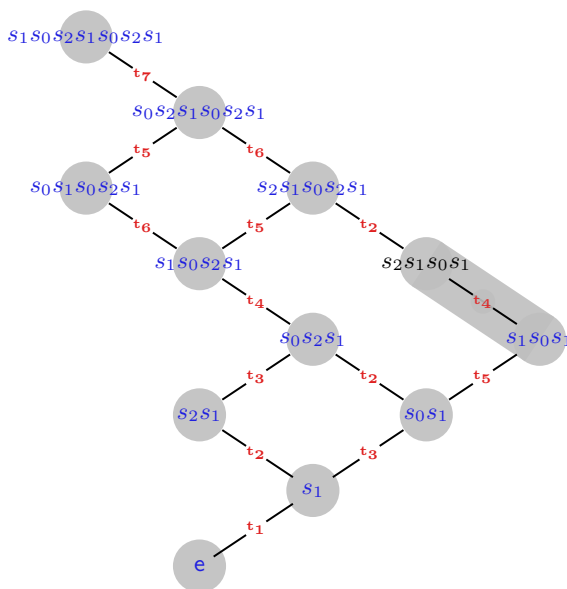


Figure 36. The lattice $\mathbf{Weak}(B_3^{\{s_0, s_2\}})$. The $(B_3^{\{s_0, s_2\}}, c)$ -aligned elements, for $c = s_0s_1s_2$, are marked in blue.

Example 3.1.1. Let $W = B_3$ and $J = \{s_0, s_2\}$. The corresponding parabolic subgroup is $(B_3)_J = \{e, s_0, s_2, s_0s_2\}$, and the left cosets of $(B_3)_J$ in B_3 are (where each element is represented by its $s_0s_1s_2$ -sorting word; see Figure 20):

$$\begin{aligned} & \{e, s_0, s_2, s_2s_0\}, \\ & \{s_1, s_1s_0, s_1s_2, s_1s_2s_0\}, \\ & \{s_0s_1, s_0s_1s_0, s_0s_1s_2, s_0s_1s_2s_0\}, \\ & \{s_2s_1, s_2s_1s_0, s_1s_2s_1, s_1s_2s_1s_0\}, \\ & \{s_0s_2s_1, s_0s_2s_1s_0, s_0s_1s_2s_1, s_0s_1s_2s_1s_0\}, \\ & \{s_1s_0s_1, s_1s_0s_1s_0, s_1s_0s_1s_2, s_1s_0s_1s_2s_0\}, \\ & \{s_1s_0s_2s_1, s_1s_0s_2s_1s_0, s_1s_0s_1s_2s_1, s_1s_0s_1s_2s_1s_0\}, \\ & \{s_2s_1s_0s_1, s_2s_1s_0s_1s_0, s_2s_1s_0s_1s_2, s_2s_1s_0s_1s_2s_0\}, \\ & \{s_0s_1s_0s_2s_1, s_0s_1s_0s_2s_1s_0, s_1s_0s_1s_0s_2s_1, s_1s_0s_1s_0s_2s_1s_0\}, \\ & \{s_2s_1s_0s_2s_1, s_2s_1s_0s_2s_1s_0, s_2s_1s_0s_1s_2s_1, s_2s_1s_0s_1s_2s_1s_0\}, \\ & \{s_0s_2s_1s_0s_2s_1, s_0s_2s_1s_0s_2s_1s_0, s_2s_1s_0s_1s_0s_2s_1, s_2s_1s_0s_1s_0s_2s_1s_0\}, \\ & \{s_1s_0s_2s_1s_0s_2s_1, s_1s_0s_2s_1s_0s_2s_1s_0, s_2s_1s_0s_2s_1s_0s_2s_1, s_2s_1s_0s_2s_1s_0s_2s_1s_0\}. \end{aligned}$$

Thus, the parabolic quotient of B_3 by $(B_3)_J$ is

$$B_3^J = \{e, s_1, s_0s_1, s_2s_1, s_0s_2s_1, s_1s_0s_1, s_1s_0s_2s_1, s_2s_1s_0s_1, s_0s_1s_0s_2s_1, s_2s_1s_0s_2s_1, s_0s_2s_1s_0s_2s_1, s_1s_0s_2s_1s_0s_2s_1\},$$

and Figure 36 shows $\mathbf{Weak}(B_3^J)$.

If we compare Example 3.1.1 with Figure 20, then we see that the weak order on $B_3^{\{s_0, s_2\}}$ is an interval in $\mathbf{Weak}(B_3)$. This is not a coincidence. In fact, since we defined parabolic

quotients to consist of minimal length representatives with respect to *left* cosets, parabolic quotients behave nicely with respect to the *left* weak order.

Theorem 3.1.2 ([30, Theorem 4.1]). *For every finite Coxeter system (W, S) and every $J \subseteq S$, the poset $\mathbf{Weak}(W^J)$ is a principal order ideal in $\mathbf{Weak}(W)$.*

We record two important corollaries of this theorem.

Corollary 3.1.3. *For every finite, irreducible Coxeter system (W, S) and every $J \subseteq S$, the poset $\mathbf{Weak}(W^J)$ is a congruence-uniform lattice.*

PROOF. This follows from Proposition 1.1.31 and Theorems 1.2.9 and 3.1.2. \square

In particular, canonical join representations can be computed in $\mathbf{Weak}(W^J)$ in the same way as in $\mathbf{Weak}(W)$; see Theorem 2.2.17.

Corollary 3.1.4. *If (W, S) is a finite Coxeter system and $J \subseteq S$, then W^J has a longest element; denoted by w_0^J .*

We define the restriction of the positive roots to W^J by

$$(3.2) \quad \Phi_{W^J}^+ \stackrel{\text{def}}{=} \{\alpha \in \Phi_W^+ \mid t_\alpha \in \text{Inv}(w_0^J)\},$$

i.e., $\Phi_{W^J}^+$ contains all positive roots corresponding to inversions of w_0^J . Note that $W_\emptyset = \{e\}$, and thus $W^\emptyset = W$ and $\Phi_{W^\emptyset}^+ = \Phi_W^+$.

3.2. Parabolic aligned elements

From now on, let (W, S) be a finite, irreducible Coxeter system, and fix an S -reduced word c for a Coxeter element $c \in W$. Let \prec_c denote the inversion order $\mathbf{Inv}(w_0(c))$ defined in Section 2.2. In Definition 2.2.6, we have defined the c -aligned elements of W via a certain forcing order on the reflections of W . We slightly adapt this definition when we move to parabolic quotients of W . We use \prec_c^J as a short-hand for $\mathbf{Inv}(w_0^J(c))$.

Definition 3.2.1 ([192, Definition 5.1.6]). *Let (W, S) be a finite, irreducible Coxeter system, let $c \in W$ be a Coxeter element for which we have fixed an S -reduced word c and let $J \subseteq S$. An element $w \in W^J$ is (W^J, c) -aligned if for all $\alpha, \beta \in \Phi_{W^J}^+$ with $\alpha \prec_c^J \beta$ and $a, b \in \mathbb{R}_{\geq 0}$ such that $a\alpha + b\beta \in \Phi_{W^J}^+$:*

$$(3.3) \quad t_{a\alpha + b\beta} \in \text{Cov}(w) \quad \text{implies} \quad t_a \in \text{Inv}(w).$$

Let $\text{Align}(W^J, c)$ denote the set of all (W^J, c) -aligned elements.

Remark 3.2.2. *In the case $J = \emptyset$, the only difference in the definition of c -aligned elements vs. (W^\emptyset, c) -aligned elements is that $t_{a\alpha + b\beta}$ can be an arbitrary inversion in Definition 2.2.6 while it must be a cover inversion in Definition 3.2.1. So, clearly, it holds that $\text{Align}(W, c) \subseteq \text{Align}(W^\emptyset, c)$. However, since $W^\emptyset = W$ it is desirable that both definitions are equivalent for $J = \emptyset$. This is trivially true if $W = I_2(m)$, and was shown to hold in [147, Lemma 5.5] if*

$W = A_n$. If $W = B_n$ or $W = D_n$, then this equality follows from [148, Lemmas 4.9 and 4.11], and it was explicitly checked by computer for $W \in \{H_3, F_4, H_4\}$. It has not yet been verified for $W \in \{E_6, E_7, E_8\}$, but is believed to be true. See also [192, Remark 5.1.8].

Example 3.2.3. Let us continue Example 2.3.9, and consider $W = B_2$ and $\mathbf{c} = s_1 s_0$. Recall that $t_1 = s_1$, $t_2 = s_1 s_0 s_1$, $t_3 = s_0 s_1 s_0$ and $t_4 = s_0$. We have explained in Example 2.3.9, that $w \in B_2$ is \mathbf{c} -aligned if whenever it has t_2 or t_3 as inversions it must have t_1 as an inversion, too. By Definition 3.2.1, $w \in B_2$ is (B_2^0, \mathbf{c}) -aligned if whenever it has t_2 or t_3 as cover inversions it must have t_1 as an inversion, too. The following table shows that $w \in B_2$ is \mathbf{c} -aligned if and only if it is (B_2^0, \mathbf{c}) -aligned.

$w \in B_2$	$\text{Inv}(w)$	$\text{Cov}(w)$	$w \in \text{Align}(B_2, \mathbf{c})$	$w \in \text{Align}(B_2^0, \mathbf{c})$
e	\emptyset	\emptyset	yes	yes
s_0	$\{t_4\}$	$\{t_4\}$	yes	yes
s_1	$\{t_1\}$	$\{t_1\}$	yes	yes
$s_0 s_1$	$\{t_1, t_2\}$	$\{t_2\}$	yes	yes
$s_1 s_0$	$\{t_4, t_3\}$	$\{t_3\}$	no	no
$s_0 s_1 s_0$	$\{t_4, t_3, t_2\}$	$\{t_2\}$	no	no
$s_1 s_0 s_1$	$\{t_1, t_2, t_3\}$	$\{t_3\}$	yes	yes
$s_0 s_1 s_0 s_1$	$\{t_1, t_2, t_3, t_4\}$	$\{t_1, t_4\}$	yes	yes

Example 3.2.4. Let $W = B_3$, and $\mathbf{c} = s_0 s_1 s_2$. If $J = \{s_0, s_2\}$, then $\mathbf{w}_o^J(\mathbf{c}) = s_1 s_0 s_2 s_1 s_0 s_2 s_1$, and the inversion set of \mathbf{w}_o^J is

$$\text{Inv}(\mathbf{w}_o^J) = \left\{ \underbrace{s_1}_{t_1}, \underbrace{s_1 s_2 s_1}_{t_2}, \underbrace{s_1 s_0 s_1}_{t_3}, \underbrace{s_1 s_0 s_2 s_1 s_0 s_2 s_1}_{t_4}, \underbrace{s_0 s_1 s_0}_{t_5}, \underbrace{s_2 s_1 s_0 s_1 s_2}_{t_6}, \underbrace{s_0 s_1 s_2 s_1 s_0}_{t_7} \right\},$$

ordered with respect to $\text{Inv}(\mathbf{w}_o^J(\mathbf{c}))$. (Note that this order is not contained in $\text{Inv}(\mathbf{w}_o(\mathbf{c}))$.) We may compute directly that

$$\begin{aligned} \alpha_{t_1} &= \alpha_1, & \alpha_{t_2} &= \alpha_1 + \alpha_2, & \alpha_{t_3} &= \alpha_0 + \alpha_1, & \alpha_{t_4} &= 2\alpha_0 + 2\alpha_1 + \alpha_2, \\ \alpha_{t_5} &= 2\alpha_0 + \alpha_1, & \alpha_{t_6} &= \alpha_0 + \alpha_1 + \alpha_2, & \alpha_{t_7} &= 2\alpha_0 + \alpha_1 + \alpha_2; \end{aligned}$$

compare Figure 14a regarding the notation. The only root in $\Phi_{B_3^J}^+$ that can be expressed as a sum of other roots in $\Phi_{B_3^J}^+$ is α_{t_4} , and we have

$$\alpha_{t_4} = \alpha_{t_1} + \alpha_{t_7} = \alpha_{t_2} + \alpha_{t_5} = \alpha_{t_3} + \alpha_{t_6}.$$

Thus, $w \in B_3^J$ is (B_3^J, \mathbf{c}) -aligned if whenever $t_4 \in \text{Cov}(w)$, then $\{t_1, t_2, t_3\} \subseteq \text{Inv}(w)$.

The twelve elements of B_3^J were computed in Example 3.1.1 and Figure 36 shows $\text{Weak}(B_3^J)$ labeled by the appropriate cover inversions. We obtain the following table.

$w \in B_3^J$	$\text{Inv}(w)$	$\text{Cov}(w)$	$w \in \text{Align}(B_3^J, \mathbf{c})$	$w \in \text{Align}(B_3, \mathbf{c})$
e	\emptyset	\emptyset	yes	yes
s_1	$\{t_1\}$	$\{t_1\}$	yes	yes
$s_0 s_1$	$\{t_1, t_3\}$	$\{t_3\}$	yes	no
$s_2 s_1$	$\{t_1, t_2\}$	$\{t_2\}$	yes	yes
$s_0 s_2 s_1$	$\{t_1, t_2, t_3\}$	$\{t_2, t_3\}$	yes	no

$s_1 s_0 s_1$	$\{t_1, t_3, t_5\}$	$\{t_5\}$	yes	no
$s_1 s_0 s_2 s_1$	$\{t_1, t_2, t_3, t_4\}$	$\{t_4\}$	yes	no
$s_2 s_1 s_0 s_1$	$\{t_1, t_3, t_4, t_5\}$	$\{t_4\}$	no	no
$s_0 s_1 s_0 s_2 s_1$	$\{t_1, t_2, t_3, t_4, t_6\}$	$\{t_6\}$	yes	no
$s_2 s_1 s_0 s_2 s_1$	$\{t_1, t_2, t_3, t_4, t_5\}$	$\{t_2, t_5\}$	yes	no
$s_0 s_2 s_1 s_0 s_2 s_1$	$\{t_1, t_2, t_3, t_4, t_5, t_6\}$	$\{t_5, t_6\}$	yes	no
$s_1 s_0 s_2 s_1 s_0 s_2 s_1$	$\{t_1, t_2, t_3, t_4, t_5, t_6, t_7\}$	$\{t_7\}$	yes	no

Since $\text{Align}(W^J, c) \subseteq W^J$ it is worthwhile considering this set under weak order.

Definition 3.2.5. Let (W, S) be a finite, irreducible Coxeter system, let $c \in W$ be a Coxeter element and let $J \subseteq S$. The (W^J, c) -Cambrian poset is

$$(3.4) \quad \mathbf{Camb}(W^J, c) \stackrel{\text{def}}{=} \mathbf{Weak}(\text{Align}(W^J, c)).$$

For $J = \emptyset$, we recover the c -Cambrian lattice from Definition 2.2.12. Since $\mathbf{Weak}(W^J)$ is an interval of $\mathbf{Weak}(W)$ with least element e and greatest element w_o^J , it follows that $\mathbf{Camb}(W^J, c)$ is a bounded poset. We conjecture a stronger property, directly generalizing Theorem 2.2.13.

Conjecture 3.2.6. Let (W, S) be a finite, irreducible Coxeter system, let $c \in W$ be a Coxeter element and let $J \subseteq S$. Then, $\mathbf{Camb}(W^J, c)$ is a lattice. Moreover, it is:

- (i) a quotient lattice of $\mathbf{Weak}(W^J)$;
- (ii) congruence uniform;
- (iii) trim.

Figure 36 shows how $\mathbf{Camb}(B_3^{\{s_0, s_2\}}, s_0 s_1 s_2)$ arises as a quotient lattice of $\mathbf{Weak}(B_3^{\{s_0, s_2\}})$. In general, however, $\mathbf{Camb}(W^J, c)$ fails to be a sublattice of $\mathbf{Weak}(W^J)$, as is detailed in the next example.

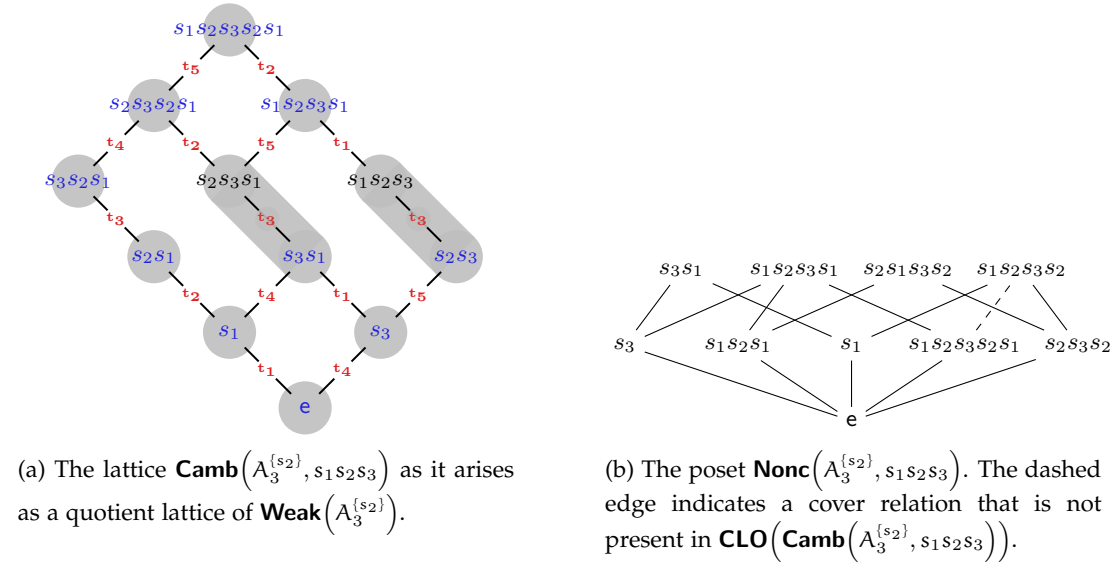
Example 3.2.7. Let $W = A_3$, $c = s_1 s_2 s_3$ and $J = \{s\}$. Then, $w_o^J(c) = s_1 s_2 s_3 s_2 s_1$, and

$$\text{Inv}(w_o^J) = \left\{ \underbrace{s_1}_{t_1}, \underbrace{s_1 s_2 s_1}_{t_2}, \underbrace{s_1 s_2 s_3 s_2 s_1}_{t_3}, \underbrace{s_3}_{t_4}, \underbrace{s_2 s_3 s_2}_{t_5} \right\}$$

where the inversions are ordered according to $\text{Inv}(w_o^J(c))$. Figure 37a shows how $\mathbf{Camb}(A_3^J, c)$ arises as a quotient lattice of $\mathbf{Weak}(A_3^J)$. The cover relations in this lattice are labeled by the appropriate cover inversions. We observe that the meet of $s_2 s_3 s_2 s_1$ and $s_1 s_2 s_3 s_1$ in $\mathbf{Weak}(A_3^J)$ is $s_2 s_3 s_1$, while the meet of these elements in $\mathbf{Camb}(A_3^J, c)$ is $s_3 s_1$.

Proposition 3.2.8. Conjecture 3.2.6(i) implies Conjecture 3.2.6(ii).

PROOF. By Theorem 3.1.2, $\mathbf{Weak}(W^J)$ is an interval of $\mathbf{Weak}(W)$, and if $\mathbf{Camb}(W^J, c)$ is a quotient lattice of $\mathbf{Weak}(W^J)$, then it is a quotient lattice of a sublattice of $\mathbf{Weak}(W)$. Now, $\mathbf{Weak}(W)$ is congruence uniform by Theorem 1.2.9, and

Figure 37. Some parabolic posets for A_3 .

congruence-uniformity is preserved under passing to sublattices and quotient lattices by Proposition 1.1.31. \square

3.3. Parabolic noncrossing partitions

In Definition 2.3.5 we have defined c -noncrossing W -partitions as the elements in the principal order ideal of $\mathbf{Abs}(W)$ generated by c . However, neither c nor the inversions of w_0^J are necessarily members of W^J . It is therefore not immediately clear which elements of $\mathbf{Abs}(W)$ should be considered parabolic analogues of c -noncrossing W -partitions.

However, READING's bijection from $\mathbf{Align}(W, c)$ to $\mathbf{Nonc}(W, c)$ extends to an isomorphism from the core label order of $\mathbf{Weak}(\mathbf{Align}(W, c))$ to $\mathbf{Nonc}(W, c)$; see Theorem 2.3.13. We are going to use an appropriate restriction of this map to define parabolic c -noncrossing W -partitions.

For $w \in \mathbf{Align}(W^J, c)$ we label the cover inversions of w according to $\mathbf{Inv}(w_0^J(c))$, i.e., we have $\mathbf{Cov}(w) = \{t_1, t_2, \dots, t_k\}$ with $t_i \prec_c^J t_j$ if and only if $i < j$. With this convention, we define a map

$$(3.5) \quad \mathbf{nc}_c^J: \mathbf{Align}(W^J, c) \rightarrow W, \quad w \mapsto t_1 t_2 \cdots t_k.$$

Definition 3.3.1 ([192, Definition 5.1.13]). *Let (W, S) be a finite, irreducible Coxeter system, let $c \in W$ be a Coxeter element and let $J \subseteq S$. We define the set of c -noncrossing W^J -partitions by*

$$\mathbf{Nonc}(W^J, c) \stackrel{\text{def}}{=} \{\mathbf{nc}_c^J(w) \mid w \in \mathbf{Align}(W^J, c)\}.$$

Moreover, we define $\mathbf{Nonc}(W^J, c) \stackrel{\text{def}}{=} \mathbf{Abs}(\mathbf{Nonc}(W^J, c))$.

Since $\mathbf{Align}(W^0, c) = \mathbf{Align}(W, c)$ by Remark 3.2.2, the map \mathbf{nc}_c^0 is identical to the map \mathbf{nc}_c defined in (2.10). Consequently, $\mathbf{Nonc}(W^0, c) = \mathbf{Nonc}(W, c)$.

Note that there is no apparent reason why \mathbf{nc}_c^J should be injective. We conjecture, however, that this is the case.

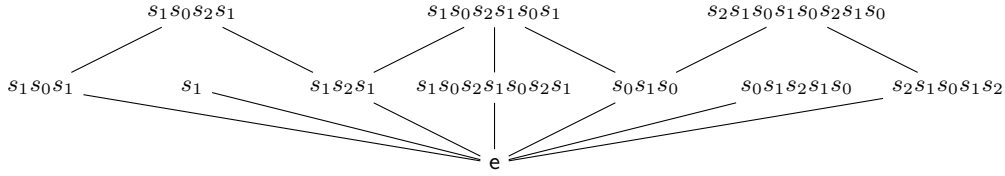


Figure 38. The poset $\mathbf{Nonc}\left(\mathbb{B}_3^{\{s_0, s_2\}}, s_0 s_1 s_2\right)$.

Conjecture 3.3.2 ([192, Section 5.1.3]). *Let (W, S) be a finite, irreducible Coxeter system, let $c \in W$ be a Coxeter element and let $J \subseteq S$. The map nc_c^J is a bijection. Consequently, $|\text{Align}(W^J, c)| = |\text{Nonc}(W^J, c)|$.*

Example 3.3.3. *We continue Example 3.2.4, and consider $W = \mathbb{B}_3$, $c = s_0 s_1 s_2$ and $J = \{s_0, s_2\}$. This example also lists the (W^J, c) -aligned elements together with their cover inversions. We thus obtain the following c -noncrossing W^J -partitions.*

$w \in \text{Align}(W^J, c)$	$\text{Cov}(w)$	$\text{nc}_c^J(w)$	$\text{nc}_c^J(w) \in W^J$
e	\emptyset	e	yes
s_1	$\{t_1\}$	s_1	yes
$s_0 s_1$	$\{t_3\}$	$s_1 s_0 s_1$	yes
$s_2 s_1$	$\{t_2\}$	$s_1 s_2 s_1$	no
$s_0 s_2 s_1$	$\{t_2, t_3\}$	$s_1 s_0 s_2 s_1$	yes
$s_1 s_0 s_1$	$\{t_5\}$	$s_0 s_1 s_0$	no
$s_1 s_0 s_2 s_1$	$\{t_4\}$	$s_1 s_0 s_1 s_2 s_1 s_0 s_1$	yes
$s_0 s_1 s_0 s_2 s_1$	$\{t_6\}$	$s_2 s_1 s_0 s_1 s_2$	no
$s_2 s_1 s_0 s_2 s_1$	$\{t_2, t_5\}$	$s_1 s_2 s_1 s_0 s_1 s_0$	no
$s_0 s_2 s_1 s_0 s_2 s_1$	$\{t_5, t_6\}$	$s_2 s_1 s_0 s_1 s_0 s_2 s_1 s_0$	no
$s_1 s_0 s_2 s_1 s_0 s_2 s_1$	$\{t_7\}$	$s_0 s_1 s_2 s_1 s_0$	no

Figure 38 shows $\mathbf{Nonc}(W^J, c)$; this poset is isomorphic to $\mathbf{CLO}(\mathbf{Camb}(W^J, c))$.

Figure 37 illustrates that Theorem 2.3.13 does not necessarily extend to parabolic quotients¹⁰. It illustrates the case $W = A_3$ and $J = \{s_2\}$. Figure 37b shows $\mathbf{Nonc}\left(A_3^{\{s_2\}}, s_1 s_2 s_3\right)$, which is not isomorphic to $\mathbf{CLO}\left(\mathbf{Camb}\left(A_3^{\{s_2\}}, s_1 s_2 s_3\right)\right)$. It is left as an exercise for the reader to verify that, however, $\mathbf{Nonc}\left(A_3^{\{s_2\}}, s_1 s_3 s_2\right) \cong \mathbf{CLO}\left(\mathbf{Camb}\left(A_3^{\{s_2\}}, s_1 s_3 s_2\right)\right)$.

Research Challenge 3.3.4. *Given a finite, irreducible Coxeter system (W, S) , characterize the sets $J \subseteq S$ and the Coxeter elements $c \in W$ such that $\mathbf{Nonc}(W^J, c) \cong \mathbf{CLO}(\mathbf{Camb}(W^J, c))$. This requires proof that Conjecture 3.2.6(ii) is satisfied.*

¹⁰Strictly speaking, we cannot even be sure at the moment that $\mathbf{CLO}(\mathbf{Camb}(W^J, c))$ exists, since congruence-uniformity (or semidistributivity for that matter) of $\mathbf{Camb}(W^J, c)$ is only conjectured.

3.4. Parabolic clusters

The definition of a parabolic generalization of the c -cluster complex of W is relatively straightforward.

Definition 3.4.1 ([192, Definition 5.1.1]). *Let (W, S) be a finite, irreducible Coxeter system, let $c \in W$ be a Coxeter element and let $J \subseteq S$. The (W^J, c) -cluster complex is the subword complex*

$$\text{Clus}(W^J, c) \stackrel{\text{def}}{=} \text{Subw}(W; \overline{cw_o(c)}, w_o^J),$$

for any S -reduced word c for c . The facets of $\text{Clus}(W^J, c)$ are the (W^J, c) -clusters.

It is immediately clear that $\text{Clus}(W^0, c) = \text{Clus}(W, c)$; see Definition 2.4.3. For easy reference and by slight abuse of notation we denote by $|\text{Clus}(W^J, c)|$ the number of facets of $\text{Clus}(W^J, c)$. Moreover, we denote by $\mathbf{Clus}(W^J, c)$ the set of facets of $\text{Clus}(W^J, c)$ ordered by \leq_{flip} .

Example 3.4.2. *We continue Example 3.3.3. For $W = B_3$, $J = \{s_0, s_2\}$ and $c = s_0s_1s_2$, we have $w_o^J(c) = s_1s_0s_2s_1s_0s_2s_1$.*

We have already computed the facets of $\text{Clus}(B_3^{\{s_0, s_2\}}, s_0s_1s_2) = \text{Subw}(B_3; \overline{cw_o(c)}, w_o^J)$ in Example 2.4.2. The poset $\mathbf{Clus}(B_3^{\{s_0, s_2\}}, s_0s_1s_2)$ is shown in Figure 24a, and it is isomorphic to $\mathbf{Camb}(B_3^{\{s_0, s_2\}}, s_0s_1s_2)$; see Figure 36.

The next two conjectures generalize Theorems 2.4.7 and 2.4.9, respectively.

Conjecture 3.4.3 ([192, Conjecture 5.1.10]). *Let (W, S) be a finite, irreducible Coxeter system, let $c \in W$ be a Coxeter element and let $J \subseteq S$. Then, $|\text{Align}(W^J, c)| = |\text{Clus}(W^J, c)|$.*

Conjecture 3.4.4 ([192, Conjectures 5.1.3 and 5.1.10]). *Let (W, S) be a finite, irreducible Coxeter system, let $c \in W$ be a Coxeter element and let $J \subseteq S$. The poset $\mathbf{Clus}(W^J, c)$ is a lattice isomorphic to the dual of $\mathbf{Camb}(W^J, c)$.*

The bijection between $\text{Align}(W, c)$ and the facets of $\text{Clus}(W, c)$ established in Theorem 2.4.7 identifies the last reflections of $w \in \text{Align}(W, c)$ with certain positions of $\overline{cw_o(c)}$. The straightforward generalization of this map to parabolic quotients is in general not injective, as is illustrated in the next example.

Example 3.4.5. *Let us continue Example 3.2.7, and consider $W = A_3$, $c = s_1s_2s_3$ and $J = \{s_2\}$. The following table lists the elements of $A_3^{\{s_2\}}$ together with their last reflections.*

$w \in A_3^J$	$w \in \text{Align}(A_3^J, c)$	last reflections of w
e	yes	$-s_1, -s_2, -s_3$
s_1	yes	$-s_2, -s_3, t_1$
s_3	yes	$-s_1, -s_2, t_4$
s_2s_1	yes	$-s_3, t_1, t_2$
s_3s_1	yes	$-s_2, t_1, t_4$

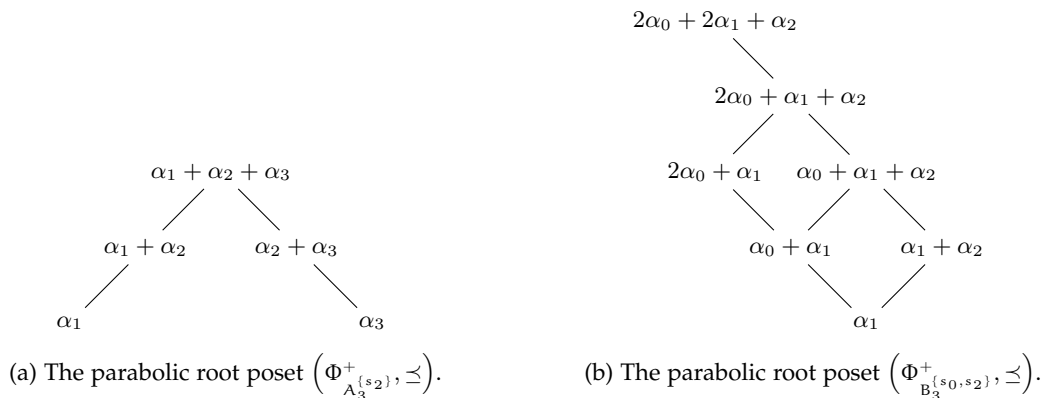


Figure 39. Some parabolic root posets.

s_2s_3	<i>yes</i>	$-s_1, t_4, t_5$
$s_3s_2s_1$	<i>yes</i>	t_1, t_2, t_3
$s_2s_3s_1$	<i>no</i>	t_1, t_3, t_4
$s_1s_2s_3$	<i>no</i>	t_3, t_4, t_5
$s_2s_3s_2s_1$	<i>yes</i>	t_1, t_3, t_4
$s_1s_2s_3s_1$	<i>yes</i>	t_3, t_4, t_5
$s_1s_2s_3s_2s_1$	<i>yes</i>	t_3, t_4, t_5

We notice that the $(A_3^{s_2}, s_1s_2s_3)$ -aligned elements $s_1s_2s_3s_1$ and $s_1s_2s_3s_2s_1$ have the same set of last reflections.

3.5. Parabolic nonnesting partitions

We conclude the constructive part of this section by generalizing the nonnesting partitions to parabolic quotients of W . Since nonnesting partitions of W are antichains in the root poset associated with W , we have to require that $W \neq H_4$; see Remark 2.5.3.

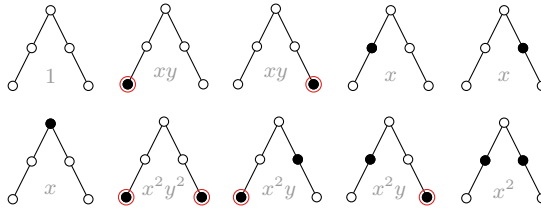
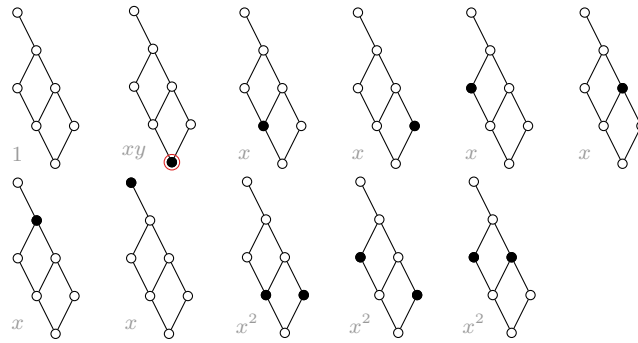
We wish to define nonnesting partitions associated with W^J as antichains in a subposet of the root poset consisting of positive roots corresponding to the inversions of w_o^J . We thus define

$$\Phi_{W^J}^+ \stackrel{\text{def}}{=} \{\alpha \in \Phi_W^+ \mid t_\alpha \in \text{Inv}(w_o^J)\},$$

and call $(\Phi_{W^J}^+, \preceq)$ the *parabolic root poset* of W^J . Figure 39 shows two instances of parabolic root posets.

By [29, Proposition 2.4.4], for every $J \subseteq S$ each element $w \in W$ has a unique factorization $w = w^J \cdot w_J$, where $w^J \in W^J$ and $w_J \in W_J$, and $\text{Inv}(w) = \text{Inv}(w^J) \uplus \text{Inv}(w_J)$. It follows that the roots in $\Phi_{W^J}^+$ are precisely the roots in the order filter of (Φ_W^+, \preceq) generated by $\{\alpha_s \mid s \in S \setminus J\} \subseteq \Pi_W$.

Definition 3.5.1. Let (W, S) be a finite, irreducible Coxeter system other than H_4 and let $J \subseteq S$. The **nonnesting W^J -partitions** are the antichains of $(\Phi_{W^J}^+, \preceq)$.

Figure 40. The ten nonnesting partitions of $A_3^{\{s_2\}}$.Figure 41. The eleven nonnesting partitions of $B_3^{\{s_0, s_2\}}$.

Figures 40 and 41 show the parabolic nonnesting partitions for $A_3^{\{s_2\}}$ and $B_3^{\{s_0, s_2\}}$, respectively. We observe that there are ten resp. eleven of them, which coincides with the number of aligned elements exhibited in Figures 36 and 37a.

However, it turns out that the number of parabolic nonnesting partitions does not always coincide with the number of parabolic aligned elements; see Table 5. By inspection of Figure 33 we notice that choosing the same subsets of minimal elements in each of the four “fake” root posets associated with H_4 yields the same number of antichains. This, together with the fact that $\text{Nonn}(W^J)$ does not depend on a choice of Coxeter element, indicates that we should use parabolic nonnesting partitions to define parabolic W -Catalan numbers.

Definition 3.5.2. Let (W, S) be a finite, irreducible Coxeter system other than H_4 and let $J \subseteq S$. The W^J -Catalan number is

$$\text{Cat}(W^J) \stackrel{\text{def}}{=} |\text{Nonn}(W^J)|.$$

Conjecture 3.5.3 ([192, Chapter 5]). Let (W, S) be a finite, irreducible Coxeter system. If W is of coincidental type, then for every Coxeter element $c \in W$ and every $J \subseteq S$:

$$\text{Cat}(W^J) = |\text{Align}(W^J, c)| = |\text{Nonc}(W^J, c)| = |\text{Clus}(W^J, c)|.$$

Tables 3 to 6 support Conjectures 3.3.2, 3.4.3 and 3.5.3 by listing the cardinalities of $\text{Align}(W^J, c)$, $\text{Nonc}(W^J, c)$, $\text{Clus}(W^J, c)$ and $\text{Nonn}(W^J)$ when W is a finite, irreducible crystallographic Coxeter group of rank 3 or 4. Table 7 lists the cardinalities of $\text{Clus}(H_4^J, c)$ and $\text{Nonn}(H_4^J)$.

3.6. Parabolic Chapoton triangles

Now that we have generalized the ordinary Catalan families together with the relevant partial orders to parabolic quotients of W , it is an intriguing challenge to generalize the F-, H- and M-triangles from Section 2.6 as well. In fact, we wish to define such polynomials in such a way that the relations from Theorem 2.6.2 remain true in the parabolic setting.

Currently, we only dare to give a general definition for the *parabolic H-triangle*. This is defined in the obvious way by:

$$(3.6) \quad \mathcal{H}_{W^J}(x, y) \stackrel{\text{def}}{=} \sum_{A \in \text{Nonn}(W^J)} x^{|A|} y^{\min(A)},$$

where $\min(A)$ denotes the number of minimal elements of $(\Phi_{W^J}^+, \preceq)$ contained in A .

Proposing candidates for parabolic analogues of the M- and F-triangles is far from clear at the moment.

Example 3.6.1. Let $W = A_3$ and $J = \{s_2\}$. Figure 40 shows the ten nonnesting A_3^J -partitions together with the term they contribute to $\mathcal{H}_{A_3^J}(x, y)$. The minimal elements per antichain are circled in red. We thus obtain

$$\mathcal{H}_{A_3^J}(x, y) = x^2 y^2 + 2x^2 y + x^2 + 2xy + 3x + 1.$$

The maximum size of an antichain in the parabolic root poset of A_3^J is 2, and applying the relations from Theorem 2.6.2 to $\mathcal{H}_{A_3^J}(x, y)$ with $r = 2$ yields

$$\mathcal{M}(x, y) = 4x^2 y^2 - 9xy^2 + 5xy + 5y^2 - 5y + 1,$$

$$\mathcal{F}(x, y) = 5x^2 + 4xy + y^2 + 9x + 4y + 4.$$

Example 3.6.2. Let $W = A_3$ and $J = \{s_2\}$. Figure 37b shows both the posets $\text{Nonc}(A_3^J, c)$ (including the dashed edge) and $\text{CLO}(\text{Camb}(A_3^J, c))$ (without the dashed edge) for $c = s_1 s_2 s_3$. It is easy to verify that

$$\mathcal{M}(x, y) = \sum_{u, v \in \text{Align}(A_3^J, c)} \mu_{\text{CLO}(\text{Camb}(A_3^J, c))}(u, v) x^{\ell_{\tau}(nc_c^l(u))} y^{\ell_{\tau}(nc_c^l(v))},$$

where $\mathcal{M}(x, y)$ is the polynomial computed in Example 3.6.1.

This indicates that a parabolic analogue of the M-triangle could perhaps be defined on the core label order of $\text{Camb}(W^J, c)$ rather than on $\text{Nonc}(W^J, c)$. This is obscured in the ordinary case, since for $J = \emptyset$ both posets are isomorphic by Theorem 2.3.13. However, $\text{CLO}(\text{Camb}(A_3^J, s_1 s_3 s_2)) \cong \text{Nonc}(A_3^J, s_1 s_3 s_2)$, which implies that a potential definition of a parabolic M-triangle will depend on the Coxeter element.

Example 3.6.3. Let $W = A_3$ and $J = \{s_2\}$. Figure 42 shows $\text{Clus}(A_3^J, c)$. For a face $A \in \text{Clus}(A_3^J, c)$, we define $n(A) = |A \cap \{1, 3\}|$ and $p(A) = |A| - 2 - n(A)$. Recall that a lattice is nuclear if the join of its atoms is the greatest element, and thus an interval in a lattice is nuclear if it is nuclear considered as a lattice. The next table lists the nuclear intervals of the flip order of $\text{Clus}(A_3^J, c)$ together with the corresponding face of $\text{Clus}(A_3^J, c)$ and the value of the two statistics n and p on these faces.

$[A, B]$ nuclear interval of $\mathbf{Clus}(A_3^J, c)$	$A \cap B \in \mathbf{Clus}(A_3^J, c)$	$n(A \cap B)$	$p(A \cap B)$
$\{1, 2, 3, 7\}, \{1, 2, 3, 7\}$	$\{1, 2, 3, 7\}$	2	0
$\{1, 2, 3, 7\}, \{2, 3, 4, 7\}$	$\{2, 3, 7\}$	1	0
$\{1, 2, 3, 7\}, \{1, 2, 7, 8\}$	$\{1, 2, 7\}$	1	0
$\{1, 2, 3, 7\}, \{2, 4, 7, 8\}$	$\{2, 7\}$	0	0
$\{2, 3, 4, 7\}, \{2, 3, 4, 7\}$	$\{2, 3, 4, 7\}$	1	1
$\{2, 3, 4, 7\}, \{3, 4, 5, 7\}$	$\{3, 4, 7\}$	1	0
$\{2, 3, 4, 7\}, \{2, 4, 7, 8\}$	$\{2, 4, 7\}$	0	1
$\{2, 3, 4, 7\}, \{4, 6, 7, 8\}$	$\{4, 7\}$	0	0
$\{1, 2, 7, 8\}, \{1, 2, 7, 8\}$	$\{1, 2, 7, 8\}$	1	1
$\{1, 2, 7, 8\}, \{2, 4, 7, 8\}$	$\{2, 7, 8\}$	0	1
$\{1, 2, 7, 8\}, \{1, 2, 8, 9\}$	$\{1, 2, 8\}$	1	0
$\{1, 2, 7, 8\}, \{2, 4, 8, 9\}$	$\{2, 8\}$	0	0
$\{3, 4, 5, 7\}, \{3, 4, 5, 7\}$	$\{3, 4, 5, 7\}$	1	1
$\{3, 4, 5, 7\}, \{4, 5, 6, 7\}$	$\{4, 5, 7\}$	0	1
$\{2, 4, 7, 8\}, \{2, 4, 7, 8\}$	$\{2, 4, 7, 8\}$	0	2
$\{2, 4, 7, 8\}, \{4, 6, 7, 8\}$	$\{4, 7, 8\}$	0	1
$\{2, 4, 7, 8\}, \{2, 4, 8, 9\}$	$\{2, 4, 8\}$	0	1
$\{2, 4, 7, 8\}, \{4, 6, 8, 9\}$	$\{4, 8\}$	0	0
$\{1, 2, 8, 9\}, \{1, 2, 8, 9\}$	$\{1, 2, 8, 9\}$	1	1
$\{1, 2, 8, 9\}, \{2, 4, 8, 9\}$	$\{2, 8, 9\}$	0	1
$\{4, 5, 6, 7\}, \{4, 5, 6, 7\}$	$\{4, 5, 6, 7\}$	0	2
$\{4, 5, 6, 7\}, \{4, 6, 7, 8\}$	$\{4, 6, 7\}$	0	1
$\{4, 6, 7, 8\}, \{4, 6, 7, 8\}$	$\{4, 6, 7, 8\}$	0	2
$\{4, 6, 7, 8\}, \{4, 6, 8, 9\}$	$\{4, 6, 8\}$	0	1
$\{2, 4, 8, 9\}, \{2, 4, 8, 9\}$	$\{2, 4, 8, 9\}$	0	2
$\{2, 4, 8, 9\}, \{4, 6, 8, 9\}$	$\{4, 8, 9\}$	0	1
$\{4, 6, 8, 9\}, \{4, 6, 8, 9\}$	$\{4, 6, 8, 9\}$	0	2

Then, we recover the polynomial $\mathcal{F}(x, y)$ from Example 3.6.1 as

$$\mathcal{F}(x, y) = \sum_{A} x^{p(A)} y^{n(A)},$$

where the sum runs over the faces of $\mathbf{Clus}(A_3^J, c)$ that arise as the intersection over nuclear intervals of $\mathbf{Clus}(A_3^J, c)$.

Example 3.6.4. Let $W = B_3$ and $J = \{s_0, s_2\}$. Figure 41 shows the eleven nonnesting B_3^J -partitions together with the term they contribute to $\mathcal{H}_{B_3^J}(x, y)$. The minimal elements per antichain are circled in red. We thus obtain

$$\mathcal{H}_{B_3^J}(x, y) = 3x^2 + xy + 6x + 1.$$

The maximum size of an antichain in the parabolic root poset of B_3^J is 2, and applying the relations from Theorem 2.6.2 to $\mathcal{H}_{B_3^J}(x, y)$ with $r = 2$ yields

$$\mathcal{M}(x, y) = 3x^2y^2 - 13xy^2 + 7xy + 10y^2 - 8y + 1,$$

$$\mathcal{F}(x, y) = 10x^2 + xy + 13x + 3.$$

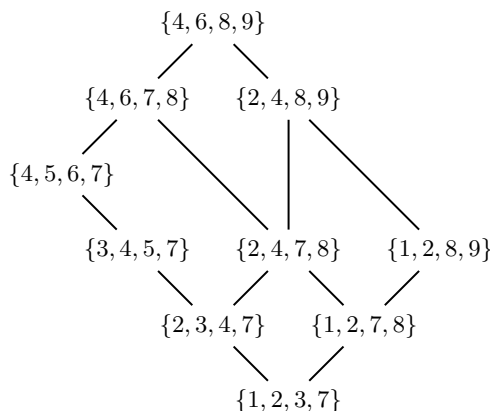
Figure 42. The flip poset $\mathbf{Clus}(A_3^{\{s_2\}}, s_1 s_2 s_3)$.

Figure 38 shows $\mathbf{Nonc}(B_3^J, c) \cong \mathbf{CLO}(\mathbf{Camb}(B_3^J, c))$ for $c = s_0 s_1 s_2$. We obtain

$$\begin{aligned} \tilde{\mathcal{M}}(x, y) &= \sum_{p, q \in \mathbf{Nonc}(B_3^J, c)} \mu_{\mathbf{Nonc}(B_3^J, c)}(p, q) x^{\ell_{\tau}(p)} y^{\ell_{\tau}(q)} \\ &= 3x^2 y^2 - 7xy^2 + 7xy + 4y^2 - 7y + 1 \\ &\neq \mathcal{M}(x, y). \end{aligned}$$

If we apply the relations from Theorem 2.6.2 to $\tilde{\mathcal{M}}(x, y)$ with $r = 2$, then we obtain

$$\begin{aligned} \tilde{\mathcal{H}}(x, y) &= x^2 y^2 + 4x^2 y - 2x^2 + 2xy + 5x + 1, \\ \tilde{\mathcal{F}}(x, y) &= 4x^2 + 6xy + y^2 + 7x + 6y + 3. \end{aligned}$$

Note that not all coefficients of $\tilde{\mathcal{H}}(x, y)$ are nonnegative, which means that it cannot enumerate antichains of some poset with respect to some statistics. Moreover, there cannot exist a poset \mathbf{P} such that

$$\mathcal{M}(x, y) = \sum_{a, b \in \mathbf{P}} \mu_{\mathbf{P}}(a, b) x^{\text{rk}(a)} y^{\text{rk}(b)},$$

because the coefficient of xy in $\mathcal{M}(x, y)$ is 7, forcing \mathbf{P} to have seven elements of rank 1. Since the constant term of $\mathcal{M}(x, y)$ is 1, \mathbf{P} has a unique minimal element. Thus, there are seven cover relations in \mathbf{P} connecting the elements of rank 0 and 1. However, the coefficient of y in $\mathcal{M}(x, y)$ (which up to sign represents this number) is -8 , forcing eight cover relations between elements of rank 0 and 1. This is clearly impossible.

The flip poset $\mathbf{Clus}(B_3^J, c)$ is shown in Figure 24a. If we consider the statistics $n(\Lambda) = |\Lambda \cap \{2\}|$ and $p(\Lambda) = |\Lambda| - 3 - n(\Lambda)$, then we obtain

$$\mathcal{F}(x, y) = \sum_{\Lambda} x^{p(\Lambda)} y^{n(\Lambda)},$$

where the sum runs once again over the faces of $\mathbf{Clus}(B_3^J, c)$ that arise as intersections over nuclear intervals of $\mathbf{Clus}(B_3^J, c)$.

Research Challenge 3.6.5. Given a finite, irreducible Coxeter system (W, S) , characterize the sets $J \subseteq S$ and the Coxeter elements $c \in W$ for which one can define polynomials $\mathcal{M}(x, y)$ and

$\mathcal{F}(x, y)$ which restrict to $\mathcal{M}_W(x, y)$ and $\mathcal{F}_W(x, y)$ for $J = \emptyset$ and which, together with $\mathcal{H}_{W^J}(x, y)$ satisfy the relations from Theorem 2.6.2 for some appropriate choice of τ (possibly depending on c and J).

We conclude this section with a few examples for which this theory is reasonably well understood.

Example 3.6.6. When $W = I_2(m)$, then this whole theory is rather easy. Since W is canonically generated by $S = \{s_1, s_2\}$, there are four parabolic quotients: $J_0 = \emptyset$, $J_1 = \{s_1\}$, $J_2 = \{s_2\}$ and $J_3 = S$. The cases J_0 and J_3 are trivial, and J_1 and J_2 behave exactly analogously. Moreover, there are two Coxeter elements $c_1 = s_1s_2$ and $c_2 = s_2s_1$, whose roles are also equivalent. So, if we consider $I_2(m)^{J_1}$, then $\text{Cat}(I_2(m)^{J_1}) = m$ because the parabolic root poset is an $(m-1)$ -chain. The set $\text{Align}(I_2(m)^{J_1}, c_1)$ equals $I_2(m)^J$ because every member of the parabolic quotient is $(I_2(m)^{J_1}, c_1)$ -aligned. Thus, $\mathbf{Camb}(I_2(m)^{J_1}, c_1)$ is an m -chain, and its core label order is an $(m-1)$ -antichain with an adjoined least element. Thus, it is isomorphic to $\mathbf{Nonc}(I_2(m)^{J_1}, c_1)$. The $(I_2(m)^{J_1}, c_1)$ -clusters are the three-element subsets of $[m+2]$ of the form $\{i, i+1, k\}$ where

$$i \in \begin{cases} \{2, 3, \dots, m+1\}, & \text{if } m \text{ is even,} \\ \{1, 2, \dots, m\}, & \text{if } m \text{ is odd;} \end{cases} \quad \text{and} \quad k = \begin{cases} 1, & \text{if } m \text{ is even,} \\ m+2, & \text{if } m \text{ is odd.} \end{cases}$$

Thus, $\mathbf{Clus}(I_2(m)^{J_1}, c_1) \cong \mathbf{Camb}(I_2(m)^{J_1}, c_1)$. Moreover, analogously to Example 3.6.3, we obtain

$$\begin{aligned} \mathcal{F}_{I_2(m)^{J_1}}(x, y) &= (m-1)x + y + m - 1, \\ \mathcal{H}_{I_2(m)^{J_1}}(x, y) &= xy + (m-2)x + 1, \\ \mathcal{M}_{I_2(m)^{J_1}}(x, y) &= (m-1)xy - (m-1)y + 1. \end{aligned}$$

These three polynomials satisfy the relations from Theorem 2.6.2.

Example 3.6.7. Let $W = H_3$. We have verified using Sage [162] that Conjectures 3.2.6, 3.3.2, 3.4.3 and 3.4.4 are true. See Table 3 in Appendix A.1 for the parabolic Catalan numbers in type H_3 .

Our computations did also resolve Research Challenge 3.3.4: the core label order of $\mathbf{Camb}(H_3^J, c)$ is isomorphic to $\mathbf{Nonc}(H_3^J, c)$ except for the cases $J = \{s_2\}$ and $c = s_1s_2s_3$ or $c = s_3s_2s_1$. Moreover, the obvious candidates for the H- and M-triangles do not satisfy the relations from Theorem 2.6.2 except for the trivial case $J = \{s_1, s_2, s_3\}$. Hence, Research Challenge 3.6.5 remains open.

Let us exemplify this in the case $J = \{s_2, s_3\}$ and $c = s_2s_1s_3$. We have

$$\mathbf{w}_c^J(c) = s_1s_2s_3s_1s_2s_3s_1s_2s_3s_1s_2s_1.$$

The inversion order $\mathbf{Inv}(w_o^J(c))$ is

$$\begin{array}{ccc}
 \underbrace{s_1}_{t_1} & \prec_c & \underbrace{s_1 s_2 s_1}_{t_2} & \prec_c & \underbrace{s_1 s_2 s_1 s_2 s_1}_{t_3} \\
 \prec_c & \underbrace{s_1 s_2 s_3 s_2 s_1}_{t_4} & \prec_c & \underbrace{s_1 s_2 s_1 s_2 s_3 s_2 s_1 s_2 s_1}_{t_5} & \prec_c & \underbrace{s_1 s_2 s_3 s_1 s_2 s_1 s_2 s_1 s_3 s_2 s_1}_{t_6} \\
 \prec_c & \underbrace{s_2 s_1 s_2}_{t_7} & \prec_c & \underbrace{s_2 s_1 s_2 s_1 s_3 s_2 s_1 s_2 s_1 s_3 s_2 s_1 s_2}_{t_8} & \prec_c & \underbrace{s_2 s_1 s_2 s_3 s_2 s_1 s_2}_{t_9} \\
 \prec_c & \underbrace{s_1 s_3 s_2 s_1 s_2 s_1 s_3}_{t_{10}} & \prec_c & \underbrace{s_2 s_1 s_3 s_2 s_1 s_2 s_1 s_3 s_2}_{t_{11}} & \prec_c & \underbrace{s_3 s_2 s_1 s_2 s_3}_{t_{12}}.
 \end{array}$$

The “forcing” of inversions that determines membership of $w \in H_3^J$ in $\text{Align}(H_3^J, c)$, see Definition 3.2.1, is the following:

$$\begin{array}{ll}
 t_2 \in \text{Cov}(w) \implies t_1 \in \text{Inv}(w), & t_3 \in \text{Cov}(w) \implies t_1 \in \text{Inv}(w), \\
 t_4 \in \text{Cov}(w) \implies t_1 \in \text{Inv}(w), & t_5 \in \text{Cov}(w) \implies \{t_1, t_2, t_3, t_4\} \subseteq \text{Inv}(w), \\
 t_6 \in \text{Cov}(w) \implies \{t_1, t_2, t_3, t_4\} \subseteq \text{Inv}(w), & t_8 \in \text{Cov}(w) \implies \{t_2, t_3, t_4, t_7\} \subseteq \text{Inv}(w), \\
 t_9 \in \text{Cov}(w) \implies t_7 \in \text{Inv}(w), & t_{10} \in \text{Cov}(w) \implies t_1 \in \text{Inv}(w), \\
 t_{11} \in \text{Cov}(w) \implies t_7 \in \text{Inv}(w).
 \end{array}$$

We thus obtain the following eighteen elements of $\text{Align}(H_3^J, c)$.

$w \in H_3^J$	$\text{Inv}(w)$	$\text{Cov}(w)$	$w \in \text{Align}(H_3^J, c)?$
e	\emptyset	\emptyset	yes
s_1	$\{t_1\}$	$\{t_1\}$	yes
$s_2 s_1$	$\{t_1, t_2\}$	$\{t_2\}$	yes
$s_3 s_2 s_1$	$\{t_1, t_2, t_4\}$	$\{t_4\}$	yes
$s_1 s_2 s_1$	$\{t_1, t_2, t_3\}$	$\{t_3\}$	yes
$s_1 s_3 s_2 s_1$	$\{t_1, t_2, t_3, t_4\}$	$\{t_3, t_4\}$	yes
$s_2 s_1 s_2 s_1$	$\{t_1, t_2, t_3, t_7\}$	$\{t_7\}$	yes
$s_2 s_1 s_3 s_2 s_1$	$\{t_1, t_2, t_3, t_4, t_5\}$	$\{t_5\}$	yes
$s_3 s_2 s_1 s_2 s_1$	$\{t_1, t_2, t_3, t_5, t_7\}$	$\{t_5\}$	no
$s_1 s_2 s_1 s_3 s_2 s_1$	$\{t_1, t_2, t_3, t_4, t_5, t_6\}$	$\{t_6\}$	yes
$s_2 s_3 s_2 s_1 s_2 s_1$	$\{t_1, t_2, t_3, t_4, t_5, t_7\}$	$\{t_4, t_7\}$	yes
$s_2 s_1 s_2 s_1 s_3 s_2 s_1$	$\{t_1, t_2, t_3, t_4, t_5, t_6, t_{10}\}$	$\{t_{10}\}$	yes
$s_1 s_3 s_2 s_1 s_3 s_2 s_1$	$\{t_1, t_2, t_3, t_4, t_5, t_6, t_7\}$	$\{t_6, t_7\}$	yes
$s_3 s_2 s_1 s_2 s_1 s_3 s_2 s_1$	$\{t_1, t_2, t_3, t_4, t_5, t_6, t_8, t_{10}\}$	$\{t_8\}$	no
$s_2 s_1 s_3 s_2 s_1 s_3 s_2 s_1$	$\{t_1, t_2, t_3, t_4, t_5, t_6, t_7, t_8\}$	$\{t_8\}$	yes
$s_2 s_3 s_2 s_1 s_2 s_1 s_3 s_2 s_1$	$\{t_1, t_2, t_3, t_4, t_5, t_6, t_7, t_8, t_{10}\}$	$\{t_7, t_{10}\}$	yes
$s_1 s_2 s_1 s_3 s_2 s_1 s_3 s_2 s_1$	$\{t_1, t_2, t_3, t_4, t_5, t_6, t_7, t_8, t_9\}$	$\{t_9\}$	yes
$s_1 s_3 s_2 s_1 s_3 s_2 s_1 s_3 s_2 s_1$	$\{t_1, t_2, t_3, t_4, t_5, t_6, t_7, t_8, t_9, t_{10}\}$	$\{t_9, t_{10}\}$	yes
$s_2 s_1 s_3 s_2 s_1 s_3 s_2 s_1 s_3 s_2 s_1$	$\{t_1, t_2, t_3, t_4, t_5, t_6, t_7, t_8, t_9, t_{10}, t_{11}\}$	$\{t_{11}\}$	yes
$s_1 s_2 s_1 s_3 s_2 s_1 s_3 s_2 s_1 s_3 s_2 s_1$	$\{t_1, t_2, t_3, t_4, t_5, t_6, t_7, t_8, t_9, t_{10}, t_{11}, t_{12}\}$	$\{t_{12}\}$	yes

W	J	$\text{Cat}(W^J)$
A_n	$J = S \setminus \{s_i\}$ for $i \in [n]$	$\binom{n+1}{i}$
B_n	$J = \{s_0, s_1, \dots, s_{n-2}\}$	$2n$
	$J = \{s_1, s_2, \dots, s_{n-1}\}$	2^n
D_n	$J = \{\bar{s}_0, s_1, s_2, \dots, s_{n-2}\}$	$2n$
	$J = \{s_1, s_2, \dots, s_{n-1}\}$	2^{n-1}
	$J = \{\bar{s}_0, s_2, \dots, s_{n-1}\}$	2^{n-1}
E_6	$J = \{s_1, s_2, s_3, s_4, s_5\}$	27
	$J = \{s_2, s_3, s_4, s_5, s_6\}$	27
E_7	$J = \{s_1, s_2, s_3, s_4, s_5, s_6\}$	56
H_3	$J = \{s_1, s_2\}$	12
$I_2(m)$	$J = \{s_1\}$	m
	$J = \{s_2\}$	m

Table 2. The subsets $J \subseteq S$ inducing a fully commutative quotient W^J as classified in [177, Theorem 6.1] together with the corresponding parabolic Catalan number. The Coxeter generators are named as in Figure 11.

Figure 43 shows $\mathbf{Camb}(H_3^J, c)$ and Figure 44 shows the corresponding core label order, which is isomorphic to $\mathbf{Nonc}(H_3^J, c)$.

The generating function of the Möbius function of the poset $\mathbf{Nonc}(H_3^J, c)$ is

$$\mathcal{M}(x, y) = 5x^2y^2 - 12xy^2 + 12xy + 7y^2 - 12y + 1.$$

The length of $\mathbf{Nonc}(H_3^J, c)$ is $r = 2$, and we obtain

$$\begin{aligned} \mathcal{H}(x, y) &= (x(y-1) + 1)^r \mathcal{M}\left(\frac{y}{y-1}, \frac{x(y-1)}{x(y-1) + 1}\right) \\ &= x^2y^2 + 8x^2y - 4x^2 + 2xy + 10x + 1. \end{aligned}$$

If we label the minimal elements in Figure 32a from left to right by s_1, s_2, s_3 , then we obtain the parabolic root poset of H_3^J by considering the order filter generated by s_1 . The generating function of the antichains according to size and containment of s_1 is

$$\tilde{\mathcal{H}}(x, y) = 5x^2 + xy + 11x + 1 \neq \mathcal{H}(x, y).$$

Remark 3.6.8. Another easy case is given when W^J is a fully commutative quotient, see [192, Section 5.2]. These are the parabolic quotients of W for which w_0^J is fully commutative, i.e., any two S -reduced words are related by a sequence of commutations. The fully commutative quotients were classified in [177, Theorem 6.1]. We include this classification in Table 2.

In this situation, any element of W^J is (W^J, c) -aligned for c a Coxeter element. Thus, $\mathbf{Camb}(W^J, c) \cong \mathbf{Weak}(W^J)$ is a distributive lattice. Then, [128, Theorem 1.1] implies that $\mathbf{CLO}(\mathbf{Camb}(W^J, c)) \cong \mathbf{Nonc}(W^J, c)$.

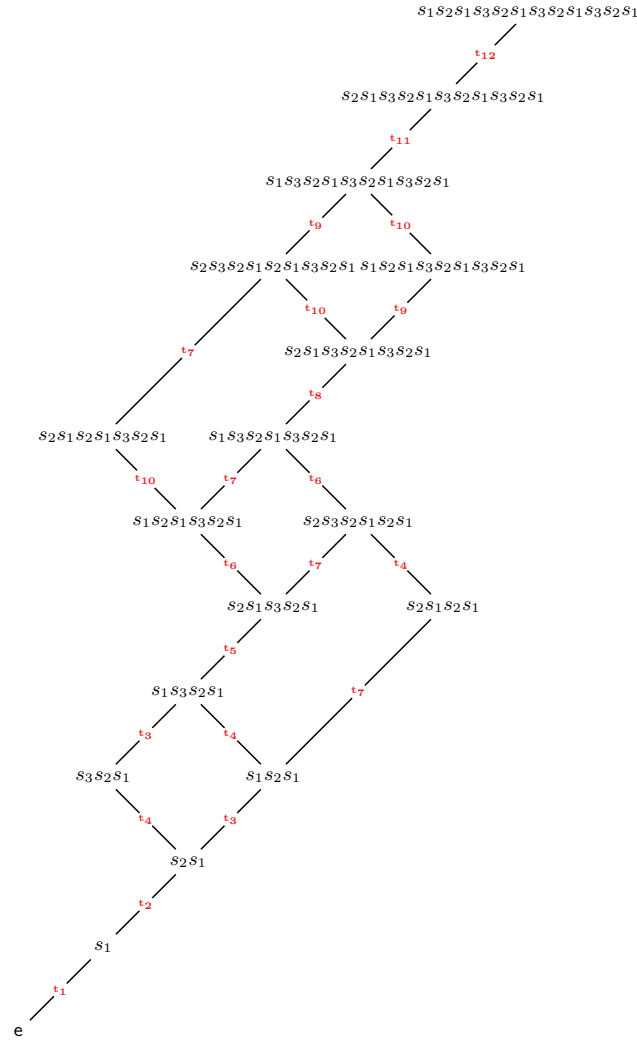


Figure 43. The lattice $\mathbf{Camb}(H_3^{\{s_2, s_3\}}, s_2 s_1 s_3)$.

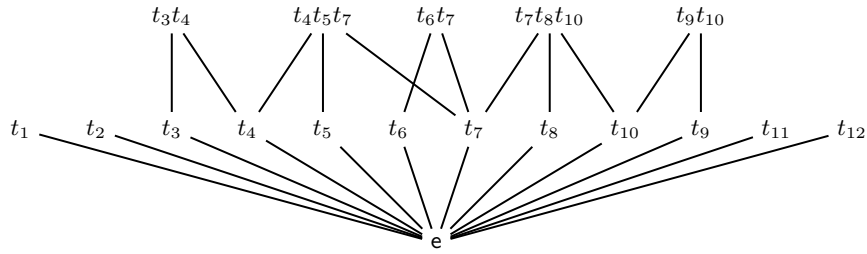


Figure 44. The poset $\mathbf{Nonc}(H_3^{\{s_2, s_3\}}, s_2 s_1 s_3)$. This is isomorphic to the core label order of $\mathbf{Camb}(H_3^{\{s_2, s_3\}}, s_2 s_1 s_3)$.

CHAPTER 4

Parabolic Cataland: Linear type A

4.1. Definitions

In Chapter 2, we have explained that most of the prototypical results that led to the definition of ordinary Cataland came from linear type A, i.e., the Coxeter group of type A_n together with the linear Coxeter element $\vec{c} = s_1 s_2 \cdots s_n$.

In this section we give combinatorial models for the sets $\text{Align}(A_n^J, \vec{c})$, $\text{Nonc}(A_n^J, \vec{c})$, $\text{Clus}(A_n^J, \vec{c})$ and $\text{Nonn}(A_n^J)$ as well as proofs of Conjectures 3.2.6, 3.3.2, 3.4.3, 3.4.4 and 3.5.3 and answers to Research Challenges 3.3.4 and 3.6.5.

The results of this section have appeared in [45, 66, 108, 130, 132, 133], some of them in collaboration with C. CEBALLOS, W. FANG, C. KRATTENTHALER, J.-C. NOVELLI and N. WILLIAMS.

4.1.1. Parabolic quotients of the symmetric group. To ease the notation, we slightly shift the index, and consider the Coxeter group A_{n-1} , which is isomorphic to the symmetric group \mathfrak{S}_n of permutations of $[n]$. Recall that the Coxeter generators of A_{n-1} are the adjacent transpositions $s_i = (i \ i+1)$ for $i \in [n-1]$. We first characterize the members of the parabolic quotients of \mathfrak{S}_n .

Lemma 4.1.1. *If $w \in \mathfrak{S}_n^J$, then $w_i < w_{i+1}$ for all $s_i \in J$.*

PROOF. Note that for $w \in \mathfrak{S}_n$ and $s_i \in S$, the one-line notation of the permutation $w' = ws_i$ equals the one-line notation of w except that the values in positions i and $i+1$ are swapped.

If $w \in \mathfrak{S}_n^J$ and $s_i \in J$, then, by (3.1), $\ell_S(ws_i) > \ell_S(w)$. This means that $\text{Inv}(ws_i) = \text{Inv}(w) \setminus \{(i, i+1)\}$, and therefore $w_i < w_{i+1}$. □

The subsets of $S = \{s_1, s_2, \dots, s_{n-1}\}$ can be identified with compositions of n . More precisely, with $J = S \setminus \{s_{i_1}, s_{i_2}, \dots, s_{i_r}\} \subseteq S$ we associate the tuple $\alpha_J \stackrel{\text{def}}{=} (\alpha_1, \alpha_2, \dots, \alpha_r)$ of n , where $\alpha_j = i_j - i_{j-1}$ and $i_0 = 0$ and $i_r = n$. Then, Lemma 4.1.1 states that the elements of \mathfrak{S}_n^J are precisely the permutations whose one-line notation can be partitioned according to α_J such that the entries per part form an increasing sequence.

Example 4.1.2. Let $W = A_3 = \mathfrak{S}_4$ and $J = \{s_2\} = \{s_1, s_2, s_3\} \setminus \{s_1, s_3\}$. The associated composition of 4 is therefore $\alpha_J = (1, 2, 1)$. The elements of \mathfrak{S}_4^J are the following, where we have colored the one-line notation according to α_J :

$$\begin{array}{llll}
 e & = & \boxed{1} \boxed{2} \boxed{3} \boxed{4}, & s_3 & = & \boxed{1} \boxed{2} \boxed{4} \boxed{3}, & s_2 s_3 & = & \boxed{1} \boxed{3} \boxed{4} \boxed{2}, \\
 s_1 & = & \boxed{2} \boxed{1} \boxed{3} \boxed{4}, & s_3 s_1 & = & \boxed{2} \boxed{1} \boxed{4} \boxed{3}, & s_1 s_2 s_3 & = & \boxed{2} \boxed{3} \boxed{4} \boxed{1}, \\
 s_2 s_1 & = & \boxed{3} \boxed{1} \boxed{2} \boxed{4}, & s_2 s_3 s_1 & = & \boxed{3} \boxed{1} \boxed{4} \boxed{2}, & s_1 s_2 s_3 s_1 & = & \boxed{3} \boxed{2} \boxed{4} \boxed{1}, \\
 s_3 s_2 s_1 & = & \boxed{4} \boxed{1} \boxed{2} \boxed{3}, & s_2 s_3 s_2 s_1 & = & \boxed{4} \boxed{1} \boxed{3} \boxed{2}, & s_1 s_2 s_3 s_2 s_1 & = & \boxed{4} \boxed{2} \boxed{3} \boxed{1}.
 \end{array}$$

* * *

Now, let $n > 0$ and let $\alpha = (\alpha_1, \alpha_2, \dots, \alpha_r)$ be a *composition* of n , i.e., $\alpha_1 + \alpha_2 + \dots + \alpha_r = n$ and $\alpha_i > 0$ for $i \in [r]$. In this case, we sometimes write $\alpha \vdash n$. Let $\bar{\alpha} = (\alpha_r, \dots, \alpha_2, \alpha_1)$ be the *reverse* composition. We define $p_0 \stackrel{\text{def}}{=} 0$ and $p_i \stackrel{\text{def}}{=} \alpha_1 + \alpha_2 + \dots + \alpha_i$ for $i \in [r]$, and consider the set

$$(4.1) \quad \mathfrak{S}_\alpha \stackrel{\text{def}}{=} \left\{ w \in \mathfrak{S}_n \mid w_i < w_{i+1} \text{ for } i \notin \{p_1, p_2, \dots, p_{r-1}\} \right\}.$$

By Lemma 4.1.1 and the reasoning before Example 4.1.2, it is clear that $\mathfrak{S}_\alpha = A_{n-1}^J$, where $J_\alpha \stackrel{\text{def}}{=} S \setminus \{s_{p_1}, s_{p_2}, \dots, s_{p_{r-1}}\}$. Thus, \mathfrak{S}_α is the *parabolic quotient* of \mathfrak{S}_n by α , and its elements are *α -permutations*.

Remark 4.1.3. If $\alpha = (1, 1, \dots, 1) \vdash n$, then $J_\alpha = \emptyset$. Therefore, $\mathfrak{S}_\alpha = \mathfrak{S}_n$, and all the definitions that follow will restrict to their ordinary linear type-A counterparts introduced in Chapter 2.

4.1.2. The longest α -permutation. The longest element of \mathfrak{S}_α is denoted by $w_{\circ; \alpha}$ and has the one-line notation:

$$(4.2) \quad \underbrace{n-p_1+1, n-p_1+2, \dots, n}_{\alpha_1} \mid \underbrace{n-p_2+1, n-p_2+2, \dots, n-p_1}_{\alpha_2} \mid \dots \mid \underbrace{1, 2, \dots, n-p_{r-1}}_{\alpha_r}.$$

We may thus compute the inversions of $w_{\circ; \alpha}$ and determine the reflections and the roots that are relevant for the definition of parabolic Catalan objects in linear type A.

We approach this a little bit differently and determine the \bar{c} -sorting word of $w_{\circ; \alpha}$. Let $\lambda = (\lambda_1, \lambda_2, \dots, \lambda_k)$ be a Ferrers shape that fits into a staircase shape of order n . We define the associated permutation by

$$(4.3) \quad w(\lambda) \stackrel{\text{def}}{=} \prod_{i=1}^k \prod_{j=1}^{\lambda_{k-i+1}} s_{n-k+i-j}$$

For a composition $\alpha = (\alpha_1, \alpha_2, \dots, \alpha_r)$, we define the associated Ferrers shape by

$$(4.4) \quad \lambda_\alpha \stackrel{\text{def}}{=} \underbrace{(p_{r-1}, p_{r-1}, \dots, p_{r-1})}_{\alpha_r} \underbrace{(p_{r-2}, p_{r-2}, \dots, p_{r-2})}_{\alpha_{r-1}} \dots \underbrace{(p_1, p_1, \dots, p_1)}_{\alpha_2}.$$

We sometimes call λ_α the *α -shape*. Clearly, λ_α fits into a staircase shape of order n .

Lemma 4.1.4 ([165, Lemma 3.2]). *For any composition α of $n > 0$, $w(\lambda_{\bar{\alpha}}) = w_{\circ; \alpha}$. In fact, $w_{\circ; \alpha}(\bar{c})$ is given by the product described in (4.3).*

The reversal of α is necessary, because we have defined c -sorting words as subwords of ${}^\infty c$; see (2.4).

Example 4.1.5. Let $\alpha = (2, 4, 1, 3) \vdash 10$. We have $p_0 = 0, p_1 = 2, p_2 = 6, p_3 = 7, p_4 = 10$. The associated α -shape is $\lambda_\alpha = (7, 7, 7, 6, 2, 2, 2, 2)$. The $\bar{\alpha}$ -shape $\lambda_{\bar{\alpha}} = (8, 8, 4, 4, 4, 4, 3)$ is the conjugation of λ_α , i.e., the reflection across the main diagonal. In order to obtain the \bar{c} -sorting word of $w_{\circ; \alpha}$ according to Lemma 4.1.4, we place the Coxeter generators $s_{n-i}, s_{n-i-1}, \dots$ from left to right in the cells of the i^{th} row (from the top) of the Ferrers shapes λ_α and $\lambda_{\bar{\alpha}}$. We may now obtain $w_{\circ; \alpha}(\bar{c})$ by reading the placed letters either from left-to-right, bottom-to-top in $\lambda_{\bar{\alpha}}$ or from top-to-bottom, right-to-left in λ_α . This is illustrated in the next picture.

If we compute $w(\lambda_{\bar{\alpha}})$ according to (4.3), then—since $\lambda = \lambda_{\bar{\alpha}} = (8, 8, 4, 4, 4, 4, 3)$ —we have $n = 10$ and $k = 7$ and obtain:

i	λ_{k-i+1}	$n - k + i$	factor
1	3	4	$s_3 s_2 s_1$
2	4	5	$s_4 s_3 s_2 s_1$
3	4	6	$s_5 s_4 s_3 s_2$
4	4	7	$s_6 s_5 s_4 s_3$
5	4	8	$s_7 s_6 s_5 s_4$
6	8	9	$s_8 s_7 s_6 s_5 s_4 s_3 s_2 s_1$
7	8	10	$s_9 s_8 s_7 s_6 s_5 s_4 s_3 s_2$

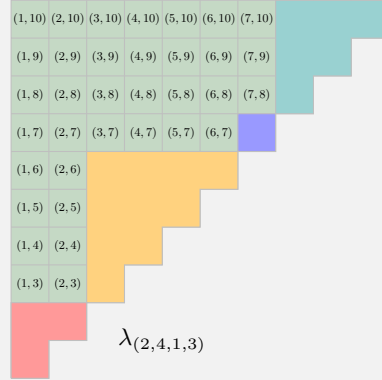
Thus,

$$w_{\circ; (2,4,1,3)}(\bar{c}) = (s_3 s_2 s_1)(s_4 s_3 s_2 s_1)(s_5 s_4 s_3 s_2)(s_6 s_5 s_4 s_3)(s_7 s_6 s_5 s_4) \\ (s_8 s_7 s_6 s_5 s_4 s_3 s_2 s_1)(s_9 s_8 s_7 s_6 s_5 s_4 s_3 s_2).$$

4.1.3. The root poset of \mathfrak{S}_α and α -Dyck paths. Let $\lambda = (n, n - 1, \dots, 1)$ be the staircase shape of order n . If we label the box in the i^{th} row and j^{th} column (read from the top-left corner) by the transposition $(j, n - i + 1)$, then we obtain the triangular poset Δ_n , defined in (2.15), inside the staircase shape. The poset Δ_n is naturally isomorphic to the root poset of type A_{n-1} , so if we restrict this labeling to the α -shape λ_α , then we recover the parabolic root

poset of $A_{n-1}^{J_\alpha} = \mathfrak{S}_\alpha$ consisting of all inversions of $w_{o;\alpha}$. Let us write Δ_α for this parabolic root poset.

Example 4.1.6. For $\alpha = (2, 4, 1, 3) \vdash 10$, the α -shape inscribed in the staircase shape of order 10 with the boxes labeled by transpositions is shown below.



Note that the α -shape is traced out by the northeast path

$$(4.5) \quad v_\alpha \stackrel{\text{def}}{=} N^{\alpha_1} E^{\alpha_1} N^{\alpha_2} E^{\alpha_2} \dots N^{\alpha_r} E^{\alpha_r};$$

the α -bounce path. Then, analogously to the situation for Dyck paths described in Section 2.5, the order ideals of Δ_α are traced out by the v_α -paths, i.e., the northeast paths weakly between v_α and $N^n E^n$. We refer to these paths as α -Dyck paths, and write $\text{Dyck}(\alpha) \stackrel{\text{def}}{=} \text{Paths}(v_\alpha)$. We obtain the first combinatorial realization in parabolic linear type A.

Proposition 4.1.7. Let $n > 0$. For any composition α of $n > 0$, the sets $\text{Nonn}(A_{n-1}^{J_\alpha})$ and $\text{Dyck}(\alpha)$ are in bijection.

Let $\text{Cat}(\alpha) \stackrel{\text{def}}{=} |\text{Dyck}(\alpha)|$ denote the α -Catalan number, which is the $A_{n-1}^{J_\alpha}$ -Catalan number from Definition 3.5.2. The complements of the order ideals of Δ_α correspond to Ferrers shapes that fit inside λ_α . The number of these Ferrers shapes can be computed by a determinantal formula of G. KREWERAS.

Theorem 4.1.8 ([110, Section 2.3.7]). If $\lambda = (\lambda_1, \lambda_2, \dots, \lambda_k)$ is a Ferrers shape, then the number of Ferrers shapes that fit inside λ is given by the determinant of the $k \times k$ -matrix whose entry in row i and column j is $\binom{\lambda_i + 1}{j - i + 1}$.

Example 4.1.9. For $\alpha = (2, 4, 1, 3)$, we have $\lambda_\alpha = (7, 7, 7, 6, 2, 2, 2, 2)$. The corresponding matrix is

$$\begin{pmatrix} 8 & 28 & 56 & 35 & 0 & 0 & 0 & 0 \\ 1 & 8 & 28 & 35 & 0 & 0 & 0 & 0 \\ 0 & 1 & 8 & 21 & 1 & 0 & 0 & 0 \\ 0 & 0 & 1 & 8 & 3 & 1 & 0 & 0 \\ 0 & 0 & 0 & 1 & 3 & 3 & 1 & 0 \\ 0 & 0 & 0 & 0 & 1 & 3 & 3 & 1 \\ 0 & 0 & 0 & 0 & 0 & 1 & 3 & 3 \\ 0 & 0 & 0 & 0 & 0 & 0 & 1 & 3 \end{pmatrix},$$

and its determinant is $\text{Cat}(\alpha) = 2415$.

If $\alpha = (t, 1, 1, \dots, 1) \vdash n$, then we can give a closed formula for the corresponding α -Catalan number.

Proposition 4.1.10. Let $n, t > 0$ and let $\alpha = (t, 1, 1, \dots, 1) \vdash n$. Then,

$$\text{Cat}(\alpha) = \frac{t+1}{n+1} \binom{2n-t}{n-t}.$$

PROOF. If α is of the given form, then $\text{Cat}(\alpha)$ essentially counts ordinary Dyck paths starting with t north steps. That such paths are counted by the formula in the statement follows from [107, Corollary 10.3.2]. \square

Computer experiments suggest the following conjecture.

Conjecture 4.1.11. Let $\alpha = (1, 2, 1, 1, \dots, 1) \vdash n$ for $n > 3$. Then,

$$\text{Cat}(\alpha) = \left(\frac{5}{n+1} + \frac{9}{n-3} \right) \binom{2n-4}{n-4}.$$

The numbers appearing in Conjecture 4.1.11 count for instance certain noncrossing partitions avoiding certain patterns [129, Lemma 3.1], see also [36] and [169, A071718].

4.1.4. \bar{c} -clusters for \mathfrak{S}_α . We now give a combinatorial model for the \bar{c} -clusters of \mathfrak{S}_α combining the ideas from [44] with those of [165]. Recall the permutation sum from (2.13), and consider the permutation

$$w_{(\alpha)} \stackrel{\text{def}}{=} 1 \oplus w_{\circ; \alpha}.$$

Since $w_{\circ; \alpha}$ is clearly 132-avoiding, Theorem 2.4.14 states that $(\text{Pipe}(w_{(\alpha)}), \leq_{\text{chute}})$ is a lattice.

As described in [44, Section 5.3], the α -Dyck paths correspond bijectively to the elements of $\text{Pipe}(w_{(\alpha)})$.

Theorem 4.1.12 ([44, Proposition 16(2)]). For every composition α of $n > 0$, there exists a bijection

$$(4.6) \quad \Psi_{\text{pipe}}: \text{Dyck}(\alpha) \rightarrow \text{Pipe}(w_{(\alpha)}).$$

We describe this bijection only briefly, and refer to [44, Section 3.2] for the details. Let $p \in \text{Dyck}(\alpha)$. Starting from the origin, we flush every lattice point on p as far right as possible

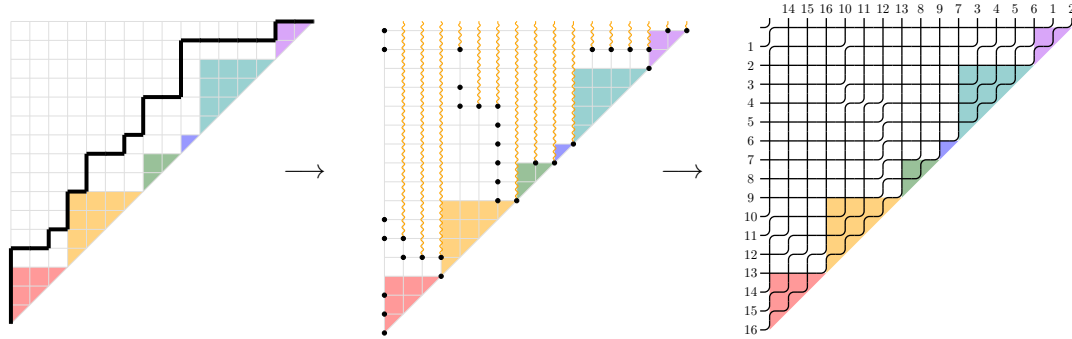


Figure 45. Right-flushing of an α -Dyck path produces a pipe dream for $w_{\langle\alpha\rangle}$; illustrated when $\alpha = (3, 4, 2, 1, 4, 2)$.

while staying inside the α -shape and avoiding blocked columns. After flushing all lattice points of y -coordinate i , every such lattice point, except for the leftmost one, blocks its column for lattice points of bigger y -coordinate. When we have flushed every lattice point of p , we replace each occupied lattice point in the α -shape by an elbow and every unoccupied lattice point by a cross. We also fill every lattice point outside the α -shape with an elbow. The inverse procedure proceeds by flushing to the left and blocking all columns except the rightmost one. Figure 45 illustrates this map.

In fact, the correspondence described in Theorem 2.4.12 can be reused to construct a bijection from $\text{Pipe}(w_{\langle\bar{\alpha}\rangle})$ to the facets of $\text{Clus}(\mathfrak{S}_\alpha, \bar{c})$.

Theorem 4.1.13. *Let α be a composition of $n > 0$. For $P \in \text{Pipe}(w_{\langle\bar{\alpha}\rangle})$, the set of labels of the boxes inside $\lambda_{\bar{\alpha}}$ containing the elbows of P is a facet of $\text{Clus}(\mathfrak{S}_\alpha, \bar{c})$, and this correspondence is bijective.*

PROOF. By Lemma 4.1.4, the \bar{c} -sorting word for $w_{\circ;\alpha}$ can be read from a particular labeling of the conjugate α -shape $\lambda_{\bar{\alpha}}$. Since the facets of $\text{Clus}(\mathfrak{S}_\alpha)$ are complements of $w_{\circ;\alpha}$ in $w_{\circ}(\bar{c})$, we can reuse the labeling of the staircase shape, see for instance Figure 26, and use the restriction of the bijection from Theorem 2.4.12 (which sends elbows to positions of the complement) to obtain a map from $\text{Pipe}(w_{\langle\bar{\alpha}\rangle})$ to the set of facets of $\text{Clus}(\mathfrak{S}_\alpha, \bar{c})$. The fact that this map is a bijection follows analogously to the proof of Theorem 2.4.12. \square

Example 4.1.14. *Let $\alpha = (2, 1, 1)$. We have $w_{\circ;\alpha} = \mathbf{3} \mathbf{4} \mathbf{2} \mathbf{1}$. Then, $\lambda_{\bar{\alpha}} = (2, 2, 1)$, and by Lemma 4.1.4 we get $w_{\circ;\alpha}(\bar{c}) = s_1 s_2 s_1 s_3 s_2$. The S -reduced words for $w_{\circ;\alpha}$ are*

$$s_2 s_1 s_3 s_2 s_3, \quad s_1 s_2 s_1 s_3 s_2, \quad s_1 s_2 s_3 s_1 s_2, \quad s_2 s_1 s_2 s_3 s_2, \quad s_2 s_3 s_1 s_2 s_3.$$

Given $Q = s_1 s_2 s_3 s_1 s_2 s_3 s_1 s_2 s_1$, we find that S -reduced words for $w_{\circ;\alpha}$ appear nine times as subwords of Q :

$$\begin{aligned} & s_1 s_2 s_3 s_1 s_2 s_3 s_1 s_2 s_1, \quad s_1 s_2 s_3 s_1 s_2 s_3 s_1 s_2 s_1, \quad s_1 s_2 s_3 s_1 s_2 s_3 s_1 s_2 s_1, \quad s_1 s_2 s_3 s_1 s_2 s_3 s_1 s_2 s_1, \\ & s_1 s_2 s_3 s_1 s_2 s_3 s_1 s_2 s_1, \quad s_1 s_2 s_3 s_1 s_2 s_3 s_1 s_2 s_1, \quad s_1 s_2 s_3 s_1 s_2 s_3 s_1 s_2 s_1, \quad s_1 s_2 s_3 s_1 s_2 s_3 s_1 s_2 s_1, \\ & s_1 s_2 s_3 s_1 s_2 s_3 s_1 s_2 s_1. \end{aligned}$$

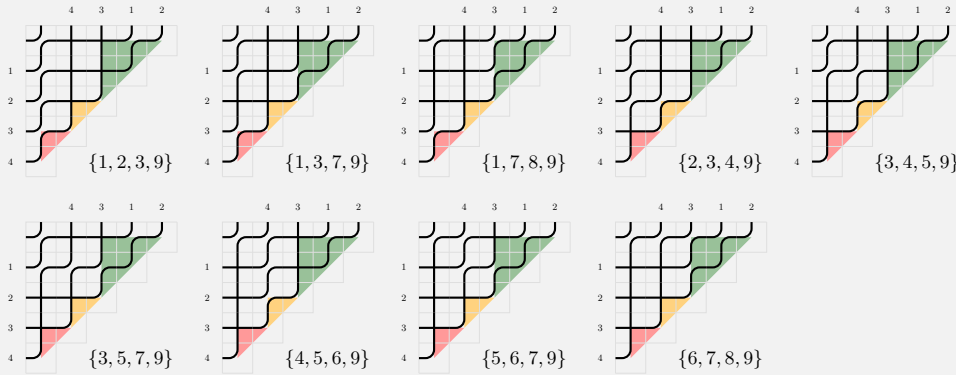
Thus, the facets of $\text{Clus}(\mathfrak{S}_\alpha, \vec{c})$ are

- $\{1, 2, 3, 9\}, \{1, 3, 7, 9\}, \{1, 7, 8, 9\}, \{2, 3, 4, 9\}, \{3, 4, 5, 9\},$
 $\{3, 5, 7, 9\}, \{4, 5, 6, 9\}, \{5, 6, 7, 9\}, \{6, 7, 8, 9\}.$

We label the staircase shape of order 5 as follows:



Mapping each elbow inside the $\bar{\alpha}$ -shape to the corresponding box label creates the correspondence between the nine pipe dreams of $w_{\bar{\alpha}}$ and the nine facets of $\text{Clus}(\mathfrak{S}_\alpha, \vec{c})$:



4.1.5. \vec{c} -aligned elements for \mathfrak{S}_α . Let $w_{\circ;\alpha}(\vec{c})$ be the \vec{c} -sorting word of $w_{\circ;\alpha}$ as defined in Lemma 4.1.4. We have explained in Example 4.1.5 how we can obtain $w_{\circ;\alpha}(\vec{c})$ from a particular labeling of λ_α . Moreover, we have explained in Example 4.1.6 how to obtain the root poset of \mathfrak{S}_α from another labeling of λ_α . If we put this together, we obtain the inversion order $\text{Inv}(w_{\circ;\alpha}(\vec{c}))$. In fact, we consider the labeling of λ_α by the α -root poset, and read the columns of same length (from left to right) as a block. The columns per block are read from right to left and inside a column we read the labels from bottom to top.

Example 4.1.15. We repeat the α -root poset inscribed in the α -shape for $\alpha = (2, 4, 1, 3)$ as shown in Example 4.1.6, but added the reading order this time. In this example, we read the columns from bottom to top in the order 2, 1, 6, 5, 4, 3, 7.

We write \prec_α for the inversion order $\mathbf{Inv}(w_{\circ;\alpha}(\bar{c}))$, and obtain

(2, 3)	\prec_α	(2, 4)	\prec_α	(2, 5)	\prec_α	(2, 6)	\prec_α	(2, 7)	\prec_α	(2, 8)	\prec_α	(2, 9)
	\prec_α	(2, 10)	\prec_α	(1, 3)	\prec_α	(1, 4)	\prec_α	(1, 5)	\prec_α	(1, 6)	\prec_α	(1, 7)
	\prec_α	(1, 8)	\prec_α	(1, 9)	\prec_α	(1, 10)	\prec_α	(6, 7)	\prec_α	(6, 8)	\prec_α	(6, 9)
	\prec_α	(6, 10)	\prec_α	(5, 7)	\prec_α	(5, 8)	\prec_α	(5, 9)	\prec_α	(5, 10)	\prec_α	(4, 7)
	\prec_α	(4, 8)	\prec_α	(4, 9)	\prec_α	(4, 10)	\prec_α	(3, 7)	\prec_α	(3, 8)	\prec_α	(3, 9)
	\prec_α	(3, 10)	\prec_α	(7, 8)	\prec_α	(7, 9)	\prec_α	(7, 10)				

This can also be verified directly using the \bar{c} -sorting word of $w_{\circ;\alpha}$ computed in Example 4.1.5.

Recall from Section 2.5 that a transposition $(i j) \in \mathfrak{S}_n$ corresponds bijectively to the positive root $\alpha_i + \alpha_{i+1} + \dots + \alpha_j$ of type A_{n-1} ¹¹. Thus, $\beta, \beta_1, \beta_2 \in \Phi_{A_{n-1}}^+$ satisfy $\beta_1 + \beta_2 = \beta$ if and only if β corresponds to the transposition $(i k)$ for some $i < k$ and $\{\beta_1, \beta_2\}$ corresponds to $\{(i j), (j k)\}$ for $i < j < k$. Such compositions of roots can be recovered in the labeling of the Ferrers shape associated with the parabolic quotient of A_{n-1} as follows: if β is the label of the cell in row a and column b , then $\{\beta_1, \beta_2\}$ is the set of labels of the cells in column b and row $a - d$ as well as in row a and column $b + d$.

With respect to the inversion order $\mathbf{Inv}(w_{\circ;\alpha}(\bar{c}))$ ¹² this means the following: if β, β_1, β_2 are roots as above, then $\beta_1 \prec_\alpha \beta \prec_\alpha \beta_2$ if β_1 corresponds to $(i j)$ and β_2 corresponds to $(j k)$. Thus, even though $\mathbf{Inv}(w_{\circ;\alpha}(\bar{c}))$ is in general *not* the lexicographic order on the set of transpositions of \mathfrak{S}_α —see Example 4.1.15—every triple of transpositions corresponding to roots $\beta, \beta_1, \beta_2 \in \Phi_{A_{n-1}}^+$ with $\beta = \beta_1 + \beta_2$ is ordered lexicographically.

Let $\alpha = (\alpha_1, \alpha_2, \dots, \alpha_r) \vdash n$. For $i \in [r]$, the set $\{p_{i-1}+1, p_{i-1}+2, \dots, p_i\}$ is the i^{th} α -region. For $a \in [n]$ we write $\text{reg}_\alpha(a) \stackrel{\text{def}}{=} i$ if $p_{i-1} < a \leq p_i$. In other words, $\text{reg}_\alpha(a) = i$ if a belongs to the i^{th} α -region.

We say that $\mathbf{Inv}(w)$ is α -aligned if $(i, k) \in \text{Cov}(w)$ implies $(i, j) \in \mathbf{Inv}(w)$ whenever $i < j < k$ and $\text{reg}_\alpha(i) < \text{reg}_\alpha(j) < \text{reg}_\alpha(k)$. The reasoning above implies the following result.

Lemma 4.1.16. *A permutation $w \in \mathfrak{S}_\alpha$ is $(\mathfrak{S}_\alpha, \bar{c})$ -aligned if and only if $\mathbf{Inv}(w)$ is α -aligned.*

¹¹In this paragraph, α_i is the i^{th} simple root of type A .

¹²Now, α is a composition again.

We now give a combinatorial interpretation of α -alignment. Recall that $(i, k) \in \text{Cov}(w)$ if $i < k$ and $w_i = w_k + 1$. If $\text{Inv}(w)$ is α -aligned, then there can be no $j \in \{i+1, i+2, \dots, k-1\}$ with $\text{reg}_\alpha(i) < \text{reg}_\alpha(j) < \text{reg}_\alpha(k)$ such that $w_j > w_i$. We thus say that $w \in \mathfrak{S}_\alpha$ has an $(\alpha, 231)$ -pattern if there exist indices $i < j < k$ with $\text{reg}_\alpha(i) < \text{reg}_\alpha(j) < \text{reg}_\alpha(k)$ such that $w_i = w_k + 1$ and $w_i < w_j$. Moreover, $w \in \mathfrak{S}_\alpha$ is $(\alpha, 231)$ -avoiding if it does not have an $(\alpha, 231)$ -pattern. We write

$$\mathfrak{S}_\alpha(231) \stackrel{\text{def}}{=} \{w \in \mathfrak{S}_\alpha \mid w \text{ is } (\alpha, 231)\text{-avoiding}\}.$$

Lemma 4.1.17. *A permutation $w \in \mathfrak{S}_\alpha$ is $(\alpha, 231)$ -avoiding if and only if $\text{Inv}(w)$ is α -aligned.*

PROOF. Suppose that $w \in \mathfrak{S}_\alpha$ is $(\alpha, 231)$ -avoiding. If $(i, k) \in \text{Cov}(w)$, then for every $j \in \{i+1, i+2, \dots, k-1\}$ with $\text{reg}_\alpha(i) < \text{reg}_\alpha(j) < \text{reg}_\alpha(k)$ we have that $(i, j) \in \text{Inv}(w_{\circ; \alpha})$ and $w_i > w_j$. Thus, $(i, j) \in \text{Inv}(w)$ for any such j , meaning that $\text{Inv}(w)$ is α -aligned. If w has an $(\alpha, 231)$ -pattern, say in positions $i < j < k$, then $(i, k) \in \text{Cov}(w)$ and $(i, j) \notin \text{Inv}(w)$. Since i and j belong to different α -regions, it follows that $(i, j) \in \text{Inv}(w_{\circ; \alpha})$, meaning that $\text{Inv}(w)$ is not α -aligned. \square

Example 4.1.18. *Let $\alpha = (1, 2, 1)$. We have listed the twelve $(1, 2, 1)$ -permutations in Example 4.1.2. We now list these permutations again together with their (cover) inversions, and we conclude which elements belong to $\mathfrak{S}_{(1,2,1)}(231)$. See also Example 3.4.5 and Figure 37a.*

$w \in \mathfrak{S}_{(1,2,1)}$	$\text{Inv}(w)$	$\text{Cov}(w)$	$w \in \mathfrak{S}_{(1,2,1)}(231)$
1 2 3 4	\emptyset	\emptyset	yes
1 2 4 3	$\{(3, 4)\}$	$\{(3, 4)\}$	yes
1 3 4 2	$\{(2, 4), (3, 4)\}$	$\{(2, 4)\}$	yes
2 1 3 4	$\{(1, 2)\}$	$\{(1, 2)\}$	yes
2 1 4 3	$\{(1, 2), (3, 4)\}$	$\{(1, 2), (3, 4)\}$	yes
2 3 4 1	$\{(1, 4), (2, 4), (3, 4)\}$	$\{(1, 4)\}$	no
3 1 2 4	$\{(1, 2), (1, 3)\}$	$\{(1, 3)\}$	yes
3 1 4 2	$\{(1, 2), (1, 4), (3, 4)\}$	$\{(1, 4)\}$	no
3 2 4 1	$\{(1, 2), (1, 4), (2, 4), (3, 4)\}$	$\{(1, 2), (2, 4)\}$	yes
4 1 2 3	$\{(1, 2), (1, 3), (1, 4)\}$	$\{(1, 4)\}$	yes
4 1 3 2	$\{(1, 2), (1, 3), (1, 4), (3, 4)\}$	$\{(1, 3), (3, 4)\}$	yes
4 2 3 1	$\{(1, 2), (1, 3), (1, 4), (2, 4), (3, 4)\}$	$\{(1, 3), (2, 4)\}$	yes

We observe that the permutation **3 2 4 1** is not 231-avoiding in the classical sense; see Section 2.2. It has two 231-patterns, one in positions $(1, 3, 4)$ and one in $(2, 3, 4)$. These are, however, not harmful in the parabolic setting, because in the first case, the “2” and the “1” do not form a descent, and in the second case, the “2” and the “3” are in the same α -region.

Remark 4.1.19. *A different notion of parabolic pattern avoidance was given at about the same time by R. PROCTOR and M. WILLIS. Following [146], for $R = \{j_1, j_2, \dots, j_r\} \subseteq [n]$ a permutation $w \in \mathfrak{S}_n$ is R -312-containing if there exists $h \in [r-1]$ and $a, b, c \in [n]$ with*

$a \leq j_h < b \leq j_{h+1} < c$ such that $w_b < w_c < w_a$. If w is not R-312-containing, then it is R-312-avoiding. PROCTOR and WILLIS suggested the name R-parabolic Catalan number for the cardinality of the set of all R-312-avoiding permutations [145]. Several combinatorial structures counted by these numbers were given in [145, 146].

It is straightforward to define R-231-avoiding permutations in the above sense. However, this definition is more restrictive than our definition of $(\alpha, 231)$ -avoidance. For instance, when $\alpha = (1, 2, 1)$, then the permutation $\boxed{3} \boxed{2} \boxed{4} \boxed{1}$ is $\{1, 3\}$ -231-containing because it contains a 231-pattern in positions (1, 3, 4). However, since the difference of the first and the last entry is bigger than 1, it is not an $((1, 2, 1), 231)$ -pattern.

4.1.6. \bar{c} -noncrossing partitions for \mathfrak{S}_α . By Definition 3.3.1, \bar{c} -noncrossing partitions for \mathfrak{S}_α are obtained by multiplying the cover inversions of the elements of \mathfrak{S}_α in order of their appearance in $\text{Inv}(w_{\circ, \alpha}(\bar{c}))$. Recall that cover inversions in type A are exactly the descents of a permutation. Drawing inspiration from the ordinary case, we wish to represent a descent (a, b) by an arc connecting nodes labeled a and b so that the descents of $w \in \mathfrak{S}_\alpha(231)$ produce a collection of noncrossing arcs of some sort.

Now, no element of \mathfrak{S}_α can have a descent (a, b) , where a and b belong to the same α -region. We thus define an ordinary partition $P \in \Pi_n$ to be an α -partition if no block of P intersects an α -region in more than one element. We write Π_α for the set of α -partitions.

However, our definition of $(\alpha, 231)$ -avoiding permutations makes it perfectly possible for $w \in \mathfrak{S}_\alpha(231)$ to have descents (a_1, b_1) and (a_2, b_2) with $a_1 < a_2 < b_1 < b_2$ —at least when either a_1 and a_2 or a_2 and b_1 belong to the same α -region. Thus, drawing the bumps corresponding to these descents analogously to the ordinary case would produce a crossing between these bumps. It turns out that the following definition makes perfect sense. An α -partition $P \in \Pi_\alpha$ is *noncrossing* if for any two bumps $(a_1, b_1), (a_2, b_2)$ of P it holds that:

- (NC1): if $a_1 < a_2 < b_1 < b_2$, then either a_1 and a_2 lie in the same α -region or b_1 and a_2 lie in the same α -region;
- (NC2): if $a_1 < a_2 < b_2 < b_1$, then a_1 and a_2 lie in different α -regions.

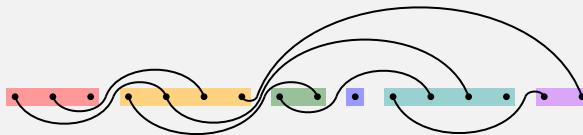
We write $\text{Nonc}(\alpha)$ for the set of noncrossing α -partitions.

If we wish to represent a noncrossing α -partition by a diagram consisting of a collection of arcs, we have to adapt the diagram of an ordinary partition as follows. We first draw n nodes labeled by $1, 2, \dots, n$ on a horizontal line. If (a, b) is a bump of $P \in \Pi_\alpha$, then we draw a curve that leaves the node labeled a to the bottom, stays below the α -region containing a , proceeds above every subsequent α -region until it enters the node labeled b from above. Such a curve is called an α -arc. Then, it is not hard to see that $P \in \Pi_\alpha$ is noncrossing if and only if its diagram can be drawn in such a way that no two arcs intersect in their interior.

Example 4.1.20. Let $\alpha = (3, 4, 2, 1, 4, 2) \vdash 16$. We consider the α -partition P , given by

$$P = \left\{ \{1, 5, 13\}, \{2, 6\}, \{3\}, \{4, 9\}, \{7, 16\}, \{8, 12\}, \{10\}, \{11, 15\}, \{14\} \right\}.$$

Its diagram, shown below, indicates that P is indeed noncrossing.



Since $\text{Nonc}(\alpha) \subseteq \Pi_n$, we may consider these partitions ordered by refinement. The resulting poset is $\mathbf{Nonc}(\alpha) \stackrel{\text{def}}{=} (\text{Nonc}(\alpha), \leq_{\text{ref}})$. At the moment, unfortunately, we do not have much to say about these posets.

Proposition 4.1.21. *For $\alpha \vdash n$, the poset $\mathbf{Nonc}(\alpha)$ is bounded if and only if $\alpha = (n)$ or $\alpha = (1, 1, \dots, 1)$.*

PROOF. If $\alpha = (n)$, then Π_α consists only of the discrete partition, i.e., the partition where every block is a singleton. If $\alpha = (1, 1, \dots, 1)$, then the full partition, i.e., the partition whose only block is $[n]$, is certainly noncrossing, and must therefore be the maximal element of $\mathbf{Nonc}(\alpha)$.

Now, conversely, let $\alpha = (\alpha_1, \alpha_2, \dots, \alpha_r)$ and suppose that $r > 1$ and $\alpha_1 > 1$. Let P_1 be the α -partition, in which the first element of each α -region is connected by an arc with the last element of the subsequent α -region. Let P_2 be the α -partition, in which the last element of each α -region is connected by an arc with the first element of the subsequent α -region. By assumption, $P_1 \neq P_2$. Clearly, P_1 and P_2 are noncrossing and maximal in $\mathbf{Nonc}(\alpha)$. This finishes the proof. \square

However, it turns out that $\mathbf{Nonc}(\alpha)$ is in general not a meet-semilattice¹³.

Example 4.1.22. *Let $\alpha = (2, 4, 3, 1)$, and consider the noncrossing α -partitions*

$$P_1 = \left\{ \{1, 3, 8, 10\}, \{2, 6, 9\}, \{4\}, \{5\}, \{7\} \right\},$$

$$P_2 = \left\{ \{1, 4, 7, 10\}, \{2, 5, 9\}, \{3\}, \{6\}, \{8\} \right\}.$$

The intersection of P_1 and P_2 is

$$P = \left\{ \{1, 10\}, \{2, 9\}, \{3\}, \{4\}, \{5\}, \{6\}, \{7\}, \{8\} \right\} \notin \mathbf{Nonc}(\alpha).$$

Moreover, if we consider

$$Q_1 = \left\{ \{1, 10\}, \{2\}, \{3\}, \{4\}, \{5\}, \{6\}, \{7\}, \{8\}, \{9\} \right\},$$

$$Q_2 = \left\{ \{1\}, \{2, 9\}, \{3\}, \{4\}, \{5\}, \{6\}, \{7\}, \{8\}, \{10\} \right\},$$

then $Q_i \in \mathbf{Nonc}(\alpha)$ and $Q_i \leq_{\text{ref}} P_j$ for $i, j \in \{1, 2\}$. Since Q_1 and Q_2 are mutually incomparable, $\mathbf{Nonc}(\alpha)$ is not a meet-semilattice.

4.1.7. α -trees. In this section we introduce a family of colored trees parametrized by a composition α that fits nicely into the linear type-A part of Parabolic Cataland. We have not mentioned trees earlier in this thesis, because we are not aware of analogues of trees in the context of Coxeter groups. However, these trees play an important role in the applications of Parabolic Cataland in linear type A to Hopf algebras and diagonal harmonics that we will present in Section 4.5.

Recall that a *tree* is a connected, acyclic graph. We usually refer to the vertices of a tree as *nodes*, and consider *rooted* trees, i.e., trees with a distinguished node, the *root*. Rooted trees allow for a “descendance” relation among its nodes. We say that a node u is a *descendant* of a node v if v lies on the unique path from the root to u . If u is a descendant of v and u and v are adjacent nodes, then u is a *child* of v and v is the *parent* of u . Nodes that have the same

¹³This counterexample was provided by a referee of [132].

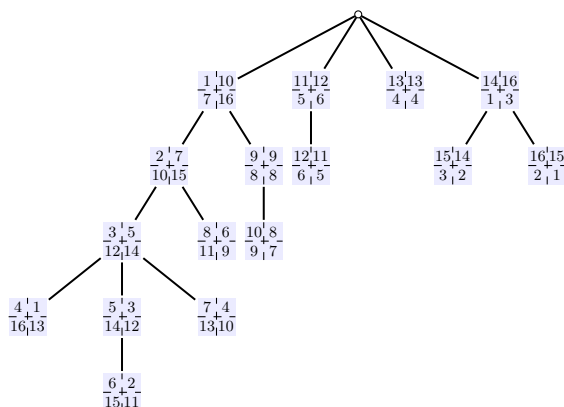


Figure 46. Illustrating the various traversals of a plane rooted tree.

parent are *siblings*. A *leaf* is a node without children. A node that is neither a leaf nor the root is *internal*.

A *plane* tree is a tree together with an embedding in the plane. For a plane rooted tree, we may therefore order the children of each node from left to right. A *left-to-right traversal* (resp. *right-to-left traversal*) of a plane rooted tree is a depth-first search starting from the root, where the children of the same node are visited from left to right (resp. from right to left). The *LR-prefix order* (resp. *LR-postfix order*) of a plane rooted tree is the linearization of its nodes, where we record the nodes in order of first (resp. last) visits in left-to-right traversal. RL-prefix and RL-postfix orders are defined analogously with respect to right-to-left traversals.

Figure 46 shows a plane rooted tree with 16 non-root nodes. The nodes are labeled according to LR-prefix order (top-left), LR-postfix order (top-right), RL-prefix order (bottom-left) and RL-postfix order (bottom-right).

Lemma 4.1.23. *For a non-root node u in a plane rooted tree T , the next node in T in the LR-postfix order is either its parent, of which u is the last child, or the left-most leaf of the subtree induced by its sibling immediately to the right.*

PROOF. This follows immediately from the definition of the LR-postfix order. \square

Now, let T be a plane rooted tree with node set V whose root node is v_o . A *partial coloring* is a map $\gamma: V' \rightarrow \mathbb{N}$ for some $V' \subseteq V \setminus \{v_o\}$. If $V' = V \setminus \{v_o\}$, then γ is a *full coloring*. A *colored tree* is a pair (T, γ) , where γ is a full coloring of a plane rooted tree T . We refer to the elements in the image of γ as γ -*colors*.

A node $v \in V \setminus \{v_o\}$ is *active* with respect to a partial coloring γ on $V' \subseteq V \setminus \{v_o\}$ if $v \notin V'$ and its parent belongs to $V' \cup \{v_o\}$.

The following algorithm attempts to color a plane rooted tree with n non-root nodes by a composition of n .

Construction 4.1.24. *Let $n > 0$ and fix a composition $\alpha = (\alpha_1, \alpha_2, \dots, \alpha_r)$ of n . Let T be a plane rooted tree with n non-root nodes. Initially, we consider the empty coloring γ_0 of T , and set $V_0 = \emptyset$. In the i^{th} step of this algorithm, we denote by A_i the set of active nodes with respect to the partial coloring γ_{i-1} .*

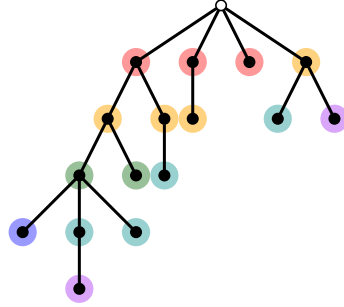


Figure 47. A plane rooted tree compatible with $\alpha = (3, 4, 2, 1, 4, 2)$.

If $|A_i| < \alpha_i$, then the algorithm fails. Otherwise, let F_i denote the set of the first α_i elements of A_i in the LR-prefix order of T . We set $V_i = V_{i-1} \uplus F_i$, and we define the partial coloring $\gamma_i: V_i \rightarrow \mathbb{N}$ by

$$\gamma_i(v) \stackrel{\text{def}}{=} \begin{cases} \gamma_{i-1}(v), & \text{if } v \in V_{i-1}, \\ i, & \text{if } v \in F_i. \end{cases}$$

If the algorithm has not failed after r steps, we return the colored tree (T, γ_r) .

A plane rooted tree T is *compatible* with α if Construction 4.1.24 does not fail. Such trees are also called *α -trees*, and we write $\text{Tree}(\alpha)$ for the set of all α -trees. The full coloring of T constructed in Construction 4.1.24 (if successful) is the *α -coloring* of T .

Figure 47 shows a plane rooted tree compatible with $\alpha = (3, 4, 2, 1, 4, 2)$. Note that this tree is not compatible with $\alpha' = (5, 3, 1, 2, 4, 1)$, because its root has less than five children. It is also not compatible with $\alpha'' = (4, 3, 6, 3)$, because Construction 4.1.24 fails in the third step.

Note that if $\alpha = (1, 1, \dots, 1) \vdash n$, then any plane rooted tree is compatible with α . Moreover, any plane rooted tree T is compatible with its *horizontal* composition $\alpha_T = (\alpha_1, \alpha_2, \dots)$, where α_i equals the number of nodes of T whose distance to the root is exactly i .

Two nodes in a tree are *comparable* if one is a descendant of the other, and *incomparable* otherwise.

Lemma 4.1.25. *Every α -tree has the following properties.*

- (i) *The color of every node is smaller than the color of its children, and the nodes of the same color are incomparable.*
- (ii) *The active nodes in each step of Construction 4.1.24 will eventually receive colors that are weakly increasing in LR-prefix order.*

PROOF. The first property follows from the fact that a node becomes active before its children do. The second property follows from the construction of the coloring, where active nodes are selected for coloring in LR-prefix order always starting from the first active node. \square

4.2. Bijections

In this section we relate the four families associated with a composition α bijectively. The results from this section have appeared in [45, 133]. In fact, we prove the following theorem, illustrated in Figure 48, bijectively.

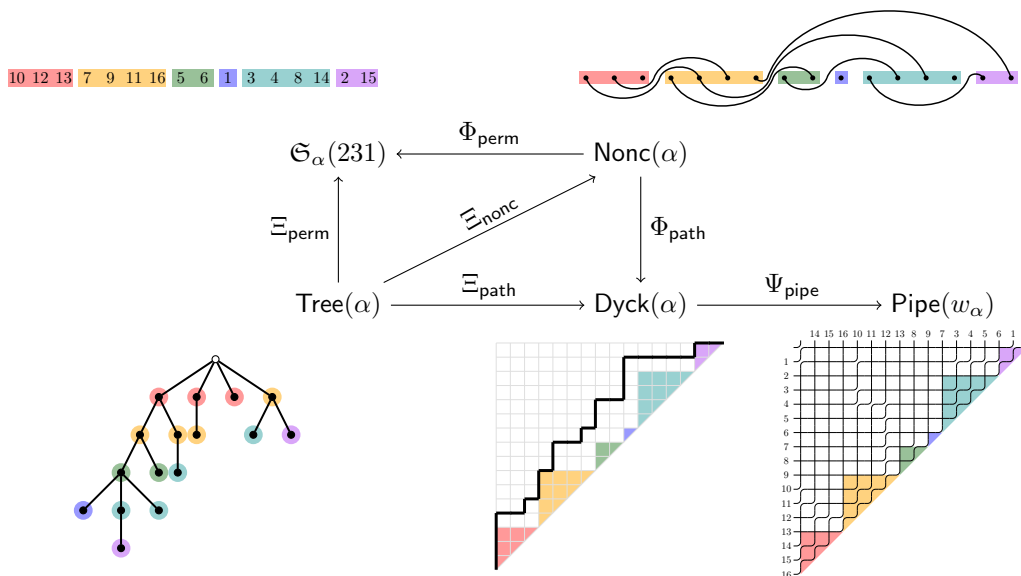


Figure 48. A commuting diagram of bijections illustrated on an example for $\alpha = (3, 4, 2, 1, 4, 2)$.

Theorem 4.2.1. *Let $n > 0$ and let α be a composition of n . Then,*

$$|\text{Dyck}(\alpha)| = |\mathfrak{S}_\alpha(231)| = |\text{Nonc}(\alpha)| = |\text{Tree}(\alpha)|.$$

4.2.1. Noncrossing α -partitions and $(\alpha, 231)$ -avoiding permutations. In this section we present a bijection from $\text{Nonc}(\alpha)$ to $\mathfrak{S}_\alpha(231)$. Recall that any partition $P \in \Pi_n$ is determined by its set of bumps. We write $\text{Bump}(P)$ for the set of bumps of P . The main result of this section states the existence of a bijection from $\text{Nonc}(\alpha)$ to $\mathfrak{S}_\alpha(231)$ that sends bumps to descents.

Theorem 4.2.2. *For every composition α of $n > 0$ there exists a bijection*

$$(4.7) \quad \Phi_{\text{perm}}: \text{Nonc}(\alpha) \rightarrow \mathfrak{S}_\alpha(231)$$

that sends bumps to descents.

In order to prove Theorem 4.2.2, we first define a partial order on the blocks of $P = \{B_1, B_2, \dots, B_k\} \in \text{Nonc}(\alpha)$. We say that a block B_j *starts below* a block B_i if there exists a bump $(a, b) \in \text{Bump}(P)$ with $a, b \in B_i$ such that $a < \min B_j < b$ and $\text{reg}_\alpha(a) < \text{reg}_\alpha(\min B_j)$. Graphically, this means that the node corresponding to the smallest element of B_j lies below the arc corresponding to (a, b) in the diagram of P . We define a binary relation $\vec{R}_P \subseteq P \times P$ by

$$\vec{R}_P \stackrel{\text{def}}{=} \{(B_i, B_j) \mid i, j \in [k], B_j \text{ starts below } B_i\}.$$

If $(B_i, B_j) \in \vec{R}_P$, then $\min B_i < \min B_j$. Therefore, \vec{R}_P is acyclic and can be extended to an order relation \vec{O}_P by taking the reflexive and transitive closure.

Proposition 4.2.3. *For every $P \in \text{Nonc}(\alpha)$, there exists a naturally associated permutation $w_P \in \mathfrak{S}_\alpha(231)$. Moreover, the bumps of P correspond to the descents of w_P .*

PROOF. Let $P \in \text{Nonc}(\alpha)$ and let B_o be the unique block of P containing 1. More precisely, let $B_o = \{a_1, a_2, \dots, a_k\}$ such that $1 = a_1 < a_2 < \dots < a_k$. Let

$$D = \bigcup \{B \in P \mid (B_o, B) \in \vec{O}_P\}$$

denote the set of elements of $[n]$ that lie in the order filter of \vec{O}_P generated by B_o . We construct an α -permutation w_P by setting $w_P(1) = |D|$, and $w_P(a_{i+1}) = w_P(a_i) - 1$ for $i \in [k-1]$. In particular, every bump of P that belongs to B_o is a descent of w_P .

Now, we break P into two smaller pieces

$$\begin{aligned} P_1 &= \{B \cap D \mid B \in P \setminus B_o\} \setminus \{\emptyset\}, \\ P_2 &= \{B \cap ([n] \setminus D) \mid B \in P \setminus B_o\} \setminus \{\emptyset\}. \end{aligned}$$

In terms of \vec{O}_P , the partition P_1 consists of the blocks strictly greater than B_o and P_2 consists of the blocks that do not belong to the order filter generated by B_o . Clearly, $P_1 \in \text{Nonc}(\alpha^{(1)})$ and $P_2 \in \text{Nonc}(\alpha^{(2)})$ for compositions $\alpha^{(1)} \vdash n_1 = |D| - k$ and $\alpha^{(2)} \vdash n_2 = n - |D|$ with $n_1, n_2 < n$. Recursively, we obtain permutations $w_{P_1} \in \mathfrak{S}_{\alpha^{(1)}}(231)$ and $w_{P_2} \in \mathfrak{S}_{\alpha^{(2)}}(231)$ from P_1 and P_2 , respectively. The initial condition for this recursion associates the identity permutation with the discrete partition.

We now embed w_{P_1} and w_{P_2} into w_P , where we have to increase the values of w_{P_2} by $|D|$. Note that the values of w_{P_1} are smaller than $|D|$; thus w_P is $(\alpha, 231)$ -avoiding. Moreover, the descents of w_P correspond to the bumps of P . By Proposition 4.3.50, any $w \in \mathfrak{S}_\alpha(231)$ is uniquely determined by $\text{Cov}(w)$. \square

Note that the proof of Proposition 4.2.3 uses Proposition 4.3.50 that is deferred to a later section. However, Proposition 4.3.50 does not use any of the results of this section.

For $P \in \text{Nonc}(\alpha)$, we set $\Phi_{\text{perm}}(P) = w_P$. Proposition 4.2.3 thus describes the action of the map Φ_{perm} and shows, in fact, that it is injective. This is illustrated in Figure 49. We now conclude the proof of Theorem 4.2.2.

PROOF OF THEOREM 4.2.2. It remains to show that Φ_{perm} is a bijection. Let $w \in \mathfrak{S}_\alpha(231)$, with $\text{Cov}(w) = \{(a_1, b_1), (a_2, b_2), \dots, (a_k, b_k)\}$. Since $w \in \mathfrak{S}_\alpha$, it follows that $\text{reg}_\alpha(a_i) \neq \text{reg}_\alpha(b_i)$ for all $i \in [k]$, and $a_i \neq a_j$ whenever $i \neq j$ as well as $b_i \neq b_j$ whenever $i \neq j$. Thus, there exists an α -partition P_w with $\text{Bump}(P_w) = \{(a_1, b_1), (a_2, b_2), \dots, (a_k, b_k)\}$.

First, assume that P_w does not satisfy (NC1). Thus, there exist indices $i, j \in [k]$ with $i < j$ such that $a_i < a_j < b_i < b_j$ and a_i, a_j, b_i lie in different α -regions. Since $w \in \mathfrak{S}_\alpha(231)$, it follows that $w_{a_i} > w_{a_j}$ (because otherwise w would have an $(\alpha, 231)$ -pattern in positions (a_i, a_j, b_i)). Since w is a permutation and $(a_i, b_i), (a_j, b_j) \in \text{Cov}(w)$, this implies $w_{b_i} = w_{a_i} - 1 > w_{a_j} > w_{b_j}$. Since $b_i < b_j$, Lemma 4.1.1 implies that b_i and b_j lie in different α -regions, too. But then, w has an $(\alpha, 231)$ -pattern in positions (a_j, b_i, b_j) , which is a contradiction. Thus, P_w satisfies (NC1).

Now, assume that P_w does not satisfy (NC2). Thus, there exist indices $i, j \in [k]$ with $i < j$ such that $a_i < a_j < b_j < b_i$ and a_i and a_j lie in the same α -region. By Lemma 4.1.1, $w_{a_i} < w_{a_j}$. Since w is a permutation and $(a_i, b_i), (a_j, b_j) \in \text{Cov}(w)$, it follows that $w_{a_j} > w_{b_j} > w_{a_i} > w_{b_i}$. Once again, Lemma 4.1.1 now implies that a_i, b_j, b_i lie in

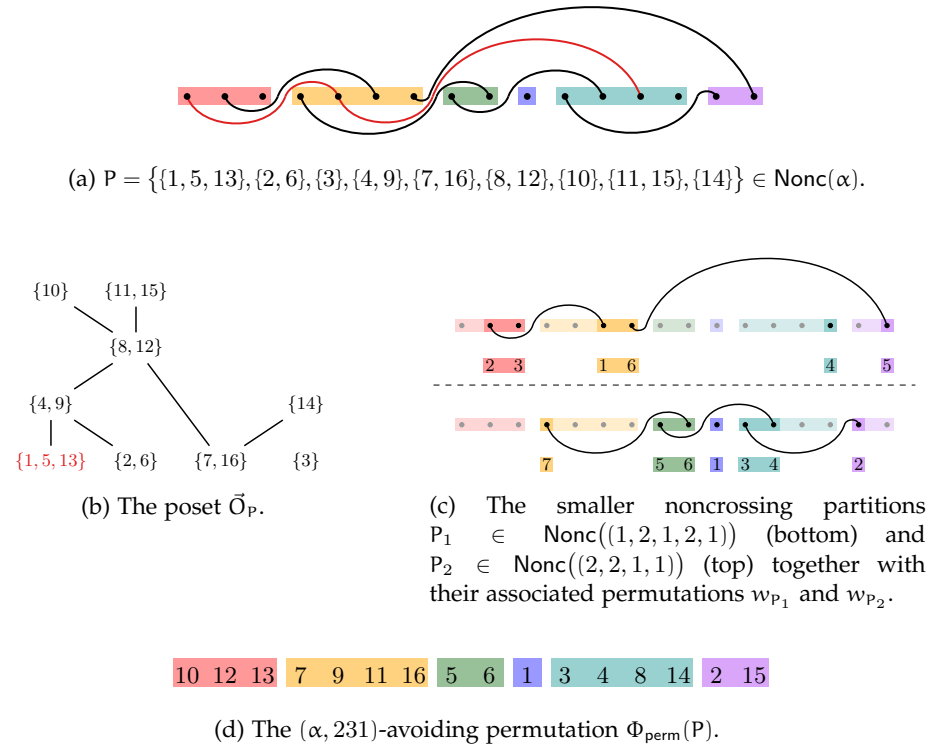


Figure 49. An illustration of the bijection Φ_{perm} for $\alpha = (3, 4, 2, 1, 4, 2)$.

three different α -regions. But then, w has an $(\alpha, 231)$ -pattern in positions (a_i, b_j, b_i) , which is a contradiction. Thus, P_w satisfies (NC2).

It follows that $P_w \in \text{Nonc}(\alpha)$. Together with Proposition 4.2.3 follows that $P_w = \Phi_{\text{perm}}^{-1}(w)$. Since $P \in \text{Nonc}(\alpha)$ is completely determined by $\text{Bump}(P)$, and $w \in \mathfrak{S}_\alpha(231)$ is completely determined by $\text{Cov}(w)$ (see Proposition 4.3.50) it follows that Φ_{perm} is a bijection. \square

4.2.2. Noncrossing α -partitions and α -Dyck paths. In this section we present a bijection from $\text{Nonc}(\alpha)$ to $\text{Dyck}(\alpha)$. Recall that $\alpha = (\alpha_1, \alpha_2, \dots, \alpha_r)$, and $p_0 = 0, p_i = \alpha_1 + \alpha_2 + \dots + \alpha_i$ for $i \in [r]$. For $p \in \text{Dyck}(\alpha)$, we denote by $\text{Valley}(p)$ the set of valleys of p , i.e., the set of coordinates (a, b) on p that are preceded by an east step and followed by a north step.

Theorem 4.2.4. For every composition α of $n > 0$ there exists a bijection

$$(4.8) \quad \Phi_{\text{path}}: \text{Nonc}(\alpha) \rightarrow \text{Dyck}(\alpha)$$

that sends bumps to valleys.

Let (a, b) in $\text{Bump}(P)$, and let $i \in [n]$. If $\text{reg}_\alpha(a) = j$, then i is *directly below* (a, b) if $p_j + 1 \leq i \leq b$ and there is no $(a', b') \in \text{Bump}(P)$ with $a' < i < b'$ such that either $\text{reg}_\alpha(a') = \text{reg}_\alpha(a)$ and $a' < a$ or $\text{reg}_\alpha(a) < \text{reg}_\alpha(a')$. Graphically, i is directly below a bump (a, b) , if $b = i$ or (a, b) is the first arc that a vertical line rising from the node labeled i intersects in the diagram of P . In Figure 49a, for instance, 4 is directly below the bump $(1, 5)$ and 10 is directly below

the bump $(8, 12)$. We say that $(a', b') \in \text{Bump}(P)$ is directly below (a, b) if a' is directly below (a, b) .

Proposition 4.2.5. *For every $P \in \text{Nonc}(\alpha)$, there exists a unique $p_P \in \text{Dyck}(\alpha)$. Moreover, the bumps of P correspond to the valleys of p_P .*

PROOF. Let $P \in \text{Nonc}(\alpha)$, and let $\text{Bump}(P) = \{(a_1, b_1), (a_2, b_2), \dots, (a_k, b_k)\}$ be ordered as follows: if $\text{reg}_\alpha(a_i) = \text{reg}_\alpha(a_{i+1})$, then $a_i < a_{i+1}$, and if $\text{reg}_\alpha(a_i) \neq \text{reg}_\alpha(a_{i+1})$, then $a_i > a_{i+1}$ (and thus $\text{reg}_\alpha(a_i) > \text{reg}_\alpha(a_{i+1})$). In other words, we parse the α -regions from right to left and record the bumps with respect to their starting node from left to right within each α -region.

Let $n_0 = n$. For $i \in [k]$, let $\text{reg}_\alpha(a_i) = j_i$. This means, that $p_{j_{i-1}} + 1 \leq a_i \leq p_{j_i}$. Thus, we may write $a_i = p_{j_{i-1}} + l_i$ for some $l_i \in [\alpha_{j_i}]$. We set $m_i = p_{j_i} + 1 - l_i$. Moreover, let d_i denote the number of elements that are directly below the bump (a_i, b_i) . Iteratively, we see that $d_i \leq n_{i-1} - p_{j_i}$, and we set $n_i = n_{i-1} - d_i$. Since the endpoint of a bump is always directly below the bump, $d_i > 0$ for all $i \in [k]$ and thus $n_1 > n_2 > \dots > n_k$.

Note that by our ordering of the bumps, we always have $j_i \geq j_{i+1}$: if $j_i = j_{i+1}$, then $l_i < l_{i+1}$ and thus $m_i > m_{i+1}$. If $j_i > j_{i+1}$, then

$$m_{i+1} = p_{j_{i+1}} + 1 - l_{i+1} < p_{j_{i+1}+1} + 1 \leq p_{j_i-1} + 1 \leq p_{j_i+1-l_i} = m_i.$$

We consider the coordinates (m_i, n_i) for $i \in [k]$. Then, (m_i, n_i) lies above the m_i^{th} east step of v_α . Since this east step has ordinate p_{j_i} , and $n_i \geq n - p_{j_i}$, it follows that (m_i, n_i) lies inside the α -shape λ_α . Thus, the set $\{(m_1, n_1), (m_2, n_2), \dots, (m_k, n_k)\}$ is the set of valleys of some (unique) α -path p_P . \square

Example 4.2.6. Let $\alpha = (3, 4, 2, 1, 4, 2)$ and let P be the noncrossing α -partition from Example 4.1.20. Then,

$$\text{Bump}(P) = \{(1, 5), (2, 6), (4, 9), (5, 13), (7, 16), (8, 12), (11, 15)\}.$$

The following table lists the values computed in the proof of Proposition 4.2.5.

i	(a_i, b_i)	j_i	l_i	d_i	m_i	n_i
1	(11, 15)	5	1	1	14	15
2	(8, 12)	3	1	3	9	12
3	(4, 9)	2	1	2	7	10
4	(5, 13)	2	2	1	6	9
5	(7, 16)	2	4	2	4	7
6	(1, 5)	1	1	2	3	5
7	(2, 6)	1	2	1	2	4

Figure 50 shows the α -path p_P constructed in Proposition 4.2.5. We have

$$\text{Valley}(p_P) = \{(14, 15), (9, 12), (7, 10), (6, 9), (4, 7), (3, 5), (2, 4)\}.$$

For $P \in \text{Nonc}(\alpha)$, we set $\Phi_{\text{path}}(P) = p_P$. Proposition 4.2.5 thus describes the action of the map Φ_{path} and shows, in fact, that it is injective. Example 4.2.6 illustrates the construction of $\Phi_{\text{path}}(P)$. We now conclude the proof of Theorem 4.2.4.

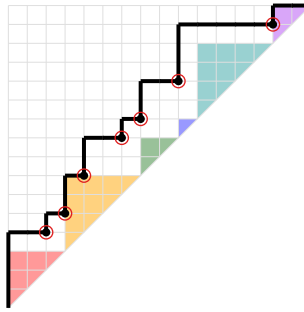


Figure 50. The α -path $\Phi_{\text{path}}(P)$, where $\alpha = (3, 4, 2, 1, 4, 2)$ and P is the noncrossing α -partition from Example 4.1.20.

PROOF OF THEOREM 4.2.4. It remains to show that Φ_{path} is a bijection. Let $p \in \text{Dyck}(\alpha)$, with $\text{Valley}(p) = \{(m_1, n_1), (m_2, n_2), \dots, (m_k, n_k)\}$ such that $m_1 > m_2 > \dots > m_k$. Since these are valleys of an α -path, it follows that $n_1 > n_2 > \dots > n_k$ and if $\text{reg}_\alpha(m_i) = j$, then $n_i \in \{p_j, p_j+1, \dots, n_{i-1}-1\}$ (where $n_0 = n$).

We draw n nodes labeled by $1, 2, \dots, n$ on a horizontal line, and group them according to α -regions. We now iteratively add arcs corresponding to the valleys of p so that after k steps we end up with an α -partition.

For $i \in [k]$, define $\text{reg}_\alpha(m_i) = j_i$. We write $m_i = p_{j_i-1} + l_i$ for some $l_i \in [\alpha_{j_i}]$, and set $a_i = p_{j_i} - l_i + 1$. Let b_i be the $(n_{i-1} - n_i)^{\text{th}}$ node after the j_i^{th} α -region that is not directly below some bump.

We claim that the collection $B = \{(a_1, b_1), (a_2, b_2), \dots, (a_k, b_k)\}$ is the collection of bumps of some noncrossing α -partition. By construction, $\text{reg}_\alpha(a_i) \neq \text{reg}_\alpha(b_i)$ for all i , and $|\{a_1, a_2, \dots, a_k\}| = k = |\{b_1, b_2, \dots, b_k\}|$. Thus B is indeed the set of bumps of some α -partition P_p . If we can guarantee that in step i there are always at least $n_{i-1} - n_i$ nodes after the j_i^{th} α -region that are not below some bump, then it is clear that P is noncrossing. But this is clear, because $n_{i-1} - p_{j_i}$ determines the number of nodes that are not already below some bump. Since $n_i \in \{p_{j_i}, p_{j_i}+1, \dots, n_{i-1}-1\}$, it follows that $n_{i-1} - n_i \in \{1, 2, \dots, n_{i-1} - p_{j_i}\}$.

It follows that $P_p \in \text{Nonc}(\alpha)$ and $\text{Bump}(P_p) = B$. The fact that the assignment $p \mapsto P_p$ is the inverse of Φ_{path} is immediate, and since the set of bumps uniquely determines a noncrossing α -partition and the set of valleys uniquely determines an α -Dyck path, the claim follows. \square

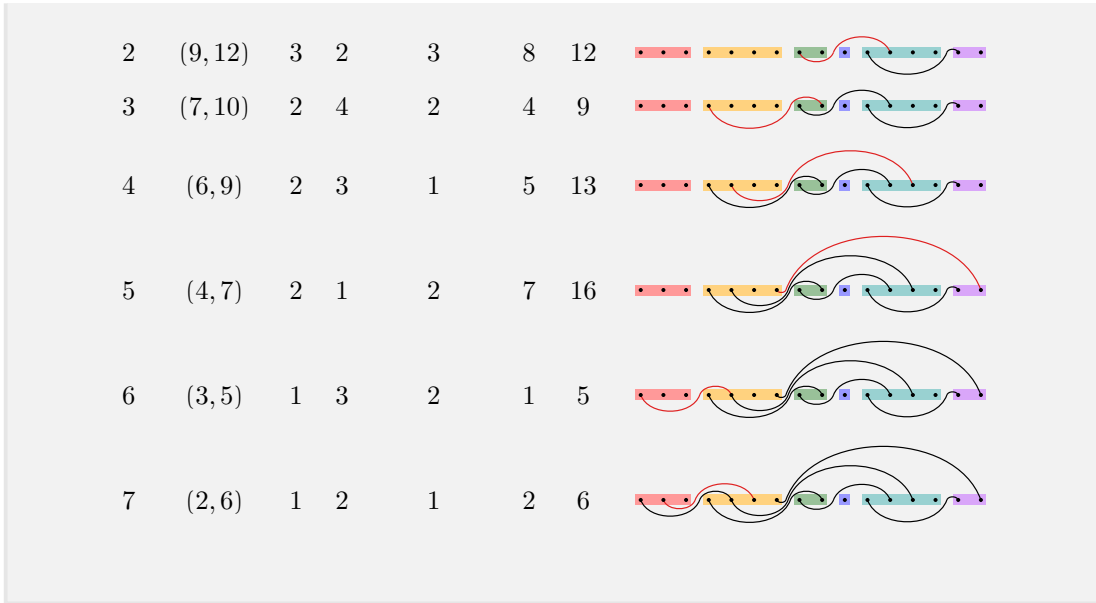
The next example illustrates the construction of a noncrossing α -partition from an α -path.

Example 4.2.7. Let $\alpha = (3, 4, 2, 1, 4, 2)$ and let p be the α -Dyck path shown in Figure 50. We have

$$\text{Valley}(p) = \{(14, 15), (9, 12), (7, 10), (6, 9), (4, 7), (3, 5), (2, 4)\}.$$

The following table lists the values computed in the proof of Theorem 4.2.4 together with the “partial” noncrossing α -partitions obtained by successively adding arcs.

i	(m_i, n_i)	j_i	l_i	$n_{i-1} - n_i$	a_i	b_i	
1	(14, 15)	5	4	1	11	15	



4.2.3. α -trees and $(\alpha, 231)$ -avoiding permutations. We next present a bijection from $\text{Tree}(\alpha)$ to $\mathfrak{S}_\alpha(231)$.

Theorem 4.2.8. *For every composition α of $n > 0$ there exists a bijection*

$$(4.9) \quad \Xi_{\text{perm}}: \text{Tree}(\alpha) \rightarrow \mathfrak{S}_\alpha(231),$$

that maps internal nodes to descents.

We prove Theorem 4.2.8 in several steps.

Proposition 4.2.9. *For every $T \in \text{Tree}(\alpha)$ there exists a naturally associated permutation $w_T \in \mathfrak{S}_\alpha(231)$. Moreover, the internal nodes of T correspond to the descents of w_T .*

PROOF. Let γ denote the α -coloring of T . We first label the non-root nodes of T in LR-postfix order and group together labels that correspond to nodes with the same color. We order nodes with the same color increasingly and order the blocks according to increasing color. This clearly produces a unique permutation $w_T \in \mathfrak{S}_\alpha$.

Now pick $i < j < k$ all in different α -regions such that $w_T(i) = w_T(k) + 1$. Let u_i, u_j, u_k denote the nodes of T that are labeled by i, j, k , respectively. It follows that $\gamma(u_i) < \gamma(u_j) < \gamma(u_k)$.

Since $w_T(i) = w_T(k) + 1$, Lemma 4.1.23 implies that u_i is either the parent of u_k or the left-most leaf of the subtree induced by the sibling of u_k on the right. In the second case, however, u_k precedes u_i in LR-prefix order, and thus u_k would become active before u_i in Construction 4.1.24. Lemma 4.1.25(ii) would yield $\gamma(u_k) \leq \gamma(u_i)$, a contradiction.

Thus, u_i is the parent of u_k and u_k is the rightmost child of u_i . This means that u_i comes before u_k in the LR-prefix order of T and that u_k is active during steps $i + 1, i + 2, \dots, u_k$ in Construction 4.1.24; in particular in step j . Since $j = \gamma(u_j) < \gamma(u_k)$

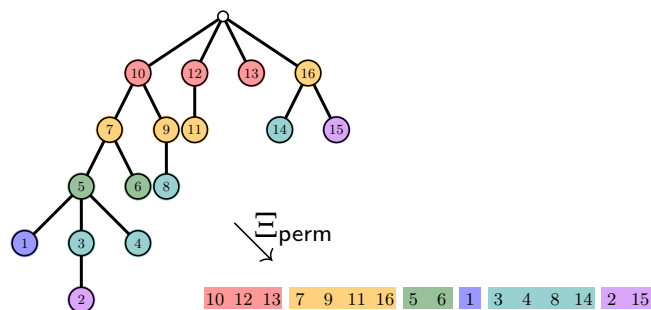


Figure 51. An α -tree labeled in LR-postfix order for $\alpha = (3, 4, 2, 1, 4, 2)$, and the associated $(\alpha, 231)$ -avoiding permutation.

the node u_j must come before u_k in LR-prefix order. However, since $w_T(i) < w_T(j)$, we know that u_j comes after u_i in LR-postfix order. Moreover, $\gamma(u_i) < \gamma(u_j)$ means that u_j is not an ancestor of u_i . Thus, u_i must come before u_j in LR-prefix order. Since u_k is the rightmost child of u_i , we conclude that u_j comes before u_k in LR-postfix order, and it follows that $w_T(j) < w_T(k)$.

We have just shown that w_T is $(\alpha, 231)$ -avoiding. Moreover, the labels of an internal node and its right-most child form a descent of w_T . The assignment $T \mapsto w_T$ is precisely the map Ξ_{perm} . \square

Figure 51 illustrates the construction from Proposition 4.2.9.

Proposition 4.2.10. *For every $w \in \mathfrak{S}_\alpha(231)$ there exists a naturally associated α -tree $T_w \in \text{Tree}(\alpha)$.*

PROOF. Let $\alpha = (\alpha_1, \alpha_2, \dots, \alpha_r) \vdash n$, and pick $w \in \mathfrak{S}_\alpha(231)$. We start with the tree T_0 that consists of a single node, labeled by $n+1$. We now insert nodes one at a time to obtain a plane rooted tree with n non-root nodes. This insertion proceeds inductively as follows. In the i^{th} step, we try to insert a node labeled by $w(i)$ into T_{i-1} . To that end, we start at the root of T_{i-1} and walk around the tree in a certain manner. Suppose that we have reached a node v of T_{i-1} labeled by a . If $w(i) < a$, then we move to the left-most child of v , otherwise we move to the first sibling of v on the right. If the destination does not exist, we create a new node in the desired place and label it by $w(i)$. After n steps we clearly obtain a plane rooted tree $T_w = T_n$. By construction, the nodes of T_w are labeled in LR-postfix order.

It remains to show that T_w is compatible with α . To that end, we define a full coloring f of T_w by setting $f(v) = \text{reg}_\alpha(w^{-1}(a))$. In other words, a node of T_w labeled by a is colored by i if the position of a in w is in the i^{th} α -region.

We now show that f is indeed the α -coloring of T_w constructed in Construction 4.1.24. First, let us consider a non-root node u whose parent v is not the root. Since v is inserted in T_w before u , we must have $f(v) \leq f(u)$. If $f(u) = f(v)$, then the labels of u and v come from indices in the same α -region, and since v is inserted before u , the label of v is smaller than the label of u . However, since u is a descendant of v , the label

of u must be smaller than the label of v , which is a contradiction. Thus, $f(v) < f(u)$. It follows that nodes of T_w whose labels come from the same α -region are incomparable. We now prove inductively that Construction 4.1.24 does not fail for T_w and that the coloring created is precisely f . More precisely, let γ_s be the labeling of T_w from Construction 4.1.24 constructed after the s^{th} step, and let f_s denote the restriction of f to values in $[s]$. We show, for $0 \leq s \leq r$, that Construction 4.1.24 does not fail in step s and that $\gamma_s = f_s$. The base case, $s = 0$, is clearly correct. Suppose that the claim is true for $s - 1$.

We first show that there are enough active nodes in step s . Since w is an α -permutation, the labels $w(i)$ for i in the s^{th} α -region are inserted in increasing order, and by the argument from the third paragraph of this proof these newly inserted nodes are incomparable. Therefore, all of them are children of the nodes in the domain of γ_s , and thus active at step s . We therefore have at least α_s active nodes, so that Construction 4.1.24 does not fail. Moreover, γ_s is well defined.

We now show that $\gamma_s = f_s$. Suppose that this is not the case, and let u_* be the first node of T_w in LR-prefix order that is in the domain of γ_s but not in that of f_s . Thus, $f(u_*) > s$. Let u_i be the parent of u_* , which is in the domain of γ_{s-1} and therefore also in the domain of f_{s-1} by induction hypothesis. Thus, $f(u_i) \leq s - 1$. Let u_k be the rightmost child of u_i (which exists since u_i has at least the child u_*). Since u_k is inserted not before u_* , we conclude $f(u_k) \geq f(u_*)$. By construction, the domains of f_s and γ_s are of the same size (namely $\alpha_1 + \alpha_2 + \dots + \alpha_s$), which means that there is a node u_j in the domain of f_s but not in the domain of γ_s . We choose u_j minimal with respect to the LR-prefix order. By induction hypothesis we have $f(u_j) \geq s$, which forces $f(u_j) = s$. By minimality, u_* precedes u_j in LR-prefix order. If u_j is a child of u_i , since u_* is inserted before u_j , we obtain a contradiction to $f(u_j) = s < f(u_*)$. As a consequence, u_j comes after u_i in LR-postfix order.

Now, let i, j, k be the indices such that u_i, u_j, u_k are labeled by $w(i), w(j), w(k)$, respectively. Since $f(u_i) \leq s - 1 < f(u_j) = s < f(u_*) \leq f(u_k)$, we have $\text{reg}_\alpha(i) < \text{reg}_\alpha(j) < \text{reg}_\alpha(k)$. Since u_k is the rightmost child of u_i we have $w(i) = w(k) + 1$ by construction, and since u_j comes after u_i in LR-postfix order we have $w(j) > w(i)$. Therefore, w has an $(\alpha, 231)$ -pattern in positions (i, j, k) , which is a contradiction.

We thus conclude that $\gamma_s = f_s$. As a consequence f is the labeling of T_w constructed in Construction 4.1.24, which means that T_w is an α -tree. \square

Proposition 4.2.10 suggests the existence of a well-defined map

$$(4.10) \quad \Lambda_{\text{perm}}: \mathfrak{S}_\alpha(231) \rightarrow \text{Tree}(\alpha), \quad w \mapsto T_w.$$

We now prove Theorem 4.2.8 by showing that Ξ_{perm} and Λ_{perm} are mutually inverse maps.

PROOF OF THEOREM 4.2.8. By Propositions 4.2.9 and 4.2.10, it remains to show that $\Xi_{\text{perm}} \circ \Lambda_{\text{perm}} = \text{id}$ and $\Lambda_{\text{perm}} \circ \Xi_{\text{perm}} = \text{id}$. Let $\alpha = (\alpha_1, \alpha_2, \dots, \alpha_r)$.

To show that $\Xi_{\text{perm}} \circ \Lambda_{\text{perm}} = \text{id}$, for $w \in \mathfrak{S}_\alpha(231)$, we consider $T = \Lambda_{\text{perm}}(w)$ and $w' = \Xi_{\text{perm}}(T)$. Let γ be the full coloring of T constructed in the proof of Proposition 4.2.10. According to this proof, γ agrees with the α -coloring of T . Therefore, the entries in each α -region of w and w' agree, and since there is a unique way to order a set of numbers increasingly, we conclude that $w = w'$.

Now, for $\Lambda_{\text{perm}} \circ \Xi_{\text{perm}} = \text{id}$, given $T \in \text{Tree}(\alpha)$, we consider $w = \Xi_{\text{perm}}(T)$ and $T' = \Lambda_{\text{perm}}(w)$. Let γ, γ' be the α -colorings of T, T' , respectively. For $s \in [r]$, let T_s, T'_s denote

the induced subtrees consisting of the nodes of color at most s in T, T' , respectively. We prove by induction on s that $T_s = T'_s$ holds for all $0 \leq s \leq r$.

The base case $s = 0$ is clear as T_0 and T'_0 consist only of the root node. Now suppose that $T_{s-1} = T'_{s-1}$ and pick a node u of T with $\gamma(u) = s$ and label $w(i)$. Let u' be the node of T' with the same label. Since entries of w in the same α -region appear increasingly, we know that every node of color s inserted in T' before u' has a smaller label than u' , and by construction no such node can be the parent of u' . It follows that the parent of u' belongs to T'_{s-1} . By induction hypothesis, it follows that the parent v of u has the same label as v' . Now, for the order of the newly inserted children of a node, see the proof of Proposition 4.2.9, the children of each node in T' are—at each step—ordered by increasing labels. Since nodes in both T and T' are labeled in LR-postfix order, we conclude $T_s = T'_s$. This completes the induction step, and we conclude $T = T_r = T'_r = T'$. \square

4.2.4. α -trees and noncrossing α -partitions. Now we present a bijection from $\text{Tree}(\alpha)$ to $\text{Nonc}(\alpha)$.

Theorem 4.2.11. *For every composition α of $n > 0$ there exists a bijection*

$$(4.11) \quad \Xi_{\text{nonc}}: \text{Tree}(\alpha) \rightarrow \text{Nonc}(\alpha)$$

that maps internal nodes to bumps.

Again, we prove Theorem 4.2.11 in several steps.

Proposition 4.2.12. *For every $T \in \text{Tree}(\alpha)$ there exists a naturally associated partition $P_T \in \text{Nonc}(\alpha)$. Moreover, the internal nodes of T correspond to the bumps of P_T .*

PROOF. Let $T \in \text{Tree}(\alpha)$. We first draw the n non-root nodes of T on a horizontal line and group them according to their color. The entries per color group are ordered with respect to the LR-prefix order of T and the color groups are sorted by increasing color. We then connect two nodes u and v by an arc if v is the rightmost child of u . The resulting diagram represents a partition P_T . By construction, every internal node of T (together with its rightmost child) corresponds to a bump of P_T .

By Lemma 4.1.25(i) there are no arcs connecting nodes with the same color, so P_T is actually an α -partition. Suppose that P_T is not noncrossing, and pick two bumps (a_1, b_1) and (a_2, b_2) that violate either (NC1) or (NC2). Let u_1, v_1, u_2, v_2 be the nodes of T corresponding to a_1, b_1, a_2, b_2 whose colors with respect to the α -coloring are c_1, d_1, c_2, d_2 .

If these bumps violate (NC1), then $a_1 < a_2 < b_1 < b_2$, but a_1, a_2, b_1 belong to three different α -regions. It follows that $c_1 < c_2 < d_1$. We conclude that u_2 precedes v_1 in LR-prefix order, since v_1 (being a child of u_1) becomes active immediately after step c_1 of Construction 4.1.24 in which u_1 receives its color. Moreover, since $c_1 < c_2$, the node u_2 is not an ancestor of u_1 . Consequently, the rightmost child of u_2 , which is v_2 , precedes v_1 in LR-prefix order, too. However, since $b_1 < b_2$ we have $d_1 \leq d_2$, which implies that v_1 precedes v_2 in LR-prefix order. This is a contradiction, and we conclude that (NC1) is not violated.

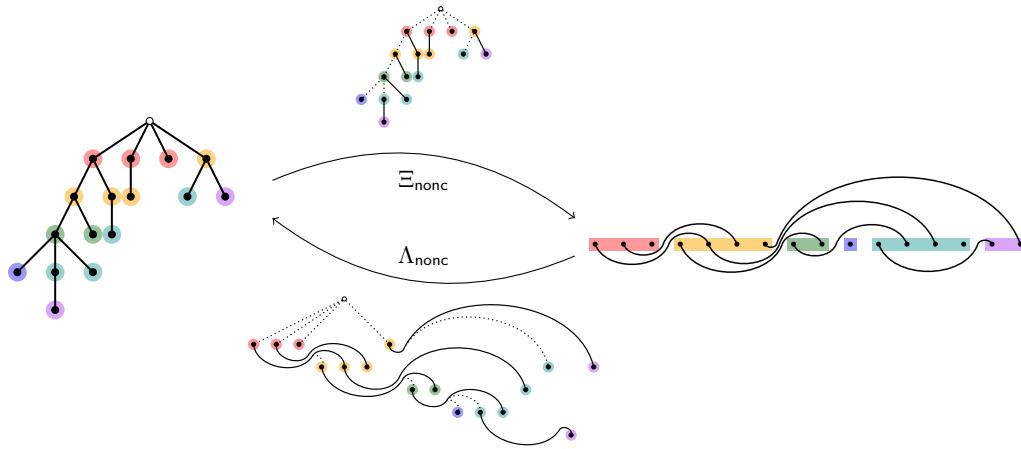


Figure 52. Illustration of the bijection from $\text{Tree}(\alpha)$ to $\text{Nonc}(\alpha)$ for $\alpha = (3, 4, 2, 1, 4, 2)$.

If these bumps violate (NC2), then $a_1 < a_2 < b_2 < b_1$ and a_1, a_2 are in the same α -region. It follows that $c_1 = c_2$ so that, by construction, u_1 precedes u_2 in LR-prefix order. Lemma 4.1.25(i) implies that u_1 and u_2 are incomparable in T , and since v_1 is the rightmost child of u_1 it precedes u_2 in LR-prefix order, too. Thus, v_1 precedes v_2 , which is the rightmost child of u_2 , in LR-prefix order. However, since $b_2 < b_1$, it follows that $d_2 \leq d_1$ which implies that v_2 precedes v_1 in LR-prefix order. This is a contradiction, and we conclude that (NC2) is not violated.

Consequently, our assumption must have been wrong and P_T is noncrossing. The assignment $T \mapsto P_T$ is precisely the map Ξ_{nonc} . \square

The process of creating a noncrossing α -partition from an α -tree is the *flattening* of T and illustrated in the top part of Figure 52.

Proposition 4.2.13. *For every $P \in \text{Nonc}(\alpha)$ there exists a naturally associated α -tree $T_P \in \text{Tree}(\alpha)$.*

PROOF. Let $P \in \text{Nonc}(\alpha)$, and label the elements of P by $1, 2, \dots, n$ from left to right. We start with a collection of $n + 1$ nodes denoted by v_0, v_1, \dots, v_n . If the element i does not lie below any bump of P , then we add an edge from v_0 to v_i making v_i a child of v_0 . If i lies directly below a bump $(a, b) \in \text{Bump}(P)$, then we add an edge from v_a to v_i making v_i a child of v_a .

Since we associate with each element of P a parent with strictly smaller index, the resulting graph is acyclic. Moreover, it has $n + 1$ nodes and n edges and therefore must be a tree. We order the children of each node by their label in increasing order and root the tree at v_0 . We thus obtain a plane rooted tree T_P . Moreover, every bump of P corresponds to a unique internal node of T_P (and its rightmost child).

We now prove that T_P is compatible with α . Suppose that $\alpha = (\alpha_1, \alpha_2, \dots, \alpha_r)$. We define a full coloring f of T_P by setting $f(v_a) = i$ if and only if $\text{reg}_\alpha(a) = i$. We now

prove that Construction 4.1.24 does not fail for T_P and that the resulting α -coloring agrees with f . We proceed by induction on the number s of coloring steps.

The elements in the first α -region do not lie below any bump of P , which means that Construction 4.1.24 does not fail in the first step. Moreover, by construction, the nodes $v_1, v_2, \dots, v_{\alpha_1}$ are the leftmost children of the root of T_P , and the partial labeling of Construction 4.1.24 assigns the color 1 to all these nodes. Hence, this partial labeling agrees with f on the nodes colored by 1. This establishes the base case $s = 1$ of our induction.

Now suppose that the induction hypothesis holds for $s - 1 < r$, and we now consider step s . For $a \in \{p_{s-1}+1, p_{s-1}+2, \dots, p_s\}$, let w be the parent of v_a . By construction, w is either the root or $w = v_{a'}$ for some $a' \leq p_{s-1}$. This implies $f(w) \leq s - 1$. Thus, v_a is active in step s of Construction 4.1.24. Since a was chosen arbitrarily, we conclude that all nodes of T_P coming from the s^{th} α -region are active in step s . This implies that Construction 4.1.24 does not fail in step s .

We now prove that the nodes corresponding to elements in the s^{th} α -region are the first active nodes in LR-prefix order at step s . Suppose that at step s there are two active nodes v_{b_1} and v_{b_2} such that v_{b_1} precedes v_{b_2} in LR-prefix order and $f(v_{b_1}) > s = f(v_{b_2})$. Consequently, $b_2 < b_1$ and $\text{reg}_\alpha(b_1) \neq \text{reg}_\alpha(b_2)$. Let v_{a_1}, v_{a_2} denote the parents of v_{b_1}, v_{b_2} , respectively. If $v_{a_1} = v_{a_2}$, then by construction we must have $b_1 < b_2$; a contradiction. If v_{a_1} is the root, then v_{b_1} also precedes v_{a_2} in LR-prefix order and it is either colored or active in the step in which v_{a_2} receives its color. By our induction hypothesis, we have $s < f(v_{b_1}) \leq f(v_{a_2}) < s$, which is a contradiction. If v_{a_2} is the root, then since b_2 is not below any bump and $b_2 < b_1$, $\text{reg}_\alpha(b_2) \leq \text{reg}_\alpha(a_1)$. In combination with the induction hypothesis, we obtain $s = f(v_{b_2}) \leq f(v_{a_1}) < s$, which is a contradiction. We conclude that b_1 and b_2 are directly below bumps (a_1, b'_1) and (a_2, b'_2) , respectively.

Since v_{b_1} and v_{b_2} are active in the s^{th} step, it follows that a_1 and a_2 are in α -regions before the s^{th} α -region, with $b_1 < b'_1$ and $b_2 < b'_2$. There are four possibilities:

(i) If $a_1 < a_2 < b'_1 < b'_2$, then either $\text{reg}_\alpha(a_1) = \text{reg}_\alpha(a_2)$ or $\text{reg}_\alpha(a_2) = \text{reg}_\alpha(b'_1)$ by (NC1). In both cases we would have $b_1 < b_2$, which is a contradiction.

(ii) If $a_1 < a_2 < b'_2 < b'_1$, then $\text{reg}_\alpha(a_1) < \text{reg}_\alpha(a_2)$ by (NC2). Thus, v_{a_1} is colored before v_{a_2} , which implies that v_{b_1} is active before v_{a_2} receives its color. Since v_{b_1} precedes v_{b_2} in LR-prefix order and v_{b_1} is not a descendant of v_{a_2} , we conclude that v_{b_1} precedes v_{a_2} in LR-prefix order, too. It follows that v_{b_1} receives its color not later than v_{a_2} , and by our induction hypothesis, we have $s < f(v_{b_1}) \leq f(v_{a_2}) < s$; a contradiction.

(iii) If $a_2 < a_1 < b'_1 < b'_2$, then $\text{reg}_\alpha(a_2) < \text{reg}_\alpha(a_1)$ by (NC2). This means that (a_1, b'_1) separates b_1 from (a_2, b'_2) . Since $f(v_{a_1}) < s = f(v_{b_2})$, we have $\text{reg}_\alpha(a_1) < \text{reg}_\alpha(b_2)$. Thus, $b_1 < b'_1 < b_2$, which is a contradiction.

(iv) If $a_2 < a_1 < b'_2 < b'_1$, then either $\text{reg}_\alpha(a_2) = \text{reg}_\alpha(a_1)$ or $\text{reg}_\alpha(a_1) = \text{reg}_\alpha(b'_2)$ by (NC2). If $\text{reg}_\alpha(a_2) = \text{reg}_\alpha(a_1)$, then v_{a_2} precedes v_{a_1} in LR-prefix order by construction, because $a_2 < a_1$. Moreover, since $f(v_{a_1}) = f(v_{a_2}) \leq s - 1$, by our induction hypothesis, these two nodes receive the same color in Construction 4.1.24. By Lemma 4.1.25(i), v_{a_1} and v_{a_2} are incomparable in T_P . Since v_{b_2} is a child of v_{a_2} , it follows that v_{b_2} precedes v_{b_1} in LR-prefix order, which is a contradiction. If $\text{reg}_\alpha(a_1) = \text{reg}_\alpha(b'_2)$, then necessarily $\text{reg}_\alpha(b_2) \leq \text{reg}_\alpha(a_1)$. By induction hypothesis, we have $s > f(v_{a_1}) \geq f(v_{b_2}) = s$, a contradiction.

We conclude that all nodes of T_P corresponding to elements from the s^{th} α -region receive color s in step s of Construction 4.1.24, which finishes the induction step. We conclude that T_P is an α -tree and f its α -coloring. \square

Proposition 4.2.13 suggests the existence of a well-defined map

$$(4.12) \quad \Lambda_{\text{nonc}}: \text{Nonc}(\alpha) \rightarrow \text{Tree}(\alpha), \quad P \mapsto T_P,$$

which is illustrated in the bottom part of Figure 52. We now prove Theorem 4.2.11 by showing that Ξ_{nonc} and Λ_{nonc} are mutually inverse maps.

PROOF OF THEOREM 4.2.11. By Propositions 4.2.12 and 4.2.13, it remains to show that $\Xi_{\text{nonc}} \circ \Lambda_{\text{nonc}} = \text{id}$ and $\Lambda_{\text{nonc}} \circ \Xi_{\text{nonc}} = \text{id}$.

To show that $\Xi_{\text{nonc}} \circ \Lambda_{\text{nonc}} = \text{id}$, for $P \in \text{Nonc}(\alpha)$, let $T = \Lambda_{\text{nonc}}(P)$ be the α -tree obtained from P as in the proof of Proposition 4.2.13 and let $P' = \Xi_{\text{nonc}}(T)$ be the noncrossing α -partition obtained from T as in the proof of Proposition 4.2.12.

Since every bump of P corresponds to an internal node of T and every internal node of T corresponds to a bump of P' , we conclude that P and P' have the same number of bumps. Let $(a, b) \in \text{Bump}(P)$. In T , the node v_a is thus the parent of the node v_b . Let i be an element of P such that v_i is a child of v_a in T . By construction, $a < i \leq b$ and $\text{reg}_\alpha(a) < \text{reg}_\alpha(i)$. Hence, v_i (weakly) precedes v_b in LR-prefix order. This is valid for every child of v_a , which implies that v_b is the rightmost child of v_a , leading to a bump $(a, b) \in \text{Bump}(P')$. We conclude $\text{Bump}(P) = \text{Bump}(P')$ and thus $P = P'$.

To show that $\Lambda_{\text{nonc}} \circ \Xi_{\text{nonc}} = \text{id}$, for $T \in \text{Tree}(\alpha)$, let γ be its α -coloring, $P = \Xi_{\text{nonc}}(T)$, $T' = \Lambda_{\text{nonc}}(P)$. We now prove that $T = T'$. For a non-leaf node u of T , let v be a child of u , let a, b be the elements of P corresponding to u, v , and let u', v' be the nodes of T' corresponding to a, b , respectively. We first show that v' is a child of u' in T' .

If u is the root, then b is not below any bump in P , meaning that u' is the root of T' and v' is one of its children by the proof of Proposition 4.2.13. We now suppose that u is not the root. If v is the rightmost child of u , then $(a, b) \in \text{Bump}(P)$, and it follows from the proof of Proposition 4.2.13 that v' is the rightmost child of u' , too.

It remains to consider the case that v is not the rightmost child of u . Let v_r be the rightmost child of u , and let b_r be the element of P corresponding to v_r . It follows that $(a, b_r) \in \text{Bump}(P)$. But now, the proof of Proposition 4.2.12 implies that b lies directly below (a, b_r) ; hence v' is a child of u' in T' . The order of the children of a node in T and T' depends only on the order of the elements of P which allows us to conclude $T = T'$. \square

4.2.5. α -trees and α -Dyck paths. Finally, we present a bijection from $\text{Tree}(\alpha)$ to $\text{Dyck}(\alpha)$.

Theorem 4.2.14. *For every composition α of $n > 0$ there exists a bijection*

$$(4.13) \quad \Xi_{\text{path}}: \text{Tree}(\alpha) \rightarrow \text{Dyck}(\alpha)$$

that maps internal nodes to valleys.

Proposition 4.2.15. *For every $T \in \text{Tree}(\alpha)$ there exists a naturally associated α -Dyck path $p_T \in \text{Dyck}(\alpha)$. Moreover, the internal nodes of T correspond to the valleys of p_T .*

PROOF. Let $\alpha = (\alpha_1, \alpha_2, \dots, \alpha_r) \vdash n$, let $p_i = \alpha_1 + \alpha_2 + \dots + \alpha_i$ for $i \in [r]$ and $p_0 = 0$. Choose $T \in \text{Tree}(\alpha)$. Let q_i denote the number of active nodes in step $i + 1$ of Construction 4.1.24 before coloring. Then, p_i denotes the number of nodes of T of color

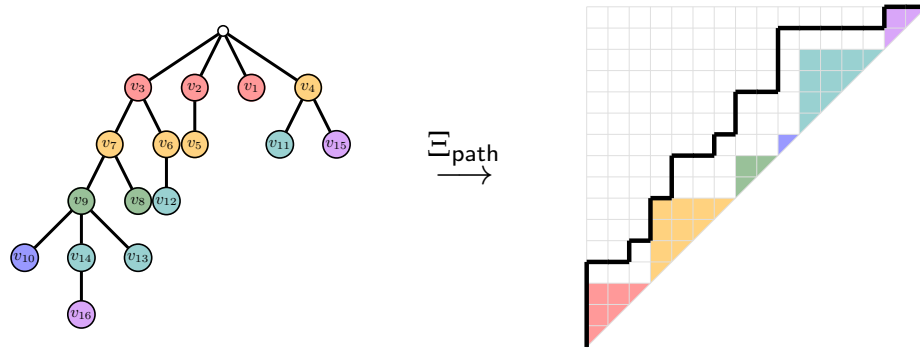


Figure 53. A labeled α -tree and its associated α -Dyck path.

$\leq i$ and q_i denotes the number of nodes of color $> i$ whose parents have color $\leq i$. It follows immediately that $p_i + q_i \leq n$ for all i .

If the rightmost child of the j^{th} internal node (from left to right) of color i is the k^{th} active node (from left to right) in the $(i+1)^{\text{st}}$ step of Construction 4.1.24 before coloring, then we mark the coordinate (a, b) in the plane, where $a = p_i - j + 1$ and $b = p_i + q_i - k$. After parsing all internal nodes of T , we return the unique northeast path p_T from $(0, 0)$ to (n, n) whose valleys are precisely at the marked coordinates. By construction, the internal nodes of T correspond to the valleys of p_T .

Moreover, since $j \leq \alpha_i$, we have $p_{i-1} < a \leq p_i$, and since $k \leq q_i$, we have $p_i \leq b < p_i + q_i$. Therefore, (a, b) is weakly above $v_\alpha = N^{\alpha_1} E^{\alpha_1} N^{\alpha_2} E^{\alpha_2} \dots N^{\alpha_r} E^{\alpha_r}$.

Since this reasoning goes through for every internal node of T , p_T is an α -Dyck path. \square

Example 4.2.16. The left side of Figure 53 shows an α -tree for $\alpha = (3, 4, 2, 1, 4, 2)$, where the nodes are labeled from right to left per color class. The following table lists the steps of Construction 4.1.24, and for each step it lists the active nodes before coloring, the internal nodes that receive a color and the valley they contribute. The internal nodes are marked in red.

$i + 1$	p_i	q_i	active nodes	internal node		rightmost child	k	valley
				of color i	j			
1	0	4	$\{v_1, v_2, v_3, v_4\}$	-	-	-	-	-
2	3	4	$\{v_4, v_5, v_6, v_7\}$	v_2	2	v_5	3	(2, 4)
				v_3	1	v_6	2	(3, 5)
				v_4	4	v_{15}	5	(4, 7)
3	7	5	$\{v_8, v_9, v_{11}, v_{12}, v_{15}\}$	v_6	2	v_{12}	3	(6, 9)
				v_7	1	v_8	2	(7, 10)
4	9	6	$\{v_{10}, v_{11}, v_{12}, v_{13}, v_{14}, v_{15}\}$	v_9	1	v_{13}	3	(9, 12)
5	10	5	$\{v_{11}, v_{12}, v_{13}, v_{14}, v_{15}\}$	-	-	-	-	-
6	14	2	$\{v_{15}, v_{16}\}$	v_{14}	1	v_{16}	1	(14, 15)

Note that, in the labeling we used, the indices of the nodes correspond to the x -coordinates of their corresponding valleys. The right side of Figure 53 shows the α -Dyck path whose valleys were computed in the above table.

Proposition 4.2.17. *For every $p \in \text{Dyck}(\alpha)$ there exists a naturally associated α -tree $T_p \in \text{Tree}(\alpha)$.*

PROOF. Let $\alpha = (\alpha_1, \alpha_2, \dots, \alpha_r)$ and let $p \in \text{Dyck}_\alpha$. Let T_0 be the plane rooted tree consisting of a single (root) node, and let f_0 be the coloring of T_0 that colors the only node of T_0 by color 0.

At the i^{th} step, we construct a (partially) colored tree T_i from T_{i-1} by adding as many children to the j^{th} node of color $i-1$ (from left to right) as there are north steps in p with x -coordinate equal to $p_{i-1} - j + 1$. After all children have been added, we extend f_{i-1} to f_i by assigning the color i to the first α_i uncolored nodes of T_i in LR-prefix order. This algorithm fails if there are not enough uncolored nodes. After r steps, we return the plane rooted tree $T_p = T_r$.

We first prove that we never run out of uncolored nodes, i.e., that the above construction never fails. For $i \in \{0, 1, \dots, r-1\}$ we denote by m_i the maximal y -coordinate of a lattice point on p that has x -coordinate p_i . Since p is weakly above v_α , we have $m_i \geq p_{i+1}$.

Next we prove by induction on $s \in [r]$ that the number of uncolored non-root nodes at the end of step s in the above construction is precisely $m_{s-1} - p_s$. The base case $s = 1$ holds, because in the first step, we add exactly m_0 children to the root and we color $\alpha_1 = p_1$ of them. Now suppose that the claim holds up until the s^{th} step of the construction. In particular, at the beginning of the $(s+1)^{\text{st}}$ step we already have $m_{s-1} - p_s$ uncolored nodes. In the $(s+1)^{\text{st}}$ step, we add $m_s - m_{s-1}$ new nodes and color α_{s+1} of all uncolored nodes. This leaves us with $m_{s-1} - p_s + m_s - m_{s-1} - \alpha_{s+1} = m_s - p_{s+1} \geq 0$ uncolored nodes. This completes the induction, and implies that the above construction never fails; in fact it produces a full coloring $f = f_r$ of T_p .

Now we prove that T_p is compatible with α by proving that f is indeed the α -coloring γ of T_p from Construction 4.1.24. Let us prove by induction on $s \in [r]$ that Construction 4.1.24 does not fail. Let f_s denote the restriction of f to the nodes of T_p that have f -color at most s , and let γ_s be the (partial) coloring of T_p obtained after the s^{th} step of Construction 4.1.24.

For the base case $s = 1$, by construction, the root of T_p has $m_0 \geq \alpha_1$ children and we have $f(v) = 1$ if and only if v is among the α_1 leftmost children of the root. It is now clear that Construction 4.1.24 does not fail at step 1 and that the same nodes receive γ -color 1.

Suppose now that the induction hypothesis holds for s . The active nodes with respect to γ_s are precisely those whose parents have γ_s -color at most s . In step $s+1$ of the above construction, we add precisely $m_s - m_{s-1}$ new nodes and after this addition, the parents of the uncolored nodes have f_s -color at most s . By induction hypothesis, the uncolored nodes with respect to f_s are precisely the active nodes with respect to γ_s . We have already shown that Construction 4.1.24 does not fail in step $s+1$, and since we color the α_{s+1} leftmost nodes in LR-prefix order by $s+1$ in both constructions, the induction step is established.

We conclude that T_p is compatible with α and that the colorings f and γ agree. \square

Remark 4.2.18. *It follows from the proof of Proposition 4.2.17 that after we have created all the nodes in the $(s + 1)^{\text{st}}$ step of Construction 4.1.24, there are $m_s - p_s$ active nodes before coloring and $m_s - p_{s+1}$ active nodes after coloring.*

We need the following auxiliary result.

Lemma 4.2.19. *Given $T \in \text{Tree}(\alpha)$, let u be an internal node of T . The number of children of u is equal to the number of consecutive north steps in $p = \Xi_{\text{path}}(T)$ immediately after the valley corresponding to u .*

PROOF. Suppose that the valley corresponding to u is at position (a, b) in the plane. Let c_1 be the number of children of u and let c_2 be the number of consecutive north steps with x -coordinate a . Suppose that u has color s and that the rightmost child of u is the j^{th} active node in LR-prefix order in the $(s + 1)^{\text{st}}$ step of Construction 4.1.24 before coloring among a total of q_s active nodes. Moreover, let m_s be the maximal y -coordinate of a lattice point on p with x -coordinate p_s . It follows from Remark 4.2.18 that $q_s = m_s - p_s$. The proof of Proposition 4.2.15 further implies that $b = p_s + q_s - j = m_s - j$.

If u is the first internal node in its color group, then $c_1 = j$. By construction, the valley (a, b) is the last valley whose x -coordinate is at most p_s , which implies that $c_2 = m_s - b = j$.

Otherwise, let u_* be the internal node of color s that immediately precedes u in LR-prefix order. Suppose that the rightmost child of u_* is the j_*^{th} active node in LR-prefix order at step $s + 1$ of Construction 4.1.24 before coloring. It follows that $c_1 = j - j_*$. Moreover, let (a_*, b_*) be the valley of p corresponding to u_* . We know that (a_*, b_*) is the valley immediately after (a, b) , and we have $c_2 = b_* - b$. Since $b_* = p_s + q_s - j_* = m_s - j_*$ by the proof of Proposition 4.2.15 we conclude that $c_2 = j_* - j$. We thus have $c_1 = c_2$ in all cases. \square

Proposition 4.2.17 suggests the existence of a well-defined map

$$(4.14) \quad \Lambda_{\text{path}}: \text{Dyck}(\alpha) \rightarrow \text{Tree}(\alpha), \quad p \mapsto T_p.$$

We now prove Theorem 4.2.14 by showing that Ξ_{path} and Λ_{path} are mutually inverse maps.

PROOF OF THEOREM 4.2.14. By Propositions 4.2.15 and 4.2.17, it remains to show that $\Xi_{\text{path}} \circ \Lambda_{\text{path}} = \text{id}$ and $\Lambda_{\text{path}} \circ \Xi_{\text{path}} = \text{id}$.

To show that $\Xi_{\text{path}} \circ \Lambda_{\text{path}} = \text{id}$, for $p \in \text{Dyck}(\alpha)$, let $T = \Lambda_{\text{path}}(p)$ be the α -tree obtained from p as in the proof of Proposition 4.2.17 and let $p' = \Xi_{\text{path}}(T)$ be the α -Dyck path obtained from T as in the proof of Proposition 4.2.15. Since every valley of p corresponds to an internal node of T , which in turn corresponds to a valley of p' , we conclude that p and p' have the same number of valleys.

Let (a, b) be a valley of p and let u be the corresponding internal node of T , which is the $(p_s - a + 1)^{\text{st}}$ node of color s in the LR-prefix order of T . Let m_s be the maximal y -coordinate of a lattice point on p with x -coordinate p_s . By Remark 4.2.18, the number of active nodes in the $(s + 1)^{\text{st}}$ step of Construction 4.1.24 (before coloring) is precisely $q_s = m_s - p_s$. The rightmost child of u is thus the $(m_s - b)^{\text{th}}$ active node of T (in LR-prefix order) at step s of Construction 4.1.24. According to the proof of Proposition 4.2.15,

the internal node u and its rightmost child contribute a valley (a', b') to p' , where $a' = p_s - (p_s - a + 1) + 1 = a$ and $b' = p_s + q_s - (m_s - b) = b$. Thus, the valleys of p and p' agree and it follows that $p = p'$.

To show that $\Lambda_{\text{path}} \circ \Xi_{\text{path}} = \text{id}$, for $T \in \text{Tree}(\alpha)$ let $p = \Xi_{\text{path}}(T)$ and $T' = \Lambda_{\text{path}}(p)$. For $s \in [r]$ let T_s, T'_s denote the induced subtrees of T and T' , respectively, consisting of nodes of color at most s . We prove by induction on s that $T_s = T'_s$ holds for all $0 \leq s \leq r$. The base case $s = 0$ is trivially true, since both trees T_0 and T'_0 consist only of a root node that is colored by 0. Suppose that $T_{s-1} = T'_{s-1}$. Suppose that u is a node of T_{s-1} that has $k > 0$ children in T . By Lemma 4.2.19, either p starts with k north steps (if u is the root) or the valley corresponding to u is followed by k north steps. According to the proof of Proposition 4.2.17, the node u' (which is either the root or the node corresponding to the previously considered valley) of T'_{s-1} also has k children. We also notice that, by construction, the positions of u and u' among all active nodes of T_{s-1} and T'_{s-1} are the same. Therefore, we have $T_s = T'_s$, which completes our induction. We conclude that $T = T_r = T'_r = T'$ and we are done. \square

We may now conclude the proof of Theorem 4.2.1.

PROOF. This follows from Theorems 4.2.2, 4.2.4, 4.2.8, 4.2.11 and 4.2.14. \square

We end this section by showing that the diagram in Figure 48 commutes.

Proposition 4.2.20. *For every $p \in \text{Dyck}(\alpha)$, we have $\Phi_{\text{path}}^{-1}(p) = \Xi_{\text{nonc}} \circ \Lambda_{\text{path}}(p)$.*

PROOF. Let $T = \Lambda_{\text{path}}(p)$, $P = \Xi_{\text{nonc}}(T)$, $P' = \Phi_{\text{path}}^{-1}(p)$. By Theorem 4.2.14, we know that every valley of p corresponds to an internal node u of T with its coordinates dictating the exact position of u and its rightmost child v in the α -regions. By Theorem 4.2.11, every such pair of nodes (u, v) corresponds to a bump $(a, b) \in \text{Bump}(P)$, where a and b are determined by the positions of u and v . Following the proof of Theorem 4.2.4, we see that (a, b) is also a bump of P' . It follows that $P = P'$. \square

Proposition 4.2.21. *For every $P \in \text{Nonc}(\alpha)$, we have $\Phi_{\text{perm}}(P) = \Xi_{\text{perm}} \circ \Lambda_{\text{nonc}}(P)$.*

PROOF. Let $T = \Lambda_{\text{nonc}}(P)$, $w = \Xi_{\text{perm}}(T)$ and $w' = \Phi_{\text{perm}}(P)$. We prove by induction on n that $w = w'$. The base case $n = 0$ is clearly true. Now suppose that our claim is true for all compositions $\alpha' \vdash n'$ with $n' < n$.

We take the block of P containing 1 and denote it by $B_\circ = \{a_1, a_2, \dots, a_k\}$ with $a_1 < a_2 < \dots < a_k$ and $a_1 = 1$. By Proposition 4.2.3, we have $w'(a_1) = w'(a_2) + 1 = \dots = w'(a_k) + k - 1$. The remaining values are determined inductively from two noncrossing α' -partitions P_1 and P_2 with strictly less than n elements each. By induction hypothesis, we have $\Phi_{\text{perm}}(P_i) = \Xi_{\text{perm}} \circ \Lambda_{\text{nonc}}(P_i)$ for $i \in \{1, 2\}$.

On the other hand, by Proposition 4.2.13, the elements of B_\circ correspond to nodes in T on the rightmost branch of the first child u of the root, i.e., the set of nodes visited from u by always moving to the rightmost child when possible. The label of u according

to Proposition 4.2.9 is always $w(1)$ and the label of the rightmost child of any node v is always one less than the label of v itself. Finally, by comparing the constructions from Propositions 4.2.3 and 4.2.13, we see that the elements contributing to $w'(1)$ are precisely the nodes in the subtree of u , and we conclude that w and w' agree on B_\circ . Now let T_2 be the induced subtree of T consisting of all the nodes that are descendants of all but the first root children, and let $w^{(2)} = \Xi_{\text{perm}}(T_2)$. Moreover, we construct a new tree T_1 from T by first deleting the root and all nodes of T_2 , and then contracting the rightmost branch of u into a new root node, while keeping the LR-prefix order of the remaining nodes. Let $w^{(1)} = \Xi_{\text{perm}}(T_1)$. The nodes of T_1 and T_2 , respectively, are in the same relative order as in T with respect to LR-postfix order. Hence, w can be reconstructed from the values $w(a_1), w(a_2), \dots, w(a_k)$, the values in $w^{(1)}$ and the values in $w^{(2)}$ increased by $w(1)$. This is precisely the way in which w' is constructed, and we conclude $w = w'$. \square

4.3. Posets

We now move to the study of various posets defined on α -Catalan families. These results have appeared in [45, 66, 132].

4.3.1. The weak order on $\mathfrak{S}_\alpha(231)$. The pattern avoidance characterization of the \bar{c} -aligned elements of \mathfrak{S}_α from Lemma 4.1.16 provides us with a good combinatorial understanding of these elements. We will now study their behaviour under weak order and eventually prove Conjecture 3.2.6 in linear type A.

The next lemma is a key result in this study, and states the existence of a well-defined projection map

$$(4.15) \quad \pi_\alpha^\downarrow: \mathfrak{S}_\alpha \rightarrow \mathfrak{S}_\alpha(231),$$

where for any $w \in \mathfrak{S}_\alpha$, $\pi_\alpha^\downarrow(w)$ is the greatest $(\alpha, 231)$ -avoiding permutation below w in weak order.

Lemma 4.3.1. *For every $w \in \mathfrak{S}_\alpha$, there exists a unique $w' \in \mathfrak{S}_\alpha(231)$ such that $\text{Inv}(w')$ is the maximal set under inclusion among all α -aligned inversion sets $\text{Inv}(u) \subseteq \text{Inv}(w)$.*

PROOF. We proceed by induction on the cardinality of $\text{Inv}(w)$. If $\text{Inv}(w) = \emptyset$, then $\text{Inv}(w)$ is α -aligned and the claim holds trivially. Suppose that $|\text{Inv}(w)| = r$, and that the claim is true for all $u \in \mathfrak{S}_\alpha$ with $|\text{Inv}(u)| < r$.

If $\text{Inv}(w)$ is already α -aligned, then we set $w' = w$ and we are done. Otherwise, Lemma 4.1.17 implies that w contains an $(\alpha, 231)$ -pattern, which means that there are indices $i < j < k$ such that $|\{\text{reg}_\alpha(i), \text{reg}_\alpha(j), \text{reg}_\alpha(k)\}| = 3$, $w_i = w_k + 1$ and $w_j > w_i$. Consider the lower cover u of w in which w_i and w_k are exchanged. In particular, we have $\text{Inv}(w) = \text{Inv}(u) \uplus \{(i, k)\}$. By the induction hypothesis, there exists some $u' \in \mathfrak{S}_\alpha$ such that $\text{Inv}(u')$ is the unique maximal α -aligned inversion set that is contained in $\text{Inv}(u)$. We claim that $w' = u'$.

In order to prove this claim, we choose some element $v \in \mathfrak{S}_\alpha$ such that $\text{Inv}(v)$ is α -aligned and $\text{Inv}(v) \subseteq \text{Inv}(w)$. By construction, we have $(i, j) \notin \text{Inv}(w)$, and hence $(i, j) \notin \text{Inv}(v)$. Since $\text{Inv}(v)$ is α -aligned it follows by definition that $v_i \neq v_k + 1$. We want to show that $\text{Inv}(v) \subseteq \text{Inv}(u)$, which amounts to showing that $(i, k) \notin \text{Inv}(v)$ because $\text{Inv}(w) \setminus \text{Inv}(u) = \{(i, k)\}$.

We assume the opposite, and in view of the argument above it follows that $v_i > v_k + 1$. Let d be the index such that $v_d = v_k + 1$, and let e be the index such that $v_i = v_e + 1$. Since $w_i = w_k + 1$, we observe the following:

- (D) either $w_d < w_k$ or $w_i < w_d$, and
 (E) either $w_e < w_k$ or $w_i < w_e$.

We have the following relations:

$$v_j > v_i > v_e \geq v_d > v_k.$$

(If $v_j < v_i$, then $(i, j) \in \text{Inv}(v) \subseteq \text{Inv}(w)$, which is a contradiction.) We now distinguish five cases.

(i) Let $d < i < k$. Then $(d, k) \in \text{Cov}(v) \subseteq \text{Inv}(w)$. It follows that $w_d > w_k$, and (D) implies $w_d > w_i$. Lemma 4.1.1 implies that d and i lie in different α -regions. Since $\text{Inv}(v)$ is α -aligned, we conclude $(d, i) \in \text{Inv}(v)$. Hence $v_i < v_d = v_k + 1 < v_i$, which is a contradiction.

(ii) Let $i < d < k$. Then $(i, d), (d, k) \in \text{Inv}(v) \subseteq \text{Inv}(w)$. It follows that $w_i > w_d > w_k$, which contradicts $(i, k) \in \text{Cov}(w)$.

(iii) Let $i < e < k$. Then $(i, e), (e, k) \in \text{Inv}(v) \subseteq \text{Inv}(w)$. It follows that $w_i > w_e > w_k$, which contradicts $(i, k) \in \text{Cov}(w)$.

(iv) Let $i < k < e$. Then $(i, e) \in \text{Cov}(v) \subseteq \text{Inv}(w)$. It follows that $w_i > w_e$, and (E) implies $w_e < w_k$. Lemma 4.1.1 implies that k and e lie in different α -regions. Since $\text{Inv}(v)$ is α -aligned, we conclude $(k, e) \in \text{Inv}(v)$. Hence $v_i = v_e + 1 < v_k + 1 < v_i$, which is a contradiction.

(v) Let $e < i < k < d$, which in particular implies that $(e, d) \in \text{Inv}(v) \subseteq \text{Inv}(w)$. Moreover, $(e, k), (i, d) \in \text{Cov}(v) \subseteq \text{Inv}(w)$. It follows that $w_i > w_d$ as well as $w_e > w_k$. Now (D) and (E) imply $w_d < w_k$ and $w_e > w_i$, respectively. Lemma 4.1.1 implies that e, i, k and d all lie in different α -regions.

Let e' be the smallest element in the α -region of e such that $v_{e'} > v_d$, and let d' be the largest element in the α -region of d such that $v_{d'} < v_{e'}$. We record that $e' \leq e < i < j < k < d \leq d'$, and we proceed by induction on $v_{e'} - v_{d'}$. If $v_{e'} = v_{d'} + 1$, then $(e', i), (e', j) \in \text{Inv}(v)$, since $\text{Inv}(v)$ is α -aligned. Lemma 4.1.1 implies that $v_e \geq v_{e'} > v_j > v_i = v_e + 1$, which is a contradiction. If $v_{e'} > v_{d'} + 1$, then there must be some index f with $v_{e'} > v_f > v_{d'} + 1$. By construction we have $v_i = v_e + 1 > v_e \geq v_{e'} > v_f$.

If $f < i$ and they do not lie in the same α -region, then we can consider the triple (f, i, d') , and obtain a contradiction by induction, since $v_f - v_{d'} < v_{e'} - v_{d'}$. If $f > i$ and they do not lie in the same α -region, then we can consider the triple (e', i, f) , and obtain a contradiction by induction, since $v_{e'} - v_f < v_{e'} - v_{d'}$. If f and i lie in the same α -region, then we have $f < i$. We can consider the triple (f, j, d') , and obtain a contradiction by induction, since $v_f - v_{d'} < v_{e'} - v_{d'}$.

We have thus shown that $(i, k) \notin \text{Inv}(v)$, which implies $\text{Inv}(v) \subseteq \text{Inv}(u)$. By the induction assumption it follows that $\text{Inv}(v) \subseteq \text{Inv}(u')$, which proves $w' = u'$. \square

For $\alpha = (1, 1, \dots, 1)$, Lemma 4.3.1 is [147, Lemma 5.6]. We obtain the lattice property of $\text{Weak}(\mathfrak{S}_\alpha(231))$ as a consequence.

Proposition 4.3.2. *For every composition α of $n > 0$, the poset $\text{Weak}(\mathfrak{S}_\alpha(231))$ is a lattice.*

PROOF. Let $u, v \in \mathfrak{S}_\alpha(231)$. By Corollary 3.1.3, $\mathbf{Weak}(\mathfrak{S}_\alpha)$ is a lattice and we denote by w the meet of u and v in $\mathbf{Weak}(\mathfrak{S}_\alpha)$. Then, $\pi_\alpha^\downarrow(w)$ is the greatest $(\alpha, 231)$ -avoiding permutation below u and v and must thus be the meet of u and v in $\mathbf{Weak}(\mathfrak{S}_\alpha(231))$. By inspection of (4.2), we see that $w_{\circ; \alpha} \in \mathfrak{S}_\alpha(231)$. Lemma 1.1.11 then implies that $\mathbf{Weak}(\mathfrak{S}_\alpha(231))$ is a lattice. \square

Let us write $\mathbf{Tam}(\alpha) \stackrel{\text{def}}{=} \mathbf{Weak}(\mathfrak{S}_\alpha)$. Since $\mathbf{Tam}(\alpha)$ is the linear type-A incarnation of a parabolic c -Cambrian lattice, we follow the ordinary case and call $\mathbf{Tam}(\alpha)$ the α -*Tamari lattice*.

We now proceed with proving Conjecture 3.2.6(i) in linear type A. To that end we define a binary relation Θ_α on \mathfrak{S}_α by

$$(4.16) \quad (w, w') \in \Theta_\alpha \quad \text{if and only if} \quad \pi_\alpha^\downarrow(w) = \pi_\alpha^\downarrow(w').$$

It is immediate that Θ_α is an equivalence relation containing exactly one $(\alpha, 231)$ -avoiding permutation per equivalence class. Moreover, π_α^\downarrow maps $w \in \mathfrak{S}_\alpha(231)$ to the least element in its equivalence class. Consequently, the equivalence classes of Θ_α each have a least element under weak order.

We wish to show that Θ_α is a congruence relation of $\mathbf{Weak}(\mathfrak{S}_\alpha)$ exhibiting $\mathbf{Weak}(\mathfrak{S}_\alpha(231))$ as a quotient lattice. Thus, we need to check the properties stated in Lemma 1.1.27.

Lemma 4.3.3. *The fibers of π_α^\downarrow are order convex, i.e., if $u \leq_{\text{weak}} w \leq_{\text{weak}} v$ and $\pi_\alpha^\downarrow(u) = \pi_\alpha^\downarrow(v)$, then $\pi_\alpha^\downarrow(u) = \pi_\alpha^\downarrow(w)$.*

PROOF. Let $u' = \pi_\alpha^\downarrow(u) = \pi_\alpha^\downarrow(v)$ and $w' = \pi_\alpha^\downarrow(w)$. Since $w' \leq_{\text{weak}} w \leq_{\text{weak}} v$, Lemma 4.3.1 implies $w' \leq_{\text{weak}} u'$. Likewise, since $u' \leq_{\text{weak}} u \leq_{\text{weak}} w$, Lemma 4.3.1 implies $u' \leq_{\text{weak}} w'$. \square

We claim that the equivalence classes of Θ_α each have a greatest element, which would prove that the equivalence classes of Θ_α are in fact intervals in $\mathbf{Weak}(\mathfrak{S}_\alpha)$. We say that $w \in \mathfrak{S}_\alpha$ has an $(\alpha, 132)$ -*pattern* if there exist indices $i < j < k$ all in different α -regions such that $w_i = w_k - 1$ and $w_k < w_j$. An α -permutation without $(\alpha, 132)$ -patterns is $(\alpha, 132)$ -*avoiding*. The proof of the following lemma is almost verbatim to the proof of Lemma 4.3.1.

Lemma 4.3.4. *For any $w \in \mathfrak{S}_\alpha$, there exists a unique minimal $(\alpha, 132)$ -avoiding permutation w' with $w \leq_{\text{weak}} w'$.*

If we denote by $\mathfrak{S}_\alpha(132)$ the set of all $(\alpha, 132)$ -avoiding permutations, then Lemma 4.3.4 implies the existence of a map

$$(4.17) \quad \pi_\alpha^\uparrow: \mathfrak{S}_\alpha \rightarrow \mathfrak{S}_\alpha(132),$$

where for any $w \in \mathfrak{S}_\alpha$, $\pi_\alpha^\uparrow(w)$ is the least $(\alpha, 132)$ -avoiding permutation above w in weak order. We now prove some auxiliary results regarding the interaction between the maps π_α^\downarrow and π_α^\uparrow .

Lemma 4.3.5. *The maps π_α^\downarrow and π_α^\uparrow are order preserving.*

PROOF. We prove this property only for π_α^\downarrow ; the reasoning for π_α^\uparrow is analogous. Let $u, v \in \mathfrak{S}_\alpha$ such that $u \leq_{\text{weak}} v$. By Lemma 4.3.1, $\pi_\alpha^\downarrow(u) \leq_{\text{weak}} u \leq_{\text{weak}} v$. Moreover, since $\pi_\alpha^\downarrow(v)$ is maximal among all $(\alpha, 231)$ -avoiding permutations below v —also by Lemma 4.3.1—it follows that $\pi_\alpha^\downarrow(u) \leq_{\text{weak}} \pi_\alpha^\downarrow(v)$. \square

Lemma 4.3.6. *Let $u, v \in \mathfrak{S}_\alpha$ with $u \leq_{\text{weak}} v$ and suppose that $\text{Inv}(v) \setminus \text{Inv}(u) = \{(i, k)\}$. The following are equivalent.*

- (i) *There exists an index $j \in \{i+1, i+2, \dots, k-1\}$ such that $v_j > v_i$.*
- (ii) $\pi_\alpha^\downarrow(u) = \pi_\alpha^\downarrow(v)$.
- (iii) $\pi_\alpha^\uparrow(u) = \pi_\alpha^\uparrow(v)$.

PROOF. If $u \leq_{\text{weak}} v$ and $\text{Inv}(v) \setminus \text{Inv}(u) = \{(i, k)\}$, then $v_i = v_{k+1}$ by construction. In particular, u is obtained from v by swapping the entries in positions i and k . If (i) holds, then v has an $(\alpha, 231)$ -pattern in positions (i, j, k) and u has an $(\alpha, 132)$ -pattern in positions (i, j, k) . Lemmas 4.3.1 and 4.3.4 then imply (ii) and (iii), respectively.

If (i) does not hold, then for any j in an α -region strictly between the α -regions containing i and k , we have $v_j < v_k$. In particular, i and k do neither participate in an $(\alpha, 231)$ -pattern of v , nor in an $(\alpha, 132)$ -pattern of u . The maximality of $\pi_\alpha^\downarrow(v)$ implies that $(i, k) \in \text{Inv}(\pi_\alpha^\downarrow(v))$. However, since $(i, k) \notin \text{Inv}(u)$ we must have $(i, k) \notin \text{Inv}(\pi_\alpha^\downarrow(u))$ implying $\pi_\alpha^\downarrow(u) \neq \pi_\alpha^\downarrow(v)$. We have shown that (ii) implies (i). The proof that (iii) implies (i) is similar. \square

Lemma 4.3.7. *If $\pi_\alpha^\downarrow(u) = \pi_\alpha^\downarrow(v)$, then $\pi_\alpha^\uparrow(u) = \pi_\alpha^\uparrow(v)$.*

PROOF. Let $u, v \in \mathfrak{S}_\alpha$. If $u \leq_{\text{weak}} v$, then the claim follows from Lemma 4.3.6. If $u \leq_{\text{weak}} v$, then the claim follows by repeated application of Lemma 4.3.6. If u and v are incomparable, we consider their meet w in $\mathbf{Weak}(\mathfrak{S}_\alpha)$. If $\pi_\alpha^\downarrow(u) = \pi_\alpha^\downarrow(v)$, then we denote this element by w' . Since w' is the maximal $(\alpha, 231)$ -avoiding permutation below u and v , it follows that $\pi_\alpha^\downarrow(w) = w'$. Since $w \leq_{\text{weak}} u$ and $w \leq_{\text{weak}} v$, we conclude $\pi_\alpha^\uparrow(u) = \pi_\alpha^\uparrow(w) = \pi_\alpha^\uparrow(v)$ using the argument above. \square

Proposition 4.3.8. *The equivalence relation Θ_α is a lattice congruence on $\mathbf{Weak}(\mathfrak{S}_\alpha)$. The corresponding quotient lattice is isomorphic to $\mathbf{Tam}(\alpha)$.*

PROOF. Lemma 4.3.1 implies that the congruence classes of Θ_α each have a least element, and Lemmas 4.3.4 and 4.3.7 imply that the congruence classes of Θ_α each have a greatest element. Lemma 4.3.3 then implies that the congruence classes of Θ_α are actually intervals of $\mathbf{Weak}(\mathfrak{S}_\alpha)$. More precisely, for $w \in \mathfrak{S}_\alpha$, the congruence class $[w]_{\Theta_\alpha}$ equals the interval $[\pi_\alpha^\downarrow(w), \pi_\alpha^\uparrow(w)]$ in $\mathbf{Weak}(\mathfrak{S}_\alpha)$. Lemma 4.3.5 implies that π_α^\downarrow and π_α^\uparrow are order-preserving maps, and the claim follows from Lemma 1.1.27 and

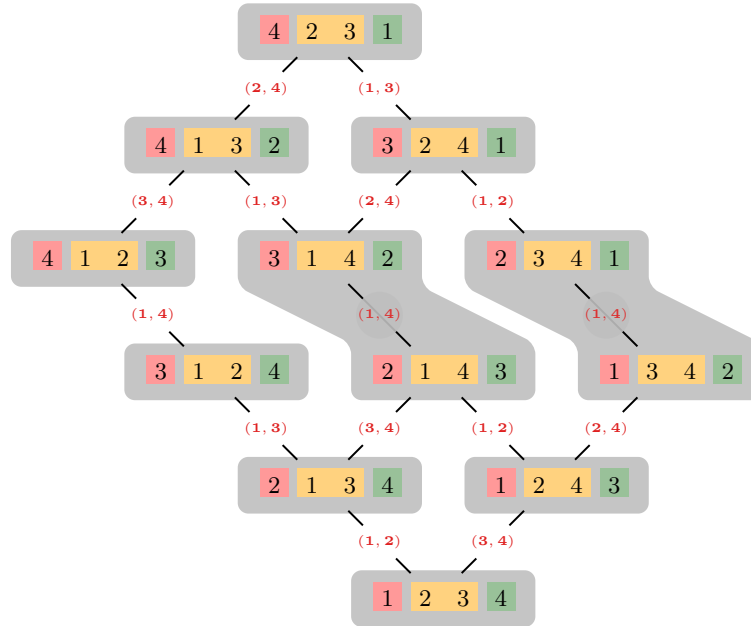


Figure 54. The $(1,2,1)$ -Tamari lattices as it arises as a quotient lattice of $\mathbf{Weak}(\mathfrak{S}_{(1,2,1)})$. The edges are labeled by λ_α , see (4.22).

the consequence of Lemma 4.3.1 that congruence classes of Θ_α are in bijection with $(\alpha, 231)$ -avoiding permutations. \square

The previous reasoning implies the following result, which is illustrated in Figure 54 for $\alpha = (1, 2, 1)$. See also Figure 37a.

Theorem 4.3.9. For every composition α of $n > 0$, $\mathbf{Tam}(\alpha)$ is a quotient lattice of $\mathbf{Weak}(\mathfrak{S}_\alpha)$.

Corollary 4.3.10. For every composition α of $n > 0$, $\mathbf{Tam}(\alpha)$ is congruence uniform and semidistributive.

PROOF. The first claim follows from Proposition 3.2.8 and Theorem 4.3.9. The second claim follows from Theorem 1.1.30(ii). \square

The fact that $\mathbf{Tam}(\alpha)$ arises from $\mathbf{Weak}(\mathfrak{S}_\alpha)$ as a quotient lattice, where the minimal elements per congruence class are $(\alpha, 231)$ -avoiding and the maximal elements per congruence class are $(\alpha, 132)$ -avoiding yields the following duality result, which is illustrated in Figure 55. Recall that for a composition $\alpha = (\alpha_1, \alpha_2, \dots, \alpha_r)$, its reverse is the composition $\bar{\alpha} = (\alpha_r, \dots, \alpha_2, \alpha_1)$.

Theorem 4.3.11. For every composition α of $n > 0$, the lattice $\mathbf{Tam}(\alpha)$ is isomorphic to the dual of $\mathbf{Tam}(\bar{\alpha})$.

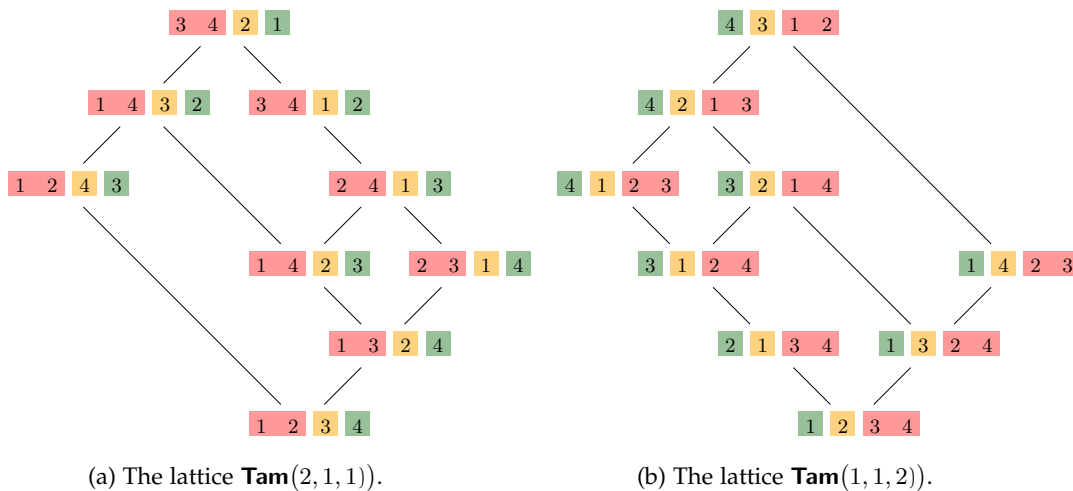


Figure 55. An illustration of Theorem 4.3.11.

PROOF. For $w \in \mathfrak{S}_n$, we define the *reverse* permutation \bar{w} by setting $\bar{w}_i \stackrel{\text{def}}{=} w_{n+1-i}$. We construct a permutation \tilde{w} from \bar{w} by reversing the order of the entries according to the $\bar{\alpha}$ -regions. Then, $\tilde{w} \in \mathfrak{S}_{\bar{\alpha}}$ if and only if $w \in \mathfrak{S}_{\alpha}$.

Now let $u, v \in \mathfrak{S}_{\alpha}$. We prove that $\text{Inv}(u) \subseteq \text{Inv}(v)$ if and only if $\text{Inv}(\tilde{u}) \supseteq \text{Inv}(\tilde{v})$. It is enough to prove one implication, because the other one is analogous. So, suppose that $\text{Inv}(u) \subseteq \text{Inv}(v)$ and choose indices $a < b$ in different $\bar{\alpha}$ -regions such that $(a, b) \notin \text{Inv}(\tilde{u})$. Let a', b' be the unique indices with $u_{a'} = \tilde{u}_a$ and $u_{b'} = \tilde{u}_b$. Since the entries in each $\bar{\alpha}$ -region are ordered linearly, and by passing from u to \tilde{u} (resp. from v to \tilde{v}) we reverse this order, we conclude that $v_{a'} = \tilde{v}_a$ and $v_{b'} = \tilde{v}_b$.

Suppose that $\text{reg}_{\bar{\alpha}}(a) = i$ and $\text{reg}_{\bar{\alpha}}(b) = j$. Since $a < b$, then $i < j$ by assumption. By construction, $\text{reg}_{\alpha}(a') = r + 1 - i$ and $\text{reg}_{\alpha}(b') = r + 1 - j$, and consequently $b' < a'$.

Since $(a, b) \notin \text{Inv}(\tilde{u})$, we must have $u_{a'} = \tilde{u}_a < \tilde{u}_b = u_{b'}$, which implies $(b', a') \in \text{Inv}(u) \subseteq \text{Inv}(v)$. This means that $\tilde{v}_b = v_{b'} > v_{a'} = \tilde{v}_a$; thus $(a, b) \notin \text{Inv}(\tilde{v})$. By contraposition, we obtain $\text{Inv}(\tilde{v}) \subseteq \text{Inv}(\tilde{u})$.

We now show that w has an $(\alpha, 231)$ -pattern if and only if \tilde{w} has an $(\bar{\alpha}, 132)$ -pattern. Once again, it is enough to prove one implication, because the other one is analogous. So, suppose that w has an $(\alpha, 231)$ -pattern in positions (i, j, k) . Let $a = w_i$, $b = w_j$, $c = w_k$. Then, $i < j < k$ belong to different α -regions, and $a < b$ and $a = c + 1$. Let i', j', k' be such that $\tilde{w}_{i'} = a$, $\tilde{w}_{j'} = b$ and $\tilde{w}_{k'} = c$. As before, we see that $k' < j' < i'$ belong to different $\bar{\alpha}$ -regions. By construction, this implies that \tilde{w} has an $(\bar{\alpha}, 132)$ -pattern in positions (k', j', i') .

Let $w \in \mathfrak{S}_{\alpha}$. By Lemma 4.3.7, the least element in the congruence class $[w]_{\Theta_{\alpha}}$ is the $(\alpha, 231)$ -avoiding permutation $\pi_{\alpha}^{\downarrow}(w)$ and the greatest element in $[w]_{\Theta_{\alpha}}$ is the $(\alpha, 132)$ -avoiding permutation $\pi_{\alpha}^{\uparrow}(w)$. Consequently, $\mathbf{Tam}(\alpha) \cong \mathbf{Weak}(\mathfrak{S}_{\alpha}(132))$, too. We have shown above that the assignment $w \mapsto \tilde{w}$ is a bijection from $\mathfrak{S}_{\alpha}(231)$ to $\mathfrak{S}_{\bar{\alpha}}(132)$, which reverses the weak order. This proves the claim. \square

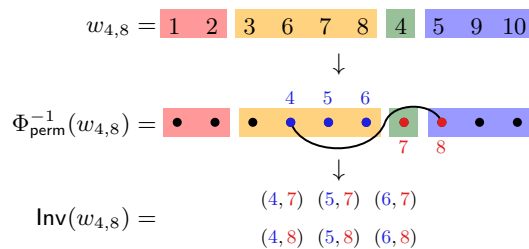


Figure 56. Illustrating the inversion set of a join-irreducible $(\alpha, 231)$ -avoiding permutation.

Example 4.3.12. Let $w =$
4
7
1
5
6
10
3
2
8
9
 $\in \mathfrak{S}_{(2,4,1,3)}$. The reverse permutation is $\bar{w} =$
9
8
2
3
10
6
5
1
7
4, and—after reordering—the associated $\bar{\alpha}$ -permutation is $\tilde{w} =$
2
8
9
3
1
5
6
10
4
7
 $\in \mathfrak{S}_{(3,1,4,2)}$. Note that w has an $(\alpha, 231)$ -pattern in positions $(1, 4, 7)$ induced by the values $\{3, 4, 5\}$ and \tilde{w} has an $(\bar{\alpha}, 132)$ -pattern in positions $(4, 6, 9)$ using the same values.

We henceforth use \leq_{α} and $<_{\alpha}$ to denote order resp. cover relations in $\mathbf{Tam}(\alpha)$; in particular when we need to distinguish them from order resp. cover relations in $\mathbf{Weak}(\mathfrak{S}_{\alpha})$. Our next goal is a description of the canonical join representations of $\mathbf{Tam}(\alpha)$. We start with a characterization of the join-irreducible elements of $\mathbf{Tam}(\alpha)$.

Proposition 4.3.13. For every $a < b$ with $\text{reg}_{\alpha}(a) < \text{reg}_{\alpha}(b)$, there exists a unique $(\alpha, 231)$ -avoiding permutation whose only descent is (a, b) ; denoted by $w_{a,b}$. Moreover,

$$(4.18) \quad \text{Inv}(w_{a,b}) = \left\{ (k, l) \mid a \leq k \leq p_j, p_j + 1 \leq l \leq b \right\}.$$

PROOF. Suppose that $\text{reg}_{\alpha}(a) = j$, and consider the permutation $w_{a,b}$ defined by

$$(4.19) \quad w_{a,b}(i) \stackrel{\text{def}}{=} \begin{cases} i, & \text{if } i < a \text{ or } i > b, \\ a + b - p_j + k, & \text{if } i = a + k \text{ for } 0 \leq k \leq p_j - a, \\ a + k - 1, & \text{if } i = p_j + k \text{ for } 1 \leq k \leq b - p_j. \end{cases}$$

It is quickly verified that $w_{a,b} \in \mathfrak{S}_{\alpha}(231)$ and that $\text{Cov}(w_{a,b}) = \{(a, b)\}$. Moreover, every other $w \in \mathfrak{S}_{\alpha}$ with $\text{Cov}(w) = \{(a, b)\}$ necessarily has an $(\alpha, 231)$ -pattern in positions (a, c, b) for some c appropriate c with $\text{reg}_{\alpha}(a) < \text{reg}_{\alpha}(c) < \text{reg}_{\alpha}(b)$.

It is immediate that the inversion set of $w_{a,b}$ is of the form given in (4.18). \square

Proposition 4.3.13 implies that the inversion set of $w_{a,b}$ can be read off easily from the noncrossing α -partition $\Phi_{\text{perm}}^{-1}(w_{a,b})$. In fact, the first components of an inversion of $w_{a,b}$ are the nodes that lie weakly to the right of a and weakly above the arc connecting nodes a and b , the second components are the nodes that lie weakly below this arc. This is illustrated in the following example in the case $n = 10$, $a = 4$, $b = 8$; see also Figure 56.

Example 4.3.14. Let $\alpha = (3, 2, 1, 2)$. Then, $w_{4,8} = \overline{1\ 2}\ \overline{3\ 6\ 7\ 8}\ \overline{4}\ \overline{5\ 9\ 10}$. Its inversion set is

$$\text{Inv}(w_{4,8}) = \{(4, 7), (4, 8), (5, 7), (5, 8), (6, 7), (6, 8)\}.$$

Lemma 4.3.15. For $w \in \mathfrak{S}_\alpha(231)$, the number of descents of w equals the number of elements of $\mathbf{Tam}(\alpha)$ covered by w .

PROOF. Let $w \in \mathfrak{S}_\alpha(231)$ and let n_w (resp. n_α) denote the number of elements of $\mathbf{Weak}(\mathfrak{S}_\alpha)$ (resp. $\mathbf{Tam}(\alpha)$) covered by w . By definition of the weak order, $n_w = |\text{Cov}(w)|$. Since $\mathbf{Weak}(\mathfrak{S}_\alpha)$ is congruence uniform (and thus semidistributive), n_w equals the number of canonical joinands of w in $\mathbf{Weak}(\mathfrak{S}_\alpha)$ by Corollary 1.1.17. If $w \in \mathfrak{S}_\alpha(231)$, then $\pi_\alpha^\downarrow(w) = w$ and Proposition 1.1.28 implies that n_w is the number of canonical joinands of w in $\mathbf{Tam}(\alpha)$, which is also n_α . \square

Corollary 4.3.16. A permutation $w \in \mathfrak{S}_\alpha(231)$ is join irreducible in $\mathbf{Tam}(\alpha)$ if and only if $w = w_{a,b}$ for some $a < b$ with $\text{reg}_\alpha(a) < \text{reg}_\alpha(b)$.

PROOF. A permutation $w \in \mathfrak{S}_\alpha(231)$ is join irreducible in $\mathbf{Tam}(\alpha)$ if and only if it covers a unique element. By Lemma 4.3.15, w is join irreducible if and only if it has a unique descent. Thus, Proposition 4.3.13 implies that w is join irreducible if and only if $w = w_{a,b}$ for some $a < b$ with $\text{reg}_\alpha(a) < \text{reg}_\alpha(b)$. \square

Corollary 4.3.17. Let $\alpha = (\alpha_1, \alpha_2, \dots, \alpha_r)$. The number of join-irreducible elements of $\mathbf{Tam}(\alpha)$ is

$$|\text{JoinIrr}(\mathbf{Tam}(\alpha))| = \sum_{j=1}^{r-1} \alpha_j \cdot (\alpha_{j+1} + \alpha_{j+2} + \dots + \alpha_r).$$

We finish this section with the proof that Conjecture 3.2.6(iii) holds in linear type A by showing that $\mathbf{Tam}(\alpha)$ is trim; and we subsequently describe the Galois graph of $\mathbf{Tam}(\alpha)$. Since $\mathbf{Tam}(\alpha)$ is semidistributive, it is enough to show that $\mathbf{Tam}(\alpha)$ is extremal by virtue of Theorem 1.1.24.

Proposition 4.3.18. For every composition α of $n > 0$, $\mathbf{Tam}(\alpha)$ is extremal.

PROOF. The semidistributivity of $\mathbf{Tam}(\alpha)$ implies in conjunction with Lemma 1.1.18 that $|\text{JoinIrr}(\mathbf{Tam}(\alpha))| = |\text{MeetIrr}(\mathbf{Tam}(\alpha))|$. The number of join-irreducible elements of $\mathbf{Tam}(\alpha)$ is given by

$$(4.20) \quad f(\alpha) \stackrel{\text{def}}{=} \sum_{j=1}^{r-1} \alpha_j \cdot (\alpha_{j+1} + \alpha_{j+2} + \dots + \alpha_r);$$

see Corollary 4.3.17. It remains to exhibit a chain in $\mathbf{Tam}(\alpha)$ consisting of $f(\alpha) + 1$ elements.

Let $\alpha = (\alpha_1, \alpha_2, \dots, \alpha_r)$. We apply induction on r . If $r = 1$, then $\alpha = (n)$ and $\mathfrak{S}_\alpha(231) = \{e\}$. Thus $\mathbf{Tam}(\alpha)$ is the singleton lattice which is trivially extremal.

Now assume that the claim is true for all compositions of n with at most $r - 1$ components, and recall that $p_j = \alpha_1 + \alpha_2 + \dots + \alpha_j$ for $j \in [r]$.

We set $v^{(0,0)} = e$ and for $k \in [n - p_1]$ we define $v^{(0,k)} = s_{p_1+k-1} \circ v^{(0,k-1)}$. This means that if the value of $v^{(0,k-1)}$ in position p_1 is a , then we move to $v^{(0,k)}$ by swapping the values a and $a + 1$. (By construction, $v_{p_1}^{(0,k-1)} = p_1 + k - 1$.) Since we do this in order from left to right, $v^{(0,k-1)} \prec_\alpha v^{(0,k)}$ and $v^{(0,k)} \in \mathfrak{S}_\alpha(231)$ for all $k \in [n - p_1]$. Then, $v^{(0,n-p_1)}$ has the one-line notation

$$\underbrace{1, 2, \dots, p_1-1, n}_{\alpha_1} \mid \underbrace{p_1, p_1+2, \dots, n-1}_{n-\alpha_1}.$$

(The vertical bar indicates the end of the first α -region.)

Now, for $i \in [p_1 - 1]$, we set $v^{(i,1)} = s_{p_1-i} \circ v^{(i-1,n-p_1)}$ (which means that we swap the values $p_1 - i$ and $p_1 - i + 1$), and for $k \in \{2, \dots, n - p_1\}$ we set $v^{(i,k)} = s_{p_1-i+k-1} \circ v^{(i,k-1)}$. As before, each of these elements is $(\alpha, 231)$ -avoiding. Then, $v^{(p_1-1,n-p_1)}$ has the one-line notation

$$\underbrace{n-p_1+1, n-p_1+2, \dots, n}_{\alpha_1} \mid \underbrace{1, 2, \dots, n-p_1}_{n-\alpha_1}.$$

This constitutes a chain of length $p_1 \cdot (n - p_1)$ from e to $v^{(p_1-1,n-p_1)}$ in $\mathbf{Tam}(\alpha)$. The interval $[v^{(p_1-1,n-p_1)}, w_{\alpha_1}]$ in $\mathbf{Tam}(\alpha)$ is isomorphic to $\mathbf{Tam}((\alpha_2, \dots, \alpha_r))$, which by induction has length $f((\alpha_2, \dots, \alpha_r))$. It follows that

$$\begin{aligned} \ell(\mathbf{Tam}(\alpha)) &= p_1 \cdot (n - p_1) + \sum_{j=2}^{r-1} \alpha_j \cdot (\alpha_{j+1} + \alpha_{j+2} + \dots + \alpha_r) \\ &= \alpha_1 \cdot (\alpha_2 + \alpha_3 + \dots + \alpha_r) + \sum_{j=2}^{r-1} \alpha_j \cdot (\alpha_{j+1} + \alpha_{j+2} + \dots + \alpha_r) \\ &= \sum_{j=1}^{r-1} \alpha_j \cdot (\alpha_{j+1} + \alpha_{j+2} + \dots + \alpha_r) \\ &= f(\alpha). \end{aligned}$$

Hence, $\mathbf{Tam}(\alpha)$ is extremal. \square

Proposition 4.3.19. *For every composition α of $n > 0$, $\mathbf{Tam}(\alpha)$ is trim.*

PROOF. This follows from Corollary 4.3.10, Proposition 4.3.18 and Theorem 1.1.24. \square

Figure 57 shows $\mathbf{Tam}(\alpha)$, for $\alpha = (2, 1, 2)$, where the nodes are labeled by both $(\alpha, 231)$ -avoiding permutations and noncrossing α -partitions, and the maximal chain constructed in the proof of Proposition 4.3.18 is highlighted.

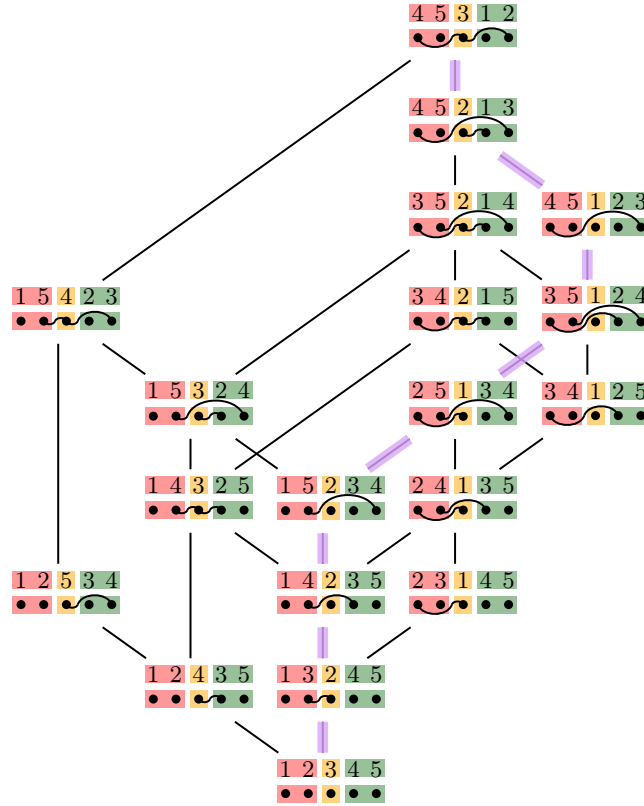


Figure 57. The lattice $\mathbf{Tam}((2, 1, 2))$.

Corollary 4.3.20. *Let C be the maximal chain constructed in the proof of Proposition 4.3.18. The label sequence $\lambda_\alpha(C)$ induces a total order on $\text{Joinrr}(\mathbf{Tam}(\alpha))$ given by the following cover relations:*

$$w_{a,b} \prec \begin{cases} w_{a,b+1}, & \text{if } p_j + 1 \leq b < n, \\ w_{a-1,p_j+1}, & \text{if } a \neq p_{j-1} + 1 \text{ and } b = n, \\ w_{p_{j+1},p_{j+1}+1}, & \text{if } a = p_{j-1} + 1 \text{ and } b = n, \end{cases}$$

if $\text{reg}_\alpha(a) = j$.

PROOF. With the notation from the proof of Proposition 4.3.18, the first $p_1 \cdot (n - p_1)$ cover relations on C are:

$$e = v^{(0,0)} \prec_\alpha v^{(0,1)} \prec_\alpha \dots \prec_\alpha v^{(0,n-p_1)} \prec_\alpha v^{(1,1)} \prec_\alpha \dots \prec_\alpha v^{(1,n-p_1)} \prec_\alpha \dots \prec_\alpha v^{(2,1)} \prec_\alpha \dots \prec_\alpha v^{(p_1-1,n-p_1)}.$$

By construction, C is also a maximal chain in $\mathbf{Weak}(\mathfrak{S}_\alpha)$ and it follows that

$$\lambda_{\text{jsd}}(v^{(i,k)}, v^{(i,k+1)}) = \begin{cases} w_{p_1,p_1+1}, & \text{if } i = k = 0, \\ w_{p_1-i-1,p_1+1}, & \text{if } 0 \leq i < p_1 - 1, k = n - p_1, \\ w_{p_1-i,p_1+k} & \text{if } 0 \leq i \leq p_1 - 1, 0 < k < n - p_1. \end{cases}$$

(If $k = n - p_1$, then we set $k + 1 = 1$.) The claim follows by induction. \square

Example 4.3.21. Let $\alpha = (2, 1, 2)$. The chain constructed in the proof of Proposition 4.3.18 is highlighted in Figure 57. The total order of the join-irreducibles of $\mathbf{Tam}((2, 1, 2))$ is

$$w_{2,3} \prec w_{2,4} \prec w_{2,5} \prec w_{1,3} \prec w_{1,4} \prec w_{1,5} \prec w_{3,4} \prec w_{3,5}.$$

Remark 4.3.22. If $\alpha = (1, 1, \dots, 1) \vdash n$, then the join-irreducibles of $\mathbf{Tam}((1, 1, \dots, 1)) = \mathbf{Tam}(n)$ correspond to all transpositions (a, b) for $1 \leq a < b \leq n$. The total order defined in Corollary 4.3.20 corresponds to the lexicographic order on these transpositions. In general, this order seems to recover the inversion order $\mathbf{Inv}(w_{\alpha; \alpha}(\vec{c}))$ for arbitrary compositions α .

Let us summarize the previous results in a handy theorem.

Theorem 4.3.23. For every composition α of $n > 0$, $\mathbf{Tam}(\alpha)$ is a congruence-uniform, trim quotient lattice of $\mathbf{Weak}(\mathfrak{S}_\alpha)$.

PROOF. This follows from Theorem 4.3.9, Corollary 4.3.10 and Proposition 4.3.19. \square

In fact, as a byproduct of the above, we have gathered almost all ingredients to describe the poset of join-irreducibles of $\mathbf{Tam}(\alpha)$.

Corollary 4.3.24. Let $w_{a,b}, w_{a',b'} \in \text{JoinIrr}(\mathbf{Tam}(\alpha))$. Then, $w_{a,b} \leq_\alpha w_{a',b'}$ if and only if a and a' belong to the same α -region and $a' \leq a < b \leq b'$.

PROOF. This an immediate consequence of Proposition 4.3.13. \square

Theorem 4.3.25. Let $n > 0$ and let $\alpha = (\alpha_1, \alpha_2, \dots, \alpha_r)$ be a composition of n . The poset of join-irreducible elements of $\mathbf{Tam}(\alpha)$ consists of $r-1$ connected components, where for $j \in [r-1]$ the j^{th} component is isomorphic to the direct product of an α_j -chain and an $(\alpha_{j+1} + \alpha_{j+2} + \dots + \alpha_r)$ -chain.

PROOF. By Corollary 4.3.24 we conclude that for $w_{a,b} \leq_{\text{weak}} w_{a',b'}$ to hold, it is necessary that a and a' belong to the same α -region. This accounts for the $r-1$ connected components of $\mathbf{Weak}(\text{JoinIrr}(\mathbf{Tam}(\alpha)))$, because a can be chosen from any but the last α -region and there is a total of r α -regions.

Now suppose that a lies in the j^{th} α -region, which means that a takes any of the values $\{p_{j-1}+1, p_{j-1}+2, \dots, p_j\}$. For any choice of a , we can pick some $b \in \{p_j+1, p_j+2, \dots, n\}$ to obtain a join-irreducible element $w_{a,b}$. Observe that whenever $a \neq p_{j-1}+1$, then $w_{a,b} \leq_{\text{weak}} w_{a-1,b}$, and we always have $w_{a,b} \leq_{\text{weak}} w_{a,b+1}$ when $b < n$. This implies

(a) The poset $\mathbf{Weak}(\text{JoinIrr}(\mathbf{Tam}(1, 2, 1)))$.(b) The poset $\mathbf{Weak}(\text{JoinIrr}(\mathbf{Tam}(2, 1, 2)))$.Figure 58. Two posets of join-irreducible α -permutations.

that the j^{th} component of $\mathbf{Weak}(\text{JoinIrr}(\mathbf{Tam}(\alpha)))$ is isomorphic to the direct product of an α_j -chain and an $(\alpha_{j+1} + \alpha_{j+2} + \dots + \alpha_r)$ -chain. \square

See Figure 58 for an illustration of Theorem 4.3.25. The next result, illustrated in Figure 59, characterizes the Galois graph of $\mathbf{Tam}(\alpha)$.

Theorem 4.3.26. *Let $n > 0$ and let α be a composition of n . The Galois graph of $\mathbf{Tam}(\alpha)$ is isomorphic to the directed graph whose vertices are the join-irreducible elements of $\mathbf{Tam}(\alpha)$ and in which there exists a directed edge $w_{a,b} \rightarrow w_{a',b'}$ if and only if $w_{a,b} \neq w_{a',b'}$ and*

- either a and a' belong to the same α -region and $a \leq a' < b' \leq b$,
- or a and a' belong to different α -regions and $a' < a < b' \leq b$, where a and b' belong to different α -regions, too.

PROOF. By definition, the vertex set of Galois($\mathbf{Tam}(\alpha)$) is $[K]$, where

$$K = |\text{JoinIrr}(\mathbf{Tam}(\alpha))| = f(\alpha)$$

and $f(\alpha)$ is defined in (4.20). There exists a directed edge $s \rightarrow t$ in Galois($\mathbf{Tam}(\alpha)$) if $s \neq t$ and $j_s \not\leq_{\alpha} m_t$, where the join- and meet-irreducible elements of $\mathbf{Tam}(\alpha)$ are ordered as in (1.7). By Corollary 4.3.10, $\mathbf{Tam}(\alpha)$ is also congruence uniform, so that Corollary 1.1.25(i) implies $s \rightarrow t$ if and only if $j_t \leq_{\alpha} j_{t*} \vee j_s$. We may thus view Galois($\mathbf{Tam}(\alpha)$) as a directed graph on the vertex set $\text{JoinIrr}(\mathbf{Tam}(\alpha))$.

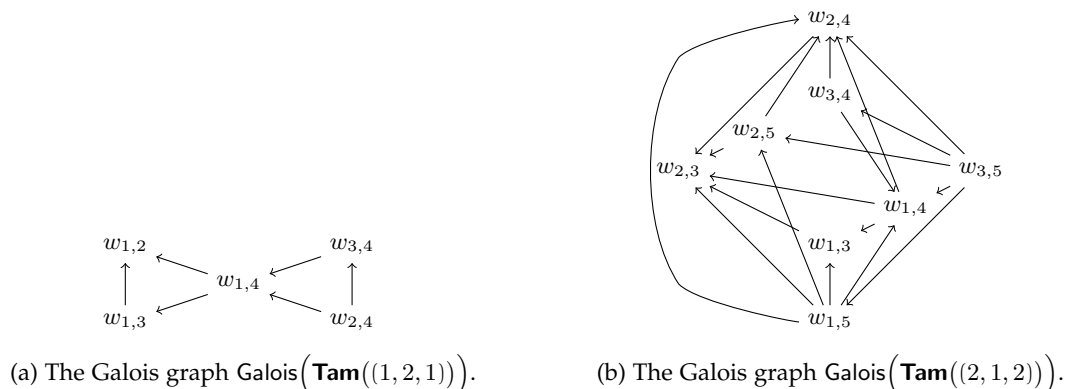
Now, pick $w_{a,b}, w_{a',b'} \in \text{JoinIrr}(\mathbf{Tam}(\alpha))$ such that $w_{a,b} \neq w_{a',b'}$ and $\text{reg}_{\alpha}(a) = i$ and $\text{reg}_{\alpha}(a') = i'$. We need to characterize when

$$(4.21) \quad w_{a',b'} \leq_{\alpha} w_{a',b'*} \vee_{\alpha} w_{a,b}.$$

For simplicity, let us write $w = w_{a,b}$, $w' = w_{a',b'}$ and $w'_* = (w_{a',b'})_*$. Let $z = w'_* \vee_{\alpha} w$. By definition, $\text{Inv}(w'_*) \cup \text{Inv}(w) \subseteq \text{Inv}(z)$. By Proposition 4.3.13, $\text{Inv}(w'_*) = \text{Inv}(w') \setminus \{(a', b')\}$. Then, (4.21) is satisfied if and only if $(a', b') \in \text{Inv}(z)$, which is the case if $(a', b') \in \text{Inv}(w)$ or if there exists $c \in \{a'+1, a'+2, \dots, b'-1\}$ such that $(a', c) \in \text{Inv}(w'_*)$ and $(c, b') \in \text{Inv}(w)$ or vice versa.

Let us first consider the case where a and a' belong to the same α -region, i.e., $i = i'$. There are two cases.

(i) Let $a \leq a'$. If $b' \leq b$, then Corollary 4.3.24 implies $w' \leq_{\alpha} w$ and (4.21) holds. If $b < b'$, then by Proposition 4.3.13, $(a', b') \notin \text{Inv}(w)$. In fact, $(c, b') \notin \text{Inv}(w)$ for any

Figure 59. Galois graphs of two α -Tamari lattices.

$c \in [n]$, and if $(a', c) \in \text{Inv}(w)$, then $p_i + 1 \leq c \leq b$. However, if $(c, b') \in \text{Inv}(w'_*)$, then $a' + 1 \leq c \leq p_i$. Thus, $(a', b') \notin \text{Inv}(z)$ so that (4.21) is not satisfied.

(ii) Let $a > a'$. If $b \leq b'$, then Corollary 4.3.24 implies $w <_\alpha w'$, so that (4.21) does not hold. If $b > b'$, then by Proposition 4.3.13, $(a', b') \notin \text{Inv}(w)$. Again, $(a', c) \notin \text{Inv}(w)$ for any $c \in [n]$, and if $(c, b') \in \text{Inv}(w)$, then $a \leq c \leq p_i$. However, if $(a', c) \in \text{Inv}(w'_*)$, then $p_i + 1 \leq c < b'$. Thus, $(a', b') \notin \text{Inv}(z)$ so that (4.21) is not satisfied.

Let us now consider the case where a and a' belong to different α -regions, i.e., $i \neq i'$. By Proposition 4.3.13, $(a', b') \notin \text{Inv}(w)$. As before, we may actually conclude $(a', c) \notin \text{Inv}(w)$ for all $c \in [n]$, and if $(c, b') \in \text{Inv}(w)$, then $a \leq c \leq p_i$ and $p_i < b' \leq b$. If $(a', c) \in \text{Inv}(w'_*)$, then $p_{i'} + 1 \leq c < b'$.

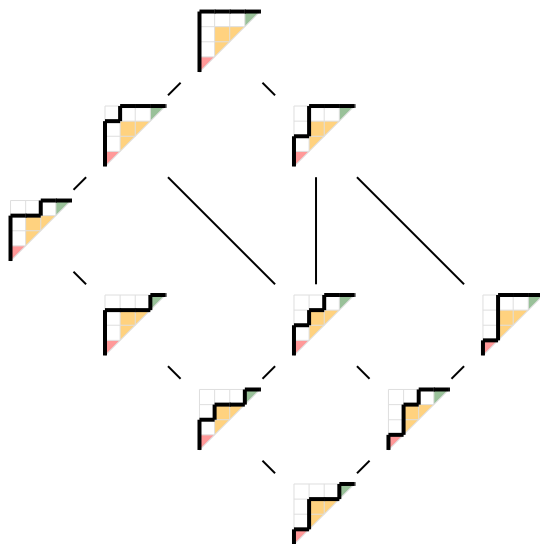
(i) If $i < i'$, then $p_i < p_{i'} + 1$. Thus, $(a', b') \notin \text{Inv}(z)$ so that (4.21) is not satisfied.

(ii) If $i > i'$, then $a' < a$. If $b' \leq p_i$, then $(c, b') \notin \text{Inv}(w)$ for any $c \in [n]$ and (4.21) cannot be satisfied. If $p_i < b'$, then we may choose $c = a$ to see that $(a', b') \in \text{Inv}(z)$ which implies (4.21). \square

4.3.2. The rotation order on $\text{Dyck}(\alpha)$. According to Section 4.1.3, the parabolic nonnesting partitions of \mathfrak{S}_α are in bijective correspondence with the northeast paths weakly above $v_\alpha = N^{\alpha_1} E^{\alpha_1} N^{\alpha_2} E^{\alpha_2} \dots N^{\alpha_r} E^{\alpha_r}$ when $\alpha = (\alpha_1, \alpha_2, \dots, \alpha_r)$. In Section 2.5.1, we have defined a natural partial order on the set of lattice paths weakly above *any* northeast path. This yields a second natural lattice structure associated with the parabolic quotient \mathfrak{S}_α ; the v_α -Tamari lattice $\mathbf{Tam}(v_\alpha) \stackrel{\text{def}}{=} (\text{Dyck}(\alpha), \leq_{v_\alpha})$.

If $\alpha = (1, 1, \dots, 1) \vdash n$, then we have seen before that $\mathbf{Tam}(v_\alpha) \cong \mathbf{Tam}(\alpha)$. Figures 60 and 61 display the lattices $\mathbf{Tam}(v_{(1,2,1)})$ and $\mathbf{Tam}(v_{(2,1,2)})$, respectively. If we compare these figures with Figures 54 and 57, then we see that this isomorphism appears to extend to parabolic quotients of the symmetric group. The main result of this section asserts that this is true in general.

Theorem 4.3.27. *For every composition α of $n > 0$, the lattices $\mathbf{Tam}(\alpha)$ and $\mathbf{Tam}(v_\alpha)$ are isomorphic.*

Figure 60. The lattice $\mathbf{Tam}(v_{(1,2,1)})$.

We prove Theorem 4.3.27 by generalizing the BW-codes from the end of Section 2.2.1. For $\alpha = (\alpha_1, \alpha_2, \dots, \alpha_r)$, let $\mathbf{Codes}(\alpha)$ denote the set of all integer tuples (c_1, c_2, \dots, c_n) with the following properties:

- (C1): $0 \leq c_i \leq n - p_{\text{reg}_\alpha(i)}$ for all $i \in [n]$;
- (C2): $c_i \leq c_{i+1}$ for all $i \in [n-1]$ such that $\text{reg}_\alpha(i) = \text{reg}_\alpha(i+1)$;
- (C3): $c_{p_a} \leq c_i - p_a + p_{\text{reg}_\alpha(i)}$ for all $i \in [p_{r-2}]$ and all $a \in \{\text{reg}_\alpha(i)+1, \text{reg}_\alpha(i)+2, \dots, r-1\}$ such that $c_i \geq p_a - p_{\text{reg}_\alpha(i)}$.

Remark 4.3.28. The statement of (C3) is directly true if $a = r$ and trivial if $i > p_{r-2}$, hence the restriction to $i \in [p_{r-2}]$ and $a < r$.

Indeed, by (C1), $c_n = 0$ so that the implication required by (C3) is trivially satisfied when $a = r$. If $i > p_{r-2}$, then $\text{reg}_\alpha(i) \geq r-1$, so that the only case one could consider is again $a = r$.

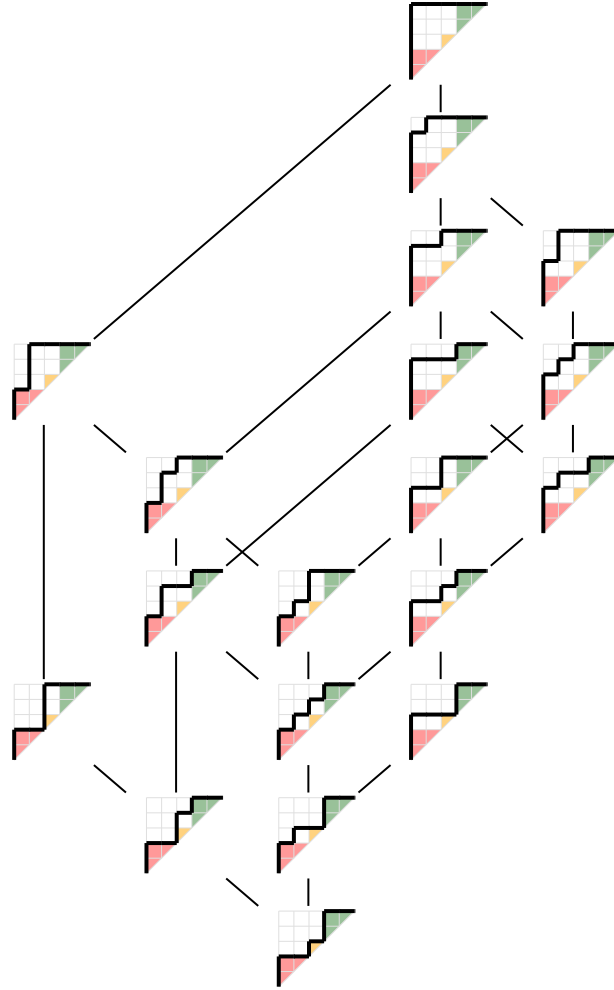
Example 4.3.29. If $\alpha = (2, 1)$, then (C1)–(C3) boil down to requiring $0 \leq c_1 \leq c_2 \leq 1$ and $c_3 = 0$ for (c_1, c_2, c_3) to belong to $\mathbf{Codes}((2, 1))$. If $\alpha = (1, 2)$, we obtain $0 \leq c_1 \leq 2$ and $0 \leq c_2 \leq c_3 \leq 0$. This means that $\mathbf{Codes}((2, 1))$ and $\mathbf{Codes}((1, 2))$ both consist of three elements.

For $\alpha = (1, 2, 1)$, conditions (C1)–(C3) imply that $\mathbf{Codes}((1, 2, 1))$ consists of tuples (c_1, c_2, c_3, c_4) with $0 \leq c_1 \leq 3$, $0 \leq c_2 \leq c_3 \leq 1$ and $c_4 = 0$. There are ten such tuples.

The componentwise order of two integer tuples $\mathbf{a} = (a_1, a_2, \dots, a_n)$ and $\mathbf{b} = (b_1, b_2, \dots, b_n)$ is defined by $\mathbf{a} \leq_{\text{comp}} \mathbf{b}$ if and only if $a_i \leq b_i$ for all $i \in [n]$. Let $\mathbf{Codes}(\alpha) \stackrel{\text{def}}{=} (\mathbf{Codes}(\alpha), \leq_{\text{comp}})$. The first step in proving Theorem 4.3.27 is the proof that $\mathbf{Tam}(\alpha)$ and $\mathbf{Codes}(\alpha)$ are isomorphic. For $w \in \mathfrak{S}_\alpha$, we define its α -code by $\text{cd}_\alpha(w) = (c_1, c_2, \dots, c_n)$, where

$$c_i \stackrel{\text{def}}{=} \max\{k \mid w_i > w_{p_{\text{reg}_\alpha(i)+1}}, w_i > w_{p_{\text{reg}_\alpha(i)+2}}, \dots, w_i > w_{p_{\text{reg}_\alpha(i)+k}}\}.$$

In other words, c_i counts the number of consecutive entries in w that are smaller than w_i starting from the first position after the α -region containing i . If $\text{cd}_\alpha(w) = (c_1, c_2, \dots, c_n)$, then

Figure 61. The lattice $\mathbf{Tam}(v_{(2,1,2)})$.

we say that w_i *sees* w_k if $0 < k - p_{\text{reg}_\alpha(i)} \leq c_i$. This means that w_i sees all positions contributing to c_i . Clearly, if w_i sees w_k , then $(i, k) \in \text{Inv}(w)$ and w_i sees exactly c_i elements for each $i \in [n]$.

Lemma 4.3.30. *For $w \in \mathfrak{S}_\alpha$, it holds that $\text{cd}_\alpha(w) \in \text{Codes}(\alpha)$.*

PROOF. Let $w \in \mathfrak{S}_\alpha$ with $\text{cd}_\alpha(w) = (c_1, c_2, \dots, c_n)$, and choose $i \in [n]$. The maximal number of inversions of w of the form (i, k) is $n - p_{\text{reg}_\alpha(i)}$, because $w_i < w_k$ for all $k \in \{i+1, i+2, \dots, p_{\text{reg}_\alpha(i)}\}$. Hence, $c_i \leq n - p_{\text{reg}_\alpha(i)}$, which establishes (C1). If $\text{reg}_\alpha(i) = \text{reg}_\alpha(i+1)$, then $w_i < w_{i+1}$ because $w \in \mathfrak{S}_\alpha$. Thus, $c_i \leq c_{i+1}$, which establishes (C2). Now let $a \in \{\text{reg}_\alpha(i)+1, \text{reg}_\alpha(i)+2, \dots, r\}$ be such that $c_i \geq p_a - p_{\text{reg}_\alpha(i)}$. In particular, w_i sees w_{p_a} , meaning that $w_i > w_{p_a}$. Hence, w_i also sees any w_k which is seen by w_{p_a} . This implies that $c_i \geq c_{p_a} + p_a - p_{\text{reg}_\alpha(i)}$, which is (C3). \square

Example 4.3.31. Let us illustrate the definition of α -codes in the case when $\alpha = (1, 2, 1)$.

$w \in \mathfrak{S}_{(1,2,1)}$	$cd_{(1,2,1)}(w)$
1 2 3 4	(0, 0, 0, 0)
1 2 4 3	(0, 0, 1, 0)
1 3 4 2	(0, 1, 1, 0)
2 1 3 4	(1, 0, 0, 0)
2 1 4 3	(1, 0, 1, 0)
2 3 4 1	(0, 1, 1, 0)
3 1 2 4	(2, 0, 0, 0)
3 1 4 2	(1, 0, 1, 0)
3 2 4 1	(1, 1, 1, 0)
4 1 2 3	(3, 0, 0, 0)
4 1 3 2	(3, 0, 1, 0)
4 2 3 1	(3, 1, 1, 0)

The red and the blue pairs indicate that the assignment $w \mapsto cd_\alpha(w)$ is in general not injective.

The previous example exhibits that in general several α -permutations have the same α -code. We will show now that all elements in a congruence class of Θ_α share an α -code.

Lemma 4.3.32. Let $u, v \in \mathfrak{S}_\alpha$ with $u \leq_{\text{weak}} v$. Then, $cd_\alpha(u) \leq_{\text{comp}} cd_\alpha(v)$, and these tuples differ by at most one element. Moreover, $cd_\alpha(u) = cd_\alpha(v)$ if and only if $\pi_\alpha^\perp(u) = \pi_\alpha^\perp(v)$.

PROOF. Let $u \leq_{\text{weak}} v$ and $cd_\alpha(u) = (a_1, a_2, \dots, a_n)$ and $cd_\alpha(v) = (b_1, b_2, \dots, b_n)$. By assumption, $\text{Inv}(v) \setminus \text{Inv}(u) = \{(i, k)\}$ for some indices $i < k$ in different α -regions such that $v_i = v_k + 1$. It follows that any entry which sees v_k must be bigger than v_i , and any entry which does not see v_i must be smaller than v_k . Thus, $a_j = b_j$ for all $j \neq i$. By construction, $u_i = v_k$ and $u_k = v_i$. Since $u_i < u_k$, we conclude that u_i never sees u_k . If v_i sees v_k , then $a_i < b_i$. This is the case precisely when every j in α -regions strictly between i and k satisfies $v_j < v_i$, which by Lemma 4.3.6 means that $\pi_\alpha^\perp(u) \neq \pi_\alpha^\perp(v)$. If v_i does not see v_k , then there exists an index j in an α -region strictly between i and k such that $v_i < v_j$, which by Lemma 4.3.6 is equivalent to $\pi_\alpha^\perp(u) = \pi_\alpha^\perp(v)$. If we choose j as small as possible with this property, then any $j' < j$ in an α -region strictly between i and k satisfies $v_i > v_{j'}$, and thus $u_i = v_k > v_{j'} = u_{j'}$, which entails $a_i = b_i$. \square

Corollary 4.3.33. If $u \leq_{\text{weak}} v$, then $cd_\alpha(u) \leq_{\text{comp}} cd_\alpha(v)$.

PROOF. This follows from repeated application of Lemma 4.3.32. \square

Lemma 4.3.34. Let $u \in \mathfrak{S}_\alpha(231)$ and $v \in \mathfrak{S}_\alpha$. If $cd_\alpha(u) \leq_{\text{comp}} cd_\alpha(v)$, then $u \leq_{\text{weak}} v$.

PROOF. Let $cd_\alpha(u) = (a_1, a_2, \dots, a_n)$ and $cd_\alpha(v) = (b_1, b_2, \dots, b_n)$ such that $cd_\alpha(u) \leq_{\text{comp}} cd_\alpha(v)$.

Assume that there exists $(i, k) \in \text{Inv}(u) \setminus \text{Inv}(v)$, and among all these inversions choose (i, k) such that $u_i - u_k$ is minimal. Since (i, k) is not an inversion of v , we have $v_i < v_k$, so that v_i does not see v_k . Since $a_i \leq b_i$ it follows that u_i does not see u_k either. Since $u_i > u_k$, $\text{reg}_\alpha(i) < \text{reg}_\alpha(k)$ and there exists a smallest index j with $\text{reg}_\alpha(i) < \text{reg}_\alpha(j) < \text{reg}_\alpha(k)$ and $u_i < u_j$. Since $u \in \mathfrak{S}_\alpha(231)$, we have that $u_i > u_k + 1$.

Now, there cannot be any element between $u_k + 1$ and $u_i - 1$ in the same α -region as u_j . Indeed, if this was the case, since $u_j > u_i$, u_{j-1} would be such an element. But, since it is seen by u_i by minimality of j , and since $b_i \geq a_i$, the value v_{j-1} would be seen by v_i , so that $v_k > v_i > v_{j-1}$. In that case, $(j-1, k)$ would be an inversion of u , not an inversion of v and would violate the minimality of (i, k) among such elements as defined earlier.

So all elements between u_k and u_i belong to α -regions different from the α -region containing u_j . Thus, among those, there is a smallest one, say u_l , (which is not u_k but can be u_i) that is on the left of u_j . This element belongs to an $(\alpha, 231)$ -pattern in u : (l, j, l') , where l' is the position of $u_l - 1$ in u , which is a contradiction.

Therefore, our assumption must have been wrong, and it follows $\text{Inv}(u) \subseteq \text{Inv}(v)$, thus $u \leq_{\text{weak}} v$ by definition. \square

Now we show that $w \mapsto cd_\alpha(w)$ is a bijection when restricted to $(\alpha, 231)$ -avoiding permutations.

Lemma 4.3.35. *If $w \in \mathfrak{S}_\alpha(231)$, then the left-most 0 in $cd_\alpha(w)$ corresponds to the position of the 1 in the one-line notation of w .*

PROOF. Let $cd_\alpha(w) = (c_1, c_2, \dots, c_n)$, and let $j_o \in [n]$ be such that $w_{j_o} = 1$. Moreover, if $j = \min\{i \mid c_i = 0\}$, then $j \leq j_o$, since $c_{j_o} = 0$. Let $w_j = a$. Since the entries in an α -region are ordered increasingly, it must necessarily be that a is the smallest element in its α -region.

Now, define $m = \min(w_1, w_2, \dots, w_j)$. Then, if $m \neq a$, since m is strictly to the left of a in w , it cannot be 1 either, so that we have a 231-pattern with the values m , a , and $m-1$ necessarily in that order in w and in different regions. Otherwise, $m = a$. If $m \neq 1$, the region of a cannot be the rightmost region of w since $a-1$ did not appear in this prefix of w . Let b be the smallest element in the $(\text{reg}_\alpha(j) + 1)^{\text{st}}$ α -region, and let $k = p_{\text{reg}(j)} + 1$, i.e., $w_k = b$. Since $c_j = 0$, we have $a < b$. We then have an $(\alpha, 231)$ -pattern with the values a , b , and $a-1$.

It follows that $j = j_o$. \square

Proposition 4.3.36. *For $c \in \text{Codes}(\alpha)$ there exists a unique $w \in \mathfrak{S}_\alpha(231)$ such that $cd_\alpha(w) = c$.*

PROOF. We proceed by induction on n . For $n \leq 3$, the claim can be checked directly, which establishes the induction base. Assume that the claim holds for all compositions of $n' < n$.

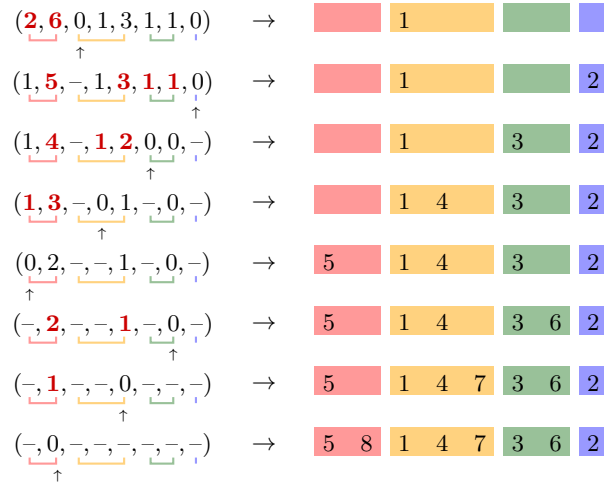


Figure 62. Decoding the $(2, 3, 2, 1)$ -code $(2, 6, 0, 1, 3, 1, 1, 0)$. The arrows indicate the left-most zero in each step; the red digits indicate the positions that see the left-most zero.

Let $\mathbf{c} = (c_1, c_2, \dots, c_n) \in \text{Codes}(\alpha)$. By definition, $c_n = 0$, which enables us to define $j_o = \min\{j \in [n] \mid c_j = 0\}$. By (C2), $j_o = p_{a-1} + 1$ for some $a \in [r]$, meaning that j_o is the first element in the a^{th} α -region.

Let $\alpha' = (\alpha'_1, \alpha'_2, \dots, \alpha'_r)$ be the unique composition of $n - 1$ which is obtained by subtracting 1 from α_a . (If $\alpha_a = 1$, then we simply remove this component.) We define $p'_b = \alpha'_1 + \alpha'_2 + \dots + \alpha'_b$, and obtain

$$p'_b = \begin{cases} p_b, & \text{if } b < a, \\ p_b - 1, & \text{if } b \geq a. \end{cases}$$

We define $\mathbf{c}' = (c'_1, c'_2, \dots, c'_{n-1})$ by setting

$$c'_i = \begin{cases} c_i, & i < j_o \text{ and } p_i < p_{a-1} - p_{\text{reg}_\alpha(i)}, \\ c_i - 1, & i < j_o \text{ and } p_i \geq p_{a-1} - p_{\text{reg}_\alpha(i)}, \\ c_{i+1}, & i \geq j_o. \end{cases}$$

It is straightforward to check that $\mathbf{c}' \in \text{Codes}(\alpha')$. By induction hypothesis, there exists a unique $w' \in \mathfrak{S}_{\alpha'}(231)$ with $\text{cd}_{\alpha'}(w') = \mathbf{c}'$.

We now “inject” 1 into w' to construct a permutation $w \in \mathfrak{S}_n$ via

$$w_i = \begin{cases} w'_i + 1, & \text{if } i < j_o, \\ 1, & \text{if } i = j_o, \\ w'_{i-1} + 1, & \text{if } i > j_o. \end{cases}$$

Since j_o is the first element in the a^{th} α -region, it follows that $w \in \mathfrak{S}_\alpha$. Assume that w has an $(\alpha, 231)$ -pattern (i, j, k) . Since $w' \in \mathfrak{S}_{\alpha'}(231)$, it must be that $k = j_o$, and $w_i = 2$. By construction, $w'_i = 1$, implying that $c'_i = 0$. Since $i < j_o$, it follows that $c_i = 0$, contradicting the choice of j_o . Thus, $w \in \mathfrak{S}_\alpha(231)$. By construction, it follows that w is the only $(\alpha, 231)$ -avoiding permutation with $\text{cd}_\alpha(w) = \mathbf{c}$. \square

The construction of the $(\alpha, 231)$ -avoiding permutation associated with $\mathbf{c} \in \text{Codes}(\alpha)$ from the proof of Proposition 4.3.36 is illustrated in Figure 62. We now prove that the α -Tamari lattice is isomorphic to the lattice of α -codes under componentwise order.

Proposition 4.3.37. *For every composition α of $n > 0$, $\mathbf{Tam}(\alpha) \cong (\text{Codes}(\alpha), \leq_{\text{comp}})$.*

PROOF. Proposition 4.3.36 establishes that $\mathfrak{S}_\alpha(231)$ and $\text{Codes}(\alpha)$ are in bijection, and Corollary 4.3.33 and Lemma 4.3.34 establish that for $u, v \in \mathfrak{S}_\alpha(231)$ we have $u \leq_{\text{weak}} v$ if and only if $\text{cd}_\alpha(u) \leq_{\text{comp}} \text{cd}_\alpha(v)$. This finishes the proof. \square

In fact, the preimages of the maps $\text{cd}_\alpha: \mathfrak{S}_\alpha \rightarrow \text{Codes}(\alpha)$ and $\pi_\alpha^\downarrow: \mathfrak{S}_\alpha \rightarrow \mathfrak{S}_\alpha(231)$ coincide.

Lemma 4.3.38. *For $u, v \in \mathfrak{S}_\alpha$ we have $\text{cd}_\alpha(u) = \text{cd}_\alpha(v)$ if and only if $\pi_\alpha^\downarrow(u) = \pi_\alpha^\downarrow(v)$.*

PROOF. Let $u, v \in \mathfrak{S}_\alpha$. Let $\text{cd}_\alpha(u) = (a_1, a_2, \dots, a_n)$ and $\text{cd}_\alpha(v) = (b_1, b_2, \dots, b_n)$. If $u \leq_{\text{weak}} v$, then the desired equivalence follows from repeated application of Lemma 4.3.32. Otherwise, u and v are incomparable. By Corollary 3.1.3, $\mathbf{Weak}(\mathfrak{S}_\alpha)$ is a lattice and thus the meet $w = u \wedge v$ exists and satisfies $w \leq_{\text{weak}} u$ and $w \leq_{\text{weak}} v$. If $\pi_\alpha^\downarrow(u) = \pi_\alpha^\downarrow(v)$, then $\pi_\alpha^\downarrow(u) = \pi_\alpha^\downarrow(w)$, by Lemma 4.3.1. It follows that $\text{cd}_\alpha(u) = \text{cd}_\alpha(w) = \text{cd}_\alpha(v)$ by Lemma 4.3.32. Conversely, let $\text{cd}_\alpha(u) = \text{cd}_\alpha(v)$. Lemma 4.3.1 implies $\pi_\alpha^\downarrow(u) \leq_{\text{weak}} u$ and $\pi_\alpha^\downarrow(v) \leq_{\text{weak}} v$. In view of the previous reasoning we find $\text{cd}_\alpha(\pi_\alpha^\downarrow(u)) = \text{cd}_\alpha(u) = \text{cd}_\alpha(v) = \text{cd}_\alpha(\pi_\alpha^\downarrow(v))$. Proposition 4.3.36 thus implies $\pi_\alpha^\downarrow(u) = \pi_\alpha^\downarrow(v)$. \square

Figure 63 shows the weak order on $\mathfrak{S}_{(1,2,1)}$ where the permutations are additionally labeled by the corresponding $(1, 2, 1)$ -codes.

Now, as a second step in proving Theorem 4.3.27, we show that $(\text{Codes}(\alpha), \leq_{\text{comp}})$ is isomorphic to $\mathbf{Tam}(v_\alpha)$. To that end, we encode v_α by an integer tuple of length $2n + 1$ by listing the y -coordinates of the lattice points on v_α in order from left to right. This *minimal* bracket vector $\mathbf{b}_{\min; \alpha}$ is thus given by

$$\mathbf{b}_{\min; \alpha}(k) \stackrel{\text{def}}{=} \begin{cases} i + p_{j-1} - 1, & \text{if } k = 2p_{j-1} + i \text{ for } 0 < i \leq \alpha_j, \\ p_j, & \text{if } k = 2p_{j-1} + \alpha_j + i \text{ for } 0 < i \leq \alpha_j, \\ n, & \text{if } k = 2n + 1. \end{cases}$$

The k^{th} *fixed* position is $f_k \stackrel{\text{def}}{=} k + 1 + p_{\text{reg}_\alpha(k+1)-1}$, which is the last position, where k appears in $\mathbf{b}_{\min; \alpha}$. In the case $k = n$, we take $f_n = 2n + 1$. We set $F \stackrel{\text{def}}{=} \{f_0, f_1, \dots, f_n\}$. A v_α -*bracket vector* is an integer tuple \mathbf{b} , whose i^{th} entry is denoted by $\mathbf{b}(i)$, satisfying

- (B1): $\mathbf{b}(f_k) = k$ for all $0 \leq k \leq n$;
- (B2): $\mathbf{b}_{\min; \alpha}(i) \leq \mathbf{b}(i) \leq n$;
- (B3): $\mathbf{b}(j) \leq \mathbf{b}(i)$ for all j with $i < j < f_{\mathbf{b}(i)}$.

Let $\text{Bracket}(\alpha)$ denote the set of v_α -bracket vectors. Given $\mathbf{b} \in \text{Bracket}(\alpha)$, we may construct a v_α -path inductively as follows: we add as many lattice points with y -coordinate k as there are entries equal to k in \mathbf{b} . These lattice points have consecutive x -coordinates with the first x -coordinate being equal to the last x -coordinate of a lattice point added at y -coordinate

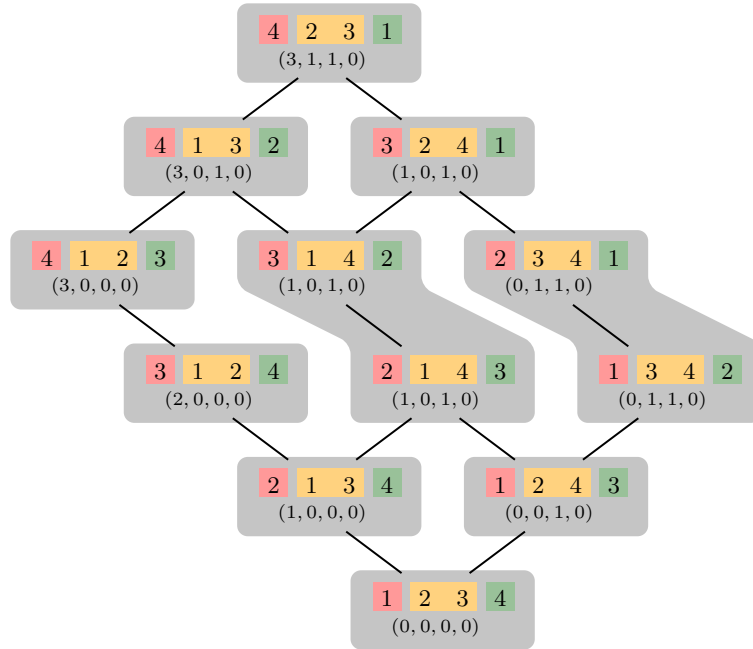
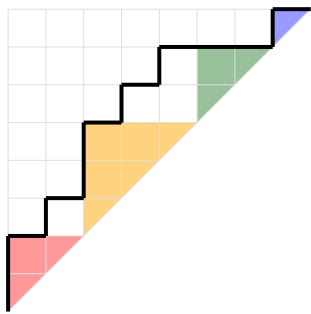
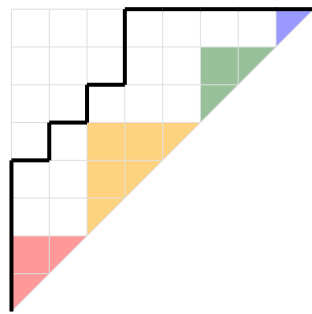


Figure 63. The weak order on $\mathfrak{S}_{(1,2,1)}$, where the permutations are additionally labeled by their $(1, 2, 1)$ -codes.



$(\mathbf{0}, 1, 3, 2, 2, \mathbf{3}, 4, 7, 6, 5, 5, \mathbf{6}, 7, 7, 7, 8, 8)$

(a) An α -Dyck path with its associated bracket vector.



$(\mathbf{0}, 1, 8, 4, 2, \mathbf{3}, 4, 8, 6, 5, 5, \mathbf{6}, 8, 8, 7, 8, 8)$

(b) Another α -Dyck path with its associated bracket vector.

Figure 64. Two α -Dyck paths for $\alpha = (2, 3, 2, 1)$. The entries in the fixed positions of the respective bracket vectors are marked in boldface.

$k - 1$ (or 0 if $k = 0$). Conversely, for $p \in \text{Dyck}(\alpha)$ we construct an integer tuple \mathbf{b} of length $2n + 1$ as follows: we fill in as many k 's as there are lattice points on p with y -coordinate k in a right-aligned fashion in the unoccupied positions of \mathbf{b} ending at the fixed position f_k . Let Ψ_{brack} denote the map that turns p to \mathbf{b} in this fashion. Figure 64 shows two $(2, 3, 2, 1)$ -Dyck paths with their associated bracket vector.

Remark 4.3.39. More generally, \mathfrak{v} -bracket vectors can be defined for arbitrary northeast paths \mathfrak{v} . The corresponding minimal bracket vector then collects the y -coordinates of the lattice points on \mathfrak{v} , and the fixed positions are defined analogously. See [44, Section 4.1].

Theorem 4.3.40 ([44, Theorem 21]). For every northeast path \mathfrak{v} , the set of \mathfrak{v} -bracket vectors under componentwise order is isomorphic to the \mathfrak{v} -Tamari lattice.

In fact, since the entries in the fixed positions are the same across all \mathfrak{v}_α -bracket vectors, we lose nothing if we delete these entries. More precisely, for $\mathbf{b} \in \text{Bracket}(\alpha)$, we define the *reduced* \mathfrak{v}_α -vector \mathbf{r} by

$$\mathbf{r}(p_{j-1} + k) \stackrel{\text{def}}{=} \mathbf{b}(2p_{j-1} + \alpha_j + k)$$

for all $k \in [\alpha_j]$ and all $j \in [r]$. It is then clear that \mathbf{r} is obtained from \mathbf{b} by removing the entries in the fixed positions. To recover \mathbf{b} from \mathbf{r} , we first insert the values of the fixed positions according to (B1) into an integer tuple of length $2n + 1$, and then insert the entries of \mathbf{r} from left to right in the empty positions of \mathbf{r} . This is clearly a bijective correspondence. Let Ω_{red} denote the “reduction” map from \mathbf{b} to \mathbf{r} and let Ω_{ext} denote its inverse. Let $\text{RedBracket}(\alpha)$ denote the set of reduced \mathfrak{v}_α -bracket vectors.

Proposition 4.3.41. A tuple $\mathbf{r} \in \mathbb{N}^n$ is a reduced \mathfrak{v}_α -bracket vector if and only if

- (R1): $p_{\text{reg}_\alpha(i)} \leq \mathbf{r}(i) \leq n$ for all $i \in [n]$;
- (R2): $\mathbf{r}(j) \leq \mathbf{r}(i)$ for all $i < j \leq p_{\text{reg}_\alpha(\mathbf{r}(i)+1)-1}$.

PROOF. Let $\mathbf{r} \in \mathbb{N}^n$ and let $\mathbf{b} = \Omega_{\text{ext}}(\mathbf{r})$. We only need to show that \mathbf{r} satisfies (R1)–(R2) if and only if \mathbf{b} satisfies (B1)–(B3).

Condition (B1) for \mathbf{b} is satisfied by construction. The equivalence between (B2) for \mathbf{b} and (R1) for \mathbf{r} is trivial given the definition of $\mathbf{b}_{\text{min};\alpha}$.

Now for the equivalence between (B3) for \mathbf{b} and (R2) for \mathbf{r} , we observe that for (B3) to hold for \mathbf{b} , for each i with $\mathbf{b}(i) = k$, we only need to check $\mathbf{b}(j) \leq k$ for all j with $i < j \leq 2p_{\text{reg}_\alpha(k+1)-1}$, since all indices from $2p_{\text{reg}_\alpha(k+1)-1} + 1$ to f_k are in F . \square

Lemma 4.3.42. For $\mathbf{r} \in \text{RedBracket}(\alpha)$, we have $\mathbf{r}(i) \geq \mathbf{r}(j)$ for all $i < j$ with $\text{reg}_\alpha(i) = \text{reg}_\alpha(j)$.

PROOF. Let $k = \mathbf{r}(i)$. By (R1), we have $k \geq p_{\text{reg}_\alpha(i)}$ and thus $p_{\text{reg}_\alpha(k+1)} - 1 \geq p_{\text{reg}_\alpha(i)+1} - 1 \geq \text{reg}_\alpha(i)$. Since $\text{reg}_\alpha(i) = \text{reg}_\alpha(j)$, we have $i < j \leq p_{\text{reg}_\alpha(i)} \leq p_{\text{reg}_\alpha(k+1)} - 1$. Then (R2) affirms that $\mathbf{r}(j) \leq k = \mathbf{r}(i)$. \square

Given any composition α , we consider the following transformation Υ which transforms $\mathbf{r} \in \text{RedBracket}(\alpha)$ into an integer tuple of length n by

$$(\Upsilon(\mathbf{r}))(i) \stackrel{\text{def}}{=} \mathbf{r}(2p_{\text{reg}_\alpha(i)} - \alpha_{\text{reg}_\alpha(i)} - i + 1) - p_{\text{reg}_\alpha(i)}.$$

Informally, we obtain $\Upsilon(\mathbf{r})$ by first splitting \mathbf{r} into regions according to α , then reverse the order of the entries in each region while subtracting p_k for entries in the k^{th} region. We claim that Υ is in fact a bijection from $\text{RedBracket}(\alpha)$ to $\text{Codes}(\alpha)$. This construction is illustrated in Figure 65.

$$\begin{array}{ccc}
(\mathbf{0}, \mathbf{1}, 8, 4, \mathbf{2}, \mathbf{3}, 4, 8, 6, 5, \mathbf{5}, \mathbf{6}, 8, 8, \mathbf{7}, 8, \mathbf{8}) & \xrightarrow{\Omega_{\text{red}}} & (8, 4, 8, 6, 5, 8, 8, 8) & \xrightarrow{\Upsilon} & (2, 6, 0, 1, 3, 1, 1, 0) \\
\text{Bracket}(\overset{\overset{\text{m}}{\text{m}}}{(2, 3, 2, 1)}) & & \text{RedBracket}(\overset{\overset{\text{m}}{\text{m}}}{(2, 3, 2, 1)}) & & \text{Codes}(\overset{\overset{\text{m}}{\text{m}}}{(2, 3, 2, 1)})
\end{array}$$

Figure 65. Illustration of the map Υ for $\alpha = (2, 3, 2, 1)$.

Proposition 4.3.43. *For every composition α of $n > 0$, the map Υ is a bijection from $\text{RedBracket}(\alpha)$ to $\text{Codes}(\alpha)$.*

PROOF. Let $\mathbf{r} \in \text{RedBracket}(\alpha)$ and let $\mathbf{c} = \Upsilon(\mathbf{r}) = (c_1, c_2, \dots, c_n)$. We need to check that \mathbf{c} satisfies (C1)–(C3). By (R1) and the definition of Υ , it is clear that \mathbf{c} satisfies (C1). Lemma 4.3.42 and the definition of Υ imply that \mathbf{c} satisfies (C2). Given that \mathbf{c} satisfies (C2), (C3) is satisfied by \mathbf{c} if we can show that for any i, j with $\text{reg}_\alpha(i) < \text{reg}_\alpha(j)$, if $c_i \geq p_{\text{reg}_\alpha(j)} - p_{\text{reg}_\alpha(i)}$, then $c_j + p_{\text{reg}_\alpha(j)} \leq c_i + p_{\text{reg}_\alpha(i)}$. Translating to \mathbf{r} , we need to check that for any i', j' with $\text{reg}_\alpha(i') < \text{reg}_\alpha(j')$, if $\mathbf{r}(i') \geq p_{\text{reg}_\alpha(j')}$, then $\mathbf{r}(j') \leq \mathbf{r}(i')$. Now suppose that $\mathbf{r}(i') \geq p_{\text{reg}_\alpha(j')}$. We then have $\text{reg}_\alpha(\mathbf{r}(i') + 1) > \text{reg}_\alpha(j')$ by definition of reg_α . As the values are integers, we have $\text{reg}_\alpha(j') \leq \text{reg}_\alpha(\mathbf{r}(i') + 1) - 1$, which means that $j' \leq p_{\text{reg}_\alpha(j')} \leq p_{\text{reg}_\alpha(\mathbf{r}(i') + 1) - 1}$, and by (R2) we have $\mathbf{r}(j') \leq \mathbf{r}(i')$. Therefore \mathbf{c} satisfies (C3), and it follows that $\mathbf{c} \in \text{Codes}(\alpha)$.

Now for the reverse direction, let $\mathbf{c} = (c_1, c_2, \dots, c_n) \in \text{Codes}(\alpha)$ and $\mathbf{r} = \Upsilon^{-1}(\mathbf{c})$. It is clear that (C1) translates directly to (R1). We only need to show that (R2) holds for \mathbf{r} . Suppose that $1 \leq i < j \leq p_{\text{reg}_\alpha(\mathbf{r}(i) + 1) - 1}$. If $\text{reg}_\alpha(i) = \text{reg}_\alpha(j)$, by the definition of Υ^{-1} and (C2), we have $\mathbf{r}(j) \leq \mathbf{r}(i)$. If $\text{reg}_\alpha(i) < \text{reg}_\alpha(j)$, then we need to check that for any $i' < j'$ such that $\text{reg}_\alpha(i') < \text{reg}_\alpha(j') \leq \text{reg}_\alpha(c_{i'} + p_{\text{reg}_\alpha(i')} + 1) - 1$, we have $c_{j'} + p_{\text{reg}_\alpha(j')} \leq c_{i'} + p_{\text{reg}_\alpha(i')}$. By (C2), we may assume that $j' = p_\alpha$ for some $\alpha \in [r]$. By the definition of reg_α , we see that $\text{reg}_\alpha(p_\alpha) \leq \text{reg}_\alpha(c_{i'} + p_{\text{reg}_\alpha(i')} + 1) - 1$ implies $p_\alpha \leq c_{i'} + p_{\text{reg}_\alpha(i')} + 1$, thus $p_\alpha \leq c_{i'} + p_{\text{reg}_\alpha(i')}$ since they are integers. By (C3), we have $c_{p_\alpha} \leq p_{i'} - p_\alpha + p_{\text{reg}_\alpha(i')}$. Therefore, \mathbf{r} satisfies (R2), and it follows that $\mathbf{r} \in \text{RedBracket}(\alpha)$. \square

We may now conclude the proof of Theorem 4.3.27.

PROOF OF THEOREM 4.3.27. We have

$$\begin{aligned}
\mathbf{Tam}(\alpha) &\stackrel{\text{Prop. 4.3.37}}{\cong} (\text{Codes}(\alpha), \leq_{\text{comp}}) \stackrel{\text{Prop. 4.3.43}}{\cong} (\text{RedBracket}(\alpha), \leq_{\text{comp}}) \\
&\stackrel{\text{trivial}}{\cong} (\text{Bracket}(\alpha), \leq_{\text{comp}}) \stackrel{\text{Thm. 4.3.40}}{\cong} \mathbf{Tam}(v_\alpha).
\end{aligned}$$

\square

Example 4.3.44. Let $\alpha = (2, 1, 1)$. The following table lists the $(\alpha, 231)$ -avoiding permutations, the associated α -codes, the resulting v_α -bracket vectors and the corresponding α -Dyck paths. In particular, we obtain a bijection from $\mathfrak{S}_\alpha(231)$ to $\text{Dyck}(\alpha)$ that sends weak order to rotation order.

Composing the bijections from Sections 4.2.1 and 4.2.2, we obtain another bijection from $\mathfrak{S}_\alpha(231)$ to $\text{Dyck}(\alpha)$. It is well worth comparing this bijection to the previous one.

$p' = \Phi_{\text{path}} \circ \Phi_{\text{perm}}^{-1}(w)$	$w \in \mathfrak{S}_{(2,1,1)}(231)$	$c = \text{cd}_{(2,1,1)}(w)$	$\mathbf{b} = (\Omega_{\text{ext}} \circ \Upsilon^{-1})(c)$	$p = \Psi_{\text{brack}}^{-1}(\mathbf{b})$
	1 2 3 4	(0, 0, 0, 0)	(0, 1, 2, 2, 2, 3, 3, 4, 4)	
	1 2 4 3	(0, 0, 1, 0)	(0, 1, 2, 2, 2, 4, 3, 4, 4)	
	1 3 2 4	(0, 1, 0, 0)	(0, 1, 3, 2, 2, 3, 3, 4, 4)	
	1 4 2 3	(0, 2, 0, 0)	(0, 1, 4, 2, 2, 3, 3, 4, 4)	
	1 4 3 2	(0, 2, 1, 0)	(0, 1, 4, 2, 2, 4, 3, 4, 4)	
	2 3 1 4	(1, 1, 0, 0)	(0, 1, 3, 3, 2, 3, 3, 4, 4)	
	2 4 1 3	(1, 2, 0, 0)	(0, 1, 4, 3, 2, 3, 3, 4, 4)	
	3 4 1 2	(2, 2, 0, 0)	(0, 1, 4, 4, 2, 3, 3, 4, 4)	
	3 4 2 1	(2, 2, 1, 0)	(0, 1, 4, 4, 2, 4, 3, 4, 4)	

Remark 4.3.45. We wish to remark that we have two different (composite) bijections from \mathfrak{S}_α to $\text{Dyck}(\alpha)$. One passes through noncrossing α -partitions (or equivalently through α -trees; see Propositions 4.2.20 and 4.2.21) and maps descents to valleys. The other one passes through α -codes and \mathfrak{v}_α -bracket vectors, but it does not seem to map descents to a local statistic on α -Dyck paths. We are not aware of a direct bijection.

Remark 4.3.46. In [45, Part 2], we have given a different proof of Theorem 4.3.27. In particular, it was shown that the bijection $\Phi_{\text{path}} \circ \Phi_{\text{perm}}^{-1} : \mathfrak{S}_\alpha(231) \rightarrow \text{Dyck}(\alpha)$ restricts to an isomorphism (of directed graphs) from the Galois graph $\text{Galois}(\mathbf{Tam}(\alpha))$ to $\text{Galois}(\mathbf{Tam}(\mathfrak{v}_\alpha)^d)$. In view of Theorem 1.1.22, the isomorphism $\mathbf{Tam}(\alpha) \cong \mathbf{Tam}(\mathfrak{v}_\alpha)^d$ follows. By Theorem 4.3.11, the claim follows. Open Problem 2.23 in [45] asks for a proof that $\Phi_{\text{path}} \circ \Phi_{\text{perm}}^{-1}$ extends to a lattice isomorphism from $\mathbf{Tam}(\alpha)$ to $\mathbf{Tam}(\mathfrak{v}_\alpha)^d$.

We conclude this section with a proof of Conjecture 3.4.4 in linear type A.

Theorem 4.3.47. *For every composition α of $n > 0$, $\mathbf{Clus}(\mathfrak{S}_\alpha, \vec{c}) \cong \mathbf{Tam}(\alpha)^d$.*

PROOF. We have seen in Theorem 4.1.13 that the set of facets of $\mathbf{Clus}(\mathfrak{S}_\alpha, \vec{c})$ is in bijection with $\text{Dyck}(\bar{\alpha})$. Moreover, it is straightforward to verify that this bijection sends chute moves to flips. We thus obtain

$$\mathbf{Clus}(\mathfrak{S}_\alpha, \vec{c}) \cong \mathbf{Tam}(v_{\bar{\alpha}}) \stackrel{\text{Thm. 4.3.27}}{\cong} \mathbf{Tam}(\bar{\alpha}) \stackrel{\text{Thm. 4.3.11}}{\cong} \mathbf{Tam}(\alpha)^d. \quad \square$$

4.3.3. The core label order of $\mathbf{Tam}(\alpha)$. By Corollary 4.3.10, $\mathbf{Tam}(\alpha)$ is a semidistributive lattice for every α , and as a consequence of Proposition 1.1.35, we may consider the core label order $\mathbf{CLO}(\mathbf{Tam}(\alpha))$. If $\alpha = (1, 1, \dots, 1) \vdash n$, then Theorem 2.3.13 implies that $\mathbf{CLO}(\mathbf{Tam}(\alpha)) \cong \mathbf{Nonc}(\alpha)$.

In this section, we study the core label sets in $\mathbf{Tam}(\alpha)$, for arbitrary α , and characterize the compositions for which $\mathbf{CLO}(\mathbf{Tam}(\alpha)) \cong \mathbf{Nonc}(\alpha)$ remains true. We first describe the labeling λ_{jstd} of $\mathbf{Tam}(\alpha)$; see Section 1.1.7.

Lemma 4.3.48. *Let $u, v \in \mathfrak{S}_\alpha(231)$ with $u \triangleleft_\alpha v$. There exists a unique $(a, b) \in \text{Cov}(v)$ such that $(a, b) \notin \text{Inv}(u)$.*

PROOF. Let $v \in \mathfrak{S}_\alpha(231)$. By Lemma 4.3.15, the number of permutations $u \in \mathfrak{S}_\alpha(231)$ with $u \triangleleft_\alpha v$ equals $|\text{Cov}(v)|$. Thus, for every $(a, b) \in \text{Cov}(v)$, there exists a unique $u \in \mathfrak{S}_\alpha(231)$ with $u \triangleleft_\alpha v$. It remains to show that $(a, b) \notin \text{Inv}(u)$. Let \hat{u} be the α -permutation that arises from v by swapping the values in positions a and b . Then, $\hat{u} \triangleleft_{\text{weak}} v$ and $(a, b) \notin \text{Inv}(\hat{u})$. By Lemma 4.3.1, $u = \pi_\alpha^\downarrow(\hat{u}) \triangleleft_\alpha v$, and $(a, b) \notin \text{Inv}(u)$ by Lemma 4.3.5. \square

Proposition 4.3.49. *Let $u, v \in \mathfrak{S}_\alpha(231)$ with $u \triangleleft_\alpha v$ and let $(a, b) \in \text{Cov}(v)$ with $(a, b) \notin \text{Inv}(u)$. Then, $(u, v) \bar{\wedge} (w_{a,b_*}, w_{a,b})$ in $\mathbf{Tam}(\alpha)$.*

PROOF. Let $v \in \mathfrak{S}_\alpha(231)$ and let $(a, b) \in \text{Cov}(v)$. Lemma 4.3.48 ensures the existence of the desired permutation u .

Suppose that $\text{reg}_\alpha(a) = j$. Since $v \in \mathfrak{S}_\alpha(231)$, $v_c \leq v_b$ for all $c \in \{p_j+1, p_j+2, \dots, b\}$. By Proposition 4.3.13, $\text{Inv}(w_{a,b}) \subseteq \text{Inv}(v)$ and thus $w_{a,b} \leq_{\text{weak}} v$.

Let \hat{u} be the α -permutation that arises from v by swapping the entries in positions a and b . Then $\hat{u} \triangleleft_{\text{weak}} v$ and $u = \pi_\alpha^\downarrow(\hat{u})$. Moreover, $\text{Inv}(\hat{u}) = \text{Inv}(v) \setminus \{(a, b)\}$ and $\text{Inv}(w_{a,b_*}) = \text{Inv}(w_{a,b}) \setminus \{(a, b)\}$. In particular, $w_{a,b_*} \in \mathfrak{S}_\alpha(231)$, and since π_α^\downarrow is a lattice map, we conclude

$$\begin{aligned} u \wedge_\alpha w_{a,b} &= \pi_\alpha^\downarrow(\hat{u}) \wedge_\alpha \pi_\alpha^\downarrow(w_{a,b}) = \pi_\alpha^\downarrow(\hat{u} \wedge_{\text{weak}} w_{a,b}) = \pi_\alpha^\downarrow(w_{a,b_*}) = w_{a,b_*}, \\ u \vee_\alpha w_{a,b} &= \pi_\alpha^\downarrow(\hat{u}) \vee_\alpha \pi_\alpha^\downarrow(w_{a,b}) = \pi_\alpha^\downarrow(\hat{u} \vee_{\text{weak}} w_{a,b}) = \pi_\alpha^\downarrow(v) = v. \end{aligned}$$

By definition, $(w_{a,b_*}, w_{a,b}) \bar{\wedge} (u, v)$ in $\mathbf{Tam}(\alpha)$. \square

Proposition 4.3.50. *For all $n > 0$ and every composition α of $n > 0$, the canonical join representation of $w \in \mathfrak{S}_\alpha(231)$ in $\mathbf{Tam}(\alpha)$ is*

$$\text{Can}(w) = \{w_{a,b} \mid (a, b) \in \text{Cov}(w)\}.$$

PROOF. This follows from Proposition 4.3.49 using Propositions 1.1.15 and 1.1.16. \square

In fact, we may use the following labeling to slightly ease the notation:

$$(4.22) \quad \lambda_\alpha: \text{Covers}(\mathbf{Tam}(\alpha)) \rightarrow \mathbb{N} \times \mathbb{N}, \quad (u, v) \mapsto \text{Cov}(v) \setminus \text{Inv}(u).$$

Lemma 4.3.48 states that for $(u, v) \in \text{Covers}(\mathbf{Tam}(\alpha))$, the set $\text{Cov}(v) \setminus \text{Inv}(u)$ has a unique element. λ_α assigns this element to the cover relation (u, v) (rather than the set containing this element). Proposition 4.3.49 implies that λ_α is equivalent to λ_{jst} for $\mathbf{Tam}(\alpha)$.

Thus, the labels under λ_α are pairs of integers in different α -regions, which themselves may be represented by α -arcs. As a consequence, the core label set of $w \in \mathfrak{S}_\alpha(231)$ can be identified with a collection of α -arcs. Proposition 4.3.50 implies, together with the bijection Φ_{perm} from Section 4.2.1, that the canonical join representation of $w \in \mathfrak{S}_\alpha(231)$ corresponds to the set of bumps of the noncrossing α -partitions $\Phi_{\text{perm}}^{-1}(w)$.

For $w \in \mathfrak{S}_\alpha(231)$, we define

$$X(w) \stackrel{\text{def}}{=} \{w_{a,b} \mid \text{there exists } B \in \Phi_{\text{perm}}^{-1}(w) \text{ with } a, b \in B\}.$$

Moreover, we abbreviate the core label sets in $\mathbf{Tam}(\alpha)$ by Sh_α rather than by $\text{Sh}_{(\mathbf{Tam}(\alpha), \lambda_\alpha)}$.

Proposition 4.3.51. *Let α be a composition of $n > 0$. For all $u \in \mathfrak{S}_\alpha(231)$, $\text{Sh}_\alpha(u) \subseteq X(u)$.*

PROOF. By Proposition 4.3.2, $\mathbf{Tam}(\alpha)$ is a quotient lattice of $\mathbf{Weak}(\mathfrak{S}_\alpha)$ by a lattice congruence Θ_α . Let $u \in \mathfrak{S}_\alpha(231)$. If $\text{Sh}_\alpha(u) = \emptyset$, then there is nothing to show. Otherwise, Proposition 1.1.15 implies that $\text{Cov}(u) = \{(a_1, b_1), (a_2, b_2), \dots, (a_t, b_t)\} \neq \emptyset$. We denote by G the subgroup of \mathfrak{S}_α generated by the transpositions corresponding to these descents.

Since $\text{Sh}_\alpha(u) \neq \emptyset$, we may pick any $w_{a,b} \in \text{Sh}_\alpha(u)$. By Lemma 1.1.38, $w_{a,b} \in \text{Sh}_{(\mathbf{Weak}(\mathfrak{S}_\alpha), \lambda_{\text{jst}})}(u)$. Since $\mathbf{Weak}(\mathfrak{S}_\alpha)$ is a principal order ideal in $\mathbf{Weak}(\mathfrak{S}_n)$ and \mathfrak{S}_n is a Coxeter group, Proposition 2.3.12 implies that $w_{a,b} \in G$ and $\text{Inv}(w_{a,b}) \subseteq \text{Inv}(u)$. Since $w_{a,b} \in G$, we may write the transposition swapping a and b as a product of the generators of G . This implies that a and b belong to the same part of $\Phi_{\text{perm}}^{-1}(u)$ and therefore $w_{a,b} \in X(u)$. \square

Example 4.3.52. *Let $\alpha = (1, 2, 1)$ and consider $u = \mathbf{3} \mathbf{2} \mathbf{4} \mathbf{1} \in \mathfrak{S}_\alpha$. Then, $\Phi_{\text{perm}}^{-1}(u) = \{1, 2, 4\}, \{3\}$ and therefore $X(u) = \{w_{1,2}, w_{1,4}, w_{2,4}\}$. The subgroup G from the proof of Proposition 4.3.51 is generated by $w_{1,2}$ and $w_{2,4}$. It follows that $X(u) \subseteq G$.*

We immediately see that $\text{Inv}(u) = \{(1, 2), (1, 4), (2, 4), (3, 4)\}$. Moreover, we obtain from Proposition 4.3.13 that

$$\text{Inv}(w_{1,2}) = \{(1, 2)\},$$

$$\text{Inv}(w_{1,4}) = \{(1, 2), (1, 3), (1, 4)\},$$

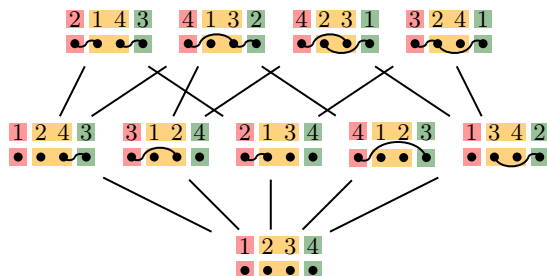


Figure 66. The poset $\mathbf{CLO}(\mathbf{Tam}((1, 2, 1)))$. This is a subset of $\mathbf{Nonc}((1, 2, 1))$, because it lacks the refinement of the partitions corresponding to $\begin{bmatrix} 4 & 1 & 2 & 3 \end{bmatrix}$ and $\begin{bmatrix} 3 & 2 & 4 & 1 \end{bmatrix}$.

$$\text{Inv}(w_{2,4}) = \{(2, 4), (3, 4)\}.$$

Thus, $\text{Inv}(w_{1,2}) \subseteq \text{Inv}(u)$ and $\text{Inv}(w_{2,4}) \subseteq \text{Inv}(u)$, but $\text{Inv}(w_{1,4}) \not\subseteq \text{Inv}(u)$. Now, since $w_{a,b} \in \text{Sh}_{(\text{Weak}(\mathfrak{S}_\alpha), \lambda_{\text{jsd}})}(u)$ if and only if $w_{a,b} \in \mathbf{G}$ and $\text{Inv}(w_{a,b}) \subseteq \text{Inv}(u)$ we conclude that $w_{1,4} \notin \text{Sh}_{(\text{Weak}(\mathfrak{S}_\alpha), \lambda_{\text{jsd}})}(u)$. By Lemma 1.1.38, $w_{1,4} \notin \text{Sh}_\alpha(u)$.

By inspection of Figure 54, we observe that $\text{Sh}_{(\text{Weak}(\mathfrak{S}_\alpha), \lambda_{\text{jsd}})}(u)$ contains the irreducible permutations $j_1 = \begin{bmatrix} 3 & 1 & 4 & 2 \end{bmatrix}$ and $j_2 = \begin{bmatrix} 2 & 3 & 4 & 1 \end{bmatrix}$, both of which contain an $(\alpha, 231)$ -pattern in positions $(1, 3, 4)$.

Figures 66 and 67 show the core label orders of $\mathbf{Tam}((1, 2, 1))$ and $\mathbf{Tam}((2, 1, 2))$, respectively. Note that the second poset is isomorphic to $\mathbf{Nonc}((2, 1, 2))$, while the first one is not isomorphic to $\mathbf{Nonc}((1, 2, 1))$. The next proposition characterizes the compositions for which equality holds in Proposition 4.3.51.

Proposition 4.3.53. *Let α be a composition of $n > 0$. Then, $\text{Sh}_\alpha(u) = X(u)$ for all $u \in \mathfrak{S}_\alpha(231)$ if and only if either $\alpha = (n)$ or $\alpha = (p, 1, 1, \dots, 1, q)$ for some integers $p, q > 0$.*

PROOF. If $\alpha = (n)$, then $\mathfrak{S}_\alpha(231) = \{e\}$ and $\text{Sh}_\alpha(e) = \emptyset = X(e)$. Now, suppose that $\alpha = (p, 1, 1, \dots, 1, q)$ for some integers $p, q > 0$. Let $u \in \mathfrak{S}_\alpha(231)$ with $\text{Cov}(u) = \{(a_1, b_1), (a_2, b_2), \dots, (a_t, b_t)\}$.

By Proposition 4.3.51, $\text{Sh}_\alpha(u) \subseteq X(u)$. In order to show the reverse inclusion, we pick $w_{a,b} \in X(u)$ and prove that $w_{a,b} \in \text{Sh}_\alpha(u)$. Using Proposition 2.3.12 as in the proof of Proposition 4.3.51 it is enough to show that $\text{Inv}(w_{a,b}) \subseteq \text{Inv}(u)$.

By definition, there exists a sequence of integers k_0, k_1, \dots, k_t such that $a = k_0$ and $b = k_t$ and (k_{i-1}, k_i) is a bump of $\Phi_{\text{perm}}^{-1}(u)$ for all $i \in [t]$. In particular, all the k_i lie in different α -regions. By Theorem 4.2.2, $(k_{i-1}, k_i) \in \text{Cov}(u)$ for all $i \in [t]$. Thus, $(a, b) \in \text{Inv}(u)$.

If $t = 1$, then $(a, b) \in \text{Cov}(u)$. By Proposition 4.3.50, $w_{a,b}$ is a canonical joinand of u , which implies $w_{a,b} \in \text{Sh}_\alpha(u)$.

If $t > 1$, then we consider two cases. If $a > p$, then

$$\text{Inv}(w_{a,b}) = \{(a, a+1), (a, a+2), \dots, (a, b)\}$$

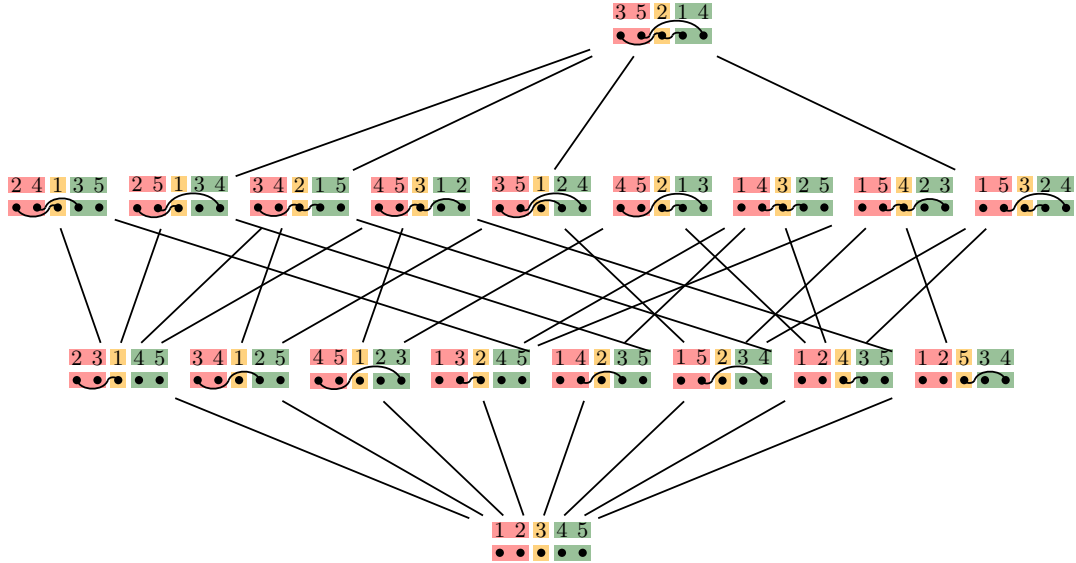


Figure 67. The poset $\mathbf{CLO}(\mathbf{Tam}((2,1,2)))$. This is also the poset $\mathbf{Nonc}((2,1,2))$.

by Proposition 4.3.13 and our assumption on the shape of α . Choose $d \in \{a+1, a+2, \dots, b\}$. By construction, there exists $(k_{i-1}, k_i) \in \text{Cov}(u)$ such that $k_{i-1} < d \leq k_i$. Since u avoids any $(\alpha, 231)$ -pattern, it follows that $u_d < u_{k_{i-1}} < u_{k_{i-2}} < \dots < u_{k_0} = u_a$. Thus, $(a, d) \in \text{Inv}(u)$. It follows that $\text{Inv}(w_{a,b}) \subseteq \text{Inv}(u)$ as desired.

If $p \leq a$, then Proposition 4.3.13 implies

$$\text{Inv}(w_{a,b}) = \{(a', b') \mid a' \in \{a, a+1, \dots, p\}, b' \in \{p+1, p+2, \dots, b\}\}.$$

As before we may show that $(a, d) \in \text{Inv}(u)$ for any $d \in \{p+1, p+2, \dots, b\}$. Since $u \in \mathfrak{S}_\alpha$, we have $u_a < u_{a'}$ for any $a' \in \{a+1, a+2, \dots, p\}$. This implies $\text{Inv}(w_{a,b}) \subseteq \text{Inv}(u)$.

We conclude that $w_{a,b} \in \text{Sh}_{(\text{Weak}(\mathfrak{S}_\alpha), \lambda_{\text{jsd}})}(u)$. Since, by construction, $w_{a,b} \in \mathfrak{S}_\alpha(231)$, it follows that $w_{a,b} \in \text{Sh}_\alpha(u)$.

Now suppose that $\alpha = (\alpha_1, \alpha_2, \dots, \alpha_r)$ is a composition of n which is not of the form $\alpha = (p, 1, 1, \dots, q)$. Then, $r \geq 3$ and there exists $k \in \{2, 3, \dots, r-1\}$ such that $p_k > p_{k-1} + 1$.

Let $a = p_{k-1}$ and consider $P \in \text{Nonc}(\alpha)$ whose only non-singleton blocks are $\{a, a+1\}$ and $\{a+1, n\}$, and let $u = \Phi_{\text{perm}}(P)$. Then, u has one-line notation

$$\underbrace{1, 2, \dots, a-1, n-\alpha_k+1}_{p_{k-1}} \mid \underbrace{n-\alpha_k, n-\alpha_k+2, \dots, n}_{\alpha_k} \mid \underbrace{a, a+1, \dots, n-\alpha_k-1}_{n-p_k}.$$

By construction, the join-irreducible permutation $w_{a,n} \in \mathfrak{S}_\alpha(231)$ is contained in $X(u)$. By Proposition 4.3.13,

$$\text{Inv}(w_{a,n}) = \{(a, a+1), (a, a+2), \dots, (a, n)\};$$

in particular $(a, p_k) \in \text{Inv}(w_{a,n})$. However, we notice in the one-line notation of u that $(a, p_k) \notin \text{Inv}(u)$, because $\alpha_k = p_k - p_{k-1} > 1$. It follows that $\text{Inv}(w_{a,n}) \not\subseteq \text{Inv}(u)$ and therefore $w_{a,n} \notin \text{Sh}_\alpha(u)$. \square

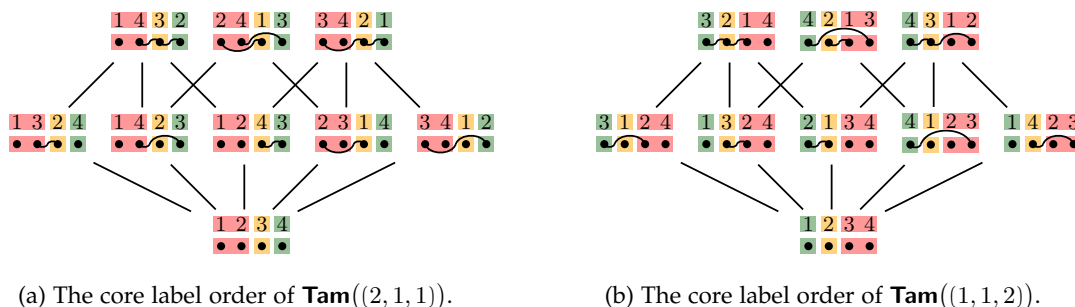


Figure 68. Reversing the composition yields isomorphic core label orders.

We summarize the main result of this section in the following theorem, whose proof we have just established. This also resolves Research Challenge 3.3.4 in linear type A.

Theorem 4.3.54. *Let α be a composition of n . Then, $\mathbf{CLO}(\mathbf{Tam}(\alpha)) \cong \mathbf{Nonc}(\alpha)$ if and only if either $\alpha = (n)$ or $\alpha = (p, 1, 1, \dots, 1, q)$ for some integers $p, q > 0$.*

We have explained in Example 4.1.22 that $\mathbf{Nonc}(\alpha)$ is not necessarily a meet-semilattice. The core label order of $\mathbf{Tam}(\alpha)$, however, always has this property.

Proposition 4.3.55. *For every composition α of $n > 0$, the poset $\mathbf{CLO}(\mathbf{Tam}(\alpha))$ is a meet-semilattice.*

PROOF. By Theorem 3.1.2, $\mathbf{Weak}(\mathfrak{S}_\alpha)$ is a principal order ideal of $\mathbf{Weak}(\mathfrak{S}_n)$, which implies that $\mathbf{CLO}(\mathbf{Weak}(\mathfrak{S}_\alpha))$ is an order ideal of $\mathbf{CLO}(\mathbf{Weak}(\mathfrak{S}_n))$. Since $\mathbf{CLO}(\mathbf{Weak}(\mathfrak{S}_n))$ is a lattice (see for instance [11, Section 4], [136] or [152, Section 4 and 5]), it follows that $\mathbf{CLO}(\mathbf{Weak}(\mathfrak{S}_\alpha))$ is a meet-semilattice. Thus, $\mathbf{Weak}(\mathfrak{S}_\alpha)$ has the intersection property by Remark 1.1.33. Since $\mathbf{Tam}(\alpha)$ is a quotient lattice of $\mathbf{Weak}(\mathfrak{S}_\alpha)$ by Theorem 4.3.9, $\mathbf{Tam}(\alpha)$ has the intersection property, too, by Proposition 1.1.39. Once again, Remark 1.1.33 implies that $\mathbf{CLO}(\mathbf{Tam}(\alpha))$ is a meet-semilattice. \square

By Theorem 4.3.11, $\mathbf{Tam}(\alpha)$ and $\mathbf{Tam}(\bar{\alpha})$ are dual to each other. Computer experiments suggest that the core label orders of these lattices are isomorphic. See Figure 68 for an illustration.

Conjecture 4.3.56. *For every composition α of $n > 0$, $\mathbf{CLO}(\mathbf{Tam}(\alpha)) \cong \mathbf{CLO}(\mathbf{Tam}(\bar{\alpha}))$.*

4.4. Chapoton triangles

In (3.6) we have proposed a straightforward generalization of the H-triangle to parabolic quotients of Coxeter groups using parabolic nonnesting partitions. In type A, the parabolic nonnesting partitions are antichains in the parabolic root poset.

We have explained in Section 4.1.3, that the α -root poset can be inscribed in the α -Ferrers shape. Our conversion from antichains in the α -root poset to α -Dyck paths takes the elements

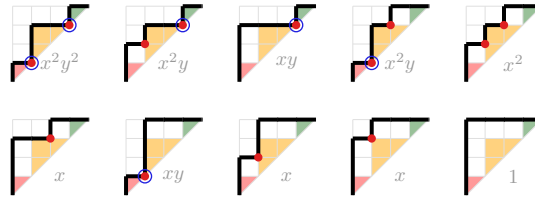


Figure 69. The $(1, 2, 1)$ -Dyck paths together with their contribution to $\mathcal{H}_{(1,2,1)}(x, y)$. Valleys are marked in red, returns are circled in blue.

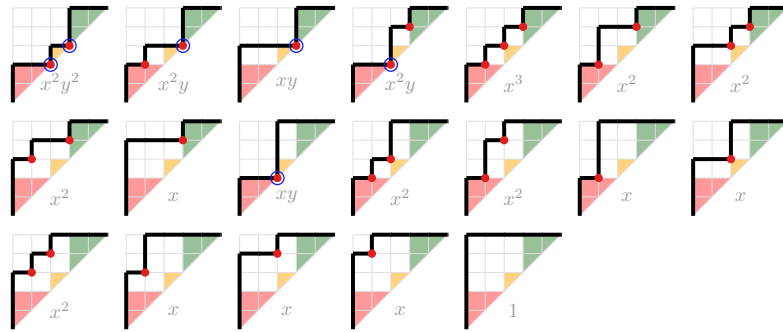


Figure 70. The $(2, 1, 2)$ -Dyck paths together with their contribution to $\mathcal{H}_{(2,1,2)}(x, y)$. Valleys are marked in red, returns are circled in blue.

of the antichain and converts them to valleys of the path. From this perspective, the parabolic H-triangle in type A takes the following form:

$$(4.23) \quad \mathcal{H}_\alpha(x, y) \stackrel{\text{def}}{=} \sum_{p \in \text{Dyck}(\alpha)} x^{\text{valley}(p)} y^{\text{return}(p)},$$

where a *return* of p is a valley of p that is also a valley of v_α .

Remark 4.4.1. In [130, Section 5], we have defined the H-triangle using certain peaks on the α -Dyck paths. This is easily seen to coincide with our previous definition as follows. An antichain in the α -root poset induces an order ideal, and the lattice path tracing out this order ideal is an α -Dyck path. The contribution of this antichain to the parabolic H-triangle defined in (3.6) then corresponds to the peak-statistics given in [130, Equation (5.2)].

Example 4.4.2. Let $\alpha = (1, 2, 1)$. Figure 69 shows the α -Dyck paths together with their contribution to $\mathcal{H}_{(1,2,1)}(x, y)$. This yields

$$\mathcal{H}_{(1,2,1)}(x, y) = x^2y^2 + 2x^2y + x^2 + 2xy + 3x + 1.$$

See also Example 3.6.1.

Example 4.4.3. Let $\alpha = (2, 1, 2)$. Figure 70 shows the α -Dyck paths together with their contribution to $\mathcal{H}_{(2,1,2)}(x, y)$. This yields

$$\mathcal{H}_{(2,1,2)}(x, y) = x^3 + x^2y^2 + 2x^2y + 6x^2 + 2xy + 6x + 1.$$

We may now use the transformations from Theorem 2.6.2 to “reengineer” combinatorial realizations for the F- and the M-triangles. We define

$$\begin{aligned} \mathcal{M}_\alpha(x, y) &\stackrel{\text{def}}{=} (1-y)^d \mathcal{H}_\alpha\left(\frac{y(x-1)}{1-y}, \frac{x}{x-1}\right) \\ \mathcal{F}_\alpha(x, y) &\stackrel{\text{def}}{=} x^d \mathcal{H}_\alpha\left(\frac{x+1}{x}, \frac{y+1}{x+1}\right). \end{aligned}$$

If we want these rational functions to be polynomials, then—by definition of $\mathcal{H}_\alpha(x, y)$ —we need to require that $d \geq \max\{\text{valley}(p) \mid p \in \text{Dyck}(\alpha)\}$. In order to avoid unnecessary redundancy we use equality there, and call the maximum number of valleys of any α -Dyck path the *degree* of α , and denote it by d_α . In view of the bijections Φ_{perm} and Φ_{path} (see Theorems 4.2.2 and 4.2.4) and of the description of the canonical join representations in $\mathbf{Tam}(\alpha)$ (see Proposition 4.3.50), we find that

$$d_\alpha = \max\{|\text{Can}(w)| \mid w \in \mathfrak{S}_\alpha(231)\} = \max\{|\text{Bump}(P)| \mid P \in \text{Nonc}(\alpha)\}.$$

With this definition, we obtain

$$\begin{aligned} \mathcal{M}_\alpha(x, y) &= \sum_{p \in \text{Dyck}(\alpha)} (x-1)^{\text{valley}(p)-\text{return}(p)} (1-y)^{d_\alpha-\text{valley}(p)} x^{\text{return}(p)} y^{\text{valley}(p)}, \\ \mathcal{F}_\alpha(x, y) &= \sum_{p \in \text{Dyck}(\alpha)} x^{d_\alpha-\text{valley}(p)} (x+1)^{\text{valley}(p)-\text{return}(p)} (y+1)^{\text{return}(p)}. \end{aligned}$$

Example 4.4.4. For $\alpha = (1, 2, 1)$, using Figure 69, we thus obtain

$$\begin{aligned} \mathcal{M}_{(1,2,1)}(x, y) &= 4x^2y^2 - 9xy^2 + 5xy + 5y^2 - 5y + 1, \\ \mathcal{F}_{(1,2,1)}(x, y) &= 5x^2 + 4xy + y^2 + 9x + 4y + 4. \end{aligned}$$

See also Examples 3.6.2 and 3.6.3.

Example 4.4.5. For $\alpha = (2, 1, 2)$, using Figure 70, we thus obtain

$$\begin{aligned} \mathcal{M}_{(2,1,2)}(x, y) &= x^3y^3 - 12x^2y^3 + 9x^2y^2 + 25xy^3 - 30xy^2 - 14y^3 + 8xy + 21y^2 - 9y + 1, \\ \mathcal{F}_{(2,1,2)}(x, y) &= 14x^3 + 4x^2y + xy^2 + 25x^2 + 4xy + 12x + 1. \end{aligned}$$

If we denote by $\text{Valley}(p)$ (resp. $\text{Return}(p)$) the *set* of valleys (resp. returns) of p , then we can rewrite the definition of the F-triangle as follows:

$$\begin{aligned} \mathcal{F}_\alpha(x, y) &= \sum_{p \in \text{Dyck}(\alpha)} x^{d_\alpha-\text{valley}(p)} (x+1)^{\text{valley}(p)-\text{return}(p)} (y+1)^{\text{return}(p)} \\ &= \sum_{p \in \text{Dyck}(\alpha)} \sum_{V \subseteq \text{Valley}(p)} x^{d_\alpha-\text{valley}(p)+|V \setminus \text{Return}(p)|} y^{|\text{V} \cap \text{Return}(p)|} \end{aligned}$$

We have already argued in Example 3.6.2 that the core label order is suited better to define a parabolic M-triangle than the poset of noncrossing partitions. We thus set

$$(4.24) \quad \tilde{\mathcal{M}}_\alpha(x, y) \stackrel{\text{def}}{=} \sum_{u, v \in \mathfrak{S}_\alpha(231)} \mu_{\text{CLO}(\text{Tam}(\alpha))}(u, v) x^{|\text{Can}(u)|} y^{|\text{Can}(v)|}.$$

Example 4.4.6. *Inspecting Figures 66 and 67, we obtain*

$$\tilde{\mathcal{M}}_{(1,2,1)}(x, y) = 4x^2y^2 - 9xy^2 + 5xy + 5y^2 - 5y + 1,$$

$$\tilde{\mathcal{M}}_{(2,1,2)}(x, y) = x^3y^3 - 4x^2y^3 + 9x^2y^2 + 5xy^3 - 22xy^2 - 2y^3 + 8xy + 13y^2 - 8y + 1.$$

In view of Examples 4.4.4 and 4.4.5, we see that $\tilde{\mathcal{M}}_{(1,2,1)}(x, y) = \mathcal{M}_{(1,2,1)}(x, y)$ but $\tilde{\mathcal{M}}_{(2,1,2)}(x, y) \neq \mathcal{M}_{(2,1,2)}(x, y)$.

Moreover, we notice that $\mathcal{M}_{(2,1,2)}(x, y)$ cannot arise as a generating function of the Möbius function of some poset. Indeed, if there were a poset \mathbf{P} such that $\mathcal{M}_{(2,1,2)}(x, y)$ arises analogously to (4.24). Then, since the constant term of $\mathcal{M}_{(2,1,2)}(x, y)$ is 1, \mathbf{P} has a unique minimal element. Since the coefficient of xy is 8, \mathbf{P} has eight elements of rank 1. However, the coefficient of y is -9 , which forces that there are nine elements covering the bottom element.

Conversely, we could also consider $\tilde{\mathcal{M}}_\alpha(x, y)$ as a starting point, and define

$$\tilde{\mathcal{H}}_\alpha(x, y) = (x(y-1) + 1)^{d_\alpha} \tilde{\mathcal{M}}_\alpha\left(\frac{y}{y-1}, \frac{x(y-1)}{x(y-1)+1}\right).$$

For $\alpha = (2, 1, 2)$, we obtain

$$\tilde{\mathcal{H}}_{(2,1,2)}(x, y) = x^3y^3 + x^3y^2 + 3x^3y + 3x^2y^2 - 4x^3 + 6x^2y + 3xy + 5x + 1.$$

Note that this polynomial has a negative coefficient.

Computer experiments suggest the following answer to Research Challenge 3.6.5 in linear type A.

Conjecture 4.4.7. *Let α be a composition of $n > 0$. Then, $\mathcal{M}_\alpha(x, y) = \tilde{\mathcal{M}}_\alpha(x, y)$ if and only if α has at most one component exceeding 1.*

We support Conjecture 4.4.7 with the following proposition, which computes the F-, H- and M-triangles in the case where $\alpha = (t, 1, 1, \dots, 1)$ for $t \geq 1$. The proof of this result uses generating functions, and requires quite some preliminary work. We have therefore decided not to present this proof here. The interested reader is referred to [108].

Proposition 4.4.8 ([108, Theorems 4.2 and 5.13]). *Let $t > 0$ and let $\alpha = (t, 1, 1, \dots, 1) \vdash n$. Then,*

$$\begin{aligned} \mathcal{F}_\alpha(x, y) &= \sum_{k=0}^{n-t} \sum_{h=0}^{n-t-k} \frac{t+h}{n} \binom{n+k-1}{k} \binom{n}{t+k+h} x^k y^h \\ \mathcal{H}_\alpha(x, y) &= \sum_{k=0}^{n-t} \sum_{h=0}^{n-t-k} \left(\binom{n-t+1}{k} \binom{t+k+h-2}{h} \right. \\ &\quad \left. - \binom{n-t}{k-1} \binom{t+k+h-1}{h} \right) x^{n-t-k} y^{n-t-k-h}, \end{aligned}$$

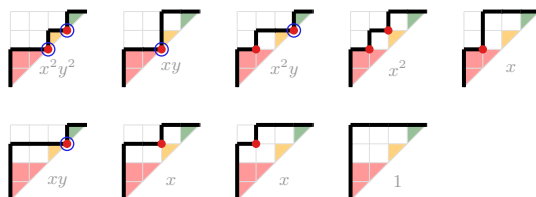


Figure 71. The $(2, 1, 1)$ -Dyck paths together with their contribution to $\mathcal{H}_{(2,1,1)}(x, y)$. Valleys are marked in red, returns are circled in blue.

$$\mathcal{M}_\alpha(x, y) = \sum_{k=0}^{n-t} \sum_{h=0}^{n-t-k} (-1)^h \frac{(t-1)(h+k) + n}{n(n-t+1)} \binom{n}{k} \binom{n-t+1}{h+k+1} \binom{n+h-1}{h} x^k y^{h+k}.$$

Example 4.4.9. We illustrate Proposition 4.4.8 in the case $\alpha = (2, 1, 1)$. Figure 71 shows the nine $(2, 1, 1)$ -Dyck paths together with their contribution to $\mathcal{H}_{(2,1,1)}(x, y)$. This yields

$$\mathcal{H}_{(2,1,1)}(x, y) = x^2y^2 + x^2y + x^2 + 2xy + 3x + 1,$$

$$\mathcal{F}_{(2,1,1)}(x, y) = 5x^2 + 3xy + y^2 + 8x + 3y + 1.$$

By inspection of Figure 68a, we compute

$$\tilde{\mathcal{M}}_{(2,1,1)}(x, y) = 3x^2y^2 - 8xy^2 + 5xy + 5y^2 - 5y + 1 = \mathcal{M}_{(2,1,1)}(x, y).$$

4.5. Applications

We now present two applications of Parabolic Cataland in linear type A. In particular, we prove a conjecture of N. BERGERON, C. CEBALLOS and V. PILAUD concerning the dimensions of the graded components of a certain Hopf algebra, and we give a combinatorial interpretation of the zeta map from diagonal harmonics. The results of this section are published in [45].

4.5.1. A Hopf algebra on pipe dreams. We briefly recall the basics on (combinatorial) Hopf algebras, and refer the interested reader to [86]. Let \mathbb{K} be a field, and let V be a \mathbb{K} -vector space. Then, V is *graded* if $V = \bigoplus_{n \geq 0} V_n$, and we call V_n the n^{th} graded component of V . Moreover, if $V_0 \cong \mathbb{K}$, then V is *connected*.

A \mathbb{K} -vector space V is an *associative \mathbb{K} -algebra* if there exists a \mathbb{K} -linear associative map $m: V \otimes V \rightarrow V$ (the *multiplication*) such that

$$m \circ (\text{id}_V \otimes m) = m \circ (m \otimes \text{id}_V)$$

and a \mathbb{K} -linear map $u: \mathbb{K} \rightarrow V$ (the *unit*) such that

$$m \circ (\text{id}_V \otimes u) = \text{id}_V = m \circ (u \otimes \text{id}_V).$$

An associative \mathbb{K} -algebra is *commutative* if m is a commutative map.

Dually, V is a *coassociative \mathbb{K} -algebra* if there exists a \mathbb{K} -linear map $\Delta: V \rightarrow V \otimes V$ (the *comultiplication*) such that

$$(\text{id}_V \otimes \Delta) \circ \Delta = (\Delta \otimes \text{id}_V) \circ \Delta$$

and a \mathbb{K} -linear map $\epsilon: V \rightarrow \mathbb{K}$ (the *counit*) such that

$$(\text{id}_V \otimes \epsilon) \circ \Delta = \text{id}_V = (\epsilon \otimes \text{id}_V) \circ \Delta.$$

A coassociative \mathbb{K} -algebra is *cocommutative* if Δ is a cocommutative map.

A *bialgebra* is an associative, coassociative \mathbb{K} -algebra such that the following compatibility conditions hold:

$$\begin{aligned} (m \otimes m) \circ (\text{id}_V \circ T \circ \text{id}_V) \circ (\Delta \otimes \Delta) &= \Delta \circ m, \\ m \circ (\epsilon \otimes \epsilon) &= \epsilon \circ m, \\ (u \otimes u) \circ \Delta &= \Delta \circ u, \\ \epsilon \circ u &= \text{id}_{\mathbb{K}}. \end{aligned}$$

where $T: V \otimes V \rightarrow V \otimes V$ given by $T(u \otimes v) = v \otimes u$ for all $u, v \in V$.

A bialgebra V is a *Hopf algebra* if there exists a \mathbb{K} -linear map $S: V \rightarrow V$ (the *antipode*) such that

$$m \circ (S \otimes \text{id}_V) \circ \Delta = u \circ \epsilon = m \circ (\text{id}_V \otimes S) \circ \Delta.$$

A subset $U \subseteq V$ is a *Hopf subalgebra* if it is a Hopf algebra in its own right, where all maps of U are the restrictions of those from V and U contains the identity of V .

Example 4.5.1. One of the most important combinatorial Hopf algebras is the *Malvenuto–Reutenauer Hopf algebra* $\mathbb{K}\mathfrak{S}$ on permutations [116]. The product of two permutations $u \in \mathfrak{S}_k$ and $v \in \mathfrak{S}_l$ is given as the formal sum over all shuffles of u, v , and the coproduct of $w \in \mathfrak{S}_n$ is given as the formal sum over all possible ways to write w as a sum $u \oplus v$ with $u \in \mathfrak{S}_i$ and $v \in \mathfrak{S}_{n-i}$.

Another important combinatorial Hopf algebra is the *Loday–Ronco Hopf algebra* $\mathbb{K}\mathcal{Y}$ on plane binary trees [115]. The coproduct of a plane binary tree T is given by the formal sum of all splits induced by the leaves of T , where a split induced by a leaf separates T into two trees, one consisting of all edges weakly to the left of the unique path from the leaf to the root, and the other consisting of all edges weakly to the right. Let T_1 and T_2 be two plane binary trees, and suppose that T_2 has s leaves. We may now split T_1 into s pieces according to a multisubsets with s elements of the leaves of T_1 , and subsequently add the i^{th} resulting factor to the i^{th} leaf of T_2 . The formal sum over all choices of such multisubsets gives the product of T_1 and T_2 .

A *global descent* of $w \in \mathfrak{S}_n$ is either 0 or $k \in [n]$ such that $\{w_i \mid i \leq k\} = \{k+1, k+2, \dots, n\}$. An *atomic* permutation is a permutation in \mathfrak{S}_n whose only global descents are 0 and n . For $u \in \mathfrak{S}_m$ and $v \in \mathfrak{S}_n$, their *swapped sum* is $u \bullet v \in \mathfrak{S}_{m+n}$ defined by

$$(4.25) \quad (u \bullet v)_i = \begin{cases} u_i + n, & \text{if } i \leq m, \\ v_{i-m}, & \text{if } i > m. \end{cases}$$

Compare this definition with the sum $u \oplus v$ defined in (2.13). It is easy to see that every permutation can be written uniquely as an iterated swapped sum of atomic permutations.

Recall the definition of a pipe dream from Section 2.4. In this section, for $w \in \mathfrak{S}_n$, we denote by $\text{Pipe}(w)$ the set of reduced pipe dreams for w with a total of $n+1$ pipes, where we add an “artificial” pipe from the topmost row to the leftmost column labeled by 0. We set

$$\text{Pipe}(\mathfrak{S}_n) \stackrel{\text{def}}{=} \{\text{Pipe}(w) \mid w \in \mathfrak{S}_n\}.$$

In [20], the graded vector space $\mathbb{K}\text{Pipe} \stackrel{\text{def}}{=} \bigoplus_n \mathbb{K}\text{Pipe}(\mathfrak{S}_n)$ was equipped with a Hopf algebra structure that we will recall next.

The coproduct on $\mathbb{K}\text{Pipe}$ is given as follows. Let $w \in \mathfrak{S}_n$ and $P \in \text{Pipe}(w)$. For a global descent k of w , we define the *untangling* $\Delta_{k, n-k}(P)$ to be the tensor of pipe dreams $P_1 \otimes P_2$, where P_1 is the restriction of P to the pipes $k+1, k+2, \dots, n$ and P_2 is the restriction of P to the first k pipes. See Figure 72 for an illustration. If k is not a global descent of w , then we set

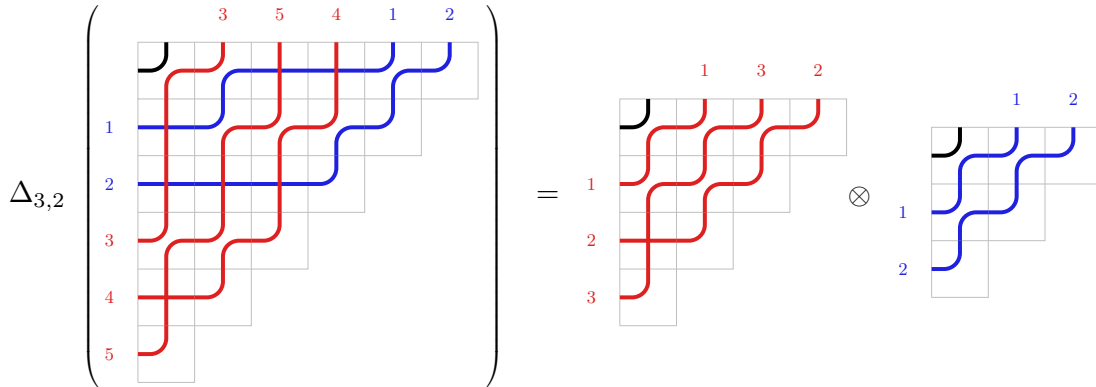


Figure 72. Untangling a pipe dream at a global descent.

$\Delta_{k,n-k}(P) = 0$. The *coproduct* on $\mathbb{K}\text{Pipe}$ is defined by $\Delta \stackrel{\text{def}}{=} \sum_{m,n \in \mathbb{N}} \Delta_{m,n}$. The counit on $\mathbb{K}\text{Pipe}$ is given by

$$\epsilon: \mathbb{K}\text{Pipe} \rightarrow \mathbb{K}, \quad P \mapsto \begin{cases} 1, & \text{if } P = \tau, \\ 0, & \text{otherwise.} \end{cases}$$

Proposition 4.5.2 ([20, Proposition 1.2.2]). *The maps Δ and ϵ equip $\mathbb{K}\text{Pipe}$ with a coassociative \mathbb{K} -algebra structure.*

The product on $\mathbb{K}\text{Pipe}$ is given as follows. Let $w_P \in \mathfrak{S}_m$ and $w_Q \in \mathfrak{S}_n$, and let $P \in \text{Pipe}(w_P)$ and $Q \in \text{Pipe}(w_Q)$. If $w_P = u_1 \bullet u_2 \bullet \dots \bullet u_s$ and $w_Q = v_1 \bullet v_2 \bullet \dots \bullet v_t$ are the factorizations of w_P and w_Q into atomic permutations, then a *•-shuffle* of w_P and w_Q is any permutation $w = w_1 \bullet w_2 \bullet \dots \bullet w_{s+t} \in \mathfrak{S}_{m+n}$ that preserves the order of the factors of both w_P and w_Q . We simplify w by adding adjacent factors belonging to the same word. If in this simplified word, there are k factors belonging to w_Q , then we untangle Q according to the positions of these factors and obtain k pipe dreams Q_1, Q_2, \dots, Q_k . The *w-tangling* of P and Q is the insertion of the factors Q_1, Q_2, \dots, Q_k into P so that the exit permutation is w . We write $P \star_w Q \in \text{Pipe}(w)$ for the resulting pipe dream. The *product* of P and Q is $m(P, Q) \stackrel{\text{def}}{=} \sum_w P \star_w Q$, where the sum ranges over all *•-shuffles* of w_P and w_Q . The unit on $\mathbb{K}\text{Pipe}$ is determined by $u(1) = \tau$.

Example 4.5.3. Let $w_P = 6752431 = 12 \bullet 1 \bullet 132 \bullet 1 \in \mathfrak{S}_7$ and $w_Q = 35412 = 132 \bullet 12 \in \mathfrak{S}_5$. The following permutations are *•-shuffles* of w_P and w_Q :

$$\begin{aligned} \bar{w} &= 11 \ 12 \ 10 \ 7 \ 9 \ 8 \ 4 \ 6 \ 5 \ 2 \ 3 \ 1 = 231 \bullet 132 \bullet 132 \bullet 12 \bullet 1, \\ \tilde{w} &= 11 \ 12 \ 8 \ 10 \ 9 \ 6 \ 7 \ 5 \ 2 \ 4 \ 3 \ 1 = 12 \bullet 35412 \bullet 52431, \end{aligned}$$

while this one is not:

$$12 \ 9 \ 11 \ 10 \ 7 \ 8 \ 5 \ 6 \ 2 \ 4 \ 3 \ 1 = 1 \bullet 132 \bullet 12 \bullet 12 \bullet 132 \bullet 1.$$

Figure 73 shows the \bar{w} -tangling and the \tilde{w} -tangling of two pipe dreams in $\text{Pipe}(w_P)$ and $\text{Pipe}(w_Q)$.

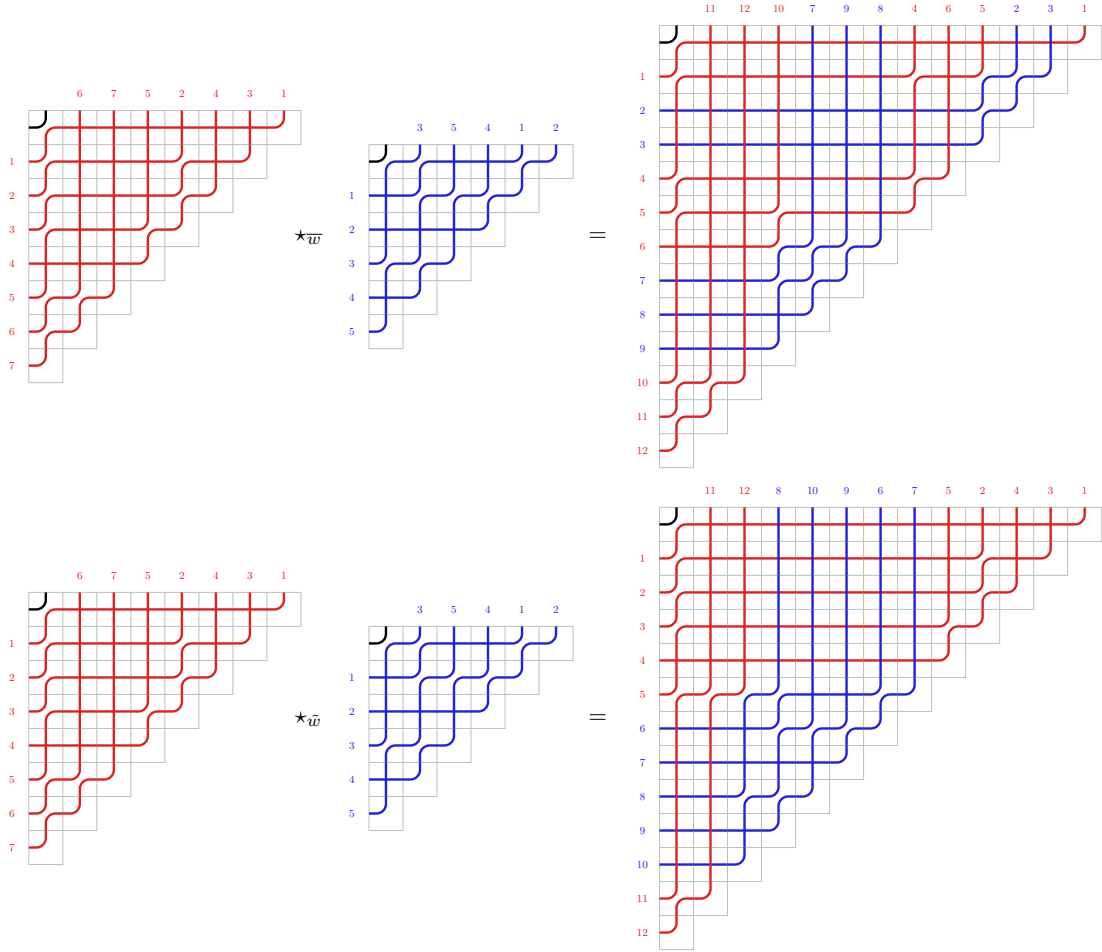


Figure 73. Two examples of the tangling of pipe dreams.

Proposition 4.5.4 ([20, Proposition 1.2.6]). *The maps m and u equip $\mathbb{K}\text{Pipe}$ with an associative \mathbb{K} -algebra structure.*

Proposition 4.5.5 ([20, Proposition 1.2.8]). *The product m and the coproduct Δ equip $\mathbb{K}\text{Pipe}$ with a graded connected Hopf algebra structure.*

We will now explain, that a certain Hopf subalgebra of $\mathbb{K}\text{Pipe}$ arises in the study of Parabolic Catalan. If S is any set of permutations, then we denote by $\text{Pipe}\langle S \rangle$ the set of pipe dreams whose exit permutations factors canonically into members of S .

Theorem 4.5.6 ([20, Theorem 2.1.1]). *For any set S of atomic permutations, the space $\mathbb{K}\text{Pipe}\langle S \rangle$ is a Hopf subalgebra of $\mathbb{K}\text{Pipe}$.*

Let id_k denote the identity permutation in \mathfrak{S}_k . Then, the set $\text{Pipe}\langle \{\text{id}_1\} \rangle$ consists of all pipe dreams whose exit permutation is $w_k = 1 \oplus k \text{ } k-1 \dots 1$ for some k . Note that by convention

we have chosen the top left corner to contain an elbow, which accounts for the first summand 1. By Theorem 2.4.12, this set collects all clusters of linear type A. The corresponding Hopf subalgebra $\mathbb{K}\text{Pipe}\langle\{\text{id}_1\}\rangle$ is isomorphic to the Loday–Ronco Hopf algebra on binary trees [20, Section 2.1.1].

By construction, for any composition $\alpha = (\alpha_1, \alpha_2, \dots, \alpha_r)$, the longest permutation $w_{\circ, \alpha}$ canonically factors as $\text{id}_{\alpha_1} \bullet \text{id}_{\alpha_2} \bullet \dots \bullet \text{id}_{\alpha_r}$, see Section 4.1.2. Therefore, any pipe dream of $w_{(\alpha)}$, see Section 4.1.4, belongs to $\text{Pipe}\langle\{\text{id}_1, \text{id}_2, \text{id}_3, \dots\}\rangle$. When computing the graded dimension of this Hopf subalgebra, the authors of [20] observed that this sequence corresponds to the sequence [169, A151498] which counts for instance certain lattice walks in the positive quarter plane, starting at the origin, ending on the x -axis and using only steps in $\{(-1, 1), (1, -1), (0, 1)\}$. Such walks were for instance considered in [32, 124, 125]. Let \nearrow_n denote the set of such walks using a total of n steps. The list of cardinalities of \nearrow_n begins as follows:

$$1, 1, 3, 12, 57, 301, 1707, 10191, 63244, 404503.$$

The main result of this section resolves [20, Conjecture 2.2.1], which describes a combinatorial interpretation of the basis of $\mathbb{K}\text{Pipe}_n\langle\{\text{id}_1, \text{id}_2, \text{id}_3, \dots\}\rangle$.

Theorem 4.5.7. *For $n > 0$, the graded dimension of $\mathbb{K}\text{Pipe}_n\langle\{\text{id}_1, \text{id}_2, \text{id}_3, \dots\}\rangle$ equals the cardinality of \nearrow_n .*

We prove Theorem 4.5.7 combinatorially by designing a bijection from the basis elements of $\mathbb{K}\text{Pipe}_n\langle\{\text{id}_1, \text{id}_2, \text{id}_3, \dots\}\rangle$ to the elements of \nearrow_n using the α -trees we have defined in Section 4.1.7.

A *marked* Dyck path is $p \in \text{Dyck}_n$ for which some north steps are marked. We denote the marked north steps by N_\bullet and the unmarked ones by N_\circ . A marked Dyck path is *level marked* if for any lattice point along this path, the number of unmarked north steps before this point does not exceed the number of east steps before this point. Let $\text{Dyck}^\bullet(n)$ denote the set of level-marked Dyck paths with a total of n steps.

We may “unfold” such a lattice walk into a level-marked Dyck path as follows. For a lattice walk in \nearrow_n , we start at the origin and successively replace each step of the form $(0, 1)$ by a marked north step, we replace each step $(-1, 1)$ by an unmarked north step and we replace each step $(1, -1)$ by an east step. See the top-left of Figure 74 for an illustration.

We now show how to obtain a level-marked Dyck path with n steps from an α -tree for any composition α of $n > 0$.

Proposition 4.5.8. *Let $\alpha \vdash n$. For every $T \in \text{Tree}(\alpha)$, there exists a naturally associated level-marked Dyck path $p_T^\bullet \in \text{Dyck}^\bullet(n)$.*

PROOF. Let γ denote the α -coloring of T . We perform a right-to-left traversal of T . Whenever we visit a new node in T with a γ -color that we have not seen before, we add a marked north step, otherwise we add an unmarked north step. When we visit a node that we have seen before, we add an east step. The resulting lattice path is denoted by p_T^\bullet .

In traversing the tree, we visit each edge twice, the first time we add a north step and the second time we add an east step. Since T has n non-root nodes, this indicates that

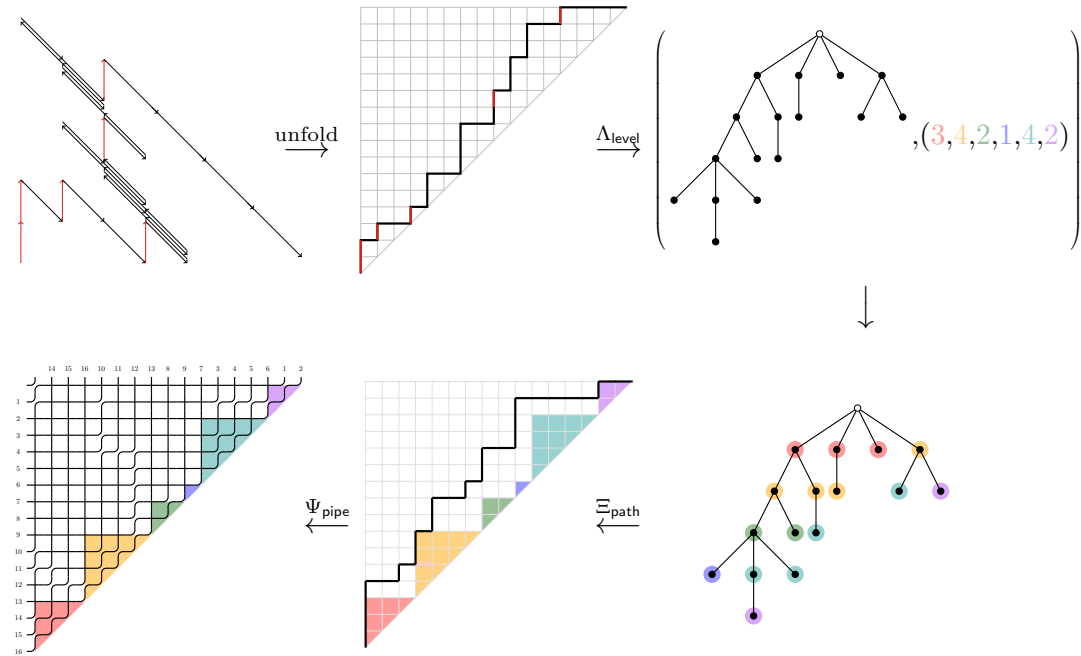


Figure 74. Illustrating the bijection from Dyck_n to $\text{Pipe}_n \langle \{id_1, id_2, id_3, \dots\} \rangle$ for $n = 16$.

p_T^\bullet has $2n$ steps and ends at (n, n) . It is also clear that there can never be a prefix which contains more east steps than north steps. Hence, $p_T^\bullet \in \text{Dyck}(n)$.

It remains to show that p_T^\bullet is level marked. Let (p, q) be the coordinate of a north step in p_T^\bullet . This north step corresponds to the first time we visit a node u in the right-to-left traversal of T . By Lemma 4.1.25(i), all nodes on the path from u to the root, including u and excluding the root, have different colors. There are exactly $q - p$ such nodes, meaning that up to (p, q) we have seen at least $q - p$ colors. Equivalently, at least $q - p$ marked north steps come before the point (p, q) which is equivalent to the defining condition of level-marked Dyck paths. Thus, $p_T^\bullet \in \text{Dyck}^\bullet(n)$. \square

Conversely, we may as well construct a colored tree from any $p^\bullet \in \text{Dyck}^\bullet(n)$.

Construction 4.5.9. Let $n > 0$ and $p^\bullet \in \text{Dyck}^\bullet(n)$ such that p^\bullet has exactly r marked north steps. We initialize our construction with the tree T_0 consisting of a single root node, the empty coloring f_0 and a list of colors $L_0 = [0]$, where 0 stands for the color of the root. Throughout this construction, we maintain a pointer on the colors. Initially, this pointer points to the 0 in L_0 . In each step of this construction, we are visiting a certain node, the **current node**. Initially, the root of T_0 is the current node.

We parse p^\bullet as a word. Suppose that p_i is the i^{th} letter of this word. We update T_{i-1} , f_{i-1} , L_{i-1} as follows.

- (i) If $p_i = N_\bullet$, then we extend T_{i-1} to T_i by adding a node v_i to the current node of T_{i-1} as its leftmost child. We set the current node of T_i to be v_i . We insert a new color c into

- L_{i-1} right after the pointer, and move the pointer to c . We extend f_{i-1} to f_i by setting $f_i(v_i) = c$.
- (ii) If $p_i = N_o$, then we extend T_{i-1} to T_i by adding a node v_i to the current node of T_{i-1} as its leftmost child. We set the current node of T_i to be v_i . We take L_i to simply be L_{i-1} with the pointer moved to the next color c' . We extend f_{i-1} to f_i by setting $f_i(v_i) = c'$.
 - (iii) If $p_i = E$, then we take T_i to simply be T_{i-1} with the current node set to the parent of the current node of T_{i-1} . We take L_i to be L_{i-1} with the pointer moved to the previous color. Since p^\bullet is a Dyck path, such a color (it may be 0 for the root) must exist. We set $f_i = f_{i-1}$.

Let f'_i be the coloring of T_i that is obtained from f_i by renaming the colors according to the first appearance in the left-to-right traversal of T_i . After $2n$ steps, we have parsed p^\bullet completely, and we output $T_{p^\bullet} = T_{2n}$ with the coloring f'_{2n} . Note that f'_{2n} uses precisely r different colors.

Lemma 4.5.10. *At the end of the i^{th} step of Construction 4.5.9, the list L_i of colors (renamed by first appearances in left-to-right traversal) is increasing. In particular, if u is a non-root node of T_i and v is a descendant of u , then $f'_i(u) < f'_i(v)$.*

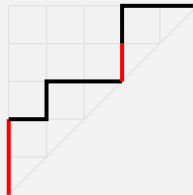
PROOF. By Construction 4.5.9, the colors in the unique shortest path from the root of T_i to v exactly coincide with the colors in L_i from the beginning of the list to the current position of the pointer, and they appear in the same order on that path and in L_i .

Now, suppose that there are two colors c_1 and c_2 such that c_1 comes after c_2 in L_i . Let u_1 be the first node in the LR-prefix order of T_i with $f'_i(u_1) = c_1$. There must be an ancestor u_2 of u_1 with $f'_i(u_2) = c_2$ by the argument in the first paragraph.

Since u_2 precedes u_1 in the LR-prefix order of T_i , it follows that $c_2 < c_1$ due to the renaming. This yields $f'_i(u_2) < f'_i(u_1)$ as desired. \square

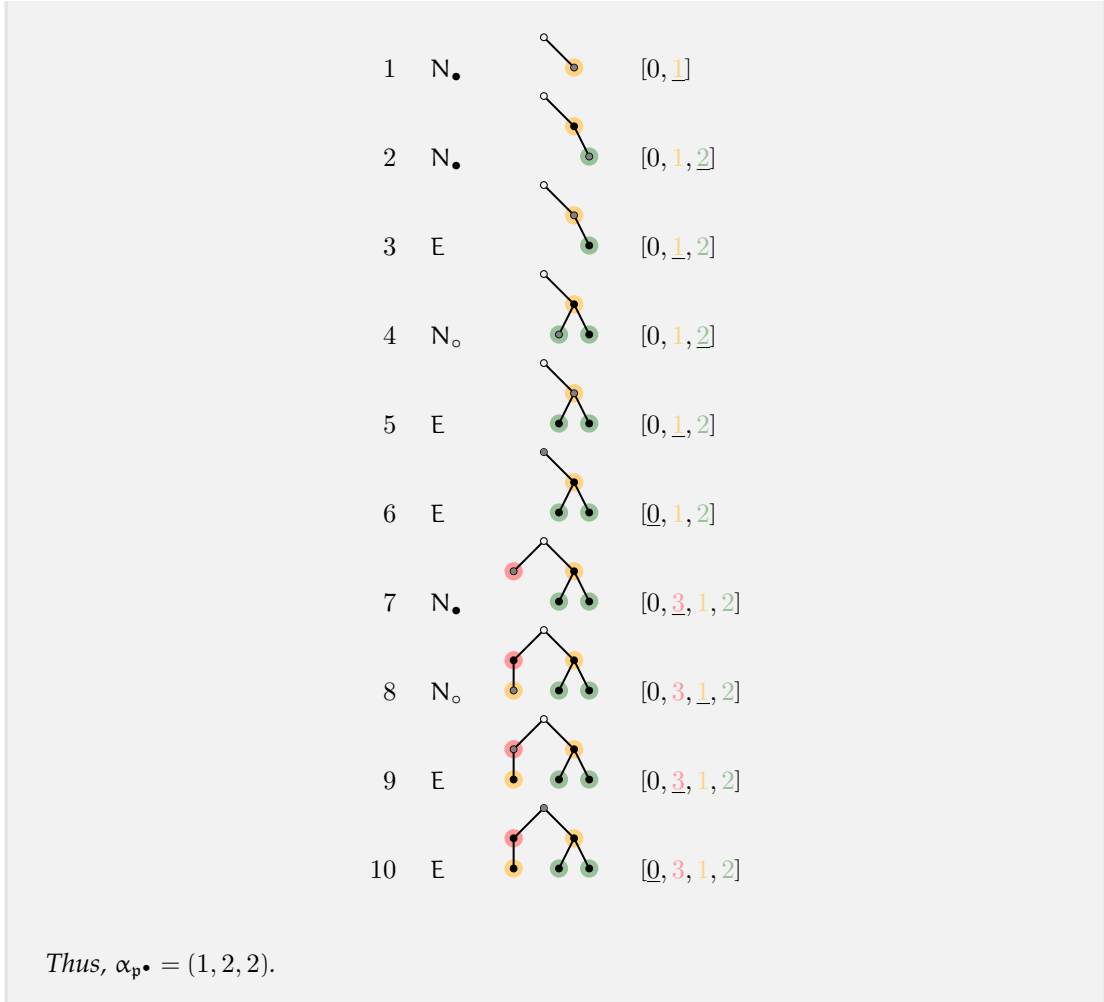
We observe that for $p^\bullet \in \text{Dyck}^\bullet(n)$, forgetting the markings determines the tree while the markings determine the coloring. More precisely, if f' is the coloring of T_{p^\bullet} obtained from Construction 4.5.9, then we set α_i to be the number of nodes of T_{p^\bullet} whose f' -color is i , and we set $\alpha_{p^\bullet} \stackrel{\text{def}}{=} (\alpha_1, \alpha_2, \dots, \alpha_r)$.

Example 4.5.11. *We illustrate Construction 4.5.9 with the path $p^\bullet = N \bullet N \bullet E N_o E E N \bullet N_o E E \in \text{Dyck}^\bullet(5)$:*



The following table lists the steps in Construction 4.5.9. The current node is marked in gray, the color currently pointed at is underlined.

i	p_i	T_i	L_i
0	-	•	<u>0</u>



Therefore, any $p^\bullet \in \text{Dyck}^\bullet(n)$ determines a pair (T, α) , where T is a plane rooted tree and α is a composition. We will see soon that in this case $T \in \text{Tree}(\alpha)$. We thus define the set of *LAC trees* by

$$(4.26) \quad \text{LAC}(n) \stackrel{\text{def}}{=} \{(T, \alpha) \mid \alpha \vdash n, T \in \text{Tree}(\alpha)\}.$$

With this notation, Proposition 4.5.8 induces a well-defined map:

$$(4.27) \quad \Xi_{\text{level}}: \text{LAC}(n) \rightarrow \text{Dyck}^\bullet(n), \quad (T, \alpha) \mapsto p_T^\bullet,$$

where $\alpha \vdash n$, $T \in \text{Tree}(\alpha)$ and p_T^\bullet is the level-marked Dyck path from Proposition 4.5.8.

We show next that Construction 4.5.9 induces the following well-defined map, which is illustrated in the top-right of Figure 74:

$$(4.28) \quad \Lambda_{\text{level}}: \text{Dyck}^\bullet(n) \rightarrow \text{LAC}(n), \quad p^\bullet \mapsto (T_{p^\bullet}, \alpha_{p^\bullet}).$$

Proposition 4.5.12. *For a level-marked Dyck path $p^\bullet \in \text{Dyck}^\bullet(n)$, let T_{p^\bullet} be the colored tree obtained from Construction 4.5.9 and let α_{p^\bullet} be the composition of n obtained from the coloring. Then, $T_{p^\bullet} \in \text{Tree}(\alpha_{p^\bullet})$.*

PROOF. Suppose that \mathbf{p}^\bullet has exactly r marked north steps, and let T be the colored tree obtained from Construction 4.5.9 and let f be the corresponding coloring. It follows that f uses exactly r colors. We have already seen before that $\alpha_{\mathbf{p}^\bullet} = (\alpha_1, \alpha_2, \dots, \alpha_r)$ is a composition of n , where α_i counts the number of nodes of T whose f -color is i .

For $s \in [r]$, let T_s be the restriction of T to the nodes of f -color at most s . We prove by induction on s that the induced subtree T'_s of T whose nodes are colored at the end of step s in Construction 4.1.24 is precisely T_s .

The base case $s = 0$ is clear, since both T_0 and T'_0 consist of a single root node. Now suppose that $T_s = T'_s$. By Lemma 4.1.25(i), we see that T'_{s+1} is connected. By Lemma 4.5.10, the f -color of any node is bigger than that of its ancestors, so T_{s+1} is also connected.

Let u be the last node with $f(u) = s + 1$ in the LR-prefix order of T . Consider a node $v \notin T'_s$ that is a child of some node in $T_s = T'_s$ while strictly preceding u in LR-prefix order. Suppose that v is created in step i of Construction 4.5.9 with L_i being the list of colors (after renaming) available just after. Note that every ancestor of v has f -color at most s so that u is in particular not an ancestor of v . Therefore, v comes after u in the right-to-left traversal of T , which means that $s + 1$ is already present in L_i . The pointer of L_i cannot be after $s + 1$, because that would imply the existence of an ancestor of v of f -color $s + 1$, which is contradiction. The pointer of L_i cannot be before $s + 1$, because otherwise, by Lemma 4.5.10 we would have the contradiction $s + 1 > f(v) > s$, because $v \notin T_s$. It follows that $f(v) = s + 1$, which holds for all nodes of $T'_{s+1} \setminus T'_s$ that come before u in LR-prefix order.

Since u is the last node in LR-prefix order that has f -color $s + 1$, no descendant of u belongs to T_{s+1} . Let X be the set of nodes in $T_{s+1} \setminus T_s$. We have just shown that X contains all the nodes $T'_{s+1} \setminus T'_s$ that precede u in LR-prefix order. Moreover, all nodes in X are active in the $(s + 1)^{\text{st}}$ step of Construction 4.1.24. Since $|X| = \alpha_{s+1}$, all the vertices in X receive color $s + 1$ in Construction 4.1.24. We conclude that $T_{s+1} = T'_{s+1}$.

This completes the induction step, and we see that T is indeed compatible with $\alpha_{\mathbf{p}^\bullet}$ and f is the $\alpha_{\mathbf{p}^\bullet}$ -coloring of T . \square

Theorem 4.5.13. *For every integer $n > 0$, the map Ξ_{level} is a bijection whose inverse is Λ_{level} .*

PROOF. In view of Propositions 4.5.8 and 4.5.12 it remains to show that $\Xi_{\text{level}} \circ \Lambda_{\text{level}} = \text{id}$ and $\Lambda_{\text{level}} \circ \Xi_{\text{level}} = \text{id}$. We observe that the map Ξ_{level} without markings and colors is a slight modification of the well-known bijection from the set of plane rooted trees with n non-root nodes to the set of Dyck paths with $2n$ steps, described for instance in [60, Appendix E.1].

To show that $\Xi_{\text{level}} \circ \Lambda_{\text{level}} = \text{id}$, for $\mathbf{p}^\bullet \in \text{Dyck}^\bullet(n)$, let $(T, \alpha) = \Lambda_{\text{level}}(\mathbf{p}^\bullet)$ and $\hat{\mathbf{p}}^\bullet = \Xi_{\text{level}}((T, \alpha))$. As mentioned before, the underlying Dyck paths \mathbf{p} and $\hat{\mathbf{p}}$ are equal, so it remains to show that the marked north steps are in the same positions. By construction, the marked north steps of \mathbf{p}^\bullet determine the right-most nodes per color in T , which in turn determine the marked north steps in $\hat{\mathbf{p}}^\bullet$ in the same way. We conclude that $\mathbf{p}^\bullet = \hat{\mathbf{p}}^\bullet$.

Conversely, to show that $\Lambda_{\text{level}} \circ \Xi_{\text{level}} = \text{id}$, for $(T, \alpha) \in \text{LAC}(n)$, let $\mathbf{p}^\bullet = \Xi_{\text{level}}((T, \alpha))$ and $(T', \alpha') = \Lambda_{\text{level}}(\mathbf{p}^\bullet)$. As before, we conclude that $T = T'$, and it remains to show that $\alpha = \alpha'$. We observe already that α has the same number of components as α' , as both are equal to the number of marked north steps in \mathbf{p}^\bullet by construction.

Let T_s, T'_s denote the subtrees of T and T' , respectively, that consist of all nodes of color at most s , including the root. We show that $T_s = T'_s$ by induction on s . The base case $s = 0$ is clear, since both T_0 and T'_0 consist of the root only. Now suppose that $T_s = T'_s$. At least one of the active nodes of T_s must belong to the set V of last nodes per color with respect to (T, α) . We denote by u the first active node in V in the LR-prefix order of T . It follows that all active nodes of T_s up to u in LR-prefix order receive color $s + 1$. The same reasoning works for T'_s as α and α' have the same number of components, and we conclude that $T_{s+1} = T'_{s+1}$. This completes the induction step, and we obtain $\alpha = \alpha'$. \square

We may now prove Theorem 4.5.7, which is illustrated in Figure 74.

PROOF. By [20, Theorem 2.1.2], a basis of $\mathbb{K}\text{Pipe}_n \langle \{\text{id}_1, \text{id}_2, \text{id}_3, \dots\} \rangle$ is given by the set of pipe dreams, whose exit permutation lies in \mathfrak{S}_n and factors into identity permutations. These are precisely the elements of $\bigcup_{\alpha \in \mathfrak{S}_n} \text{Pipe}(w_\alpha)$. Using the concatenation $\Lambda_{\text{path}} \circ \Psi_{\text{pipe}}^{-1}$, we see that this basis is in bijection with $\text{LAC}(n)$. Theorem 4.5.13 states that $\text{LAC}(n)$ and \mathcal{N}_n are in bijection, finishing the proof. \square

4.5.2. A zeta map from diagonal harmonics. The second application of Parabolic Cataland concerns certain rings of invariant polynomials under an \mathfrak{S}_n -action. Our explanation of the underlying theory mainly follows [87]. Recall from Remark 2.1.4 that if W is a finite Coxeter group, the ring A^W of (real or complex) polynomials invariant under a certain W -action is again a polynomial algebra.

Let us have a closer look at this when $W = \mathfrak{S}_n$ is the symmetric group. Let $A = \mathbb{C}[x_1, x_2, \dots, x_n]$ be the ring of complex polynomials in n variables. The usual \mathfrak{S}_n -action on A is given by

$$w \cdot f(x_1, x_2, \dots, x_n) \stackrel{\text{def}}{=} f(x_{w_1}, x_{w_2}, \dots, x_{w_n})$$

for $w \in \mathfrak{S}_n$ and $f \in A$. The invariant ring

$$A^{\mathfrak{S}_n} \stackrel{\text{def}}{=} \{f \in A \mid w \cdot f = f \text{ for all } w \in \mathfrak{S}_n\}$$

is the ring of *symmetric functions* and is for instance generated by the *power sum symmetric functions*

$$\pi_k \stackrel{\text{def}}{=} \sum_{i=1}^n x_i^k$$

for $k \in [n]$ [87]. The ring of *coinvariants* is the quotient $R^{(1)} \stackrel{\text{def}}{=} A/(\pi_1, \pi_2, \dots, \pi_n)$, which inherits a grading $R^{(1)} = R_0^{(1)} \oplus R_1^{(1)} \oplus R_2^{(1)} \oplus \dots$, where $R_k^{(1)}$ is spanned by all homogeneous polynomials in x_1, x_2, \dots, x_n of degree k . Since $\pi_1, \pi_2, \dots, \pi_n$ are algebraically independent, it follows that $\dim_{\mathbb{C}}(R^{(1)}) = n!$ and

$$(4.29) \quad \sum_{k=0}^n \dim_{\mathbb{C}}(R_k^{(1)}) q^k = \prod_{i=1}^{n-1} (1 + q + q^2 + \dots + q^i).$$

Now, π_k has degree k , so that the exponents of \mathfrak{S}_n are $e_i = i$ for $i \in [n]$. Thus (4.29) recovers precisely the type-A case¹⁴ of the generating series $W_S(q)$; see Theorem 2.1.1.

The *Vandermonde determinant* $V_n \stackrel{\text{def}}{=} \prod_{1 \leq i < j \leq n} (x_i - x_j)$ provides a different perspective to $R^{(1)}$. Let $H^{(1)}$ denote the complex vector space spanned by V_n and all its partial derivatives; the

¹⁴Note the index shift, i.e., \mathfrak{S}_n is isomorphic to A_{n-1} .

space of *harmonic polynomials*. It was shown in [90] that, for all n , $R^{(1)}$ and $H^{(1)}$ are isomorphic as \mathbb{C} -vector spaces.

A. GARSIA and M. HAIMAN generalized the above construction to two sets of variables [79]. More precisely, let $B = \mathbb{C}[x_1, x_2, \dots, x_n, y_1, y_2, \dots, y_n]$. Then, \mathfrak{S}_n acts *diagonally* on B by

$$w \cdot f(x_1, x_2, \dots, x_n, y_1, y_2, \dots, y_n) \stackrel{\text{def}}{=} f(x_{w_1}, x_{w_2}, \dots, x_{w_n}, y_{w_1}, y_{w_2}, \dots, y_{w_n})$$

for $w \in \mathfrak{S}_n$ and $f \in B$. As before, we denote by $B^{\mathfrak{S}_n}$ the ring of invariant polynomials under this diagonal action. Analogous to the case of one set of variables, we may consider *polarized power sum symmetric functions*

$$\pi_{h,k} \stackrel{\text{def}}{=} \sum_{i=1}^n x_i^h y_i^k$$

for $h, k \in \mathbb{N}$. Then, $B^{\mathfrak{S}_n}$ is generated by the $\pi_{h,k}$ as long as $h + k \geq 0$ [87], and the quotient ring of *diagonal coinvariants* is $R^{(2)} \stackrel{\text{def}}{=} B^{(2)}/I$, where

$$I \stackrel{\text{def}}{=} \langle \pi_{h,k} \mid \text{for all } h, k \in \mathbb{N} \text{ with } h + k > 0 \rangle.$$

Remarkably, $\dim_{\mathbb{C}}(R^{(2)}) = (n+1)^{n-1}$ is the number of trees with n labeled nodes [91]. Moreover, $R^{(2)} = \bigoplus_{i,j} R_{ij}^{(2)}$, where $R_{ij}^{(2)}$ is spanned by all polynomials homogeneous of degree i in the x -variables and degree j in the y -variables. The ring of *diagonal harmonics* is defined by

$$H^{(2)} \stackrel{\text{def}}{=} \left\{ f \in B \mid \sum_{i=1}^n \frac{\partial^h}{x_i^h} \frac{\partial^k}{y_i^k} f = 0 \text{ for all } h, k \in \mathbb{N} \text{ with } h + k > 0 \right\}.$$

We wish to turn our attention to the *alternating* component of $H^{(2)}$, i.e.,

$$H^{(2)\epsilon} \stackrel{\text{def}}{=} \{ f \in H^{(2)} \mid w \cdot f = (-1)^{|\text{Inv}(w)|} f \text{ for all } w \in \mathfrak{S}_n \},$$

because $\dim_{\mathbb{C}}(H^{(2)\epsilon}) = \text{Cat}(n)$ [78]. The *bigraded Hilbert series* of $H^{(2)\epsilon}$ is defined by

$$\mathcal{H}_n^{\epsilon}(q, t) \stackrel{\text{def}}{=} \sum_{i,j \geq 0} t^i q^j \dim_{\mathbb{C}}(H_{ij}^{(2)\epsilon}),$$

where $H_{ij}^{(2)\epsilon}$ denotes the bigraded components of $H^{(2)\epsilon}$. Note that $\mathcal{H}_n^{\epsilon}(1, 1) = \dim_{\mathbb{C}}(H^{(2)\epsilon}) = \text{Cat}(n)$. The series $\mathcal{H}_n^{\epsilon}(q, t)$ is usually called the *q, t-Catalan number* [78], and is by definition symmetric in the variables q and t . There are two intriguing combinatorial interpretations of $\mathcal{H}_n^{\epsilon}(q, t)$ in terms of Dyck paths.

Recall from Section 2.5 that a Dyck path is a northeast path that fits inside a staircase shape and its area is the number of boxes below the path. A Dyck path $p \in \text{Dyck}(n)$ is *bounce* if it can be written as $p = N^{i_1} E^{i_1} N^{i_2} E^{i_2} \dots N^{i_r} E^{i_r}$, where $i_1 + i_2 + \dots + i_r = n$. The name “bounce” comes from the fact that a bounce path goes north for a while, then goes east until it hits the diagonal, from which it bounces off and goes north again, then goes east until it hits the diagonal once more, and so on.

With any $p \in \text{Dyck}(n)$ we can associate a canonical bounce path p_{bounce} that essentially “bounces” between the path and the diagonal. Say that the bounce path of p hits the diagonal in the coordinates $(i_0, i_0), (i_1, i_1), \dots, (i_r, i_r)$, where $i_0 = 0$ and $i_r = n$. Then, the *bounce parameters* of p are the x -coordinates $0 = i_0, i_1, \dots, i_r = n$ of the contact points of p_{bounce} with the main diagonal. The *bounce statistic* of p is defined by $\text{bounce}(p) \stackrel{\text{def}}{=} \sum_{k=1}^{r-1} (n - i_k)$.

For $p \in \text{Dyck}(n)$, let a_i denote the number of boxes in the i^{th} row of the staircase shape containing p which lie below p . We call the vector $\mathbf{a}(p) \stackrel{\text{def}}{=} (a_1, a_2, \dots, a_n)$ the *area vector*. Then, clearly, $\text{area}(p) = a_1 + a_2 + \dots + a_n$. Moreover, the *div ν statistic* of p is

$$\text{div}\nu(p) \stackrel{\text{def}}{=} \left| \left\{ (i, j) \mid 1 \leq i < j \leq n, a_i \in \{a_j, a_j + 1\} \right\} \right|.$$

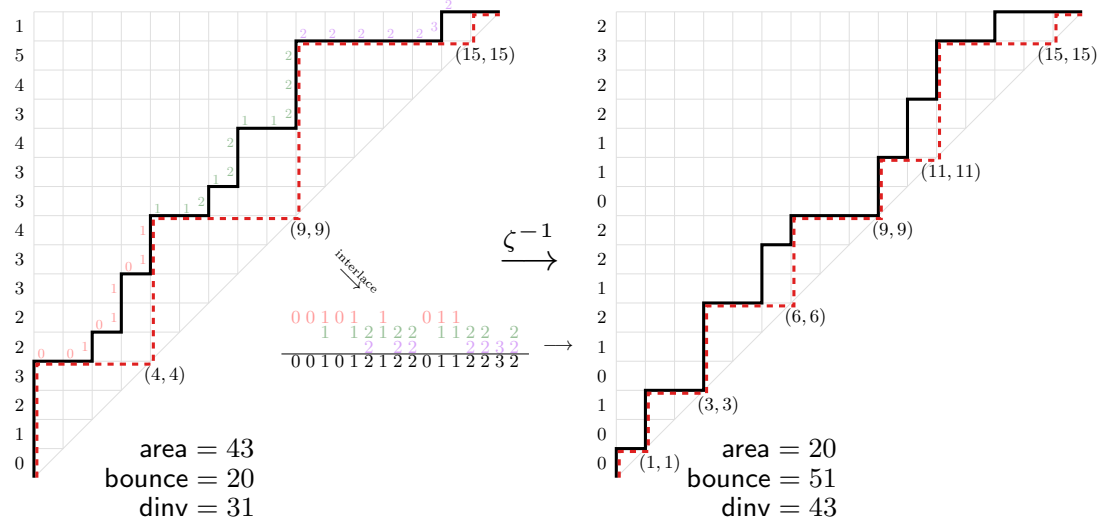


Figure 75. A Dyck path and its image under the inverse zeta map. The area vectors are written to the left and the bounce paths are drawn in dashed red. In the left path, we have labeled the steps as described in Construction 4.5.16.

In other words, $\text{dinv}(p)$ counts the pairs of rows of the same length as well as the pairs of rows which differ by one with the longer row below the shorter. See Figure 75 for an illustration of these statistics. These statistics may be used to combinatorially realize $\mathcal{H}_n^e(q, t)$.

Theorem 4.5.14 ([87, Chapter 3]). *For every $n > 0$, it holds that*

$$\begin{aligned} \mathcal{H}_n^e(q, t) &= \sum_{p \in \text{Dyck}(n)} q^{\text{area}(p)} t^{\text{bounce}(p)} \\ &= \sum_{p \in \text{Dyck}(n)} q^{\text{dinv}(p)} t^{\text{area}(p)}. \end{aligned}$$

Example 4.5.15. *For $n = 4$, Figure 76 lists the fourteen Dyck paths of semilength 4 together with the values of the statistics area, bounce and dinv. This yields*

$$\mathcal{H}_4^e(q, t) = q^6 + q^5t + q^4t^2 + q^3t^3 + q^2t^4 + qt^5 + t^6 + q^4t + q^3t^2 + q^2t^3 + qt^4 + q^3t + q^2t^2 + qt^3$$

in two different ways in accordance with Theorem 4.5.14.

The phenomenon described in Theorem 4.5.14 is explained bijectively via the so-called *zeta map* ζ . This is a bijection on $\text{Dyck}(n)$ which sends the pair of statistics $(\text{area}, \text{bounce})$ to $(\text{dinv}, \text{area})$. Let us briefly recall the construction of the inverse of ζ following [2] and [87, Proof of Theorem 3.15]; this map is illustrated in Figure 75. The interested reader is referred to [6, 42, 184, 188] for further background and variants of the zeta map.

Construction 4.5.16. *Let $p' \in \text{Dyck}(n)$, let p'_{bounce} denote its bounce path with bounce parameters i_0, i_1, \dots, i_r . For $k \in [r]$, we denote by $\vec{p}_k = (i_{k-1}, i_k)$ the peak of p'_{bounce} at height i_k . By construction, \vec{p}_k is also on p' . The number of steps between \vec{p}_k and \vec{p}_{k+1} is*

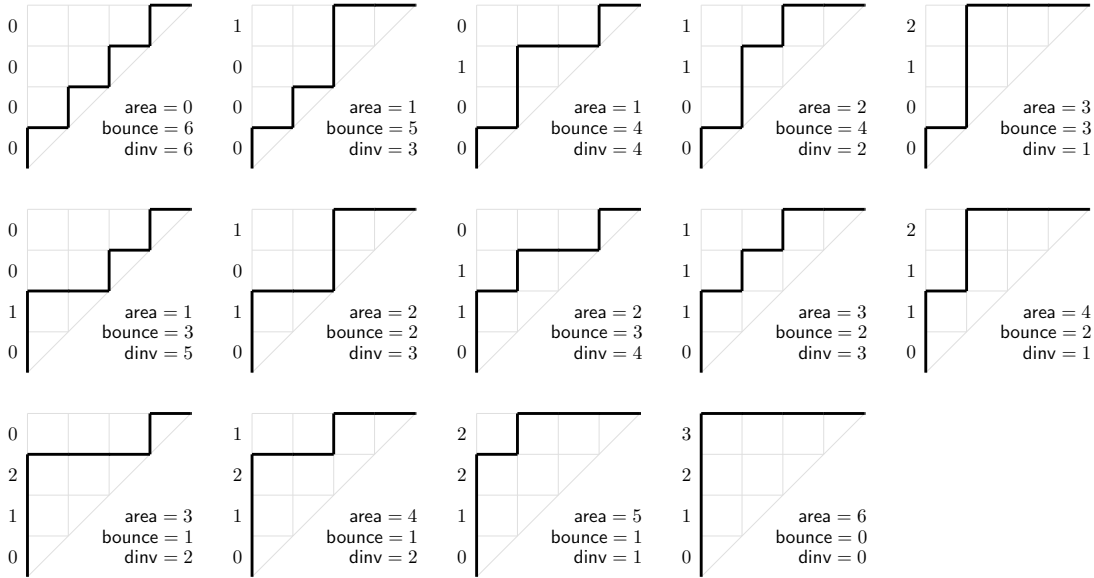


Figure 76. The fourteen Dyck paths of semilength 4 together with various statistics.

$(i_k - i_{k-1}) + (i_{k+1} - i_k) = i_{k+1} - i_k$. For $k \in [r - 1]$, the sequence $\mathbf{a}^{(k)}$ arises from the subpath of p' between \vec{p}_k and \vec{p}_{k+1} by replacing each east step by $k - 1$ and each north step by k . We fashion these $r - 1$ sequences together by interlacing the sequence $\mathbf{a}^{(k)}$ and $\mathbf{a}^{(k+1)}$ for all $k \in [r - 1]$, where we insert the values $k - 1$ and $k + 1$ relative to the values k so that we never put a $k - 1$ directly before a $k + 1$. The resulting sequence \mathbf{a} has precisely n entries, $i_{k+1} - i_k$ of which are equal to k for $k \in \{0, 1, \dots, r - 1\}$.

Proposition 4.5.17 ([87, Proof of Theorem 3.15]). For $p' \in \text{Dyck}(n)$, the sequence \mathbf{a} obtained by Construction 4.5.16 is the area vector of some Dyck path $p \in \text{Dyck}(n)$, and we have $\zeta(p) = p'$.

Now, let $p \in \text{Dyck}(n)$ and let p_{bounce} denote its bounce path. If p_{bounce} hits the diagonal in the coordinates $(i_0, i_0), (i_1, i_1), \dots, (i_r, i_r)$, then by construction $p \in \text{Dyck}((i_1, i_2, \dots, i_r))$. Thus, for any $p \in \text{Dyck}(n)$ there is a naturally associated pair (p, α) , where $\alpha \vdash n$. Using the bijection Λ_{path} from (4.14) this pair maps into $\text{LAC}(n)$ and by means of the bijection Ξ_{level} from (4.27) we obtain a level-marked Dyck path $p^\bullet \in \text{Dyck}^\bullet(n)$ associated with p .

For $p_1, p_2 \in \text{Dyck}(n)$ we say that the pair (p_1, p_2) is *nested* if p_1 always stays weakly below p_2 , and we refer to p_1 as the *bottom* path and to p_2 as the *top* path of such a nested pair. By construction, for any $p \in \text{Dyck}(n)$, (p_{bounce}, p) is indeed a nested pair of Dyck paths. We define the set of *bounce pairs* by

$$\text{BouncePair}(n) \stackrel{\text{def}}{=} \{(p_1, p_2) \in \text{Dyck}(n) \times \text{Dyck}(n) \mid (p_1, p_2) \text{ is nested and } p_1 \text{ is bounce}\}.$$

The right side of Figure 77 shows the elements of $\text{BouncePair}(3)$.

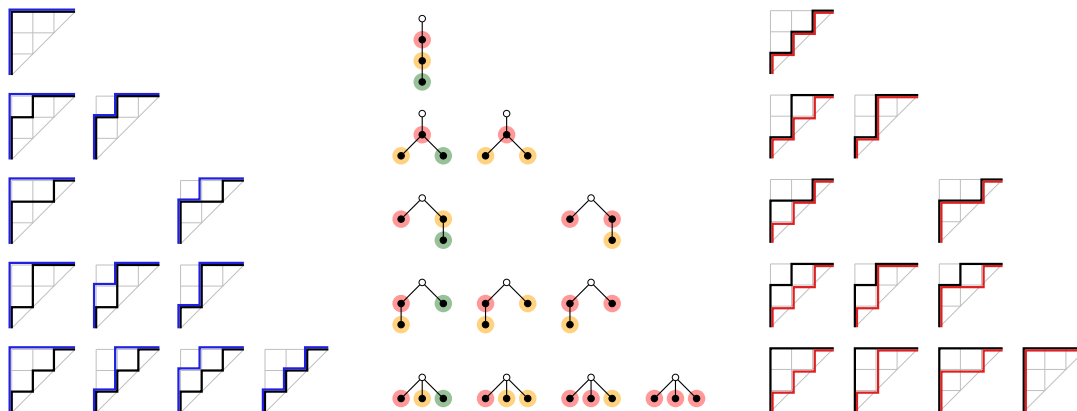


Figure 77. The sets $\text{SteepPair}(3)$, $\text{LAC}(3)$ and $\text{BouncePair}(3)$ arranged according to Λ_{steep} and Ξ_{bounce} .

We will now explain that any level-marked Dyck path can be described by a particular nested pair of Dyck paths, too. A Dyck path is *steep* if it does not contain two consecutive east steps, except possibly at the end. Let us consider the set of *steep pairs* defined by

$$\text{SteepPair}(n) \stackrel{\text{def}}{=} \{(p_1, p_2) \in \text{Dyck}(n) \times \text{Dyck}(n) \mid (p_1, p_2) \text{ is nested and } p_2 \text{ is steep}\}.$$

The left side of Figure 77 shows the elements of $\text{SteepPair}(3)$. Eventually, we describe a bijection from $\text{SteepPair}(n)$ to $\text{BouncePair}(n)$; see Theorem 4.5.19.

Given a level-marked Dyck path $p^\bullet \in \text{Dyck}^\bullet(n)$, we denote by $\vartheta(p)$ the pair (p_1, p_2) , where p_1 is p^\bullet without the marking, and p_2 is obtained from p^\bullet by forgetting the east steps, replacing each marked north step N_\bullet by a northstep N and each unmarked north step N_\circ by a valley EN , and adding as many east steps at the end as necessary. Clearly, (p_1, p_2) is a pair of Dyck paths. In fact, it is a nested pair of Dyck paths where the top path is steep, and every steep pair is obtained in this way.

Proposition 4.5.18 ([20, Section 2.2.3]). *The map $\vartheta: \text{Dyck}^\bullet(n) \rightarrow \text{SteepPair}(n)$ is a bijection.*

In view of Theorem 4.5.13 and Proposition 4.5.18, the following map is thus a bijection:

$$(4.30) \quad \Xi_{\text{steep}}: \text{LAC}(n) \rightarrow \text{SteepPair}(n), \quad (T, \alpha) \mapsto \vartheta(\Xi_{\text{level}}((T, \alpha)));$$

its inverse is denoted by Λ_{steep} . The top of Figure 78 illustrates Ξ_{steep} .

Let $\alpha = (\alpha_1, \alpha_2, \dots, \alpha_r) \vdash n$. If $T \in \text{Tree}(\alpha)$, then $(T, \alpha) \in \text{LAC}(n)$. Moreover, the path $p_T = \Xi_{\text{path}}(T)$, see Proposition 4.2.15, belongs to $\text{Dyck}(\alpha)$, which is the set of all Dyck paths lying weakly above $v_\alpha = N^{\alpha_1} E^{\alpha_1} N^{\alpha_2} E^{\alpha_2} \dots N^{\alpha_r} E^{\alpha_r}$. By construction v_α is bounce, which implies that $(v_\alpha, p) \in \text{BouncePair}(n)$. If Ξ_{bounce} denotes the assignment $(T, \alpha) \mapsto (v_\alpha, p)$, then we obtain a bijection

$$(4.31) \quad \Xi_{\text{bounce}}: \text{LAC}(n) \rightarrow \text{BouncePair}(n), \quad (T, \alpha) \mapsto (v_\alpha, \Xi_{\text{path}}(T)),$$

whose inverse is denoted by Λ_{bounce} . The bottom of Figure 78 illustrates Ξ_{bounce} . We may then concatenate these maps to obtain a bijection

$$(4.32) \quad \Gamma: \text{SteepPair}(n) \rightarrow \text{BouncePair}(n), \quad (p_1, p_2) \mapsto \Xi_{\text{bounce}}(\Lambda_{\text{steep}}(p_1, p_2)).$$

Figure 78 illustrates this map on an example for $n = 16$, and Figure 77 shows the bijective correspondence between $\text{SteepPair}(3)$ and $\text{BouncePair}(3)$.

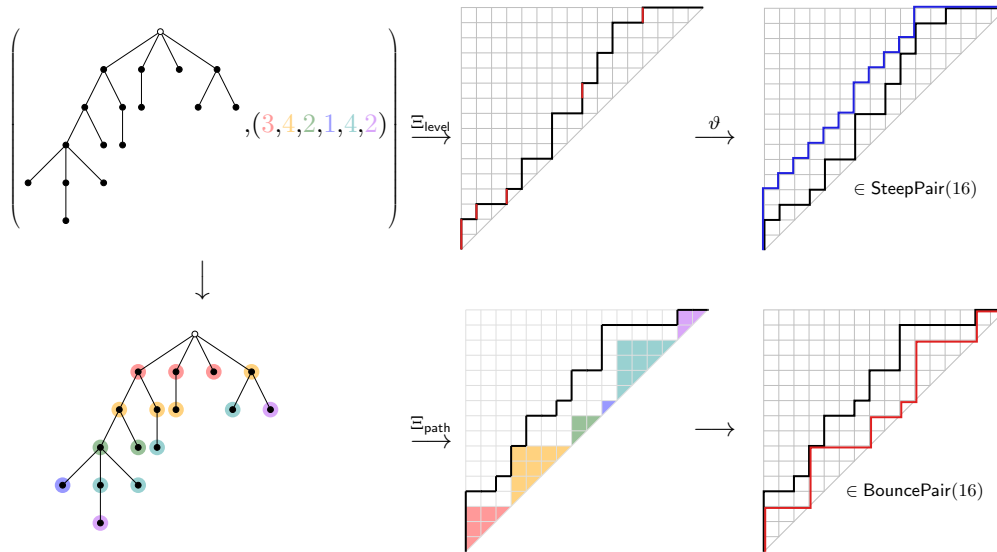


Figure 78. Illustration of the map Γ from $\text{SteepPair}(n)$ to $\text{BouncePair}(n)$ for $n = 16$.

Theorem 4.5.19. For $n > 0$ and every $r \in [n]$, the map Γ is a bijection from

- the set of nested pairs (p_1, p_2) of Dyck paths of semilength n , where p_2 is steep ending with exactly r east steps with y -coordinate equal to n , to
- the set of nested pairs (p'_1, p'_2) of Dyck paths of semilength n , where p'_1 is bounce and touches the main diagonal exactly $r + 1$ times.

PROOF. We have already argued that Γ is a bijection. Let $(p_1, p_2) \in \text{SteepPair}(n)$ where p_2 ends with r east steps, and let $(p'_1, p'_2) = \Gamma((p_1, p_2))$. By construction, the parameter r corresponds to the number of marked north steps of the level-marked Dyck path $\vartheta^{-1}(p_1, p_2)$, and by Construction 4.5.9 this equals the number of components of the composition α obtained by $(T, \alpha) = \Lambda_{\text{steep}}((p_1, p_2))$. The way that p'_1 is obtained from α makes clear that p'_1 touches the main diagonal exactly $r + 1$ times. \square

Perhaps somewhat surprisingly, the map Γ generalizes the zeta map ζ appearing in Construction 4.5.16. We have already argued that any $p \in \text{Dyck}(n)$ has a naturally associated bounce path p_{bounce} . There is also a naturally associated steep path p_{steep} , obtained as follows: we start at the origin and move north until, for the first time, we can add an east step while still staying weakly above p . We continue with at least one north step until we reach another coordinate where we may add an east step while still staying weakly above p . We continue in this manner until we reach y -coordinate n . We then finish by adding as many east steps as necessary to reach coordinate (n, n) . The left side of Figure 79 shows a Dyck path $p \in \text{Dyck}(16)$ whose associated steep path is marked in dashed blue.

As remarked in Section 4.1.7, any plane rooted tree T admits a horizontal composition $\alpha_T = (\alpha_1, \alpha_2, \dots)$, where α_i equals the number of nodes of T whose distance to the root is exactly i . In this setting, the *level vector* of T , denoted by $\mathbf{a}(T)$, is obtained by marking the levels of the nodes of T in right-to-left traversal.

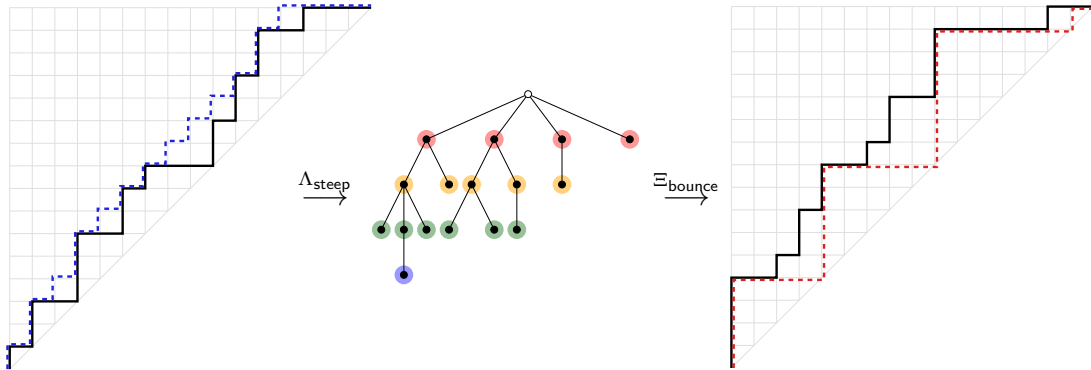


Figure 79. The zeta map is a restriction of Γ . Compare with Figure 75.

We now show that for any $p \in \text{Dyck}(n)$ there exists a unique plane binary tree T , such that $\Lambda_{\text{steep}}((p, p_{\text{steep}})) = (T, \alpha_T)$ and $\Xi_{\text{bounce}}((T, \alpha_T)) = (p'_{\text{bounce}}, p')$ such that $p' = \zeta(p)$; see Theorem 4.5.22. This is illustrated in Figure 79; see also Figure 75.

Proposition 4.5.20. *For every $n > 0$, the map Ξ_{steep} restricts to a bijection from*

- *the set of pairs (T, α_T) , where T is a plane rooted tree with n non-root nodes, to*
- *the set of pairs (p, p_{steep}) , where $p \in \text{Dyck}(n)$.*

Moreover, if $(p, p_{\text{steep}}) = \Xi_{\text{steep}}((T, \alpha_T))$, then $\mathbf{a}(p) = \mathbf{a}(T)$.

PROOF. Recall that $\Xi_{\text{steep}} = \vartheta \circ \Xi_{\text{level}}$. Let T be a plane rooted tree with n non-root nodes and let $\alpha_T \vdash n$ be its horizontal composition. Let $p^\bullet = \Xi_{\text{level}}((T, \alpha_T))$ be the associated level-marked Dyck path and let $(p_1, p_2) = \vartheta(p^\bullet)$ be the steep pair associated with p^\bullet . Let $\mathbf{a}(p_1) = (a_1, a_2, \dots, a_n)$ be the area vector of p_1 . Recall that p_1 is obtained from p^\bullet by forgetting the marking. The proof proceeds in three steps.

We first show that $\mathbf{a}(p_1) = \mathbf{a}(T)$. By Proposition 4.5.8, p_1 is obtained from the left-to-right traversal of T : whenever we visit a new node, we add a north step; every time we go back up one level, we add an east step. The contribution of a north step to the area vector of p_1 is therefore equal to the number of north steps preceding it minus the number of east steps preceding it. This is clearly the distance (in T) of the corresponding node from the root.

We now prove that $T \in \text{Tree}(\alpha_T)$ if and only if p^\bullet is such that the j^{th} north step is marked whenever $a_i < a_j$ for all $i < j$.

Observe that for every $p \in \text{Dyck}(n)$, there is a unique way to mark its north steps such that the above condition is satisfied. Moreover, every plane rooted tree has exactly one horizontal composition. Since the set of Dyck paths with $2n$ steps is in bijection with the set of plane rooted trees with n non-root nodes (see for instance [60, Appendix E.1]) and the map Ξ_{level} is a bijection, it remains to show that whenever $T \in \text{Tree}(\alpha_T)$, the image $p^\bullet = \Xi_{\text{level}}((T, \alpha_T))$ has the desired property.

The color of a node in T equals its level, and by Proposition 4.5.8, every time we reach the first node of a certain level in right-to-left traversal, we add a marked north step to p^\bullet . All other north steps correspond to unmarked north steps. Since a north step contributes an entry to the area vector which is equal to the level of its corresponding

node, the marked north steps in p^\bullet are exactly those that contribute an entry a_j with $a_i < a_j$ for all $i < j$.

We finally prove that p_2 is the steep path of p_1 if and only if p^\bullet is such that the j^{th} north step is marked whenever $a_i < a_j$ for all $i < j$.

This is straightforward in view of the following alternative description of the steep path of p_1 . We parse p_1 as follows: in the beginning, for each north step, we write down NE until we reach a north step that contributes a 1 to the area vector of p_1 ; in this case we write down NN. We then continue to append copies of NE for each north step until we reach one that contributes a 2 to the area vector, for which we append NN again. We continue this process until we have written down a total of n N-letters, and we finish by adding the necessary number of E-letters at the end.

The word so written corresponds to the steep path of p_1 and its valleys are precisely the entries a_j of the area vector of p_1 with $a_i < a_j$ for all $i < j$. By the construction before Proposition 4.5.18, the valleys of p_2 correspond precisely to the marked north steps of p^\bullet .

These three claims together show that $T \in \alpha_T$ if and only if $\Xi_{\text{steep}}((T, \alpha_T)) = (p_1, p_{1\text{steep}})$ and that $a(T) = a(p_1)$. \square

Proposition 4.5.21. *For every $n > 0$, the map Λ_{bounce} restricts to a bijection from*

- *the set of pairs (p_{bounce}, p) , where $p \in \text{Dyck}(n)$, to*
- *the set of pairs (T, α_T) , where T is a plane rooted tree with n non-root nodes.*

Moreover, if $(T, \alpha_T) = \Lambda_{\text{bounce}}(p_{\text{bounce}}, p)$, then $a(\zeta^{-1}(p)) = a(T)$.

PROOF. Let $\alpha = (\alpha_1, \alpha_2, \dots, \alpha_r) \vdash n$, let $(v_\alpha, p) \in \text{BouncePair}(n)$ and let $(T, \alpha) = \Lambda_{\text{bounce}}(v_\alpha, p)$. For $i \in [r]$, recall that $p_i = \alpha_1 + \alpha_2 + \dots + \alpha_i$ and that q_i denotes the number of active nodes at the beginning of the $(i+1)^{\text{st}}$ step of Construction 4.1.24. By definition $p_0 = 0$ and q_0 is the number of root children in T . If $\alpha = \alpha_T$, then $q_i = \alpha_{i+1}$ for $i \in [r-1]$. The proof proceeds in two steps.

We first show that $\alpha = \alpha_T$ if and only if $v_\alpha = p_{\text{bounce}}$. As in the second part of the proof of Proposition 4.5.20 we exploit the bijection from plane rooted trees with n non-root nodes to Dyck paths with $2n$ steps. Since p_{bounce} is uniquely determined by p , it suffices to prove that $\alpha = \alpha_T$ implies $v_\alpha = p_{\text{bounce}}$. By assumption v_α is weakly below p , so that we need to show that each peak of v_α touches p at the initial point of an east step of p . Equivalently, we need to show that, for each $i \in [r-1]$, the path p has a valley with coordinates (a, b) such that $p_{i-1} < a \leq p_i$ and $b = p_i$. This valley corresponds to the rightmost internal node of color i , say u , which is the j^{th} node of color i for some $j \in [\alpha_i]$. Since we have assumed that $\alpha = \alpha_T$, it follows that the rightmost child of u is the rightmost node of color $i+1$, which is the α_{i+1}^{st} active node in the i^{th} step of Construction 4.1.24. By definition of Ξ_{bounce} , we see that $p_{i-1} < a = p_i - j + 1 \leq p_i$ and $b = p_i + q_i - \alpha_{i+1} = p_i$ as desired.

We now show that $\alpha = \alpha_T$ implies $a(\zeta^{-1}(p)) = a(T)$.

Let $p' = \zeta^{-1}(p)$ as described in Construction 4.5.16. The path p_{bounce} touches the diagonal at $(0, 0) = (p_0, p_0), (p_1, p_1), \dots, (p_r, p_r) = (n, n)$. Therefore, $a(p')$ has exactly $p_{i+1} - p_i = \alpha_{i+1}$ entries equal to i for $0 \leq i \leq r-1$, which is exactly the number of entries equal to i in $a(T)$.

For $i \in [r-1]$ we denote by $\mathbf{a}_i(p')$ and $\mathbf{a}_i(T)$ the restrictions of $\mathbf{a}(p')$ and $\mathbf{a}(T)$ to the values $\{i-1, i\}$, respectively. It remains to show that $\mathbf{a}_i(p') = \mathbf{a}_i(T)$.

The vector $\mathbf{a}_i(T)$ can be obtained from the right-to-left traversal of T : each time we reach a new node at level $i-1$, we add a value $i-1$ and each time we add a new node at level i , we add a value i .

The vector $\mathbf{a}_i(p') = \mathbf{a}_i(\zeta^{-1}(p))$ can be obtained from the subpath of p between (p_{i-1}, p_i) and (p_i, p_{i+1}) by replacing each east step by $i-1$ and each north step by i . Recall that $T = \Lambda_{\text{path}}(p)$ as described in Proposition 4.2.17. By Lemma 4.2.19, for $j \in [\alpha_i]$, the number of north steps in p with x -coordinate $p_{i-1} + j$ equals the number of children of the j^{th} node of color i in the right-to-left traversal of T . From this, we deduce that $\mathbf{a}_i(T) = \mathbf{a}_i(p')$. \square

We now obtain the announced result.

Theorem 4.5.22. *For $n > 0$, the map Γ restricts to a bijection from*

- *the set of nested steep pairs (p, p_{steep}) , where $p \in \text{Dyck}(n)$, to*
- *the set of nested bounce pairs (p'_{bounce}, p') , where $p' \in \text{Dyck}(n)$.*

Moreover, if $\Gamma((p, p_{\text{steep}})) = (p'_{\text{bounce}}, p')$, then $\zeta(p) = p'$.

PROOF. Propositions 4.5.20 and 4.5.21 imply that Γ restricts to the desired bijection, and states that $\mathbf{a}(p) = \mathbf{a}(\zeta^{-1}(p'))$. Since the area vector uniquely determines a Dyck path, we conclude $\zeta(p) = p'$. \square

Remark 4.5.23. *We may as well obtain the equivalent descriptions of $\mathcal{H}_n^e(q, t)$ in terms of (area, bounce) and (dinv, area) stated in Theorem 4.5.14 directly using our bijections.*

Let $\alpha = (\alpha_1, \alpha_2, \dots, \alpha_r)$ and let T be the unique plane rooted tree which satisfies $\alpha_T = \alpha$. Consider $\Xi_{\text{steep}}(T, \alpha_T) = (p, p_{\text{steep}})$ and $\Xi_{\text{bounce}}(T, \alpha_T) = (p'_{\text{bounce}}, p')$. Since p is simply $\Xi_{\text{level}}((T, \alpha_T))$ without markings, we know that each north step corresponds to a non-root node of T , with the corresponding entry in the area vector $\text{area}(p)$ being the level of that node. Therefore, we have (summing over all non-root nodes):

$$\text{area}(p) = \sum_{u \in T} \text{level}(u) = \sum_{u \in T} \sum_{v \text{ above } u} 1 = \sum_{v \in T} \sum_{u \text{ below } v} 1 = \sum_{i=1}^{r-1} (n - b_i) = \text{bounce}(p').$$

The pairs contributing to $\text{dinv}(p)$ correspond to pairs of nodes (u, v) such that v comes before u in the right-to-left traversal of T and $\text{level}(v) - \text{level}(u) \in \{0, 1\}$. Now, if we order the nodes in T first by increasing level and then by occurrence in the right-to-left traversal, then each node can be identified with an integer between 1 and n . It follows that the cells below p' correspond precisely to the pairs contributing to $\text{dinv}(p)$, and we see that $\text{area}(p') = \text{dinv}(p)$.

Remark 4.5.24. *The bigraded Hilbert series of the full module $H^{(2)}$ of diagonal harmonics admits a combinatorial interpretation as a sum over two types of labeled Dyck paths using some modifications of the statistics dinv , area , and bounce . This was conjectured in [88] (see also [87, Conjecture 5.2]) and recently proven in [39]. Our constructions can be used to recover these interpretations by adding appropriate labels to the α -trees with respect to a horizontal*

composition. See [45, Section 3.3.4] for the details and some illustrations. Generalizing Theorem 4.5.19 to a labeled setting currently remains open.

CHAPTER 5

Epilogue

In this thesis, we have first given a broad overview of *Cataland*, i.e., the entirety of combinatorial families associated with finite, irreducible Coxeter groups enumerated by the Coxeter–Catalan numbers, their order-theoretic structures and their interactions. We have then recalled a generalization to parabolic quotients of finite, irreducible Coxeter groups, and we have posed a number of conjectures and research challenges. In linear type A we have answered most of these questions, we have given concrete combinatorial realizations of the *parabolic* Catalan families and we have uncovered two intriguing applications of the theory to certain combinatorial Hopf algebras and to the theory of diagonal harmonics.

In this epilogue, we outline four potential streams of follow-up research together with various concrete research questions.

5.1. Arbitrary type A

The next step towards proving any of Conjectures 3.2.6, 3.3.2, 3.4.3, 3.4.4 and 3.5.3 is evidently to extend the constructions from linear type A to arbitrary type A .

Let us briefly review what happens combinatorially for ordinary Catalan families, when we consider arbitrary Coxeter elements in type A . Recall that any choice of Coxeter element induces an acyclic orientation of the Coxeter graph of A_{n-1} ; see Theorem 1.2.14. Recall further that the Coxeter graph of A_{n-1} is a path of length n , whose nodes correspond to the adjacent transpositions $(i \ i+1)$ for $i \in [n-1]$, where two adjacent transpositions are connected by an edge if and only if they do not commute. Thus, any $i \in \{2, 3, \dots, n-1\}$ can be identified with the edge $\{(i-1 \ i), (i \ i+1)\}$. We represent the orientation of such an edge from $(i-1 \ i)$ to $(i \ i+1)$ by writing \bar{i} ; we represent the other orientation by writing \dot{i} . In other words, an (acyclic) orientation of the Coxeter graph of A_{n-1} (and therefore a Coxeter element of A_{n-1}) determines a map

$$\varepsilon: \{2, 3, \dots, n-1\} \rightarrow \{-1, 1\}, \quad i \mapsto \begin{cases} 1, & \text{if } \bar{i}, \\ -1, & \text{if } \dot{i}; \end{cases}$$

a so-called *barring* of $\{2, 3, \dots, n-1\}$ —where -1 represents an underbar and 1 represents an overbar; see Figure 80.

N. READING then proposed the following combinatorial model for the c -aligned elements of A_{n-1} . Given any barring ε , a permutation $w \in \mathfrak{S}_n$ is *$\bar{2}31$ -avoiding* (resp. *$31\bar{2}$ -avoiding*) with respect to ε if there do not exist indices $i < j < k$ such that $w_k < w_i < w_j$ (resp. $w_j < w_i < w_k$) and $\varepsilon(j) = 1$ (resp. $\varepsilon(j) = -1$).

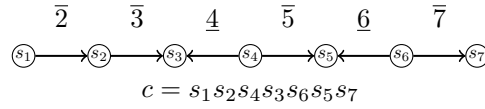


Figure 80. An acyclic orientation, a Coxeter element and a barring for A_7 .

Proposition 5.1.1 ([148, Lemma 4.8]). *Let $n > 0$ and let ε be a barring of $\{2, 3, \dots, n - 1\}$. Let c be the Coxeter element corresponding to ε . Then $w \in \mathfrak{S}_n$ is c -aligned if and only if w is both $\bar{2}31$ - and $31\bar{2}$ -avoiding.*

We now generalize this construction to parabolic type A. Let $\alpha = (\alpha_1, \alpha_2, \dots, \alpha_r)$ be a composition of n . An α -barring is a map $\varepsilon: \{2, 3, \dots, r - 1\} \rightarrow \{-1, 1\}$. We indicate ε in the one-line notation of \mathfrak{S}_α by putting an overbar over the *whole* i^{th} α -region if and only if $\varepsilon(i) = 1$ and an underbar below the *whole* i^{th} α -region otherwise.

Then, $w \in \mathfrak{S}_\alpha$ has an $(\alpha, \bar{2}31)$ -pattern (resp. $(\alpha, 31\bar{2})$ -pattern) if there exist indices $i < j < k$ with $\text{reg}_\alpha(i) < \text{reg}_\alpha(j) < \text{reg}_\alpha(k)$ such that $w_i = w_k + 1$ and $w_i < w_j$, $\varepsilon(\text{reg}_\alpha(j)) = 1$ (resp. $w_k > w_j$, $\varepsilon(\text{reg}_\alpha(j)) = -1$). A permutation without $(\alpha, \bar{2}31)$ -patterns (resp. $(\alpha, 31\bar{2})$ -patterns) is $(\alpha, \bar{2}31)$ -avoiding (resp. $(\alpha, 31\bar{2})$ -avoiding). We write $\text{Sort}(\alpha, \varepsilon)$ for the set of (α, ε) -sortable elements, i.e., all α -permutations that are simultaneously $(\alpha, \bar{2}31)$ - and $(\alpha, 31\bar{2})$ -avoiding.

Given what we have seen in Chapter 4, the (α, ε) -sortable elements appear to be a suitable combinatorial model for the (W^J, c) -aligned elements in type A. Since the Coxeter graph of A_{n-1} is a path with $n - 1$ nodes, Theorem 1.2.14 implies that the number of Coxeter elements of A_{n-1} is 2^{n-2} . However, given a composition $\alpha = (\alpha_1, \alpha_2, \dots, \alpha_r)$ there are only 2^{r-2} α -barrings, and in most cases $r < n$. This discrepancy is indeed relevant as the next example shows.

Example 5.1.2. *Let $n = 4$ and $\alpha = (1, 2, 1)$. There are two α -barrings ε and $-\varepsilon$, where $\varepsilon(2) = 1$. The two lattices $\mathbf{Weak}(\text{Sort}(\alpha, \varepsilon))$ and $\mathbf{Weak}(\text{Sort}(\alpha, -\varepsilon))$ are shown in Figure 81. Note that each lattice is dual to the other. Let $\mathbf{c} = s_2s_3s_1$ be a Coxeter element of A_3 , and choose $J = \{s_2\}$. Then $\mathbf{w}_o^J(\mathbf{c}) = s_3s_1s_2s_3s_1$, whose inversion set is*

$$\text{Inv}(\mathbf{w}_o^J) = \{s_1, s_3, s_1s_2s_3s_2s_1, s_2s_3s_2, s_1s_2s_1\};$$

see also Example 3.2.7. The (W^J, \mathbf{c}) -aligned elements are the following:

$$\begin{aligned} & \mathbf{e}, & s_1, & s_3, & s_2s_1, & s_2s_3, \\ & s_3s_1, & s_2s_3s_1, & s_1s_2s_3s_1, & s_3s_2s_3s_1, & s_3s_1s_2s_3s_1. \end{aligned}$$

Figure 82 shows the lattice $\mathbf{Camb}(W^J, \mathbf{c})$, which is not isomorphic to any of the lattices from Figure 81.

Therefore, the (α, ε) -sortable elements do not fully explain the parabolic aligned elements in type A. Nevertheless, we still think that the (α, ε) -elements possess an interesting combinatorial structure. We pose a few conjectures.

Conjecture 5.1.3. *Let α be a composition of $n > 0$ and let $\varepsilon, \varepsilon_1, \varepsilon_2$ be α -barrings. Then,*

- (i) $|\text{Sort}(\alpha, \varepsilon_1)| = |\text{Sort}(\alpha, \varepsilon_2)|$;
- (ii) *The poset $\mathbf{Weak}(\text{Sort}(\alpha, \varepsilon))$ is a congruence-uniform, trim lattice;*

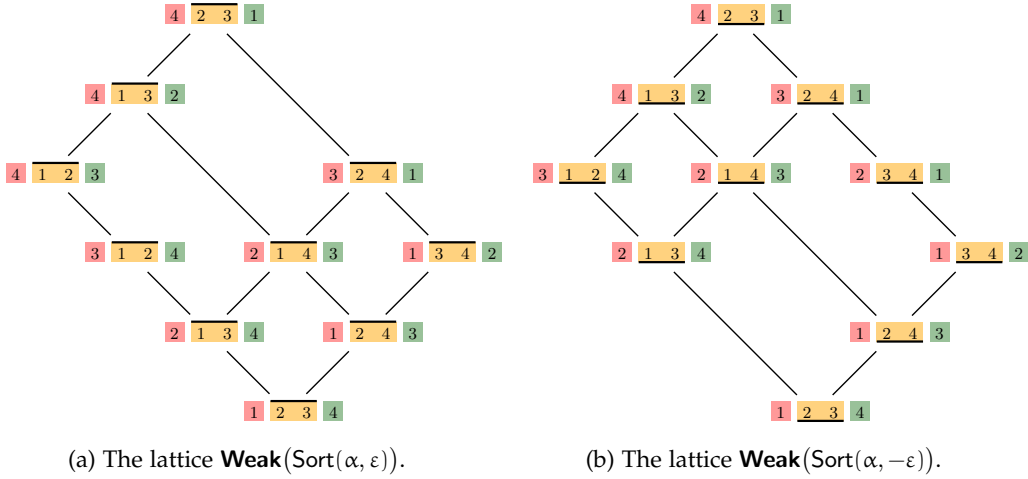


Figure 81. The two posets of (α, ε) -sortable permutations for $\alpha = (1, 2, 1)$.

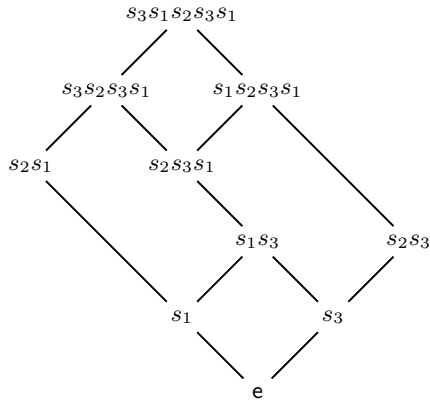


Figure 82. The lattice $\mathbf{Camb}(A_3^{\{s_2\}}, s_2 s_3 s_1)$.

- (iii) The poset $\mathbf{Weak}(\text{Sort}(\alpha, \varepsilon))$ is a quotient lattice of $\mathbf{Weak}(\mathfrak{S}_\alpha)$;
- (iv) $\mathbf{Weak}(\text{Sort}(\alpha, \varepsilon)) \cong \mathbf{Weak}(\text{Sort}(\alpha, -\varepsilon))^d$.

For $w \in \mathfrak{S}_\alpha$, we say that $\text{Inv}(w)$ is (α, ε) -aligned if for all $i < j < k$ with $\text{reg}_\alpha(i) < \text{reg}_\alpha(j) < \text{reg}_\alpha(k)$:

- if $\varepsilon(\text{reg}_\alpha(j)) = 1$, then $(i, k) \in \text{Cov}(w)$ implies $(i, j) \in \text{Inv}(w)$;
- if $\varepsilon(\text{reg}_\alpha(j)) = -1$, then $(i, k) \in \text{Cov}(w)$ implies $(j, k) \in \text{Inv}(w)$.

Lemma 5.1.4. An α -permutation is (α, ε) -sortable if and only if $\text{Inv}(w)$ is (α, ε) -aligned.

PROOF. The proof is essentially verbatim to the proof of Lemma 4.1.16. □

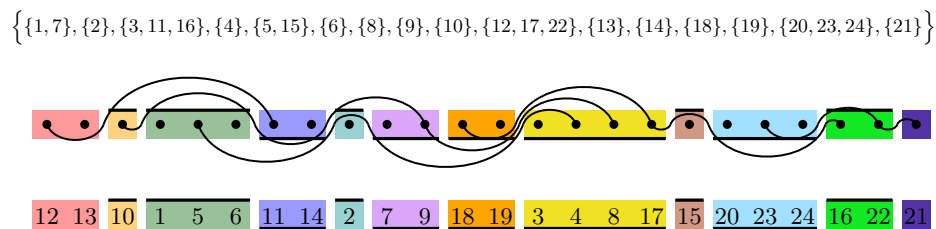


Figure 83. A ε -noncrossing α -partition together with its diagram and an (α, ε) -sortable permutation.

Analogously to the noncrossing α -partitions from Section 4.1.6, we conjecture that the set of cover inversions of the (α, ε) -sortable permutations can be modeled as certain α -partitions that can be drawn in a noncrossing fashion.

Let $P \in \Pi_\alpha$. Once again, we draw n nodes labeled by $1, 2, \dots, n$ on a horizontal line. If (a, b) is a bump of P , then we draw a curve that leaves the node labeled a to the bottom, stays below the α -region containing a , proceeds *above* every subsequent overbarred α -region and *below* every subsequent underbarred α -region until it enters the node labeled b from above. If such a drawing is possible such that no two arcs cross, then we call P ε -noncrossing. We denote by $\text{Nonc}(\alpha, \varepsilon)$ the set of all ε -noncrossing α -partitions. Figure 83 illustrates this definition and the following conjecture.

Conjecture 5.1.5. *For every composition α of $n > 0$ and every α -barring ε , there exists a bijection*

$$\Phi: \text{Nonc}(\alpha, \varepsilon) \rightarrow \text{Sort}(\alpha, \varepsilon)$$

that sends bumps to descents.

We conjecture the following complicated but explicit characterization of the ε -noncrossing α -partitions.

Conjecture 5.1.6. *An α -partition $P \in \Pi_\alpha$ is ε -noncrossing if and only if any two bumps $(a, b), (a', b') \in \text{Bump}(P)$ satisfy the following conditions:*

- if $a < a' < b < b'$, then
 - if $\text{reg}_\alpha(a) = \text{reg}_\alpha(a')$, then $\text{reg}_\alpha(b) = \text{reg}_\alpha(b')$ or $\varepsilon(\text{reg}_\alpha(b)) = 1$;
 - if $\text{reg}_\alpha(a) < \text{reg}_\alpha(a')$, then $\text{reg}_\alpha(a') = \text{reg}_\alpha(b)$ or:
 - * if $\text{reg}_\alpha(b) = \text{reg}_\alpha(b')$, then $\varepsilon(\text{reg}_\alpha(a')) = -1$;
 - * if $\text{reg}_\alpha(b) < \text{reg}_\alpha(b')$, then $\varepsilon(\text{reg}_\alpha(a')) \neq \varepsilon(\text{reg}_\alpha(b))$;
- if $a < a' < b' < b$, then
 - if $\text{reg}_\alpha(a) = \text{reg}_\alpha(a')$, then $\text{reg}_\alpha(b) \neq \text{reg}_\alpha(b')$ or $\varepsilon(\text{reg}_\alpha(b')) = -1$;
 - if $\text{reg}_\alpha(a) < \text{reg}_\alpha(a')$, then:
 - * if $\text{reg}_\alpha(b') = \text{reg}_\alpha(b)$, then $\varepsilon(\text{reg}_\alpha(a')) = 1$;
 - * if $\text{reg}_\alpha(b') < \text{reg}_\alpha(b)$, then $\varepsilon(\text{reg}_\alpha(a')) = \varepsilon(\text{reg}_\alpha(b'))$.

We have seen in Example 5.1.2 that the various sets $\text{Sort}(\alpha, \varepsilon)$ do not fully explain the (W^J, c) -aligned elements in type A. However, we may extend ε to a map from $\{2, 3, \dots, r-1\}$ to $\{-1, 0, 1, 2\}$ where 0 indicates no bar and 2 indicates both an overbar and an underbar. If we encode this extension into the diagrams of a ε -noncrossing α -partition by requiring that an

α -arc may never pass an α -region without bars and it may pass an α -region with both bars on either side, then we obtain a parabolic analogue of the permutrees introduced in [142].

5.2. Linear type B

Let us now suggest a combinatorial model for linear type B. The constructions from this section stem from work in progress with W. FANG and J.-C. NOVELLI.

We observe in Figure 11 that the Coxeter graph of B_n is a path with n nodes, where the first edge is labeled by 4. Thus, there are *two* linear orientations, corresponding to the Coxeter elements $\bar{c} = s_0 s_1 \cdots s_{n-1}$ and $\bar{c}' = s_{n-1} s_{n-2} \cdots s_0$.

As we have explained in Example 1.2.3, we may realize the Coxeter group B_n as the group of sign-symmetric permutations of $\pm[n] = \{-n, \dots, -2, -1, 1, 2, \dots, n\}$. There are two types of transpositions in B_n : those that swap two entries i and j (and their negative counterparts¹⁵), i.e., $((i j)) \stackrel{\text{def}}{=} (i j)(-i -j)$ and those that swap the sign of an entry i , i.e., $[[i]] \stackrel{\text{def}}{=} (i -i)$. With this notation, the simple transpositions in B_n are $s_0 = [[1]]$ and $s_i = ((i i+1))$ for $i \in [n-1]$.

Combinatorially, we realize the elements of B_n with their *long one-line notation*, i.e., we represent $w \in B_n$ by the string

$$w_{-n} w_{-n+1} \cdots w_{-1} w_1 \cdots w_{n-1} w_n,$$

where $w_i = w(i)$ for $i \in \pm[n]$. For stylistic reasons, it will be more pleasant if we represent negative values in the long one-line notation by an overbar rather than a minus sign¹⁶. Then, a *type-B inversion* of w is either a pair $(-i, i)$ for $i \in [n]$ such that $w_i < w_{-i}$ or two pairs $(i, j)(-j, -i)$ with $i < j$ such that $w_i > w_j$ (and symmetrically $w_{-j} < w_{-i}$)¹⁷. A *type-B descent* of w is an inversion $(-i, i)$ with $w_i = -1$ or an inversion $(i, j)(-j, -i)$ with $w_i = w_j + 1$.

Since we consider right inversions, we obtain the following characterization.

Lemma 5.2.1. *Let $w \in B_n$ and let $a, b \in [n]$ with $a < b$. Then:*

- $[[a]] \in \text{Inv}(w)$ if and only if $w_a < 0$;
- $((a b)) \in \text{Inv}(w)$ if and only if $w_a > w_b$;
- $((-b a)) \in \text{Inv}(w)$ if and only if $w_{-a} > w_b$.

Moreover,

- $[[a]] \in \text{Cov}(w)$ if and only if $w_a = -1$;
- $((a b)) \in \text{Cov}(w)$ if and only if $w_a = w_b + 1$;
- $((-b a)) \in \text{Cov}(w)$ if and only if $w_{-a} = w_b + 1$.

Example 5.2.2. *Let $n = 9$, and consider $w = s_0 s_1 s_2 s_7 s_5 s_3 s_2 s_0$. Then,*

$$w = -9, -7, -8, -5, -6, 1, -3, -4, 2, -2, 4, 3, -1, 6, 5, 8, 7, 9.$$

Then,

$$\text{Inv}(w) = \{[[1]], [[4]], ((2 3)), ((2 4)), ((3 4)), ((5 6)), ((7 8)), ((-4 1))\},$$

and

$$\text{Cov}(w) = \{[[4]], ((2 3)), ((5 6)), ((7 8))\}.$$

¹⁵Note that this notation does not imply that i and j have the same sign.

¹⁶This is not to be confused with the barring from the previous section.

¹⁷Once again, this does not imply that i and j have the same sign.

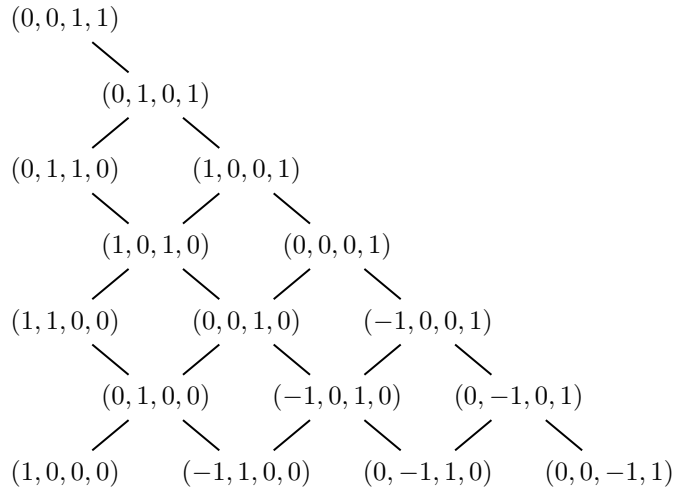


Figure 84. The root poset of type B_4 realized by vectors in \mathbb{R}^4 .

Let us briefly comment on the geometric representation of B_n . Let $V = \mathbb{R}^n$ and let e_i denote the i^{th} unit vector. The roots of B_n are

$$\Phi_{B_n} = \{ \pm e_i \mid i \in [n] \} \uplus \{ \pm(e_i \pm e_j) \mid 1 \leq i < j \leq n \}.$$

We consider the following choice of positive roots

$$\Phi_{B_n}^+ = \{ e_i \mid i \in [n] \} \uplus \{ -e_i + e_j \mid 1 \leq i < j \leq n \} \uplus \{ e_i + e_j \mid 1 \leq i < j \leq n \}$$

and we identify a root e_i with the transposition $[[i]]$, a root $-e_i + e_j$ with the transposition $((i j))$ and a root $e_i + e_j$ with the transposition $((-i j))$. Figure 84 shows the root poset $(\Phi_{B_4}^+, \preceq)$; see also Figure 14a.

We now recall a combinatorial description of the \vec{c} -aligned elements of B_n , where $\vec{c} = s_0 s_1 \cdots s_{n-1}$. The \vec{c} -sorting word of w_o has length n^n and is

$$w_o(\vec{c}) = s_{n-1} \cdots s_1 s_0 s_{n-1} \cdots s_1 s_0 \cdots s_{n-1} \cdots s_1 s_0 = (s_{n-1} \cdots s_1 s_0)^n.$$

The corresponding inversion order can be described as follows. Given $a \in [n]$, we consider the ordered list of pairs

$$(a, -a), (a, -a-1), \dots, (a, -n), (a, 1), (a, 2), \dots, (a, a-1).$$

The n possible rows are arranged in an $n \times n$ array (increasingly with respect to first components). If we now read from top to bottom, left to right, then we obtain the inversion order $\mathbf{Inv}(w_o(\vec{c}))$ by identifying a pair $(a, -a)$ with the transposition $[[a]]$, a pair (a, b) for $a > b > 0$ with the transposition $((b a))$ and a pair $(a, -b)$ for $a < b$ with the transposition $((-b a))$.

Example 5.2.3. Let $n = 4$. Then $\vec{c} = s_0 s_1 s_2 s_3$ and

$$w_o(\vec{c}) = s_3 s_2 s_1 s_0 s_3 s_2 s_1 s_0 s_3 s_2 s_1 s_0 s_3 s_2 s_1 s_0.$$

The previously mentioned array is

$$\begin{array}{cccc} (1, -1) & (1, -2) & (1, -3) & (1, -4) \\ (2, -2) & (2, -3) & (2, -4) & (2, 1) \\ (3, -3) & (3, -4) & (3, 1) & (3, 2) \\ (4, -4) & (4, 1) & (4, 2) & (4, 3) \end{array}$$

The inversion order $\text{Inv}(w_{\vec{c}})$ is

$$\begin{array}{ccccccc} \llbracket 1 \rrbracket & \prec_{\vec{c}} & ((-2 \ 1)) & \prec_{\vec{c}} & ((-3 \ 1)) & \prec_{\vec{c}} & ((-4 \ 1)) \\ & \prec_{\vec{c}} & \llbracket 2 \rrbracket & \prec_{\vec{c}} & ((-3 \ 2)) & \prec_{\vec{c}} & ((-4 \ 2)) & \prec_{\vec{c}} & ((1 \ 2)) \\ & & \prec_{\vec{c}} & \llbracket 3 \rrbracket & \prec_{\vec{c}} & ((-4 \ 3)) & \prec_{\vec{c}} & ((1 \ 3)) & \prec_{\vec{c}} & ((2 \ 3)) \\ & & & \prec_{\vec{c}} & \llbracket 4 \rrbracket & \prec_{\vec{c}} & ((1 \ 4)) & \prec_{\vec{c}} & ((2 \ 4)) & \prec_{\vec{c}} & ((3 \ 4)). \end{array}$$

We may thus characterize the \vec{c} -aligned elements of B_n via their inversion sets.

Lemma 5.2.4. *Let $w \in B_n$. Then, $w \in \text{Align}(B_n, \vec{c})$ if and only if for every $1 \leq a < b \leq n$ it holds that*

- if $\llbracket a \rrbracket \in \text{Cov}(w)$, then $\llbracket c \rrbracket \in \text{Inv}(w)$ for all $1 \leq c < a$;
- if $((a \ b)) \in \text{Cov}(w)$, then $((a \ c)) \in \text{Inv}(w)$ for all $a < c < b$;
- if $((-b \ a)) \in \text{Cov}(w)$, then
 - $\llbracket a \rrbracket \in \text{Inv}(w)$,
 - $((-c \ a)) \in \text{Inv}(w)$ for all $1 \leq c < b$, $c \neq a$,
 - $((-b \ c)) \in \text{Inv}(w)$ for all $1 \leq c < a$.

PROOF. This follows from Definition 2.2.6 and the representation of the roots of B_n as vectors in \mathbb{R}^n . \square

We wish to realize the \vec{c} -aligned elements of B_n combinatorially in terms of pattern avoidance. A signed permutation $w \in B_n$ has a *type-B 231-pattern* if there exist indices $-n \leq i < j < k \leq n$ such that either $w_i = w_k + 1$ or $w_i = 1, w_k = -1$, as well as $w_j > w_i$ and $j, k > 0$. In other words, we look for ordinary 231-patterns in the long one-line notation of w with the requirement that the positions of the '2' and the '1' are positive. We write $B_n(231)$ for the set of sign-symmetric permutations without type-B 231-patterns.

Example 5.2.5. *Let $n = 5$ and consider the signed permutation*

$$u = \bar{4} \ \bar{3} \ \bar{5} \ 1 \ 2 \ \bar{2} \ \bar{1} \ 5 \ 3 \ 4.$$

The inversions of u are

$$(3, 4)(-4, -3), \quad (3, 5)(-5, -3), \quad (-2, 1)(-1, 2), \quad (-1, 1), \quad (-2, 2).$$

and the descents are $(-2, 2)$ and $(3, 5)(-5, -3)$.

In the Coxeter presentation, u admits the S -reduced factorization $s_0 s_4 s_3 s_1 s_0$. Thus,

$$\text{Inv}(u) = \left\{ \llbracket 1 \rrbracket, \llbracket 2 \rrbracket, ((-2 \ 1)), ((3 \ 4)), ((3 \ 5)) \right\} \quad \text{and} \quad \text{Cov}(u) = \left\{ \llbracket 2 \rrbracket, ((3 \ 5)) \right\}.$$

Comparing this with Lemma 5.2.4, we note that u is \vec{c} -aligned.

On the other hand, consider the signed permutation

$$v = 2 \bar{3} 5 \bar{1} \bar{4} \mathbf{4} 1 \bar{5} 3 \bar{2}.$$

The inversions of v are

$$\begin{aligned} (1, 2)(-2, -1), & \quad (1, 3)(-3, -1), \quad (1, 4)(-4, -1), \quad (1, 5)(-5, -1), \quad (2, 3)(-3, -2), \\ (2, 5)(-5, -2), & \quad (4, 5)(-5, -4), \quad (-1, 3)(-3, 1), \quad (-2, 3)(-3, 2), \quad (-4, 3)(-3, 4), \\ (-2, 5)(-5, 2), & \quad (-3, 5)(-5, 3), \quad (-5, 5), \quad (-3, 3), \end{aligned}$$

and the descents are

$$(1, 4)(-4, -1), \quad (-1, 3)(-3, 1), \quad (-2, 5)(-5, 2).$$

In the Coxeter presentation, v admits the S -reduced factorization

$$s_1 s_0 s_1 s_4 s_3 s_2 s_1 s_0 s_3 s_1 s_4 s_3 s_2 s_1.$$

Thus,

$$\begin{aligned} \text{Inv}(v) &= \left\{ ((1 \ 2)), ((1 \ 3)), ((1 \ 4)), ((1 \ 5)), ((2 \ 3)), ((2 \ 5)), ((4 \ 5)), ((-3 \ 1)), ((-3 \ 2)), \right. \\ &\quad \left. ((-3 \ 4)), ((-3 \ 5)), ((-5 \ 2)), \llbracket 3 \rrbracket, \llbracket 5 \rrbracket \right\}, \\ \text{Cov}(v) &= \left\{ ((1 \ 4)), ((-3 \ 1)), ((-5 \ 2)) \right\}. \end{aligned}$$

Comparing this with Lemma 5.2.4, we observe that v is not \bar{c} -aligned, because for instance $((-3 \ 1)) \in \text{Cov}(v)$ but $\llbracket 1 \rrbracket \notin \text{Inv}(v)$. This manifests in the type-B 231-pattern in positions $(-1, 1, 3)$ highlighted above in boldface.

Lemma 5.2.6 ([148, Lemma 4.9]). *A signed permutation $w \in B_n$ is \bar{c} -aligned if and only if w does not have a type-B 231-pattern.*

PROOF. This is immediate from Lemmas 5.2.1 and 5.2.4. □

Analogously to type A, the subsets $J \subseteq \{s_1, s_2, \dots, s_{n-1}\}$ correspond bijectively to compositions of n (where the components are determined by the complement of J). Thus, the subsets $J \subseteq \{s_0, s_1, \dots, s_{n-1}\}$ correspond to *signed* compositions of n , which are compositions of n with a possible 0-component in the first position. This 0-component, denoted by α_0 , is present if and only if $s_0 \in J$.

Suppose that α has r non-0-components. If we define $p_i \stackrel{\text{def}}{=} \alpha_1 + \alpha_2 + \dots + \alpha_i$ for $i \in [r]$, then we can partition $\pm[n]$ symmetrically according to α :

$$\begin{cases} \left\{ \pm\{1, \dots, p_1\}, \pm\{p_1+1, \dots, p_2\}, \dots, \pm\{p_{r-1}+1, \dots, p_r\} \right\}, & \text{if } 0 \notin \alpha, \\ \left\{ \{-p_1, \dots, -1, 1, \dots, p_1\}, \pm\{p_1+1, \dots, p_2\}, \dots, \pm\{p_{r-1}+1, \dots, p_r\} \right\}, & \text{if } 0 \in \alpha. \end{cases}$$

Thus, we partition $\pm[n]$ into $2r$ parts if $0 \notin \alpha$ and into $2r - 1$ parts if $0 \in \alpha$. In both cases, however, we use r colors.

The parts of this partition are *type-B α -regions*, and an α -region is *positive* if it contains only positive entries. The *zero-region*, if present, is the unique α -region containing both positive and negative entries. The positive α -region containing p_i is the i^{th} α -region.

The parabolic quotient of B_n determined by α consists of all sign-symmetric permutations $w \in B_n$, where the entries in each α -region are in increasing order. We denote this set by B_α .

Example 5.2.7. For $n = 3$ we have $S = \{s_0, s_1, s_2\}$. We consider $J^{(1)} = \{s_0, s_2\} = S \setminus \{s_1\}$ and $J^{(2)} = \{s_1\} = S \setminus \{s_0, s_2\}$. The corresponding compositions are $\alpha^{(1)} = (0, 1, 2)$ and $\alpha^{(2)} = (2, 1)$. The set $B_{\alpha^{(1)}}$ consists of the following twelve elements:

$\bar{3} \bar{2} \bar{1} 1 2 3, \bar{3} \bar{1} \bar{2} 2 1 3, \bar{3} 1 \bar{2} 2 \bar{1} 3, \bar{2} \bar{1} \bar{3} 3 1 2,$
 $\bar{3} 2 \bar{1} 1 \bar{2} 3, \bar{2} 1 \bar{3} 3 \bar{1} 2, \bar{1} 2 \bar{3} 3 \bar{2} 1, \bar{2} 3 \bar{1} 1 \bar{3} 2,$
 $1 2 \bar{3} 3 \bar{2} \bar{1}, \bar{1} 3 \bar{2} 2 \bar{3} 1, 1 3 \bar{2} 2 \bar{3} \bar{1}, 2 3 \bar{1} 1 \bar{3} \bar{2}.$

The set $B_{\alpha^{(2)}}$ consists of the following 24 elements:

$\bar{3} \bar{2} \bar{1} 1 2 3, \bar{3} \bar{2} 1 \bar{1} 2 3, \bar{2} \bar{3} \bar{1} 1 3 2, \bar{2} \bar{3} 1 \bar{1} 3 2,$
 $\bar{3} \bar{1} 2 \bar{2} 1 3, \bar{1} \bar{3} 2 2 3 1, \bar{3} 1 2 \bar{2} \bar{1} 3, 1 \bar{3} \bar{2} 2 3 \bar{1},$
 $\bar{1} \bar{3} 2 \bar{2} 3 1, \bar{2} \bar{1} 3 \bar{3} 1 2, 1 \bar{3} 2 \bar{2} 3 \bar{1}, \bar{2} 1 3 \bar{3} \bar{1} 2,$
 $2 \bar{3} \bar{1} 1 3 \bar{2}, \bar{1} \bar{2} 3 \bar{3} 2 1, 2 \bar{3} 1 \bar{1} 3 \bar{2}, 1 \bar{2} 3 \bar{3} 2 \bar{1},$
 $\bar{1} 2 3 \bar{3} \bar{2} 1, 3 \bar{2} \bar{1} 1 2 \bar{3}, 2 \bar{1} 3 \bar{3} 1 \bar{2}, 3 \bar{2} 1 \bar{1} 2 \bar{3},$
 $1 2 3 \bar{3} \bar{2} \bar{1}, 3 \bar{1} 2 \bar{2} 1 \bar{3}, 2 1 3 \bar{3} \bar{1} \bar{2}, 3 1 2 \bar{2} \bar{1} \bar{3}.$

Definition 5.2.8. Let $n > 0$ and let α be a signed composition of n . Let $w \in B_\alpha$. Then, w has a **type-B $(\alpha, 231)$ -pattern** if and only if there exist indices $i < j < k$ such that:

- $0 \notin \alpha$ and
 - $0 < i < j < k$ with i, j, k in different α -regions, $w_i < w_j$ and $w_i = w_k + 1$, or
 - $0 < i < j$ with i, j in different α -regions, $w_j = -1$ and $w_i > 0$, or
 - $i < 0 < j < k$ with j, k in different α -regions, $w_i < w_j$ and $w_i = w_k + 1$;
- $0 \in \alpha$ and
 - $0 < i < j < k$ with i, j, k in different α -regions, $w_i < w_j$ and $w_i = w_k + 1$, or
 - $i < 0 < j < k$ with j, k in different α -regions, $w_i = 1, w_k = -1$, and
 - * $w_j > 0$ if $j > p_1$,
 - * $w_j < 0$ if $j \leq p_1$, or
 - $i < 0 < j < k$ with j, k in different α -regions, $w_i = w_k + 1$, and
 - * $w_j > w_i$ if $j > p_1$,
 - * $w_j < w_i$ if $j \leq p_1$.

We write $B_{\alpha(231)}$ for the subset of B_α consisting of those permutations without type-B $(\alpha, 231)$ -patterns.

Example 5.2.9. Let $n = 3$ and $J^{(1)} = \{s_0, s_2\}$. Then, $\alpha^{(1)} = (0, 1, 2)$. The longest element of $B_{\alpha^{(1)}}$ is $w_{\alpha^{(1)}} = \bar{2} \bar{3} \bar{1} 1 \bar{3} \bar{2}$, and has \bar{c} -sorting word $w_{\alpha^{(1)}}(\bar{c}) = s_1 s_0 s_2 s_1 s_0 s_2 s_1$. The corresponding inversion order is

$\underbrace{((1 \ 2))}_{t_1} \prec_{\bar{c}} \underbrace{((1 \ 3))}_{t_2} \prec_{\bar{c}} \underbrace{[[2]]}_{t_3} \prec_{\bar{c}} \underbrace{((-3 \ 2))}_{t_4} \prec_{\bar{c}} \underbrace{((-2 \ 1))}_{t_5} \prec_{\bar{c}} \underbrace{[[3]]}_{t_6} \prec_{\bar{c}} \underbrace{((-3 \ 1))}_{t_7}.$

The “forcing” of inversions that determines the membership in $\text{Align}(B_{\alpha^{(1)}}, \bar{c})$ described in Lemma 5.2.4 amounts to the following implications for any $w \in B_{\alpha^{(1)}}$:

$$\begin{aligned} t_2 \in \text{Cov}(w) &\implies t_1 \in \text{Inv}(w), & t_3 \in \text{Cov}(w) &\implies t_1 \in \text{Inv}(w), \\ t_4 \in \text{Cov}(w) &\implies \{t_1, t_2, t_3\} \subseteq \text{Inv}(w), & t_5 \in \text{Cov}(w) &\implies \{t_1, t_3\} \subseteq \text{Inv}(w), \\ t_5 \in \text{Cov}(w) &\implies \{t_2, t_3\} \subseteq \text{Inv}(w), & t_7 \in \text{Cov}(w) &\implies \{t_2, t_5, t_6\} \subseteq \text{Inv}(w). \end{aligned}$$

The next table lists the twelve elements of $B_{\alpha^{(1)}}$ together with their inversion and descent sets and their membership in $\text{Align}(B_{\alpha^{(1)}}, \bar{c})$. If possible, we have highlighted a type-B $(\alpha^{(1)}, 231)$ -pattern.

$w \in B_{\alpha^{(1)}}$	$\text{Inv}(w)$	$\text{Cov}(w)$	$w \in B_{\alpha^{(1)}}(231)$
$\bar{3} \bar{2} \bar{1} 1 2 3$	\emptyset	\emptyset	yes
$\bar{3} \bar{1} \bar{2} 2 1 3$	$\{t_1\}$	$\{t_1\}$	yes
$\bar{3} 1 \bar{2} 2 \bar{1} 3$	$\{t_1, t_3\}$	$\{t_3\}$	yes
$\bar{2} \bar{1} \bar{3} 3 1 2$	$\{t_1, t_2\}$	$\{t_2\}$	yes
$\bar{3} 2 \bar{1} 1 \bar{2} 3$	$\{t_1, t_3, t_5\}$	$\{t_5\}$	yes
$\bar{2} 1 \bar{3} 3 \bar{1} 2$	$\{t_1, t_2, t_3\}$	$\{t_2, t_3\}$	yes
$\bar{1} 2 \bar{3} 3 \bar{2} 1$	$\{t_1, t_2, t_3, t_4\}$	$\{t_4\}$	yes
$\bar{2} 3 \bar{1} 1 \bar{3} 2$	$\{t_1, t_3, t_4, t_5\}$	$\{t_4\}$	no
$1 2 \bar{3} 3 \bar{2} \bar{1}$	$\{t_1, t_2, t_3, t_4, t_6\}$	$\{t_6\}$	yes
$\bar{1} 3 \bar{2} 2 \bar{3} 1$	$\{t_1, t_2, t_3, t_4, t_5\}$	$\{t_2, t_5\}$	yes
$1 3 \bar{2} 2 \bar{3} \bar{1}$	$\{t_1, t_2, t_3, t_4, t_5, t_6\}$	$\{t_5, t_6\}$	yes
$2 3 \bar{1} 1 \bar{3} \bar{2}$	$\{t_1, t_2, t_3, t_4, t_5, t_6, t_7\}$	$\{t_7\}$	yes

Figure 85 shows the lattice $\text{Weak}(B_{\alpha^{(1)}}(231))$. Compare this lattice with the flip lattice from Figure 24a. Note that the subword complex considered in Example 2.4.2 is the parabolic cluster complex of B_3 with respect to $J^{(1)}$.

Example 5.2.10. Let $n = 3$ and $J^{(2)} = \{s_1\}$. Then, $\alpha^{(2)} = (2, 1)$. The longest element of $B_{\alpha^{(2)}}$ is $w_{o; \alpha^{(2)}} = \bar{3} 1 2 \bar{2} \bar{1} \bar{3}$, and has \bar{c} -sorting word $w_{o; \alpha^{(2)}}(\bar{c}) = s_2 s_1 s_0 s_1 s_0 s_2 s_1 s_0$. The corresponding inversion order is

$$\underbrace{[1]}_{t_1} \prec_{\bar{c}} \underbrace{[(-2 1)]}_{t_2} \prec_{\bar{c}} \underbrace{[(-3 1)]}_{t_3} \prec_{\bar{c}} \underbrace{[2]}_{t_4} \prec_{\bar{c}} \underbrace{[(-3 2)]}_{t_5} \prec_{\bar{c}} \underbrace{[3]}_{t_6} \prec_{\bar{c}} \underbrace{[(2 3)]}_{t_7} \prec_{\bar{c}} \underbrace{[(1 3)]}_{t_8}.$$

The “forcing” of inversions that determines the membership in $\text{Align}(B_{\alpha^{(2)}}, \bar{c})$ described in Lemma 5.2.4 amounts to the following implications for any $w \in B_{\alpha^{(2)}}$:

$$\begin{aligned} t_2 \in \text{Cov}(w) &\implies t_1 \in \text{Inv}(w), & t_3 \in \text{Cov}(w) &\implies \{t_1, t_2\} \subseteq \text{Inv}(w), \\ t_4 \in \text{Cov}(w) &\implies t_1 \in \text{Inv}(w), & t_5 \in \text{Cov}(w) &\implies \{t_2, t_3, t_4\} \subseteq \text{Inv}(w), \\ t_6 \in \text{Cov}(w) &\implies \{t_1, t_4\} \subseteq \text{Inv}(w), & t_8 \in \text{Cov}(w) &\implies t_7 \in \text{Inv}(w). \end{aligned}$$

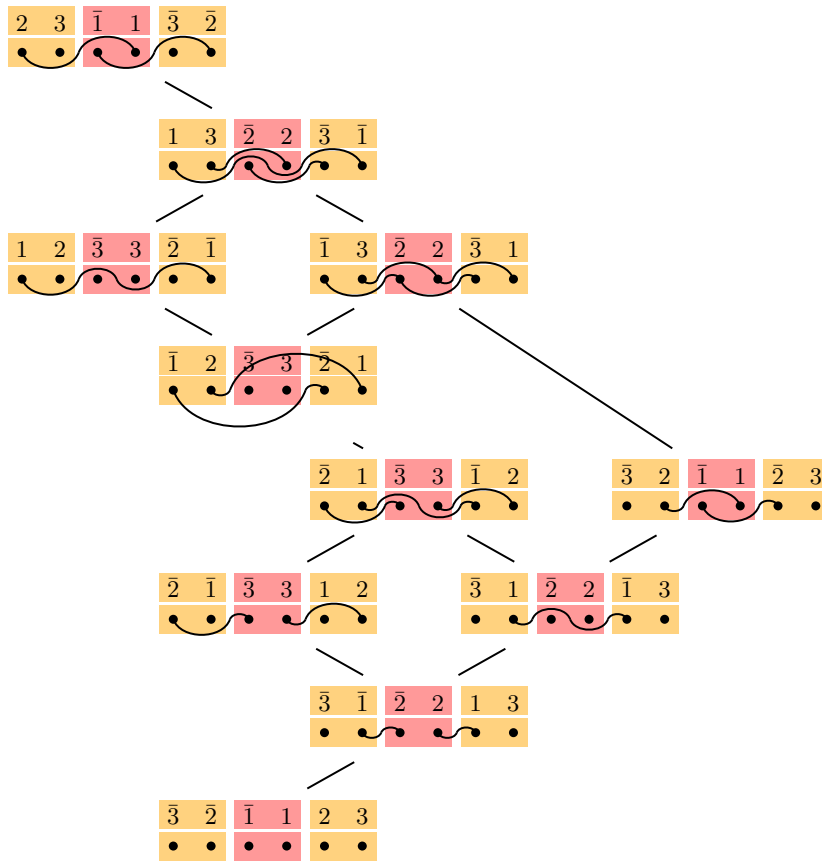


Figure 85. The lattice $\mathbf{Weak}(B_{\alpha(1)}(231))$.

The next table lists the 24 elements of $B_{\alpha(2)}$ together with their inversion and descent sets and their membership in $\mathbf{Align}(B_{\alpha(2)}, \bar{c})$. If possible, we have highlighted a type-B $(\alpha^{(2)}, 231)$ -pattern.

$w \in B_{\alpha(2)}$	$\text{Inv}(w)$	$\text{Cov}(w)$	$w \in B_{\alpha(2)}(231)$
$\bar{3} \bar{2} \bar{1} \ 1 \ 2 \ 3$	\emptyset	\emptyset	yes
$\bar{3} \bar{2} \ 1 \ \bar{1} \ 2 \ 3$	$\{t_1\}$	$\{t_1\}$	yes
$\bar{2} \ \bar{3} \ \bar{1} \ 1 \ 3 \ 2$	$\{t_7\}$	$\{t_7\}$	yes
$\bar{2} \ \bar{3} \ 1 \ \bar{1} \ 3 \ 2$	$\{t_1, t_7\}$	$\{t_1, t_7\}$	yes
$\bar{3} \ \bar{1} \ 2 \ \bar{2} \ 1 \ 3$	$\{t_1, t_2\}$	$\{t_2\}$	yes
$\bar{1} \ \bar{3} \ \bar{2} \ 2 \ 3 \ 1$	$\{t_7, t_8\}$	$\{t_8\}$	yes
$\bar{3} \ 1 \ 2 \ \bar{2} \ \bar{1} \ 3$	$\{t_1, t_2, t_4\}$	$\{t_4\}$	yes
$1 \ \bar{3} \ \bar{2} \ 2 \ \mathbf{3} \ \bar{1}$	$\{t_6, t_7, t_8\}$	$\{t_6\}$	no
$\bar{1} \ \bar{3} \ \mathbf{2} \ \bar{2} \ \mathbf{3} \ 1$	$\{t_1, t_3, t_7\}$	$\{t_3\}$	no
$\bar{2} \ \bar{1} \ 3 \ \bar{3} \ 1 \ 2$	$\{t_1, t_2, t_3\}$	$\{t_3\}$	yes

1	3	2	2	3	1	$\{t_1, t_3, t_6, t_7\}$	$\{t_6\}$	no
2	1	3	3	1	2	$\{t_1, t_2, t_3, t_4\}$	$\{t_3, t_4\}$	yes
2	3	1	1	3	2	$\{t_3, t_6, t_7, t_8\}$	$\{t_3\}$	no
1	2	3	3	2	1	$\{t_1, t_2, t_3, t_7\}$	$\{t_2, t_9\}$	yes
2	3	1	1	3	2	$\{t_1, t_3, t_6, t_7, t_8\}$	$\{t_1, t_8\}$	yes
1	2	3	3	2	1	$\{t_1, t_2, t_3, t_6, t_8\}$	$\{t_2, t_6\}$	no
1	2	3	3	2	1	$\{t_1, t_2, t_3, t_4, t_5\}$	$\{t_5\}$	yes
3	2	1	1	2	3	$\{t_3, t_5, t_6, t_7, t_8\}$	$\{t_5\}$	no
2	1	3	3	1	2	$\{t_1, t_2, t_3, t_5, t_6, t_7\}$	$\{t_5\}$	no
3	2	1	1	2	3	$\{t_1, t_3, t_5, t_6, t_7\}$	$\{t_1, t_5\}$	no
1	2	3	3	2	1	$\{t_1, t_2, t_3, t_4, t_5, t_6\}$	$\{t_6\}$	yes
3	1	2	2	1	3	$\{t_1, t_2, t_3, t_5, t_6, t_7, t_8\}$	$\{t_2, t_8\}$	yes
2	1	3	3	1	2	$\{t_1, t_2, t_3, t_4, t_5, t_6, t_7\}$	$\{t_4, t_7\}$	yes
3	1	2	2	1	3	$\{t_1, t_2, t_3, t_4, t_5, t_6, t_7, t_8\}$	$\{t_4, t_8\}$	yes

Figure 86 shows the lattice $\mathbf{Weak}(B_{\alpha^{(2)}}(231))$.

These examples and further computer experiments suggest that Conjecture 3.2.6 is true in linear type B.

Conjecture 5.2.11. *For every signed composition α of $n > 0$, the poset $\mathbf{Weak}(B_{\alpha}(231))$ is a trim, congruence-uniform lattice. Moreover, it is a quotient lattice of $\mathbf{Weak}(B_{\alpha})$.*

We expect that the proof of Conjecture 5.2.11 is essentially analogous to its type-A counterpart.

While we do not have an explicit description of analogues of parabolic noncrossing partitions in linear type B, we may define such objects via Definition 3.3.1. More precisely, for $w \in B_{\alpha}(231)$ we define P_w to be the set of connected components of the graph on $\pm[n]$ where i and j are connected if (i, j) or (j, i) is a descent of w . In Figures 85 and 86 we have suggested a way to draw these partitions in a noncrossing fashion. In ordinary type B, noncrossing arc diagrams modeling descents have been suggested for instance in [13, Section 3.2] and [135, Part II.2]. Type-B noncrossing partitions were introduced in [157].

Let $\mathbf{Nonc}^B(\alpha)$ denote the set of partitions obtained in such a way and let $\mathbf{Nonc}^B(\alpha) \stackrel{\text{def}}{=} (\mathbf{Nonc}^B(\alpha), \leq_{\text{ref}})$. With this notation, we observe that the poset in Figure 87 is isomorphic to the refinement order on the involved partitions, while this is not the case for the poset in Figure 88. Computer experiments suggest the following answer to Research Challenge 3.3.4 in linear type B.

Conjecture 5.2.12. *Let α be a signed composition of $n > 0$. Then, $\mathbf{CLO}(\mathbf{Weak}(B_{\alpha}(231))) \cong \mathbf{Nonc}^B(\alpha)$ if and only if either $\alpha = (n)$, $\alpha = (0, n-1, 1)$, or $\alpha = (p, 1, 1, \dots, 1, q)$ for $p \in \{0, 1\}$, $q \geq 1$.*

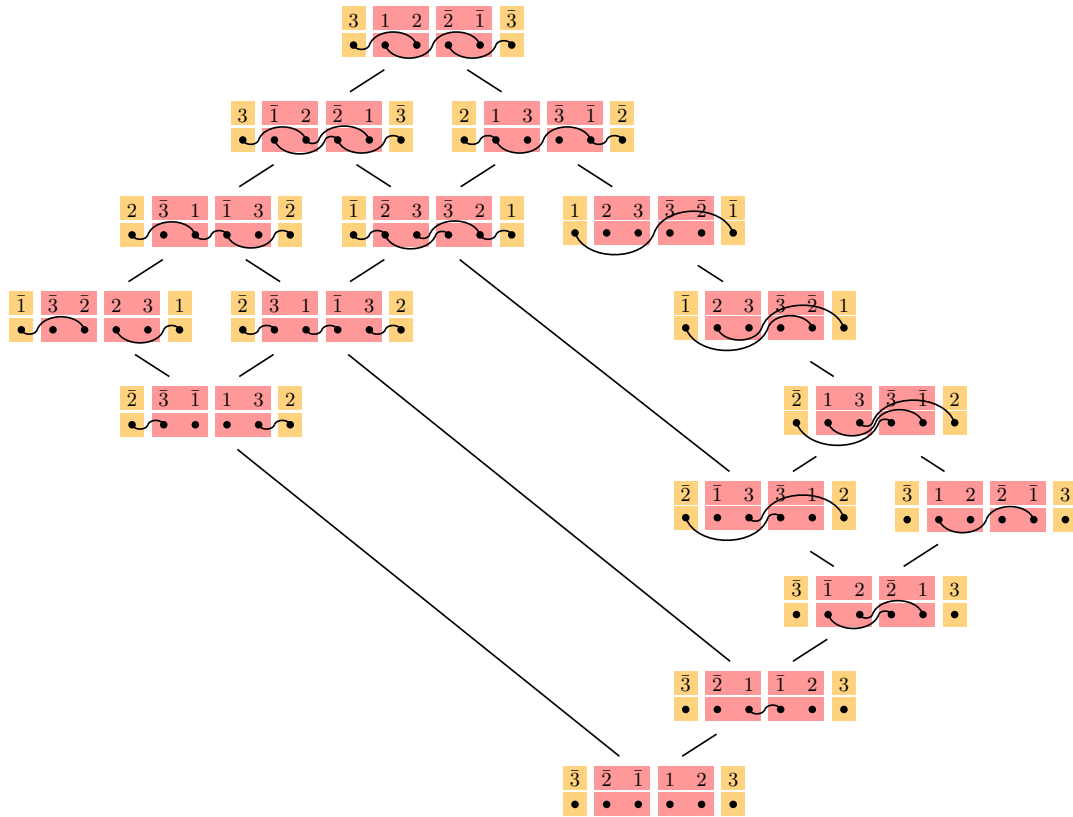


Figure 86. The lattice $\mathbf{Weak}(B_{\alpha(2)}(231))$.

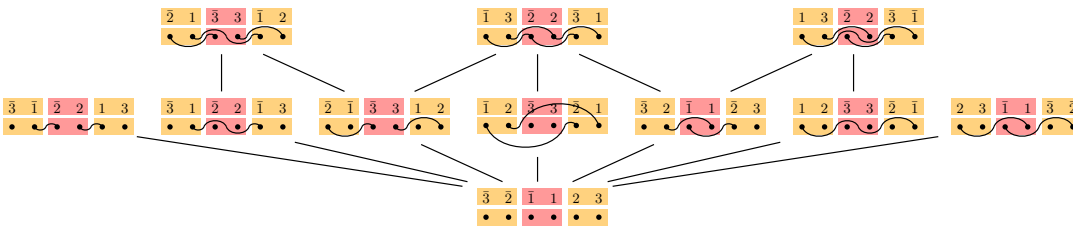


Figure 87. The core label order of $\mathbf{Weak}(B_{\alpha(1)}(231))$. This is also the refinement order on the displayed partitions.

Similarly to type A, we may realize nonnesting partitions in type B as certain lattice paths. By reflecting the root poset of B_n on a vertical axis and rotating by 45 degrees counterclockwise, each order ideal in $(\Phi_{B_n}^+, \preceq)$ determines a northeast path using a total of $2n$ steps, staying weakly above the diagonal $x = y$ and ending on the diagonal $y = 2n - x$; see Figure 89.

Let $\text{Dyck}^B(n)$ denote the set of such northeast paths. We observe that we may complete any such path by adding its mirror image by reflection across $y = 2n - x$. This in fact produces a *centrally symmetric* Dyck path of semilength $2n$.

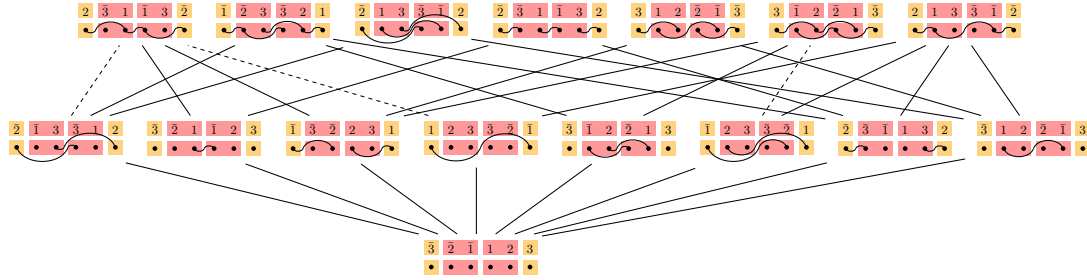


Figure 88. The core label order of $\text{Weak}(B_{\alpha(2)}(231))$. The dashed edges indicate missing refinement relations.

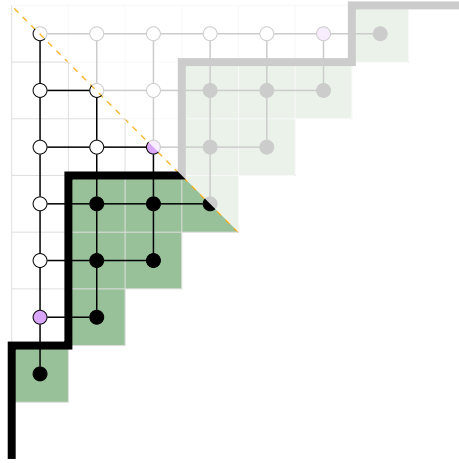


Figure 89. Interpreting order ideals in the type-B root posets as centrally symmetric Dyck paths.

Analogously to type A, parabolic root posets can be obtained using a suitable bounce path. Let α be a signed composition of n whose non-0 components are $\alpha_1, \alpha_2, \dots, \alpha_r$ from left to right. The *type-B α -bounce path* is

$$v_\alpha^B \stackrel{\text{def}}{=} \begin{cases} N^{\alpha_r} E^{\alpha_r} \dots N^{\alpha_2} E^{\alpha_2} N^{\alpha_1} E^{\alpha_1}, & \text{if } 0 \notin \alpha, \\ N^{\alpha_r} E^{\alpha_r} \dots N^{\alpha_2} E^{\alpha_2} N^{2\alpha_1}, & \text{if } 0 \in \alpha. \end{cases}$$

Now, let $\text{Dyck}^B(\alpha)$ denote the set of all lattice paths in $\text{Dyck}^B(n)$ staying weakly above v_α^B . Figures 90 and 91 display the sets $\text{Dyck}^B((0, 1, 2))$ and $\text{Dyck}^B((2, 1))$.

Let $p \in \text{Dyck}^B(\alpha)$. A *type-B valley* is either a coordinate on p which is preceded by an east step and followed by a north step, or the coordinate at which p ends if it is preceded by an east step. A *type-B return* is a type-B valley of p which is also a type-B valley of v_α^B . In Figures 90 and 91 we have marked the type-B valleys in red and the type-B returns are circled in blue. With this notation, we may define the *type-B H-triangle* by:

$$(5.1) \quad \mathcal{H}_\alpha^B(x, y) \stackrel{\text{def}}{=} \sum_{p \in \text{Dyck}^B(\alpha)} x^{\text{valley}(p)} y^{\text{return}(p)}.$$

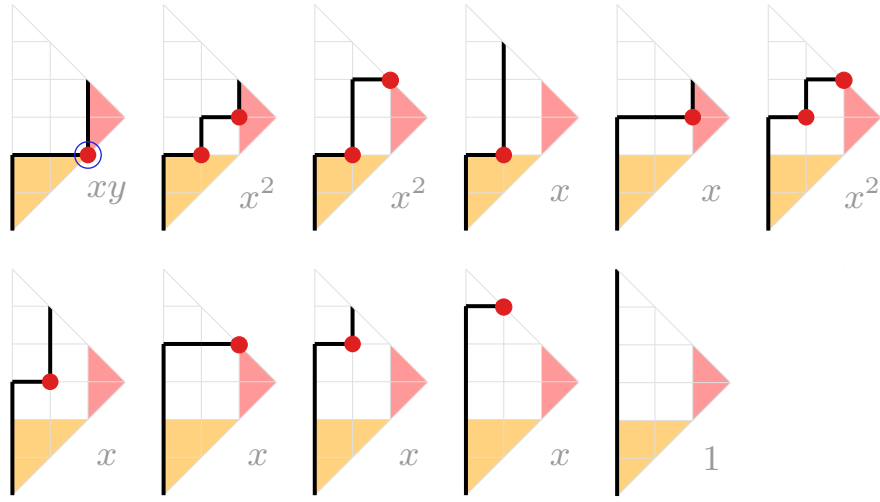


Figure 90. The parabolic type-B Dyck paths for $\alpha = (0, 1, 2)$.

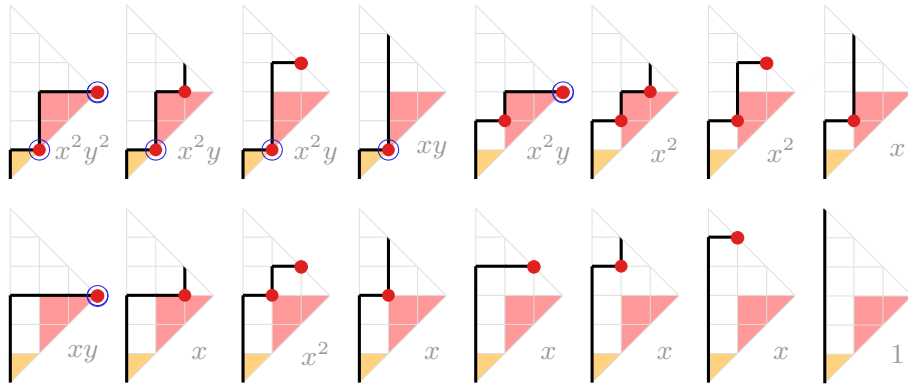


Figure 91. The parabolic type-B Dyck paths for $\alpha = (2, 1)$.

As in linear type A, we define the *type-B M-triangle* using the core label order:

$$(5.2) \quad \tilde{\mathcal{M}}_{\alpha}^B(x, y) \stackrel{\text{def}}{=} \sum_{u, v \in \mathcal{B}_{\alpha}(231)} \mu_{\text{CLO}(\text{Weak}(\mathcal{B}_{\alpha}(231)), \lambda_{\text{jsd}})}(u, v) x^{|\text{Can}(u)|} y^{|\text{Can}(v)|}.$$

We consider once again the degree parameter

$$d = \max\{\text{valley}(p) \mid p \in \text{Dyck}^B(\alpha)\},$$

and conjecture the following answer to Research Challenge 3.6.5 in linear type B.

Conjecture 5.2.13. *Let α be a signed composition of $n > 0$. Then,*

$$\mathcal{H}_{\alpha}^B(x, y) = (x(y-1) + 1)^d \tilde{\mathcal{M}}_{\alpha}^B \left(\frac{y}{y-1}, \frac{x(y-1)}{x(y-1) + 1} \right)$$

if and only if $\alpha = (n)$, $\alpha = (0, n)$, $\alpha = (0, n-1, 1)$, $\alpha = (1, 1, \dots, 1)$, or $\alpha = (1, 1, \dots, 1, 2, 1, 1, \dots, 1)$.

Example 5.2.14. Let $\alpha = (0, 1, 2)$. Using Figure 90, we obtain

$$\mathcal{H}_{(0,1,2)}^{\mathbb{B}}(x, y) = 3x^2 + xy + 6x + 1,$$

and we see that the degree is $d = 2$. From Figure 87 we may compute

$$\tilde{\mathcal{M}}_{(0,1,2)}^{\mathbb{B}}(x, y) = 3x^2y^2 - 7xy^2 + 7xy + 4y^2 - 7y + 1.$$

We have

$$\begin{aligned} (x(y-1)+1)^d \tilde{\mathcal{M}}_{(0,1,2)}^{\mathbb{B}}\left(\frac{y}{y-1}, \frac{x(y-1)}{x(y-1)+1}\right) &= x^2y^2 + 4x^2y - 2x^2 + 2xy + 5x + 1 \\ &\neq \mathcal{H}_{(0,1,2)}^{\mathbb{B}}(x, y). \end{aligned}$$

See also Example 3.6.4.

Example 5.2.15. Let $\alpha = (2, 1)$. Using Figure 91, we obtain

$$\mathcal{H}_{(2,1)}^{\mathbb{B}}(x, y) = x^2y^2 + 3x^2y + 3x^2 + 2xy + 6x + 1,$$

and we see that the degree is $d = 2$. From Figure 88 we may compute

$$\tilde{\mathcal{M}}_{(2,1)}^{\mathbb{B}}(x, y) = 7x^2y^2 - 17xy^2 + 8xy + 10y^2 - 8y + 1.$$

We have

$$\begin{aligned} (x(y-1)+1)^d \tilde{\mathcal{M}}_{(2,1)}^{\mathbb{B}}\left(\frac{y}{y-1}, \frac{x(y-1)}{x(y-1)+1}\right) &= x^2y^2 + 3x^2y + 3x^2 + 2xy + 6x + 1 \\ &= \mathcal{H}_{(2,1)}^{\mathbb{B}}(x, y). \end{aligned}$$

Let end this section with a few enumerative conjectures.

Conjecture 5.2.16. Let $\alpha = (1, 1, \dots, 1, 2)$ be a signed composition of $n > 0$. The zeta polynomial of $\mathbf{CLO}(\mathbf{Weak}(B_{\alpha}(231)))$ is

$$\frac{(2n-1)q - n}{n-1} \binom{nq-2}{n-2}.$$

Consequently,

$$|B_{\alpha}(231)| = \frac{3n-2}{n} \binom{2n-2}{n-1}.$$

By inspection of Table 1, we notice that the cardinality of $B_{\alpha}(231)$, when $\alpha = (1, 1, \dots, 1, 2)$, equals the type-D Catalan number.

Conjecture 5.2.17. Let α be a signed composition of $n > 0$. Then,

$$|B_{\alpha}(231)| = \begin{cases} 2^t \binom{2(n-t)+5}{n-t}, & \text{if } \alpha = (t, 1, 1, \dots, 1), \\ \binom{2n}{n-t}, & \text{if } \alpha = (0, t, 1, 1, \dots, 1). \end{cases}$$

5.3. (α, m) -Tamari lattices

We now present a possible extension of the m -Tamari lattices of [18] towards parabolic quotients. Recall the definition of the ring $H^{(2)}$ of diagonal harmonics in two sets of variables. Without going into too much detail, we may as well consider rings $H^{(r)}$ of diagonal harmonics in r sets of variables [18, 90].

M. HAIMAN conjectured in [90, Section 2.8] that for $r = 3$:

$$\dim_{\mathbb{C}}(H^{(3)}) = 2^n(n+1)^{n-2},$$

$$\dim_{\mathbb{C}}(H^{(3)\epsilon}) = \frac{2}{n(n+1)} \binom{4n+1}{n-1},$$

while the situation for $r \geq 4$ becomes much more complicated.

If we fix $r = 3$, then F. BERGERON and L.-F. PRÉVILLE-RATELLE introduced a *higher* variant of the space of diagonal harmonics. Let

$$C = \mathbb{C}[x_1, x_2, \dots, x_n, y_1, y_2, \dots, y_n, z_1, z_2, \dots, z_n]$$

and let \mathfrak{S}_n act on C by permuting the x -, y - and z -variables simultaneously. Let $C^{\mathfrak{S}_n}$ denote the ring of invariant polynomials of C and let C^ϵ denote the set of alternating polynomials. The ring of *higher trivariate diagonal harmonics* is defined by

$$H^{(3;m)} \stackrel{\text{def}}{=} ((C^\epsilon)^m) \cap ((C^\epsilon)^{m-1} C^{\mathfrak{S}_n})^\perp$$

with respect to a certain scalar product. The following values for the dimensions of these spaces were conjectured in [18]:

$$\dim_{\mathbb{C}}(H^{(3;m)}) = (m+1)^n(mn+1)^{n-2},$$

$$\dim_{\mathbb{C}}(H^{(3;m)\epsilon}) = \frac{m+1}{n(mn+1)} \binom{(m+1)^2n+m}{n-1}.$$

Remark 5.3.1. *In the bivariate case, M. HAIMAN proved in [91] that*

$$\dim_{\mathbb{C}}(H^{(2;m)}) = (mn+1)^{n-1},$$

$$\dim_{\mathbb{C}}(H^{(2;m)\epsilon}) = \frac{1}{mn+1} \binom{(m+1)n}{n}.$$

These formulas are well known: the first one counts for instance m -parking functions of size n and the second one recovers the Fuß-Catalan numbers, counting for instance m -divisible noncrossing partitions of $[n]$ or $(m+2)$ -angulations of a convex $(mn+2)$ -gon.

In order to realize the bigraded Hilbert series of these spaces, F. BERGERON and L.-F. PRÉVILLE-RATELLE introduced the *m -Tamari lattice*. In our notation, this is the lattice $\mathbf{Tam}(v_m)$, where $v_m \stackrel{\text{def}}{=} ((NE^m)^n)$. The bigraded Hilbert series in question can then be expressed (conjecturally) as sums over all m -Dyck paths, i.e., the elements of $\text{Paths}(v_m)$, with respect to certain statistics generalizing dinv and area and using the interval structure of $\mathbf{Tam}(v_m)$. We refer the interested reader to [18] for the concrete statements and definitions.

We now propose a parabolic analogue of the m -Tamari lattice. Given $\alpha = (\alpha_1, \alpha_2, \dots, \alpha_r) \vdash n$, we consider the *(α, m) -bounce path*

$$v_{\alpha, m} \stackrel{\text{def}}{=} N^{\alpha_1} E^{m\alpha_1} N^{\alpha_2} E^{m\alpha_2} \dots N^{\alpha_r} E^{m\alpha_r}.$$

The *(α, m) -Tamari lattice* is the lattice $\mathbf{Tam}(\alpha, m) \stackrel{\text{def}}{=} \mathbf{Tam}(v_{\alpha, m})$. This way, for $\alpha = (1, 1, \dots, 1)$, we recover the m -Tamari lattice and for $m = 1$ we recover $\mathbf{Tam}(\alpha)$ by Theorem 4.3.27.

If $\alpha = (t, 1, 1, \dots, 1) \vdash n$, then the lattice paths in $\text{Paths}(v_{\alpha, m})$ can be enumerated in closed form.

Proposition 5.3.2. *Let $m, n, t > 0$ and let $\alpha = (t, 1, 1, \dots, 1) \vdash n$. Then,*

$$|\text{Paths}(v_{\alpha, m})| = \frac{mt + 1}{mn + 1} \binom{(m+1)n - t}{n - t}.$$

PROOF. By construction, the elements of $\text{Paths}(v_{\alpha, m})$ for $\alpha = (t, 1, 1, \dots, 1) \vdash n$ may be viewed equivalently as those northeast paths starting at $(0, 0)$, ending at $(mn, n - t)$ and staying weakly above the line $x = my$. The number of these paths was computed in [107, Theorem 10.4.5] to be

$$\frac{mt + 1}{mn + n - t + 1} \binom{mn + n - t + 1}{n - t} = \frac{mt + 1}{mn + 1} \binom{(m+1)n - t}{n - t}. \quad \square$$

For $p \in \text{Paths}(v_{\alpha, m})$ we define an *m-valley* to be a valley of p whose x -coordinate is divisible by m . Let $\text{Valley}_m(p)$ denote the set of all m -valleys of p and let $\text{valley}_m(p) \stackrel{\text{def}}{=} |\text{Valley}_m(p)|$. Note that by construction of $v_{\alpha, m}$ every return of p is an m -valley.

We define the *H-triangle* of $\mathbf{Tam}(\alpha, m)$ by

$$\mathcal{H}_{\alpha}^{(m)}(x, y) \stackrel{\text{def}}{=} \sum_{p \in \text{Paths}(v_{\alpha, m})} x^{\text{valley}_m(p)} y^{\text{return}(p)}.$$

Example 5.3.3. *Let $m = 2, n = 4, t = 2$. Figure 92 shows the 25 elements of $\text{Paths}(v_{(2,1,1),2})$, and Figure 93 shows $\mathbf{Tam}((2, 1, 1), 2)$.*

Moreover, we have marked valleys and returns for each path in Figure 92, where the non 2-valleys are hatched. We thus obtain

$$\mathcal{H}_{(2,1,1)}^{(2)}(x, y) = x^2y^2 + x^2y + x^2 + 5xy + 8x + 9.$$

We are currently unaware of a permutation model for $\mathbf{Tam}(\alpha, m)$. However, drawing inspiration from the cases $m = 1$ and $\alpha = (1, 1, \dots, 1)$ we strongly suspect that we can realize $\mathbf{Tam}(\alpha, m)$ using particular m -chains of $\mathbf{Tam}(\alpha)$. This was achieved for $\alpha = (1, 1, \dots, 1)$ in [143, Section 4.2].

For $\alpha = (t, 1, 1, \dots, 1) \vdash n$ we may, however, suggest a noncrossing partition model generalizing the case $\alpha = (1, 1, \dots, 1)$. In fact, there is enumerative evidence that we should consider the set $\text{Nonc}(\alpha, m)$ of noncrossing α -partitions of $[mn]$ where each block has cardinality divisible by m and no block contains more than one element of $[t]$. Using a generating function approach we have (jointly with C. KRATTENTHALER) computed the cardinality of $\text{Nonc}(\alpha, m)$ in [108].

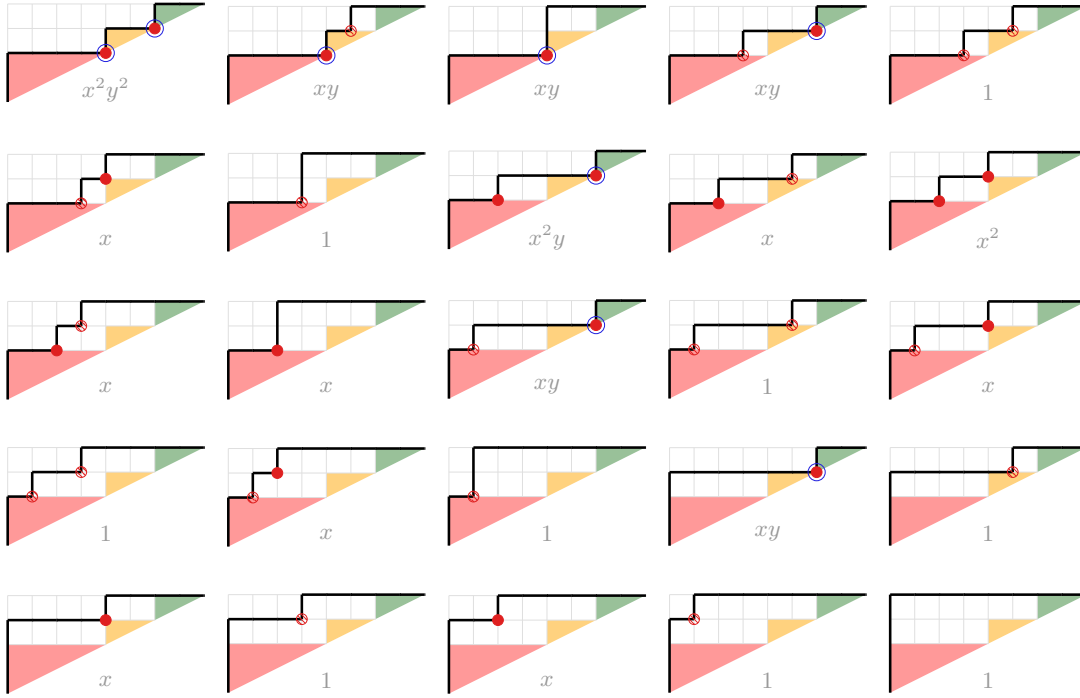


Figure 92. The elements of $\text{Paths}(v_{\alpha,2})$ for $\alpha = (2, 1, 1)$. The valleys are marked in red, the returns are circled in blue. Each path is also labeled by the term it contributes to the H-triangle.

Proposition 5.3.4 ([108, Theorem 3.1]). *Let $m, n, t > 0$ and let $\alpha = (t, 1, 1, \dots, 1) \vdash n$. Then,*

$$|\text{Nonc}(\alpha, m)| = \frac{mt + 1}{mn + 1} \binom{(m+1)n - t}{n - t}.$$

Thus, Propositions 5.3.2 and 5.3.4 imply that for all m, t :

$$|\text{Nonc}((t, 1, 1, \dots, 1), m)| = |\text{Paths}(v_{(t,1,1,\dots,1),m})|.$$

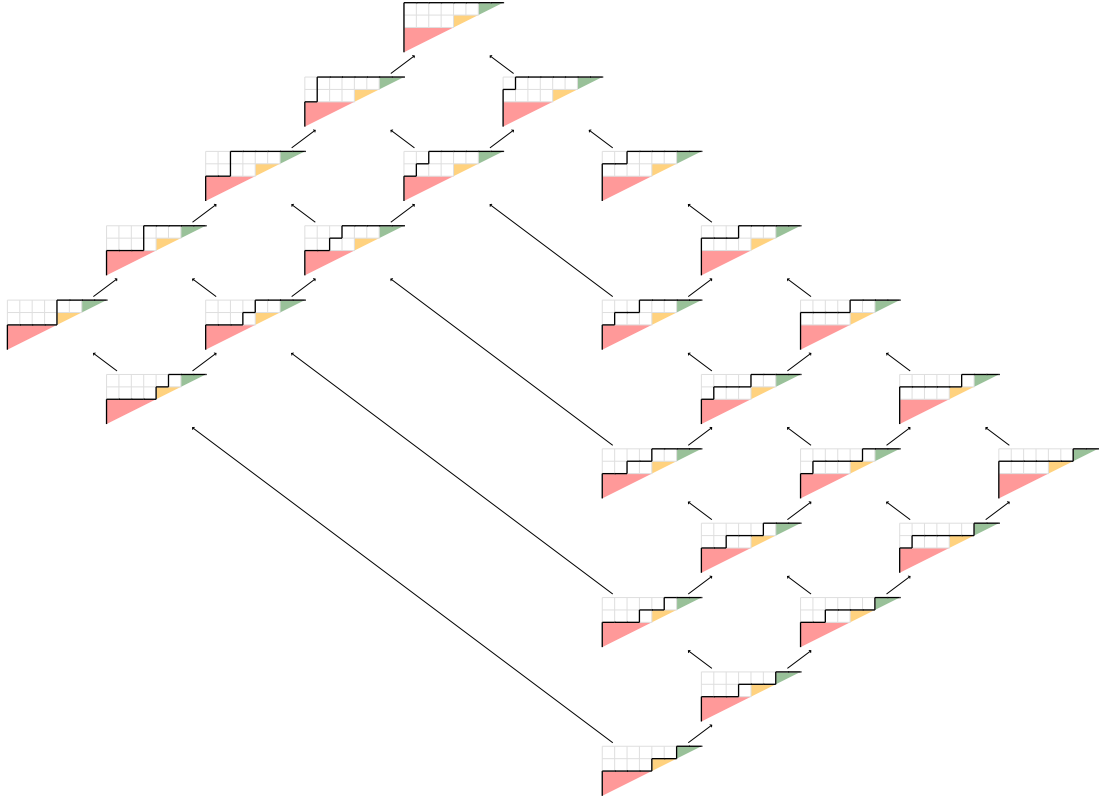
We are not aware of a bijective proof of this fact. In [108], we did as well compute the corresponding M-triangle of $\text{Nonc}(\alpha, m)$, defined by

$$\tilde{\mathcal{M}}_{\alpha}^{(m)}(x, y) \stackrel{\text{def}}{=} \sum_{P, Q \in \text{Nonc}(\alpha, m)} \mu_{\text{Nonc}(\alpha, m)}(P, Q) x^{|\text{Bump}(P)|} y^{|\text{Bump}(Q)|}.$$

Using Theorem 2.6.2, we define F- and H-triangles by

$$\begin{aligned} \tilde{\mathcal{F}}_{\alpha}^{(m)}(x, y) &\stackrel{\text{def}}{=} y^{n-t} \tilde{\mathcal{M}}_{\alpha}^{(m)}\left(\frac{y+1}{y-x}, \frac{y-x}{y}\right), \\ \tilde{\mathcal{H}}_{\alpha}^{(m)}(x, y) &\stackrel{\text{def}}{=} (x(y-1)+1)^{n-t} \tilde{\mathcal{M}}_{\alpha}^{(m)}\left(\frac{y}{y-1}, \frac{x(y-1)}{x(y-1)+1}\right). \end{aligned}$$

We have the following result, see also Proposition 4.4.8.

Figure 93. The lattice $\mathbf{Tam}((2, 1, 1), 2)$.

Proposition 5.3.5 ([108, Theorems 4.2 and 5.13]). Let $m, n, t > 0$ and let $\alpha = (t, 1, 1, \dots, 1) \vdash n$. Then,

$$\begin{aligned} \tilde{\mathcal{F}}_{\alpha}^{(m)}(x, y) &= \sum_{k=0}^{n-t} \sum_{h=0}^{n-t-k} \frac{t+h}{n} \binom{mn+k-1}{k} \binom{n}{t+k+h} x^k y^h \\ \tilde{\mathcal{H}}_{\alpha}^{(m)}(x, y) &= \sum_{k=0}^{n-t} \sum_{h=0}^{n-t-k} \left(\binom{mn-t+1}{k} \binom{t+k+h-2}{h} \right. \\ &\quad \left. - m \binom{mn-t}{k-1} \binom{t+k+h-1}{h} \right) x^{n-t-k} y^{n-t-k-h}, \\ \tilde{\mathcal{M}}_{\alpha}^{(m)}(x, y) &= \sum_{k=0}^{n-t} \sum_{h=0}^{n-t-k} (-1)^h \frac{(m-1)nt + (t-1)(h+k) + n}{n(mn-t+1)} \\ &\quad \cdot \binom{n}{k} \binom{mn-t+1}{(m-1)n+h+k+1} \binom{mn+h-1}{h} x^k y^{h+k}. \end{aligned}$$



Figure 94. The elements of $\text{Nonc}((2, 1, 1), 2)$.

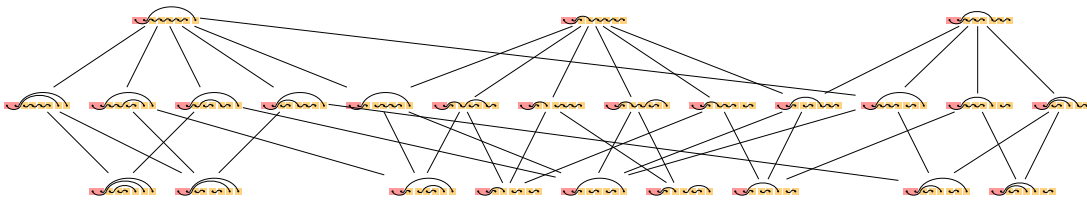


Figure 95. The poset $\text{Nonc}((2, 1, 1), 2)$.

Example 5.3.6. Let $m = 2, n = 4, t = 2$. Figure 94 shows the 25 elements of $\text{Nonc}((2, 1, 1), 2)$, and Figure 95 shows $\text{Nonc}((2, 1, 1), 2)$. We may compute directly or using Proposition 5.3.5 that

$$\tilde{\mathcal{M}}_{(2,1,1)}^{(2)}(x, y) = 3x^2y^2 - 16xy^2 + 13xy + 18y^2 - 26y + 9.$$

We obtain

$$\begin{aligned} \tilde{\mathcal{H}}_{(2,1,1)}^{(2)}(x, y) &= x^2y^2 + x^2y + x^2 + 5xy + 8x + 9 \\ &= \mathcal{H}_{(2,1,1)}^{(2)}(x, y); \end{aligned}$$

see Example 5.3.3.

Conjecture 5.3.7. Let $m, n, t > 0$ and let $\alpha = (t, 1, 1, \dots, 1) \vdash n$. Then,

$$\tilde{\mathcal{H}}_{\alpha}^{(m)}(x, y) = \mathcal{H}_{\alpha}^{(m)}(x, y).$$

Remark 5.3.8. By inspection of Proposition 5.3.2, we observe that the ordinary case, i.e., $\alpha = (1, 1, \dots, 1)$, also recovers the Fuß–Catalan numbers, see Remark 5.3.1.

There is yet another generalization of ordinary Catalan objects that is much more in line with the constructions of Chapter 2. The “ m -eralized” c -cluster complexes of a finite, irreducible Coxeter group W were introduced in [71], m -divisible c -noncrossing W -partitions were introduced in

[4] and an “*m*-eralized” version of the *c*-sortable elements was introduced in [180]. Each of these families is enumerated by the *W*-Fuß–Catalan number

$$\text{Cat}^{(m)}(W) \stackrel{\text{def}}{=} \prod_{d \in \text{Deg}(W)} \frac{d + m h_W}{d}.$$

It turns out that the “*m*-eralized” \bar{c} -Cambrian lattices in type *A* are only isomorphic to the *m*-Tamari lattices of [18] when *m* = 1. This raises the question if we can define a parabolic analogue of the “*m*-eralized” Catalan families from [180]. To that end it seems necessary to lift parabolic quotients of *W* into the corresponding braid group.

5.4. Parabolic multicusters

An intriguing generalization of the *c*-cluster complex of a finite Coxeter group *W* was first considered in [43]; see also [19, 138, 178]: the *c*-multicuster complex is, for $k \geq 1$, defined by:

$$(5.3) \quad \text{Clus}(W, c, k) \stackrel{\text{def}}{=} \text{Subw}(W; \mathbf{c}^k \overline{\mathbf{w}_o(\mathbf{c})}, \mathbf{w}_o),$$

where \mathbf{c}^k is the *k*-fold concatenation of the chosen *S*-reduced word for *c*. Clearly, for *k* = 1 we recover the *c*-cluster complex of *W*; see Definition 2.4.3. However, in contrast to Theorem 2.4.9, for *k* > 1 the flip order on $\text{Clus}(W, c, k)$ is in general not a lattice.

Example 5.4.1. Let $W = A_2$, $\mathbf{c} = s_1 s_2$ and $k = 2$. We consider

$$Q = \mathbf{c}^2 \overline{\mathbf{w}_o(\mathbf{c})} = s_1 s_2 s_1 s_2 s_1 s_2 s_1.$$

The fourteen occurrences of *S*-reduced words for the longest element of A_2 in *Q* are:

$$\begin{aligned} & s_1 s_2 s_1 s_2 s_1 s_2 s_1, \quad s_1 s_2 s_1 s_2 s_1 s_2 s_1, \\ & s_1 s_2 s_1 s_2 s_1 s_2 s_1, \quad s_1 s_2 s_1 s_2 s_1 s_2 s_1, \\ & s_1 s_2 s_1 s_2 s_1 s_2 s_1, \quad s_1 s_2 s_1 s_2 s_1 s_2 s_1, \quad s_1 s_2 s_1 s_2 s_1 s_2 s_1, \quad s_1 s_2 s_1 s_2 s_1 s_2 s_1. \end{aligned}$$

Thus, the facets of $\text{Clus}(A_2, c, 2)$ are:

$$\begin{aligned} & \{1, 2, 3, 4\}, \quad \{1, 2, 3, 7\}, \quad \{1, 2, 4, 5\}, \quad \{1, 2, 5, 6\}, \quad \{1, 2, 6, 7\}, \\ & \{1, 3, 4, 7\}, \quad \{1, 4, 5, 7\}, \quad \{1, 5, 6, 7\}, \quad \{2, 3, 4, 5\}, \quad \{2, 3, 5, 6\}, \\ & \{2, 3, 6, 7\}, \quad \{3, 4, 5, 6\}, \quad \{3, 4, 6, 7\}, \quad \{4, 5, 6, 7\}. \end{aligned}$$

The poset $\mathbf{Clus}(A_2, c, 2)$ is shown in Figure 96. We observe that, for instance, $\{1, 4, 5, 7\}$ and $\{3, 4, 6, 7\}$ do not have a meet.

It is not too much a leap to consider parabolic versions of the multicuster complex, see also [192, Remark 4.5.8]. The (W^J, c) -multicuster complex is

$$\text{Clus}(W^J, c, k) \stackrel{\text{def}}{=} \text{Subw}(W; \mathbf{c}^k \overline{\mathbf{w}_o(\mathbf{c})}, \mathbf{w}_o^J).$$

For $J = \emptyset$, there is a nice formula for the number of facets of $\text{Clus}(W, c, k)$ when *W* is of coincidental type, i.e., when $W \in \{A_n, B_n, H_3, I_2(m)\}$.

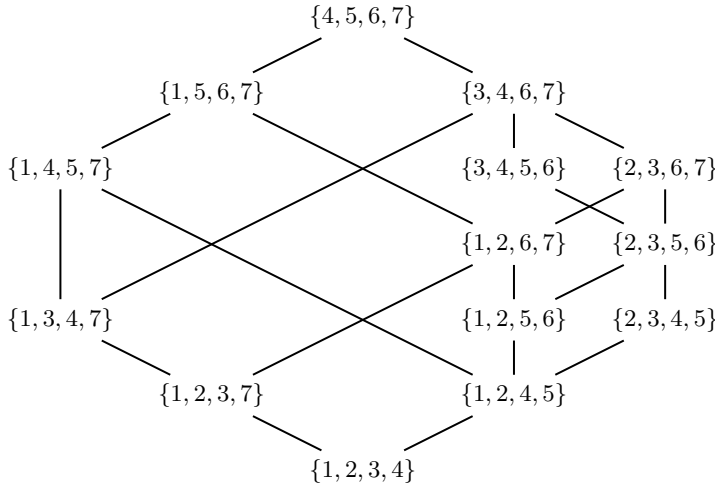


Figure 96. The flip poset $\mathbf{Clus}(A_2, c, 2)$.

Theorem 5.4.2 ([43, Section 9]). *Let (W, S) be a finite, irreducible Coxeter system with Coxeter number h , and let $c \in W$ be a Coxeter element. If W is of coincidental type, then for $k \geq 1$, the number of facets of $\mathbf{Clus}(W, c, k)$ is given by*

$$\prod_{j=0}^{k-1} \prod_{d \in \text{Deg}(W)} \frac{d + h + 2j}{d + 2j}.$$

In linear type A , computer experiments suggest the following formula for the number of facets of $\mathbf{Clus}(\mathfrak{S}_\alpha, \bar{c}, k)$, when $\alpha = (t, 1, 1, \dots, 1) \vdash n$ for $t \geq 1$.

Conjecture 5.4.3. *Let $n, k, t > 0$ and let $\alpha = (t, 1, 1, \dots, 1) \vdash n$. For any Coxeter element c of \mathfrak{S}_n , the number of facets of $\mathbf{Clus}(\mathfrak{S}_\alpha, c, k)$ is*

$$2 \prod_{j=0}^{n-t-1} \frac{\binom{k+t+j}{t}}{2^{\binom{2j+t}{t}}} \frac{\binom{2k+2j+t}{4j-2(n-t)+1}}{\binom{2(n-t)-2j+\lceil \frac{n-t}{2} \rceil - 3}{2j - \lceil \frac{n-t}{2} \rceil}}.$$

Here we have to evaluate the expression “ $\frac{0}{0}$ ” occurring in the second factor for $j \leq \lceil \frac{n-t}{2} \rceil$ as 1.

Example 5.4.4. *We illustrate Conjecture 5.4.3 in the case $n = 4$, $t = 3$ and $k = 2$. We choose $c = s_2 s_1 s_3$ and obtain*

$$Q = c^2 \overline{w_o(c)} = s_2 s_1 s_3 s_2 s_1 s_3 s_2 s_1 s_3 s_2 s_1 s_3.$$

Since $\alpha = (3, 1)$, the longest element $w_{o,\alpha}$ is **2 3 4 1** and has only one S -reduced word, namely $s_1 s_2 s_3$. This word appears ten times as a subword of Q :

- $s_2 s_1 s_3 s_2 s_1 s_3 s_2 s_1 s_3 s_2 s_1 s_3$, $s_2 s_1 s_3 s_2 s_1 s_3 s_2 s_1 s_3 s_2 s_1 s_3$, $s_2 s_1 s_3 s_2 s_1 s_3 s_2 s_1 s_3 s_2 s_1 s_3$,
- $s_2 s_1 s_3 s_2 s_1 s_3 s_2 s_1 s_3 s_2 s_1 s_3$, $s_2 s_1 s_3 s_2 s_1 s_3 s_2 s_1 s_3 s_2 s_1 s_3$, $s_2 s_1 s_3 s_2 s_1 s_3 s_2 s_1 s_3 s_2 s_1 s_3$,
- $s_2 s_1 s_3 s_2 s_1 s_3 s_2 s_1 s_3 s_2 s_1 s_3$, $s_2 s_1 s_3 s_2 s_1 s_3 s_2 s_1 s_3 s_2 s_1 s_3$, $s_2 s_1 s_3 s_2 s_1 s_3 s_2 s_1 s_3 s_2 s_1 s_3$,
- $s_2 s_1 s_3 s_2 s_1 s_3 s_2 s_1 s_3 s_2 s_1 s_3$.

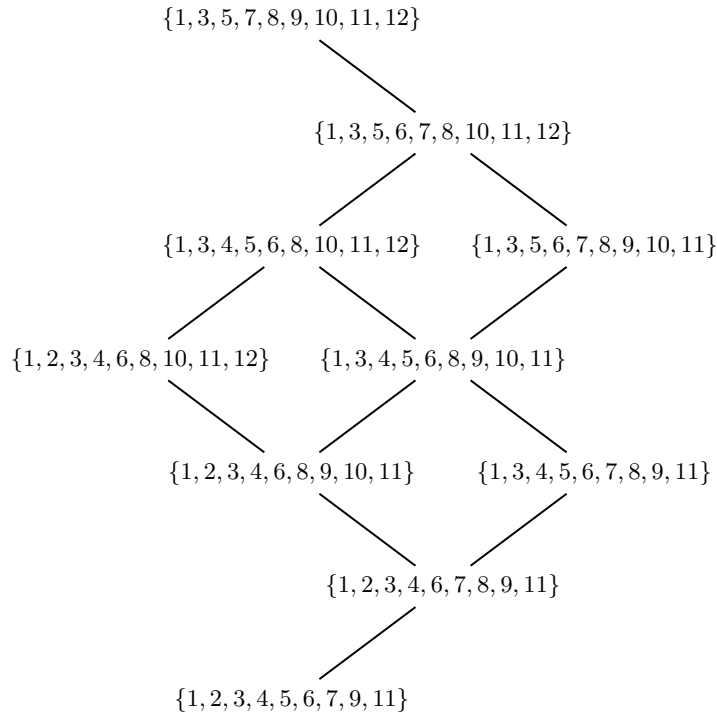


Figure 97. The flip poset of $\text{Clus}(\mathfrak{S}_\alpha, c, 2)$ for $\alpha = (3, 1)$ and $c = s_2 s_1 s_3$.

Thus, $\text{Clus}(\mathfrak{S}_\alpha, c, 2)$ has the following ten facets:

$\{1, 3, 5, 7, 8, 9, 10, 11, 12\}$, $\{1, 3, 5, 6, 7, 8, 10, 11, 12\}$, $\{1, 3, 4, 5, 6, 8, 10, 11, 12\}$,
 $\{1, 3, 5, 6, 7, 8, 9, 10, 11\}$, $\{1, 3, 4, 5, 6, 8, 9, 10, 11\}$, $\{1, 3, 4, 5, 6, 7, 8, 9, 11\}$,
 $\{1, 2, 3, 4, 6, 8, 10, 11, 12\}$, $\{1, 2, 3, 4, 6, 8, 9, 10, 11\}$, $\{1, 2, 3, 4, 6, 7, 8, 9, 11\}$,
 $\{1, 2, 3, 4, 5, 6, 7, 9, 11\}$.

The flip poset $\mathbf{Clus}(\mathfrak{S}_\alpha, c, 2)$ is shown in Figure 97.

For $n = 4$, $t = 2$, $k = 2$, we obtain a total of 40 parabolic multiclusters, which indicates that the parabolic multiclusters and the elements of the (α, m) -Tamari lattices are indeed structurally different.

APPENDIX A

Data

The indices in the tables in Appendices A.1 and A.2 correspond to the labels in Figure 11, unless otherwise stated. The tables in Appendix A.2 were previously presented in [192, Section 5.4.3], but were (re-)computed independently.

A.1. Parabolic Catalan numbers in rank 3

J	$ \text{Align}(W^J, c) = \text{Nonc}(W^J, c) $ $W = A_3$	$ \text{Clus}(W^J, c) = \text{Nonn}(W^J) $ $W = B_3$	$ \text{Nonc}(W^J, c) = \text{Clus}(W^J, c) = \text{Nonn}(W^J) $ $W = H_3$
\emptyset	14	20	32
$\{s_1\}$	9	15	27
$\{s_2\}$	10	16	28
$\{s_3\}$	9	14	25
$\{s_1, s_2\}$	4	6	12
$\{s_1, s_3\}$	6	11	22
$\{s_2, s_3\}$	4	8	18
$\{s_1, s_2, s_3\}$	1	1	1

Table 3. The various parabolic Catalan numbers in types A_3 , B_3 and H_3 . These numbers are independent of the choice of Coxeter element. In type B_3 , we have labeled the nodes of the Coxeter graph, see Figure 11, from left to right by s_1, s_2, s_3 .

A.2. Parabolic Catalan numbers in rank 4

J	Align(W ^J , c) = Nonc(W ^J , c) = Clus(W ^J , c) = Nonn(W ^J)	
	W = A ₄	W = B ₄
∅	42	70
{s ₁ }	28	56
{s ₂ }	32	60
{s ₃ }	32	58
{s ₄ }	28	50
{s ₁ , s ₂ }	14	28
{s ₁ , s ₃ }	22	48
{s ₁ , s ₄ }	19	41
{s ₂ , s ₃ }	17	40
{s ₂ , s ₄ }	22	44
{s ₃ , s ₄ }	14	30
{s ₁ , s ₂ , s ₃ }	5	8
{s ₁ , s ₂ , s ₄ }	10	22
{s ₁ , s ₃ , s ₄ }	10	26
{s ₂ , s ₃ , s ₄ }	5	16
{s ₁ , s ₂ , s ₃ , s ₄ }	1	1

Table 4. The various parabolic Catalan numbers in types A₄ and B₄. These numbers are independent of the choice of Coxeter element. In type B₄, we have labeled the nodes of the Coxeter graph, see Figure 11, from left to right by s₁, s₂, s₃, s₄.

J	Align(D ₄ ^J , c) = Nonc(D ₄ ^J , c) = Clus(D ₄ ^J , c)				Nonn(D ₄ ^J)
	c = s̄ ₀ s ₁ s ₂ s ₃	c = s̄ ₀ s ₂ s ₁ s ₃	c = s̄ ₀ s ₃ s ₂ s ₁	c = s̄ ₀ s ₁ s ₃ s ₂	
	c = s ₃ s ₂ s̄ ₀ s ₁	c = s ₁ s ₃ s ₂ s̄ ₀	c = s ₁ s ₂ s̄ ₀ s ₃	c = s ₂ s̄ ₀ s ₁ s ₃	
∅					50
{s̄ ₀ }					36
{s ₁ }					36
{s ₂ }					42
{s ₃ }					36
{s̄ ₀ , s ₁ }					27
{s̄ ₀ , s ₂ }	21	22	21	22	22
{s̄ ₀ , s ₃ }					27
{s ₁ , s ₂ }	21	21	22	22	22
{s ₁ , s ₃ }					27
{s ₂ , s ₃ }	22	21	21	22	22
{s̄ ₀ , s ₁ , s ₂ }					8
{s̄ ₀ , s ₁ , s ₃ }					21
{s̄ ₀ , s ₂ , s ₃ }					8
{s ₁ , s ₂ , s ₃ }					8
{s̄ ₀ , s ₁ , s ₂ , s ₃ }					1

Table 5. The various parabolic Catalan numbers in type D₄.

J	Align(F ₄ ^J , c) = Nonc(F ₄ ^J , c) = Clus(F ₄ ^J , c)				Nonn(F ₄ ^J)
	c = s ₁ s ₂ s ₃ s ₄	c = s ₂ s ₃ s ₄ s ₁	c = s ₄ s ₁ s ₂ s ₃	c = s ₃ s ₄ s ₁ s ₂	
∅					105
{s ₁ }					85
{s ₂ }					95
{s ₃ }					95
{s ₄ }					85
{s ₁ , s ₂ }					65
{s ₁ , s ₃ }					79
{s ₁ , s ₄ }					71
{s ₂ , s ₃ }	57	62	62	62	63
{s ₂ , s ₄ }					79
{s ₃ , s ₄ }					65
{s ₁ , s ₂ , s ₃ }					24
{s ₁ , s ₂ , s ₄ }					57
{s ₁ , s ₃ , s ₄ }					57
{s ₂ , s ₃ , s ₄ }					23
{s ₁ , s ₂ , s ₃ , s ₄ }					1

Table 6. The various parabolic Catalan numbers in type F₄.

J	Clus(H ₄ ^J , c)	Nonn(H ₄ ^J)
∅	280	280
{s ₁ }	266	266
{s ₂ }	270	270
{s ₃ }	266	266
{s ₄ }	248	248
{s ₁ , s ₂ }	209	210
{s ₁ , s ₃ }	256	256
{s ₁ , s ₄ }	239	239
{s ₂ , s ₃ }	245	245
{s ₂ , s ₄ }	242	242
{s ₃ , s ₄ }	216	216
{s ₁ , s ₂ , s ₃ }	95	106
{s ₁ , s ₂ , s ₄ }	197	198
{s ₁ , s ₃ , s ₄ }	212	212
{s ₂ , s ₃ , s ₄ }	191	191
{s ₁ , s ₂ , s ₃ , s ₄ }	1	1

Table 7. The various parabolic Catalan numbers in type H₄. These numbers are independent of the choice of Coxeter element. The cardinality of Nonn(H₄^J) is computed using the four posets in Figure 33, all of which give the same numbers.

A.3. Answers to Research Challenge 3.3.4 in rank 4

	$c = s_1s_2s_3s_4$		$c = s_2s_3s_4s_1$		$c = s_4s_1s_2s_3$		$c = s_3s_1s_2s_4$	
	$c = s_4s_3s_2s_1$		$c = s_4s_3s_1s_2$		$c = s_3s_2s_4s_1$		$c = s_4s_2s_3s_1$	
$J = \emptyset$	yes	yes	yes	yes	yes	yes	yes	yes
$J = \{s_1\}$	yes	yes	yes	yes	yes	yes	yes	yes
$J = \{s_2\}$	no	no	no	yes	yes	no	yes	yes
$J = \{s_3\}$	no	no	yes	no	no	yes	yes	yes
$J = \{s_4\}$	yes	yes	yes	yes	yes	yes	yes	yes
$J = \{s_1, s_2\}$	yes	no	yes	no	yes	no	yes	no
$J = \{s_1, s_3\}$	no	no	yes	no	no	yes	yes	yes
$J = \{s_1, s_4\}$	yes	yes	yes	yes	yes	yes	yes	yes
$J = \{s_2, s_3\}$	no	no	no	no	no	no	no	no
$J = \{s_2, s_4\}$	no	no	yes	yes	yes	no	yes	yes
$J = \{s_3, s_4\}$	yes	yes	yes	yes	yes	yes	yes	yes
$J = \{s_1, s_2, s_3\}$	yes	yes	yes	yes	yes	yes	yes	yes
$J = \{s_1, s_2, s_4\}$	yes	no	yes	no	yes	no	yes	no
$J = \{s_1, s_3, s_4\}$	yes	yes	yes	yes	yes	yes	yes	yes
$J = \{s_2, s_3, s_4\}$	yes	yes	yes	yes	yes	yes	yes	yes
$J = \{s_1, s_2, s_3, s_4\}$	yes	yes	yes	yes	yes	yes	yes	yes

Table 8. Answers to Research Challenge 3.3.4 for the crystallographic Coxeter groups of rank 4. The entries “yes” and “no” refer to the answer of the question “Is $\mathbf{CLO}(\mathbf{Camb}(W^J, c)) \cong \mathbf{Nonc}(W^J, c)$?”.

Bibliography

- [1] Murad Alim, Sergio Cecotti, Clay Córdova, Sam Espahbodi, Ashwin Rastogi, and Cumrun Vafa, *BPS quivers and spectra of complete $\mathcal{N}=2$ quantum field theories*, Communications in Mathematical Physics **323** (2013), 1185–1227. [↑2](#)
- [2] George E. Andrews, Christian Krattenthaler, Luigi Orsina, and Paolo Papi, *ad-nilpotent \mathfrak{b} -ideals in $\mathfrak{sl}(n)$ having a fixed class of nilpotence: Combinatorics and enumeration*, Transactions of the American Mathematical Society **354** (2002), 3835–3853. [↑152](#)
- [3] Federico Ardila, Felipe Rincón, and Lauren K. Williams, *Postroids and non-crossing partitions*, Transactions of the American Mathematical Society **368** (2016), 337–363. [↑1](#)
- [4] Drew Armstrong, *Generalized noncrossing partitions and combinatorics of Coxeter groups*, Memoirs of the American Mathematical Society **202** (2009). [↑1](#), [56](#), [182](#)
- [5] Drew Armstrong, *The sorting order on a Coxeter group*, Journal of Combinatorial Theory, Series A **116** (2009), 1285–1305. [↑3](#)
- [6] Drew Armstrong, Nicholas A. Loehr, and Gregory S. Warrington, *Sweep maps: a continuous family of sorting algorithms*, Advances in Mathematics **284** (2015), 159–185. [↑152](#)
- [7] Drew Armstrong, Christian Stump, and Hugh Thomas, *A uniform bijection between nonnesting and noncrossing partitions*, Transactions of the American Mathematical Society **365** (2013), 4121–4151. [↑57](#)
- [8] Christos A. Athanasiadis, *On noncrossing and nonnesting partitions for classical reflection groups*, The Electronic Journal of Combinatorics **5** (1998), Research article R42, 16 pages. [↑57](#)
- [9] Christos A. Athanasiadis, *On some enumerative aspects of generalized associahedra*, European Journal of Combinatorics **28** (2007), 1208–1215. [↑61](#)
- [10] Christos A. Athanasiadis and Victor Reiner, *Noncrossing partitions for the group D_n* , SIAM Journal on Discrete Mathematics **18** (2004), 397–417. [↑2](#), [44](#), [45](#), [46](#)
- [11] Erin Bancroft, *The shard intersection order on permutations* (2011), available at [arXiv:1103.1910](#). [↑137](#)
- [12] Emily Barnard, *The canonical join complex*, The Electronic Journal of Combinatorics **26** (2019), Research article P1.24, 25 pages. [↑13](#), [14](#)
- [13] Emily Barnard, *The canonical join complex of the Tamari lattice*, Journal of Combinatorial Theory, Series A **174** (2020), Article 105207, 27 pages. [↑14](#), [172](#)
- [14] Emily Barnard and Nathan Reading, *Coxeter-biCatalan combinatorics*, Journal of Algebraic Combinatorics **47** (2018), 241–300. [↑18](#), [63](#)
- [15] Barbara Baumeister, Kai-Uwe Bux, Friedrich Götze, Dawid Kielak, and Henning Krause, *Non-crossing partitions*. In: Spectral Studies and Topological Methods in Mathematics

- (Michael Baake, Friedrich Götze, and Werner Hoffmann, eds.), European Mathematical Society (2019), 235–274. ↑1
- [16] H. W. Becker, *Planar rhyme schemes*, Bulletin of the American Mathematical Society **28** (1952). ↑1
- [17] Nantel Bergeron and Sara C. Billey, *RC-graphs and Schubert polynomials*, Experimental Mathematics **2** (1993), 13 pages. ↑50, 52
- [18] François Bergeron and Louis-François Prévaille-Ratelle, *Higher trivariate diagonal harmonics via generalized Tamari posets*, Journal of Combinatorics **3** (2012), 317–341. ↑176, 177, 182
- [19] Nantel Bergeron, Cesar Ceballos, and Jean-Philippe Labbé, *Fan realizations of type A subword complexes and multi-associahedra of rank 3*, Discrete and Computational Geometry **54** (2015), 195–231. ↑49, 182
- [20] Nantel Bergeron, Cesar Ceballos, and Vincent Pilaud, *Hopf dreams and diagonal harmonics* (2019), available at [arXiv:1807.03044](https://arxiv.org/abs/1807.03044). ↑4, 142, 143, 144, 145, 150, 154
- [21] David Bessis, *The dual braid monoid*, Annales Scientifiques de l'École Normale Supérieure **36** (2003), 647–683. ↑2, 30, 45, 46
- [22] David Bessis and Ruth Corran, *Non-crossing partitions of type (e, e, r)* , Advances in Mathematics **202** (2006), 1–49. ↑2
- [23] David Bessis, *Finite complex reflection arrangements are $K(\pi, 1)$* , Annals of Mathematics **181** (2015), 809–904. ↑2
- [24] Philippe Biane, *Some properties of crossings and partitions*, Discrete Mathematics **175** (1997), 41–53. ↑2, 44
- [25] Sara Billey and Mark Haiman, *Schubert polynomials for the classical groups*, Journal of the American Mathematical Society **8** (1995), 443–482. ↑51
- [26] Garrett Birkhoff, *Applications of lattice algebra*, Proceedings of the Cambridge Philosophical Society **30** (1934), 115–122. ↑13
- [27] Garrett Birkhoff, *Rings of sets*, Duke Mathematical Journal **3** (1937), 443–454. ↑12
- [28] Joan S. Birman, Ki Hyoung Ko, and Sang Jin Lee, *A new approach to the word and conjugacy problem in the braid groups*, Advances in Mathematics **139** (1998), 322–353. ↑2, 30
- [29] Anders Björner and Francesco Brenti, *Combinatorics of Coxeter Groups*, Springer, New York, 2005. ↑22, 28, 29, 30, 36, 71
- [30] Anders Björner and Michelle L. Wachs, *Generalized quotients in Coxeter groups*, Transactions of the American Mathematical Society **308** (1988), 1–37. ↑65
- [31] Anders Björner and Michelle L. Wachs, *Shellable nonpure complexes and posets II*, Transactions of the American Mathematical Society **349** (1997), 3945–3975. ↑3, 35, 41, 42
- [32] Mireille Bousquet-Mélou and Marni Mishna, *Walks with small steps in the quarter plane*. In: Algorithmic Probability and Combinatorics (Manuel E. Lladser, Robert S. Maier, Marni Mishna, and Andrew Rechnitzer, eds.), American Mathematical Society (2010), 1–39. ↑145
- [33] Thomas Brady, *A partial order on the symmetric group and new $K(\pi, 1)$'s for the braid groups*, Advances in Mathematics **161** (2001), 20–40. ↑2, 44
- [34] Thomas Brady and Colum Watt, *$K(\pi, 1)$'s for Artin groups of finite type*, Geometriae Dedicata **94** (2002), 225–250. ↑2
- [35] Thomas Brady and Colum Watt, *Non-crossing partition lattices in finite real reflection groups*, Transactions of the American Mathematical Society **360** (2008), 1983–2005. ↑2, 46
- [36] Melody Bruce, Michael Dougherty, Max Hlavacek, Ryu Kudo, and Ian Nicolas, *A decomposition of parking functions by undesired spaces*, The Electronic Journal of Combinatorics **23** (2016), Research article P3.32, 22 pages. ↑85
- [37] Aslak Bakke Buan, Robert Marsh, Markus Reineke, Idun Reiten, and Gordana Todorov, *Tilting theory and cluster combinatorics*, Advances in Mathematics **204** (2006), 572–618. ↑2

- [38] Philippe Caldero and Bernhard Keller, *From triangulated categories to cluster algebras II*, *Annales Scientifiques de l'École Normale Supérieure* **39** (2006), 983–1009. ↑2
- [39] Erik Carlsson and Anton Mellit, *A proof of the shuffle conjecture*, *Journal of the American Mathematical Society* **31** (2018), 661–697. ↑158
- [40] Nathalie Caspard, Claude Le Conte de Poly-Barbut, and Michel Morvan, *Cayley lattices of finite Coxeter groups are bounded*, *Advances in Applied Mathematics* **33** (2004), 71–94. ↑29
- [41] Sabin Cautis and David M. Jackson, *The matrix of chromatic joins and the Temperley–Lieb algebra*, *Journal of Combinatorial Theory, Series B* **89** (2003), 109–155. ↑1
- [42] Cesar Ceballos, Tom Denton, and Christopher R. H. Hanusa, *Combinatorics of the zeta map on rational Dyck paths*, *Journal of Combinatorial Theory, Series A* **141** (2016), 33–77. ↑152
- [43] Cesar Ceballos, Jean-Phillipe Labbé, and Christian Stump, *Subword complexes, cluster complexes, and generalized multi-associahedra*, *Journal of Algebraic Combinatorics* **39** (2014), 17–51. ↑49, 63, 182, 183
- [44] Cesar Ceballos, Arnau Padrol, and Camilo Sarmiento, *The ν -Tamari lattice, via ν -trees, ν -bracket vectors, and subword complexes*, *The Electronic Journal of Combinatorics* **27** (2020), Research article P1.14, 31 pages. ↑4, 54, 85, 130
- [45] Cesar Ceballos, Wenjie Fang, and Henri Mühle, *The steep-bounce zeta map in Parabolic Cataland*, *Journal of Combinatorial Theory, Series A* **172** (2020), Article 105210, 59 pages. ↑81, 93, 110, 132, 141, 159
- [46] Frédéric Chapoton, *Enumerative properties of generalized associahedra*, *Séminaire Lotharingien de Combinatoire* **51** (2004), Research article B51b, 16 pages. ↑59
- [47] Frédéric Chapoton, *Sur le nombre de réflexions pleines dans les groupes de Coxeter finis*, *Bulletin of the Belgian Mathematical Society* **13** (2006), 585–596. ↑59
- [48] Claude Chevalley, *Invariants of finite groups generated by reflections*, *American Journal of Mathematics* **77** (1955), 778–782. ↑34
- [49] Claude Chevalley, *Sur certains groupes simples*, *Tohoku Mathematical Journal* **7** (1955), 14–66. ↑33
- [50] Camille Combe and Samuele Giraudo, *Three Fuss–Catalan posets in interaction and their associative algebras* (2020), available at [arXiv:2007.02378](https://arxiv.org/abs/2007.02378). ↑42
- [51] Alessandro Conflitti and Ricardo Mamede, *On noncrossing and nonnesting partitions of type D*, *Annals of Combinatorics* **15** (2011), 637–654. ↑57
- [52] Harold S. M. Coxeter, *The complete enumeration of finite groups of the form $R_i^2 = (R_i R_j)^{k_{ij}} = 1$* , *Journal of the London Mathematical Society* **10** (1935), 21–25. ↑23, 24
- [53] Harold S. M. Coxeter, *The product of the generators of a finite group generated by reflections*, *Duke Mathematical Journal* **XVII** (1951), 765–782. ↑30, 34
- [54] Michael Cuntz and Christian Stump, *On root posets for noncrystallographic root systems*, *Mathematics of Computation* **84** (2015), 485–503. ↑57, 58
- [55] Brian A. Davey, Werner Poguntke, and Ivan Rival, *A characterization of semi-distributivity*, *Algebra Universalis* **5** (1975), 72–75. ↑13
- [56] Brian A. Davey and Hilary A. Priestley, *Introduction to Lattices and Order*, Cambridge University Press, Cambridge, 2002. ↑7
- [57] Alan Day, *Characterizations of finite lattices that are bounded-homomorphic images or sublattices of free lattices*, *Canadian Journal of Mathematics* **31** (1979), 69–78. ↑19
- [58] Harm Derksen, Jerzy Weyman, and Andrei Zelevinsky, *Quivers with potentials and their representations I: Mutations*, *Selecta Mathematica* **14** (2008), 59–119. ↑2
- [59] Harm Derksen, Jerzy Weyman, and Andrei Zelevinsky, *Quivers with potentials and their representations II: Applications to cluster algebras*, *Journal of the American Mathematical Society* **23** (2010), 749–790. ↑2

- [60] Emeric Deutsch, *Dyck path enumeration*, Discrete Mathematics **204** (1999), 167–202. [↑149, 156](#)
- [61] Matthew J. Dyer, *On the weak order of Coxeter groups*, Canadian Journal of Mathematics **71** (2019), 299–336. [↑37](#)
- [62] Paul H. Edelman and Curtis C. Greene, *Balanced tableaux*, Advances in Mathematics **63** (1987), 42–99. [↑63](#)
- [63] Henrik Eriksson and Kimmo Eriksson, *Conjugacy of Coxeter elements*, The Electronic Journal of Combinatorics **16** (2009), Research article R4, 7 pages. The Björner Festschrift. [↑31](#)
- [64] Marcel Ern e, Jobst Heitzig, and J urgen Reinhold, *On the number of distributive lattices*, The Electronic Journal of Combinatorics **9** (2002), Research article R24, 23 pages. [↑19](#)
- [65] Laura Escobar and Karola M esz aros, *Subword complexes via triangulations of root polytopes*, Algebraic Combinatorics **1** (2018), 395–414. [↑52](#)
- [66] Wenjie Fang, Henri M uhle, and Jean-Christophe Novelli, *A consecutive Lehmer code for parabolic quotients of the symmetric group*, The Electronic Journal of Combinatorics **28** (2021), Research article P3.53, 28 pages. [↑81, 110](#)
- [67] Alex Fink and Benjamin I. Giraldo, *Bijections between noncrossing and nonnesting partitions for classical reflection groups*, Portugaliae Mathematica **67** (2009), 369–401. [↑57](#)
- [68] Vladimir Fock and Alexander Goncharov, *Moduli spaces of local systems and higher Teichm uller theory*, Publications Math ematiques de l’Institut Hautes  Etudes Scientifiques **103** (2006), 1–211. [↑2](#)
- [69] Vladimir Fock and Alexander Goncharov, *The quantum dilogarithm and representations of quantum cluster quivers*, Inventiones Mathematicae **175** (2009), 223–286. [↑2](#)
- [70] Sergey Fomin and Anatol N. Kirillov, *The Yang–Baxter equation, symmetric functions, and Schubert polynomials*, Discrete Mathematics **153** (1996), 123–143. [↑50](#)
- [71] Sergey Fomin and Nathan Reading, *Generalized cluster complexes and Coxeter combinatorics*, International Mathematics Research Notices **44** (2005), 2709–2757. [↑2, 181](#)
- [72] Sergey Fomin and Andrei Zelevinsky, *Cluster algebras I: Foundations*, Journal of the American Mathematical Society **15** (2002), 497–529. [↑2](#)
- [73] Sergey Fomin and Andrei Zelevinsky, *Cluster algebras II: Finite type classification*, Inventiones Mathematicae **154** (2003), 63–121. [↑2](#)
- [74] Sergey Fomin and Andrei Zelevinsky, *Y-systems and generalized associahedra*, Annals of Mathematics **158** (2003), 977–1018. [↑2, 40, 49](#)
- [75] Ralph Freese, Jaroslav Je ek, and James B. Nation, *Free Lattices*, American Mathematical Society, Providence, 1995. [↑7, 13, 14, 18](#)
- [76] Nenosuke Funayama and Tadasi Nakayama, *On the distributivity of a lattice of lattice congruences*, Proceedings of the Imperial Academy of Tokyo **18** (1942), 553–554. [↑18](#)
- [77] Davide Gaiotto, Gregory Moore, and Andrew Neitzke, *Wall-crossing, Hitchin systems, and the WKB approximation*, Advances in Mathematics **234** (2013), 239–403. [↑2](#)
- [78] Adriano M. Garsia and Mark Haiman, *A remarkable q, t-Catalan sequence and q-Lagrange inversion*, Journal of Algebraic Combinatorics **5** (1996), 191–244. [↑151](#)
- [79] Adriano M. Garsia and Mark Haiman, *Some natural bigraded S_n -modules and q, t-Kostka coefficients*, The Electronic Journal of Combinatorics **2** (1996), Research article 24, 60 pages. The Foata Festschrift. [↑151](#)
- [80] Frank A. Garside, *The braid group and other groups*, The Quarterly Journal of Mathematics **20** (1969), 235–254. [↑2, 30](#)
- [81] Michael Gekhtman, Michael Shapiro, and Alek Vainshtein, *Cluster algebras and Poisson geometry*, Moscow Mathematical Journal **3** (2003), 899–934. [↑2](#)
- [82] Michael Gekhtman, Michael Shapiro, and Alek Vainshtein, *Cluster algebras and Weil–Petersson forms*, Duke Mathematical Journal **127** (2005), 291–311. [↑2](#)

- [83] Michael Gekhtman, Michael Shapiro, and Alek Vainshtein, *On the properties of the exchange graph of a cluster algebra*, *Mathematics Research Letters* **15** (2008), 321–330. [↑2](#)
- [84] George Grätzer, *General Lattice Theory*, Academic Press, New York, 1978. [↑7](#)
- [85] George Grätzer, *Lattice Theory: Foundation*, Springer, Basel, 2011. [↑18](#)
- [86] Darij Grinberg and Victor Reiner, *Hopf algebras in combinatorics* (2020), available at [arXiv:1409.8356](#). [↑141](#)
- [87] James Haglund, *The q, t-Catalan Numbers and the Space of Diagonal Harmonics*, The American Mathematical Society, Providence, RI, 2008. [↑3](#), [150](#), [151](#), [152](#), [153](#), [158](#)
- [88] James Haglund and Nicholas A. Loehr, *A conjectured combinatorial formula for the Hilbert series for diagonal harmonics*, *Discrete Mathematics* **298** (2005), 198–204. [↑158](#)
- [89] Mark Haiman, *Dual equivalence with applications, including a conjecture of Proctor*, *Discrete Mathematics* **99** (1992), 79–113. [↑63](#)
- [90] Mark Haiman, *Conjectures on the quotient ring by diagonal harmonics*, *Journal of Algebraic Combinatorics* **3** (1994), 17–76. [↑151](#), [176](#), [177](#)
- [91] Mark Haiman, *Vanishing theorems and character formulas for the Hilbert scheme of points in the plane*, *Inventiones Mathematicae* **149** (2002), 371–407. [↑151](#), [177](#)
- [92] Zachary Hamaker, Rebecca Patrias, Oliver Pechenik, and Nathan Williams, *Doppelgängers: Bijections of plane partitions*, *International Mathematics Research Notices* **2020** (2020), 487–540. [↑63](#)
- [93] Christine E. Heitsch, *Combinatorics on plane trees, motivated by RNA secondary structure configurations*. Preprint available at [people.math.gatech.edu/~heitsch/Pubs/plane.pdf](#). [↑1](#)
- [94] David Hernandez and Bernard Leclerc, *Cluster algebras and quantum affine algebras*, *Duke Mathematical Journal* **154** (2010), 265–341. [↑2](#)
- [95] Sam Hopkins, *Minuscule doppelgängers, the coincidental down-degree expectations property, and rowmotion*, *Experimental Mathematics* (2020), 53 pages. To appear. [↑63](#)
- [96] Sam Hopkins, *Order polynomial product formulas and poset dynamics* (2020), available at [arXiv:2006.01568](#). [↑63](#)
- [97] James E. Humphreys, *Reflection Groups and Coxeter Groups*, Cambridge University Press, Cambridge, 1990. [↑22](#), [24](#), [26](#), [31](#)
- [98] Colin Ingalls and Hugh Thomas, *Noncrossing partitions and representations of quivers*, *Compositio Mathematica* **145** (2009), 1533–1562. [↑38](#)
- [99] Emma Yu Jin and Christian M. Reidys, *Combinatorial design of pseudoknot RNA*, *Advances in Applied Mathematics* (2009), 135–151. [↑1](#)
- [100] Myrto Kallipoliti and Henri Mühle, *On the topology of the Cambrian semilattices*, *The Electronic Journal of Combinatorics* **20** (2013), Research article P48, 21 pages. [↑41](#)
- [101] Donald E. Knuth, *The Art of Computer Programming Volume 1: Fundamental Algorithms*, 3rd ed., Addison-Wesley, Reading, MA, 1997. [↑3](#), [35](#), [37](#)
- [102] Allen Knutson and Ezra Miller, *Subword complexes in Coxeter groups*, *Advances in Mathematics* **184** (2004), 161–176. [↑3](#), [48](#), [49](#)
- [103] Allen Knutson and Ezra Miller, *Gröbner geometry of Schubert polynomials*, *Annals of Mathematics* **161** (2005), 1245–1318. [↑3](#), [48](#)
- [104] Yuji Kodama and Lauren Williams, *KP solitons, total positivity, and cluster algebras*, *Proceedings of the National Academy of Sciences of the USA* **108** (2011), 8984–8989. [↑2](#)
- [105] Christian Krattenthaler, *The F-triangle of the generalised cluster complex*. In: *Topics in Discrete Algorithms* (Martin Klazar, Jan Kratochvíl, Martin Loeb, Jiří Matoušek, Pavel Valtr, and Robin Thomas, eds.), Springer (2006), 93–126. [↑61](#)
- [106] Christian Krattenthaler, *The M-triangle of generalised non-crossing partitions for the types E_7 and E_8* , *Séminaire Lotharingien de Combinatoire* **54** (2006), Research article B54I, 34 pages. [↑61](#)

- [107] Christian Krattenthaler, *Lattice path enumeration*. In: Handbook of Enumerative Combinatorics (Miklós Bóna, ed.), CRC Press, Boca Raton-London-New York (2015), 589–678. [↑85, 178](#)
- [108] Christian Krattenthaler and Henri Mühle, *The rank enumeration of certain parabolic non-crossing partitions* (2019), available at [arXiv:1910.13244](#). [↑81, 140, 178, 179, 180](#)
- [109] Christian Krattenthaler and Thomas W. Müller, *Decomposition numbers for finite Coxeter groups and generalised non-crossing partitions*, Transactions of the American Mathematical Society **362** (2006), 2723–2787. [↑61](#)
- [110] Germain Kreweras, *Sur une classe de problèmes de dénombrement liés au treillis des partitions des entiers*, Cahiers du Bureau Universitaire de Recherche Opérationnelle **6** (1965), 5–105. [↑84](#)
- [111] Germain Kreweras, *Sur les partitions non croisées d'un cycle*, Discrete Mathematics **1** (1972), 333–350. [↑1, 43, 45, 46](#)
- [112] Derrick H. Lehmer, *Teaching combinatorial tricks to a computer*. In: Combinatorial Analysis (Richard Bellman and Marshall Hall Jr, eds.), Proceedings of Symposia in Applied Mathematics (1960), 179–194. [↑42](#)
- [113] Shu-Chung Liu, *Left-Modular Elements and Edge-Labelings*, Ph.D. Thesis, Michigan State University, 1999. [↑16](#)
- [114] Shu-Chung Liu and Bruce E. Sagan, *Left-modular elements of lattices*, Journal of Combinatorial Theory, Series A **91** (2000), 369–385. [↑16](#)
- [115] Jean-Louis Loday and María O. Ronco, *Hopf algebra of the planar binary trees*, Advances in Mathematics **139** (1998), 293–309. [↑42, 142](#)
- [116] Claudia Malvenuto and Christophe Reutenauer, *Duality between quasi-symmetric functions and the Solomon descent algebra*, Journal of Algebra **177** (1995), 967–982. [↑142](#)
- [117] Ricardo Mamede, *A bijection between noncrossing and nonnesting partitions of type A, B and C*, Contributions to Discrete Mathematics **6** (2011), 70–90. [↑57](#)
- [118] George Markowsky, *Primes, irreducibles and extremal lattices*, Order **9** (1992), 265–290. [↑15, 16](#)
- [119] Robert Marsh, Markus Reineke, and Andrei Zelevinsky, *Generalized associahedra via quiver representations*, Transactions of the American Mathematical Society **355** (2003), 4171–4186. [↑49](#)
- [120] Hideya Matsumoto, *Générateurs et relations des groupes de Weyl généralisés*, Comptes Rendus de l'Académie des Sciences **258** (1964), 3419–3422. [↑30](#)
- [121] Jon McCammond, *Noncrossing partitions in surprising locations*, American Mathematical Monthly **113** (2006), 598–610. [↑1](#)
- [122] Ralph McKenzie, *Equational bases and nonmodular lattice varieties*, Transactions of the American Mathematical Society **174** (1972), 1–43. [↑18](#)
- [123] Peter McNamara and Hugh Thomas, *Poset edge-labelings and left modularity*, European Journal of Combinatorics **27** (2006), 101–113. [↑16](#)
- [124] Stephen Melcer and Marni Mishna, *Singularity analysis via the iterated kernel method*, Combinatorics, Probability and Computing **23** (2014), 861–888. [↑145](#)
- [125] Marni Mishna and Andrew Rechnitzer, *Two non-holonomic lattice walks in the quarter plane*, Theoretical Computer Science **410** (2009), 3616–3630. [↑145](#)
- [126] Henri Mühle, *SB-labelings, distributivity, and Bruhat order on sortable elements*, The Electronic Journal of Combinatorics **22** (2015), Research article P2.40, 14 pages. [↑63](#)
- [127] Henri Mühle, *Trimness of closed intervals in Cambrian semilattices*, Comptes Rendus—Mathématique **354** (2016), 113–120. [↑41](#)
- [128] Henri Mühle, *Meet-Distributive lattices have the intersection property* (2018), available at [arXiv:1810.01528](#). [↑78](#)
- [129] Henri Mühle, *Two posets of noncrossing partitions coming from undesired parking spaces*, Revista Colombiana de Matemáticas **52** (2018), 65–86. [↑85](#)

- [130] Henri Mühle, *Ballot-noncrossing partitions*, Séminaire Lotharingien de Combinatoire **82B** (2019), Conference paper 7, 12 pages. ↑[81](#), [138](#)
- [131] Henri Mühle, *The core label order of a congruence-uniform lattice*, Algebra Universalis **80** (2019), Research article 10, 22 pages. ↑[19](#)
- [132] Henri Mühle, *Noncrossing arc diagrams, Tamari lattices, and parabolic quotients of the symmetric group*, Annals of Combinatorics **25** (2021), 307–344. ↑[17](#), [81](#), [91](#), [110](#)
- [133] Henri Mühle and Nathan Williams, *Tamari lattices for parabolic quotients of the symmetric group*, The Electronic Journal of Combinatorics **26** (2019), Research article P4.34, 28 pages. ↑[81](#), [93](#)
- [134] Andrew Neitzke, *Cluster-like coordinates in supersymmetric quantum field theory*, Proceedings of the National Academy of Sciences of the USA **111** (2014). ↑[2](#)
- [135] Arnau Padrol, Vincent Pilaud, and Julian Ritter, *Shard polytopes* (2020), available at [arXiv:2007.01008](https://arxiv.org/abs/2007.01008). ↑[172](#)
- [136] T. Kyle Petersen, *On the shard intersection order of a Coxeter group*, SIAM Journal on Discrete Mathematics **27** (2013), 1880–1912. ↑[137](#)
- [137] Matthieu Picantin, *Explicit presentations for the dual braid monoids*, Comptes Rendus de l'Académie des Sciences Paris, Série I **334** (2002), 843–848. ↑[2](#)
- [138] Vincent Pilaud and Michel Pocchiola, *Multitriangulations, pseudotriangulations and primitive sorting networks*, Discrete and Computational Geometry **48** (2012), 142–191. ↑[49](#), [182](#)
- [139] Vincent Pilaud and Francisco Santos, *The brick polytope of a sorting network*, European Journal of Combinatorics **33** (2012), 632–662. ↑[49](#)
- [140] Vincent Pilaud and Christian Stump, *EL-labelings and canonical spanning trees for subword complexes*. In: Discrete Geometry and Optimization (Karoly Bezdek, Antoine Deza, and Yinyu Ye, eds.), Springer (2013), 213–248. ↑[50](#)
- [141] Vincent Pilaud and Christian Stump, *Brick polytopes of spherical subword complexes and generalized associahedra*, Advances in Mathematics **276** (2015), 1–61. ↑[3](#), [49](#), [50](#)
- [142] Vincent Pilaud and Viviane Pons, *Permutrees*, Algebraic Combinatorics **1** (2018), 173–224. ↑[3](#), [165](#)
- [143] Viviane Pons, *A lattice on decreasing trees: the metasylovester lattice*, Discrete Mathematics & Theoretical Computer Science (2015), 381–392. Proceedings of the 27th Conference on Formal Power Series and Algebraic Combinatorics. ↑[178](#)
- [144] Louis-François Prévaille-Ratelle and Xavier Viennot, *The enumeration of generalized Tamari intervals*, Transactions of the American Mathematical Society **369** (2017), 5219–5239. ↑[4](#), [57](#)
- [145] Robert A. Proctor and Matthew J. Willis, *Parabolic Catalan numbers count flagged Schur functions and their appearances as type A Demazure characters (key polynomials)*, Discrete Mathematics & Theoretical Computer Science **19** (2017), Research article 15, 27 pages. ↑[90](#)
- [146] Robert A. Proctor and Matthew J. Willis, *Convexity of tableau sets for type A Demazure characters (key polynomials), parabolic Catalan numbers*, Discrete Mathematics & Theoretical Computer Science **20** (2018), Research article 3, 20 pages. ↑[89](#), [90](#)
- [147] Nathan Reading, *Cambrian lattices*, Advances in Mathematics **205** (2006), 313–353. ↑[3](#), [18](#), [65](#), [111](#)
- [148] Nathan Reading, *Clusters, Coxeter-sortable elements and noncrossing partitions*, Transactions of the American Mathematical Society **359** (2007), 5931–5958. ↑[3](#), [37](#), [38](#), [45](#), [49](#), [66](#), [162](#), [168](#)
- [149] Nathan Reading, *Sortable elements and Cambrian lattices*, Algebra Universalis **56** (2007), 411–437. ↑[3](#), [38](#), [39](#), [40](#)
- [150] Nathan Reading, *Chains in the noncrossing partition lattice*, SIAM Journal on Discrete Mathematics **22** (2008), 875–886. ↑[63](#)

- [151] Nathan Reading, *Cambrian fans*, Journal of the European Mathematical Society **11** (2009), 407–447. ↑40
- [152] Nathan Reading, *Noncrossing partitions and the shard intersection order*, Journal of Algebraic Combinatorics **33** (2011), 483–530. ↑3, 19, 47, 137
- [153] Nathan Reading, *Noncrossing arc diagrams and canonical join representations*, SIAM Journal on Discrete Mathematics **29** (2015), 736–750. ↑14, 43
- [154] Nathan Reading and David Speyer, *Sortable elements in infinite Coxeter groups*, Transactions of the American Mathematical Society **363** (2011), 699–761. ↑3, 29, 38, 40, 41
- [155] Nathan Reading, David E. Speyer, and Hugh Thomas, *The fundamental theorem of finite semidistributive lattices*, Selecta Mathematica **27** (2021), Research article 59, 53 pages. ↑13
- [156] Christian M. Reidys and Rita R. Wang, *Shapes of RNA pseudoknot structures*, Journal of Computational Biology **17** (2010), 1575–1590. ↑1
- [157] Victor Reiner, *Non-crossing partitions for classical reflection groups*, Discrete Mathematics **177** (1997), 195–222. ↑2, 4, 35, 44, 45, 46, 56, 172
- [158] Victor Reiner, Anne V. Shepler, and Eric Sommers, *Invariant theory for coincidental complex reflection groups*, Mathematische Zeitschrift (2020), 24 pages. To appear. ↑63
- [159] Claus Michael Ringel, *The Catalan combinatorics of the hereditary Artin algebras*. In: Recent Developments in Representation Theory (Alex Martsinkovsky, Gordana Todorov, and Kiyoshi Igusa, eds.), American Mathematical Society, Providence, RI (2016), 58–185. ↑1
- [160] Gian-Carlo Rota, *On the foundations of combinatorial theory I: Theory of Möbius functions*, Zeitschrift für Wahrscheinlichkeitstheorie und verwandte Gebiete **2** (1964), 340–368. ↑10, 15
- [161] Martin Rubey, *Maximal 0–1-fillings of moon polyominoes with restricted chain lengths and rc-graphs*, Advances in Applied Mathematics **48** (2012), 290–305. ↑52
- [162] The Sage Developers, *Sage Mathematics Software System (Version 9.1)*, 2020. <http://www.sagemath.org>. ↑76
- [163] Joshua S. Scott, *Grassmannians and cluster algebras*, Proceedings of the London Mathematical Society **92** (2003), 345–380. ↑2
- [164] Johann A. Segner, *Enumeratio modorum quibus figurae planae rectilineae per diagonales dividuntur in triangula*, Novi Commentarii Academiae Scientiarum Imperialis Petropolitanae **VII** (1761), 203–210. ↑55
- [165] Luis Serrano and Christian Stump, *Maximal fillings of moon polyominoes, simplicial complexes, and Schubert polynomials*, The Electronic Journal of Combinatorics **19** (2012), Research article P16, 18 pages. ↑49, 83, 85
- [166] Geoffrey C. Shephard and John A. Todd, *Finite unitary reflection groups*, Canadian Journal of Mathematics **6** (1954), 274–304. ↑33
- [167] Jian-Yi Shi, *The enumeration of Coxeter elements*, Journal of Algebraic Combinatorics **6** (1997), 161–171. ↑30
- [168] Rodica Simion, *Noncrossing partitions*, Discrete Mathematics **217** (2000), 397–409. ↑1
- [169] Neil J. A. Sloane, *The On-line Encyclopedia of Integer Sequences*, 2020. ↑85, 145
- [170] Louis Solomon, *The orders of finite Chevalley groups*, Journal of Algebra **3** (1966), 376–393. ↑33
- [171] Roland Speicher, *Multiplicative functions on the lattice of non-crossing partitions and free convolution*, Mathematische Annalen **298** (1994), 611–628. ↑1
- [172] Roland Speicher, *Free probability theory and non-crossing partitions*, Séminaire Lotharingien de Combinatoire **39** (1997), Survey article B39c, 38 pages. ↑1
- [173] Tonny A. Springer, *Regular elements of finite reflection groups*, Inventiones Mathematicae **25** (1974), 159–198. ↑30
- [174] Richard P. Stanley, *On the number of reduced decompositions of elements of Coxeter groups*, The European Journal of Combinatorics **5** (1984), 359–372. ↑63

- [175] Richard P. Stanley, *Enumerative Combinatorics, Vol. 1*, 2nd ed., Cambridge University Press, Cambridge, 2011. ↑[9](#), [10](#)
- [176] James D. Stasheff, *Homotopy associativity of H-spaces II*, Transactions of the American Mathematical Society **108** (1963), 293–312. ↑[2](#)
- [177] John R. Stembridge, *On the fully commutative elements of Coxeter groups*, Journal of Algebraic Combinatorics **5** (1996), 353–385. ↑[78](#)
- [178] Christian Stump, *A new perspective on k-triangulations*, Journal of Combinatorial Theory, Series A **118** (2011), 1794–1800. ↑[49](#), [182](#)
- [179] Christian Stump, *More bijective Catalan combinatorics on permutations and signed permutations*, Journal of Combinatorics **4** (2013), 419–447. ↑[57](#)
- [180] Christian Stump, Hugh Thomas, and Nathan Williams, *Cataland: Why the Fuss?*, Memoirs of the American Mathematical Society (2020), 132 pages. To appear. ↑[47](#), [182](#)
- [181] Robin Sulzgruber and Marko Thiel, *On parking functions and the zeta map in types B, C and D*, The Electronic Journal of Combinatorics **25** (2018), Research article P1.8, 82 pages. ↑[4](#)
- [182] Dov Tamari, *Monoïdes Préordonnés et Chaînes de Malcev*, Thèse de Mathématiques, Université de Paris, 1951. ↑[42](#)
- [183] Marko Thiel, *On the H-triangle of generalised nonnesting partitions*, European Journal of Combinatorics **39** (2014), 244–255. ↑[61](#)
- [184] Marko Thiel, *From Anderson to zeta*, Advances in Applied Mathematics **81** (2016), 156–201. ↑[152](#)
- [185] Hugh Thomas, *Graded left modular lattices are supersolvable*, Algebra Universalis **53** (2005), 481–489. ↑[16](#)
- [186] Hugh Thomas, *An analogue of distributivity for ungraded lattices*, Order **23** (2006), 249–269. ↑[16](#), [17](#)
- [187] Hugh Thomas, *The Tamari lattice as it arises in quiver representations*. In: Associahedra, Tamari Lattices and related Structures (Folkert Müller-Hoissen, Jean Marcel Pallo, and Jim Stasheff, eds.), Springer, Basel (2012), 281–291. ↑[1](#)
- [188] Hugh Thomas and Nathan Williams, *Sweeping up zeta*, Selecta Mathematica **24** (2018), 2003–2034. ↑[152](#)
- [189] Hugh Thomas and Nathan Williams, *Rowmotion in slow motion*, Proceedings of the London Mathematical Society **119** (2019), 1149–178. ↑[15](#), [17](#)
- [190] Jacques Tits, *Le problème des mots dans les groupes de Coxeter*. In: Symposia Mathematica, Istituto Nazionale di Alta Matematica, Rome (1969), 175–185. ↑[30](#)
- [191] Eleni Tzanaki, *Faces of generalized cluster complexes and noncrossing partitions*, SIAM Journal on Discrete Mathematics **22** (2008), 15–30. ↑[61](#)
- [192] Nathan Williams, *Cataland*, Ph.D. Thesis, University of Minnesota, 2013. ↑[33](#), [43](#), [63](#), [65](#), [66](#), [68](#), [69](#), [70](#), [72](#), [78](#), [182](#), [185](#)
- [193] Alexander Woo, *Catalan numbers and Schubert polynomials for $w = 1(n+1) \dots 2$* (2004), available at [arXiv:0407160](#). ↑[52](#)

Index

— Symbols —

α -coloring	93
α -partition	90
α -arc	90
noncrossing	90
α -permutation	82
$(\alpha, 132)$ -avoiding	112
$(\alpha, 132)$ -pattern	112
$(\alpha, 231)$ -avoiding	89
$(\alpha, 231)$ -pattern	89
α -code	123
α -region	88
α -tree	93
\mathbb{K} -algebra	
antipode	142
associative	141
bialgebra	142
coassociative	141
cocommutative	141
commutative	141
comultiplication	141
counit	141
Hopf algebra	142
Hopf subalgebra	142
multiplication	141
unit	141

— A —

absolute order	28
acyclic relation	7
aligned element	37
last reflection	49
parabolic	65

— C —

Cambrian congruence	40
Cambrian lattice	38
parabolic	67
canonical join complex	14
Catalan family	35
Catalan number	35
α -Catalan number	84
q, t -Catalan number	151
Coxeter–Catalan number	35
parabolic	72
Cataland	33
cluster complex	49
cluster	49
parabolic	70
cluster	70
composition	82
reverse	82
core label order	20
Coxeter element	30
barring	161
final generator	31
initial generator	31
linear	41
rotation	31
Coxeter graph	23
orientation	30
Coxeter group	<i>see</i> Coxeter system
Coxeter matrix	22
Coxeter system	23
absolute length	28
braid move	30
coincidental	63

Coxeter generators	23		
Coxeter length	28		
crystallographic	24		
degrees	34		
exponents	34		
finite	23		
geometric representation	26		
inversion order	36		
irreducible	23		
longest element	28		
nil move	30		
orientation	30		
parabolic quotient	63		
fully commutative	78		
parabolic subgroup	63		
postfix order	27		
rank	23		
reflecting hyperplane	25		
sorting word	36		
word property	30		
— D —			
Demazure product	48		
directed graph			
mutation	31		
orthogonal pair	15		
maximal	15		
sink	31		
source	31		
Dyck path	55		
α -Dyck path	84		
area vector	151		
bounce path	151		
bounce statistic	151		
dinv	151		
level marked	145		
marked	145		
nested	153		
steep	154		
— F —			
F-triangle	60		
Ferrers shape	50		
α -shape	82		
staircase	50		
— G —			
Galois graph	15		
— H —			
H-triangle	60		
parabolic	73		
— L —			
lattice	10		
atom	12		
Boolean lattice	11		
canonical joinand	13		
coatom	12		
congruence	18		
congruence uniform	18		
core	19		
distributive	12		
extremal	15		
homomorphism	18		
join representation	13		
join-irreducible element	12		
join-semidistributive	13		
spherical	15		
labeled	19		
left-modular	16		
left-modular element	16		
meet-irreducible element	12		
meet-semidistributive	13		
nuclear	12		
nucleus	19		
quotient	18		
semidistributive	13		
sublattice	12		
trim	16		
— M —			
M-triangle	60		
map			
order preserving	8		
Möbius function	10		
— N —			
noncrossing partition	44		
parabolic	68		
nonnesting partition	57		
parabolic	71		
northeast path	55		
α -bounce path	84		
ν -Tamari lattice	57		
ν_α -Tamari lattice	122		
area	55		
bracket vector	128		
peak	55		
return	138		
reverse	55		
rotation	57		
valley	55		

— O —	
order relation	7
ordinary partition	<i>see</i> set partition
— P —	
partially ordered set	<i>see</i> poset
permutation	
231-avoiding	35
231-pattern	35
•-shuffle	143
atomic	142
BW-code	41
descent	42
global descent	142
inversion set	35
α -aligned	88
aligned	35
Lehmer code	42
reverse	115
stack-sortable	38
sum	54
swapped sum	142
pipe dream	50
chutable rectangle	52
chute move	52
coproduct	143
product	143
reduced	51
poset	7
antichain	56
atom	9
bounded	8
chain	9
maximal	9
saturated	9
coatom	9
cover relation	8
perspective	12
diagram	8
dual	8
edge-labeling	8
core labeling	20
finitary	29
graded	9
greatest element	9
interval	9
join	11
join-semilattice	11
least element	9
length	9
lower bound	8
lower bounded	8
maximal element	8
meet	11
meet-semilattice	11
minimal element	8
multichain	9
size	9
order filter	9
order ideal	9
rank function	9
triangular	56
upper bound	8
upper bounded	8
zeta polynomial	9
power set	11
— R —	
reflection	26
(right) inversion	28
cover inversion	41
simple reflection	25
root poset	27
parabolic	71
root system	26
almost positive roots	49
negative roots	26
positive roots	26
root order	27
simple root	26
— S —	
set partition	43
block	43
bump	43
noncrossing	43
nonnesting	55
refinement	43
subword complex	48
flip	50
symmetric function	150
polarized power sum	151
power sum	150
symmetric group	35
parabolic quotient	82
— T —	
Tamari lattice	42, 57
α -Tamari lattice	112
tree	91
active node	92
colored	92

coloring			
full	92	descendant	91
partial	92	internal node	92
horizontal composition	93	parent	91
LAC tree	148	sibling	92
leaf	92	traversal	
LR-postfix order	92	left-to-right	92
LR-prefix order	92	right-to-left	92
node	91		
plane	92	— V —	
RL-postfix order	92	Vandermonde determinant	150
RL-prefix order	92	vector space	
root	91	connected	141
rooted	91	graded	141
child	91		
		— W —	
		weak order	28

Declaration

Erklärung gemäß §6 Abs. 2, Ziffer 2 der Habilitationsordnung

Hiermit versichere ich, dass ich die vorliegende Arbeit selbst und ohne unzulässige Hilfe Dritter und ohne andere als die darin angegebenen Hilfsmittel angefertigt habe. Die aus fremden Quellen wörtlich oder inhaltlich übernommenen Stellen wurden als solche gekennzeichnet.

Bei allen eingereichten gemeinschaftlichen Arbeiten erstreckt sich meine Mitarbeit auf sämtliche Aspekte des Forschungsprozesses, einschließlich der Ideenfindung, der Ausarbeitung und der Dokumentation der Ergebnisse.

Es wurden zuvor keine Habilitationsvorhaben unternommen.

Ich erkenne die Habilitationsordnung des Bereiches Mathematik und Naturwissenschaften der Technischen Universität Dresden vom 12. Dezember 2010, in der geänderten Fassung mit Gültigkeit vom 23. Januar 2019, an.

Henri Mühle